

ANALYSIS OF B CELL RESPONSES TO BLOOD-STAGE MALARIA ANTIGENS IN HUMANS FOLLOWING IMMUNIZATION WITH CANDIDATE VACCINES AND CONTROLLED HUMAN MALARIA INFECTION

Thesis submitted for the degree of Doctor of Philosophy Clinical Medicine

Trinity Term 2014

Sean Christopher Elias

Hertford College

Word Count ≈49,000 (excl. Bibliography, Figures and Tables)

Abstract

The apicomplexan parasite *Plasmodium falciparum* is the causative agent of the most severe and deadly form of human malaria. The production of an efficacious malaria vaccine is seen as one of the key steps towards the eradication of the disease, however to date only one candidate has progressed to application for licensure. Candidate malaria vaccines target the different stages of the *P. falciparum* lifecycle through induction of a functional immune response. Vaccines targeting the blood-stage parasite require induction of high titre neutralising antibodies. To achieve this, vaccine regimens have been designed specifically to maximise antibody induction and maintenance in humans. The ultimate test of any candidate vaccine is clinical efficacy and controlled human malaria infection (CHMI) is a powerful tool for measuring this. This model can also be used to study how vaccine induced antigen-specific components of the immune system respond to native antigen exposure in the context of parasitic infection

In this Thesis I describe the induction and maintenance of B cell responses, including memory B cells (mBC) and antibody secreting cells (ASC) to the candidate blood-stage malaria antigens MSP1 and AMA1 following vaccination with a variety of regimens and CHMI. These B cell populations along with peripheral blood T follicular helper (Tfh) cells correlate strongly with antibody induction. Within these populations I have identified a number of phenotypically distinct subsets which contribute to a functional response to vaccine and/or parasite antigen. From single cell sorting of ASC at day seven post-boost I have managed to produce the first fully human monoclonal antibodies (hmAbs) specific for AMA1, one of which shows significant growth inhibitory activity (GIA).

Despite promise the vaccine candidates MSP1 and AMA1 have been disappointing in terms of human efficacy. In this Thesis I have attempted to provide explanations on a cellular level as to why there is such disparity between pre-clinical and human data and ultimately why these candidates may have failed to provide efficacy. Such work will provide a strong basis for analysing future clinical trials of alternative candidate blood-stage vaccines and allow accurate characterisation of immune correlates and clinical efficacy when it is achieved.

Acknowledgements

First and mostly I would like to thank my supervisor Simon Draper, not only for the opportunity for this DPhil but for his endless support throughout the process. In particular I thank you for always being available to answer my 'quick questions' and for providing encouragement and solutions when things got tough. I think each and every one of your students past and present would agree that there is no better supervisor out there and I look forward to continuing learning from you as I go on to start my first post-doc.

Secondly I would like to thank our Institute Director Adrian Hill. Fresh from my undergraduate degree you gave me the opportunity to work as an RA at the Jenner Institute which has now been home for the last 6 fantastic years (and still counting). During that time despite your jet-setting lifestyle you have always been incredibly supportive and encouraging.

The clinical trials run by the Jenner Institute have been an integral part of my DPhil and so I would like to thank all those who have worked on them over the years. In particular for their work on the blood-stage clinical trials I would like to thank Prateek Choudhary, Kathryn Milne, Fenella Halstead, Susanne Hodgson, Chris Duncan and Ruth Payne. I big thanks also to the liver-stage team especially Katherine Collins, Carly Bliss, Georgina Bowyer and Katie Ewer. I also thank the hundreds of volunteers who participated in our trials, without you we could not do the work we do (and my figures would be rather empty).

There are many more to thank at the Jenner Institute outside of the clinical trials team. Huge thanks must go out to Daniel Alanine for his help with the development of the CPEC cloning and mAb production, arguably the most difficult part of this Thesis. I would also like to say a big thanks to Drew Worth, not only for all the MoFlo sorting of B cells but for general help with all flow cytometry work. Many thanks must also go to all the blood-stage lab team members past and present especially Sumi Biswas, Simone de Cassan, Joe Illingworth, David Llewellyn, Sandy Douglas and Rebecca Brown. Others who have provided ideas and solutions during my DPhil include Nick Edwards, Alex Spencer and Tess Lambe. A massive Jenner thanks also to Julie Furze, who keeps the whole place running like a well-oiled engine. Special thanks must go to Louisa Rose, Rachel Tanner, Lynda Coughlan and particularly Matthew Dicks for providing endless entertainment and banter over the years.

Next I would like to thank all my collaborators across the University of Oxford. Firstly for helping set up the initial mBC ELISPOTs, being my transfer examiner and talking B cells over coffee I would like to thank Elizabeth Clutterbuck. For invaluable help in getting the BCR PCR set up and working correctly, a big thanks to Alain Townsend and Pramila Rijal. I look forward to working together again in the upcoming Ebola trials. For proposing the Tfh cell part of my DPhil (again over coffee) and for being my transfer examiner I would like to thank Persephone Borrow, and for setting up the Tfh flow panel and helping me run the hundreds of Tfh samples, Cecilia Chui. I also would like to thank Clare Grant for setting up the Oxford B cell meeting and all the attendees for their feedback and suggestions (and for providing the coffee and biscuits… I'm seeing a trend here).

Outside of the lab the biggest of thanks must go to Amr El-Labban and Constantine Garagounis. The hours playing, watching and talking football with your guys have been very well spent and the best possible distraction from work. On that note a big thanks to all my mates in the Magdalen MCR football and cricket teams and the Medicine cricket team too.

Last but not least I would like to thank my family especially my Mum and Dad, without your nature and nurture I would not have made it to where I am now. From a young age you all encouraged my love of science and nature and have maintained that encouragement throughout school, my undergraduate degree and my DPhil.

Publications arising from this Thesis

The following manuscripts contain work described in this Thesis:

Sean C. Elias, Prateek Choudhary, Simone C. de Cassan, Sumi Biswas, Katharine A. Collins, Fenella D. Halstead, Carly M. Bliss, Katie J. Ewer, Susanne H. Hodgson, Christopher J. A. Duncan, Adrian V. S. Hill and Simon J. Draper. "*Analysis of human B-cell responses following ChAd63-MVA MSP1 and AMA1 immunization and controlled malaria infection"* Immunology, 2014, 141, 628–644

Susanne H. Hodgson, Prateek Choudhary, Sean C. Elias, Kathryn H. Milne, Thomas W. Rampling, Sumi Biswas, Ian D. Poulton, Kazutoyo Miura, Alexander D. Douglas, Daniel G. W. Alanine, Joseph J. Illingworth, Simone C. de Cassan, Alfredo Nicosia, Carole A. Long, Sarah Moyle, Eleanor Berrie, Alison M. Lawrie, Yimin Wu, Ruth D. Ellis, Adrian V. S. Hill and Simon J. Draper. *"Combining viral vectored and protein-in-adjuvant vaccines against the blood-stage malaria antigen AMA1 - Report on a Phase Ia clinical trial"* Molecular Therapy, 2014, accepted article.

Table of Contents

Abstract 2

Acknowledgements 3

Publications arising from this Thesis 5

List of Figures 12

List of Tables 14

List of Abbreviations 15

1. Introduction 20

1.1. Malaria and Natural Immunity 20

1.1.1. Malaria Lifecycle 20

1.1.2. Pathology of Malaria 23

1.1.3. Acquisition of Naturally-Acquired Immunity 23

1.2. Malaria Immunity 25

1.2.1. Innate Immunity 25

1.2.2. T cell-Mediated Immunity 27

1.2.3. Antibody-Mediated Immunity 28

1.2.4. Parasite-Mediated Evasion of Natural Immunity 37

1.3. Need for a Malaria Vaccine 39

1.3.1. Aim of Malaria Vaccines 39

1.3.2. Targets for Malaria Vaccines 40

1.3.3. Vaccine Delivery Platforms 46

1.3.4. Adjuvants 50

1.4. Controlled Human Malaria Infection (CHMI) 52

1.4.1. CHMI Delivery 52

1.4.2. Testing Vaccine Efficacy with CHMI 52

1.4.3. CHMI as a Vaccine Platform 53
1.5. Immunological Assays 54
1.5.1. ELISPOT 54
1.5.2. ELISA 55
1.5.3. Flow Cytometry 56
1.5.4. Production of Monoclonal Antibodies 57
1.5.5. Assay of Growth Inhibitory Activity 58
1.6. Thesis Aims & Outlines 60
1.6.1. Aims 60
1.6.2. Outlines 61
2. Materials and Methods 62
2.1. Materials 62
2.1.1. Reagents 62
2.1.2. Buffers and Solutions 65
2.1.3. Flow Cytometry Antibodies 66
2.1.4. Primers 68
2.1.5. Laboratory Consumables 71
2.1.6. Electronic Equipment 72
2.2. Clinical Vaccines 73
2.2.1. Vaccine manufacture 73
2.2.2. MSP1 73
2.2.3. AMA1 74
2.3. Recombinant Protein and Peptides 75
2.3.1. MSP1 75
2.3.2. AMA1 75
2.4. Clinical Trials 76

2.4.1. VAC036 76
2.4.2. VAC037 77
2.4.3. VAC039 78
2.4.4. VAC044 79
2.4.5. VAC049 80
2.5. Clinical Immunology 81
2.5.1. Blood Separation 81
2.5.2. IFN-γ ELISPOT 81
2.5.3. mBC ELISPOT 82
2.5.4. ASC ELISPOT 83
2.5.5. MSP1 and AMA1 ELISA 84
2.5.6. IFN-γ ELISA 84
2.5.7. MIG ELISA 85
2.6. Flow Cytometry 86
2.6.1. B cell Phenotyping 86
2.6.2. Single Cell ASC Sorting 88
2.6.3. Antigen-Specific Cell Staining 89
2.6.4. Tfh Cell Staining 90
2.7. Monoclonal Antibody Production 93
2.7.1. Single Cell PCR 93
2.7.2. Circular Polymerase Extension Cloning (CPEC) 95
2.7.3. Plasmid Sequencing 96
2.7.4. Transformation of E. coli 96
2.7.5. Transfection and mAb screen 96
2.7.6. Western Blot of mAbs 97
2.7.7. Assay of Growth Inhibitory Activity (GIA) 97

2.8. Statistics 99

3. B cell induction following ChAd63-MVA MSP1 and AMA1 immunisation and controlled human malaria infection 100

3.1. Introduction 100

3.2. Results 103

3.2.1. ChAd63-MVA prime-boost vaccination induces antigen-specific mBC responses 103

3.2.2. Controlled P. falciparum infection induces mBC to $MSP1_{19}$ but not AMA1 in unvaccinated infectivity control volunteers 106

3.2.3. Controlled P. falciparum infection boosts the vaccine-induced mBC response 112

3.2.4. MSP1 and AMA1 vaccine co-administration induces mBC responses to both antigens ... 115

3.2.5. $MSP1_{19}$-specific mBC responses correlate with antibodies post-MVA vaccination but not following CHMI 118

3.2.6. Migratory ASC can be detected 7 days following MVA booster vaccination but were not observed at selected time-points during and post-CHMI 120

3.3. Discussion 123

4. Phenotypic characterisation of B cell subsets during CHMI 130

4.1. Introduction 130

4.2. Results 134

4.2.1. Relative populations of different B cell subsets do not significantly change during CHMI 134

4.2.2. A decrease in $CXCR3^+$ B cells in the peripheral blood was observed at the point of diagnosis 138

4.2.3. The inflammatory cytokines IFN-γ and CXCL9 may contribute to possible migration of $CXCR3^+$ B cells away from the periphery. 141

4.2.4. Functional response to blood-stage parasite antigen likely drives production of IFN-γ. .. 143

4.3. Discussion 145

5. Single B cell sorting 151

5.1. Introduction 151
5.2. Results 155
5.2.1. Optimisation of single B cell MoFlo sorting of ASC at 7 days post-boost 155
5.2.2. Antigen-specific B cell staining for the blood-stage antigens MSP1 and AMA1 163
5.3. Discussion 168
6. Production and Characterisation of Human Monoclonal Antibodies 172
6.1. Authorship Statement 172
6.2. Introduction 172
6.3. Results 176
6.3.1. RT-PCR, Nested PCR and identification of heavy and light chains genes of the BCR 176
6.3.2. Circular Polymerase Extension Cloning (CPEC) of heavy and light chain genes into expression vectors 179
6.3.3. HEK293 transfection and screening for antigen-specific IgG 181
6.3.4. Sequence analysis of AMA1-specific human mAbs 184
6.3.5. Assay of Growth Inhibitory Activity (GIA) 185
6.4. Discussion 187
7. Association of peripheral blood T follicular helper cell populations with vaccine induced antibody and B cell responses 191
7.1. Authorship Statement 191
7.2. Introduction 191
7.3. Results 198
7.3.1. B cell responses induced by 'mixed-modality' regimens 198
7.3.2. Baseline Tfh responses do not predict immune response post-prime. 203
7.3.3. Tfh populations induced following booster vaccination correlate with peak post-boost immune responses. 209
7.4. Discussion 218

8. Discussion and Future Directions 223
8.1. Summary 223
8.2. Conclusions 225
8.2.1. B cell responses to candidate blood-stage malaria antigens mostly follow classical kinetics following vaccination. 225
8.2.2. CHMI provides a unique insight into the differences between how B cells respond to live parasite antigen compared to vaccine antigen. 226
8.2.3. Peripheral blood Tfh cells have been described for the first time following malaria vaccination and distinct populations correlate with different aspects of the antibody and B cell response. 227
8.2.4. Functional human mAbs can be isolated from volunteers vaccinated with candidate blood-stage malaria antigens 229
8.3. Future Directions 230
8.3.1. The role of B cell ELISPOT in future clinical trial immuno-monitoring 230
8.3.2. Maximising the investigative potential of CHMI 230
8.3.3. Relationships and interactions between B cell and Tfh populations 231
8.3.4. The future of MSP1 and AMA1 as candidate malaria vaccine candidates 232
8.3.5. Improving the identification and isolation of antigen-specific B cells 234
8.3.6. Production of mAb targeting alternative blood-stage malaria antigens 234
8.4. Final Remarks 236
References 237

List of Figures

Figure 1.1: *Plasmodium falciparum* lifecycle and vaccine targets. 22
Figure 1.2: Interactions between the innate and adaptive immune system in response to malaria. 26
Figure 1.3: T-dependent development of B cell subsets in a primary response in mice. 36
Figure 1.4: Vaccine candidates on the *Plasmodium* merozoite and sporozoite 41
Figure 1.5: MSP1 processing on the merozoite surface during development and erythrocyte invasion. 43
Figure 1.6: Role of AMA1 and RH proteins in erythrocyte invasion. 45
Figure 2.1: MSP1 vaccine insert 73
Figure 2.2: AMA1 vaccine insert 74
Figure 3.1: Phase I/IIa vaccine trial timelines 102
Figure 3.2: mBC responses over time in volunteers receiving ChAd63-MVA MSP1 or AMA1 prime-boost vaccination. 106
Figure 3.3: mBC responses in control unvaccinated volunteers receiving mosquito vectored CHMI. 110
Figure 3.4: mBC responses in control unvaccinated volunteers receiving cryopreserved parasite CHMI. 111
Figure 3.5: mBC responses in vaccinated volunteers receiving CHMI. 115
Figure 3.6: mBC responses in volunteers receiving both vaccines and CHMI. 117
Figure 3.7: Relationship between peripheral mBC responses and serum IgG in vaccinees before and after CHMI. 119
Figure 3.8: Measurement of $MSP1_{19}$-specific peripheral blood ASC post MVA vaccination and CHMI. 122
Figure 4.1: B cell gating strategy. 136
Figure 4.2: B cell subset composition of total B cell pool over time. 137
Figure 4.3: $CXCR3^+$ mBC in peripheral blood during blood-stage infection. 139
Figure 4.4: CXCR3 expression on other B cell subsets. 140
Figure 4.5: Serum levels of IFN-γ and CXCL9 before and during CHMI. 142
Figure 4.6: Serum IFN-γ at DoD differs across groups receiving pre-erythrocytic or blood-stage viral vectored vaccines 144
Figure 5.1: Phenotypic identification of ASC at 7 days post-boost from fresh blood. 158
Figure 5.2: Phenotypic characterisation of ASC derived from culture of mBC. 159
Figure 5.3: Proportions of IgG^+ and antigen-specific cells within cultured B cell populations. 160

Figure 5.4: Effect of B cell enrichment on MoFlo gating of B cell subsets. 161
Figure 5.5: Ratio of AMA1^{+} and IgG^{+} plasma cells detected by ASC ELISPOT post MoFlo sort. 162
Figure 5.6: Comparison of different fluorochromes in the detection of antigen-specific classical mBC. 165
Figure 5.7: Effect of B cell enrichment on antigen-specific staining of classical mBC. 166
Figure 5.8: Use of dual staining in the detection of antigen-specific classical mBC. 167
Figure 6.1: Positive nested PCR products from screen of volunteer #1017 at d63. 178
Figure 6.2: Circular Polymerase Extension Cloning. 180
Figure 6.3: mAb ELISA Screen 182
Figure 6.4: Western Blot of the mAbs C2(H1K4) and D2(H3L8). 183
Figure 6.5: Assay of Growth Inhibitory Activity (GIA) 186
Figure 7.1: Interactions and signalling between Tfh cells and B cells during a T cell-dependent antibody response. 197
Figure 7.2: Measurement of AMA1-specific peripheral blood ASC, post- boost in mixed modality vaccine regimens. 200
Figure 7.3: Relationship between peripheral ASC responses and serum IgG following AMA1 vaccination. 201
Figure 7.4: Measurement of AMA1-specific peripheral blood mBC in mixed-modality vaccine regimens. 202
Figure 7.5: Peripheral blood Tfh gating strategy. 207
Figure 7.6: Comparing CD4^{+} Tfh cell populations at baseline and post-boost. 213
Figure 7.7: Comparison of the composition of the CXCR5^{+}/CD45RO^{+}subset pre-/post-vaccination. 214
Figure 7.8: Quantification and phenotypic characterisation of antigen-specific CD154^{+} and IL-21^{+} cells. 217

List of Tables

Table 2.1: VAC036 Group Summary 76
Table 2.2: VAC037 Group Summary 77
Table 2.3: VAC039 Group Summary 78
Table 2.4: VAC044 Group Summary 79
Table 2.5: VAC049 Group Summary 80
Table 2.6: B cell flow antibody panel 87
Table 2.7: MoFlo antibody panel 89
Table 2.8: Tfh CD154 staining panel 91
Table 2.9: Tfh IL-21 staining panel 91
Table 2.10: Tfh extracellular and intracellular staining panel 92
Table 2.11: RT-PCR Master Mix 93
Table 2.12: Nested PCR Master Mix 94
Table 4.1: B cell phenotypic markers and relative expression on B cell subsets. 135
Table 6.1: Volunteer #1017 ASC ELISPOT responses 177
Table 6.2: Sequencing information of AMA1-specific human mAbs 184
Table 7.1: Correlations between baseline Tfh subsets and post adenoviral prime antibody/ mBC responses. 208
Table 7.2: Correlations between Th lineage subsets and antibody/B cell responses post-boost. 216

List of Abbreviations

AAV	Adeno-Associated Virus
Ab	Antibody
ADCI	Antibody-Dependant Cellular Inhibition
AdHu5	Human Adenovirus Serotype 5
ADRB	Antibody-Dependant Respiratory Burst
AMA1	Apical Membrane Antigen 1
APC	Antigen Presenting Cell
ASC	Antibody Secreting Cell
BCR	B Cell Receptor
BNAbs	Broadly-Neutralising Antibodies
C-1	One day before day of Challenge
CCR	Chemokine Receptor
CD	Cluster of Differentiation
CDR	Complementarity Determining Region
ChAd63	Chimpanzee Adenovirus 63
CPEC	Circular Polymerase Extension Cloning

CSP	Circumsporozoite Protein
CSR	Class Switch Recombination
CXCL	C-X-C Chemokine Ligand
CXCR	C-X-C Chemokine Receptor
DARC	Duffy Antigen Receptor for Chemokines
DC	Dendritic Cell
dDC	Dermal Dendritic Cell
dLN	Draining Lymph nodes
DoD	Day of Diagnosis
DT	Diphtheria Toxoid
EBA175	Erythrocyte Binding Antigen 175
EBV	Epstein-Barr Virus
ELISA	Enzyme-Linked Immunosorbent Assay
ELISPOT	Enzyme-Linked Immunosorbent Spot Assay
EPI	Expanded Programme of Immunisation
FDC	Follicular Dendritic Cell
FSC	Forward Scatter

GC	Germinal Centre
GIA	Growth Inhibition Activity
GLURP	Glutamate Rich Protein
GST	Glutathione *S*-Transferase
Hct	haematocrit
HEK293	Human Embryonic Kidney 293 Cells
hmAb	Human Monoclonal Antibody
ICOS	Inducible T-cell COStimulator
IFN-γ	Interferon-gamma
Ig	Immunoglobulin
IL	Interleukin
IEs	Infected Erythrocytes
L/D	Live/Dead
LLPC	Long Lived Plasma Cell
mAb	Monoclonal Antibody
mBC	Memory B cell
mDC	Myeloid Dendritic Cell

MHC	Major Histocompatibility Complex
MIG	Monokine Induced by Gamma Interferon
MSP1	Merozoite Surface Protein 1
MVA	Modified Vaccinia Virus Ankara
NAI	Naturally-Acquired Immunity
O.D.	Optical Density
PB	Plasmablast
PBMC	Peripheral Blood Mononuclear Cells
PBS	Phosphate Buffered Saline
PC	Plasma Cell
PCR	Polymerase Chain Reaction
PD-1	Programmed Cell Death 1
pDC	Plasmocytoid Dendritic Cell
PEI	Polyethylenimine
PfEMP1	*P. falciparum* erythrocyte membrane protein 1
PMA	Phorbol 12-myristate 13-acetate
PvDBP	*Plasmodium vivax* Duffy Binding Protein

PWM	Pokeweed Mitogen
qPCR	Quantitative PCR
RH5	Reticulocyte-Binding Protein Homologue 5
RON	Rhoptry Neck Protein
RT-PCR	Reverse-Transcription Polymerase Chain Reaction
SA-ALP	Streptavidin-Alkaline Phosphatase
SAC	*Staphylococcus aureus* Cowans Strain Pansorbin cells
SEB	Staphylococcal enterotoxin B
SHM	Somatic Hypermutation
SLPC	Short Lived Plasma Cell
SSC	Side Scatter
Tfh	T Follicular Helper Cell
TLR	Toll-Like Receptor
TNF-α	Tumour Necrosis Factor- alpha
TRAP	Thrombospondin-Related Adhesion Protein
TT	Tetanus Toxoid
VSA	Variant Surface Antigens

1. Introduction

1.1. Malaria and Natural Immunity

The apicomplexan parasite *Plasmodium falciparum* is the causative agent of the most severe and deadly form of human malaria. Global estimates suggest there were around 200 million cases, and 660,000 deaths from *Plasmodium falciparum* malaria in 2010 [1]. Four other species within the genus *Plasmodium* can also cause malaria in humans. *P.vivax* has a larger geographical distribution than *P. falciparum* but is responsible for lower rates of mortality [2], whilst infections with *P. malariae & P. ovale* are much less commonly reported [3]. In recent years there have also been a small number of reports of human infections of *P. knowlesi*, a monkey malaria [4, 5]. Despite reports over the last decade of a global reduction in mortality associated with malaria, the disease still poses a significant burden in developing countries particularly those in sub-Saharan Africa. Here mortality remains high, particularly in children below the age of 5 years and has high socio-economic costs [6].

1.1.1. Malaria Lifecycle

Malaria is spread to humans through the bite of an infected female mosquito of the genus *Anopheles*, with *A. gambiae* the principle vector of *P. falciparum* malaria in sub-Saharan Africa. There are three main stages of the parasite lifecycle; the liver-stage, the blood-stage and the mosquito-stage (Figure 1.1) each of which involves different cellular targets and invasion pathways [7, 8]. During feeding mosquitoes penetrate the skin with their proboscis to locate blood vessels and release saliva containing substances to prevent coagulation, vasoconstriction and inflammation [9]. Haploid sporozoite-stage parasites enter the host in the saliva of the mosquito and upon entry to the bloodstream migrate to the liver in a number of minutes. Here the sporozoite infects hepatocytes within which it undergoes asexual reproduction producing a hepatic schizont over a period of typically seven days during which the host is asymptomatic. In infections with *P.vivax* and *P. ovale* the parasite may undergo transformation to a

dormant liver-stage form known as a hypnozoite which can survive for a number of years and result in future relapses of infection [10]. After seven days the liver schizonts rupture releasing thousands of merozoite parasites into the bloodstream. Merozoites target host erythrocytes and following invasion of these cells undergo further asexual replication, first forming 'ring' stage trophozoites followed by mature trophozoites and eventually erythrocytic schizonts over a period of 48 hours in the case of *P. falciparum*. These schizonts then rupture releasing up to 20 merozoites into the blood which can infect further erythrocytes in a cyclical manner. It is at this stage after a number of cycles that the clinical manifestations of malaria arise. Following an indeterminate number of cycles some merozoites differentiate into male and female gametocytes. Recent studies have shown that expression of the DNA-binding protein AP2-G correlates with gametocyte formation, whilst forward and reverse genetics studies have shown this protein is essential for sexual stage differentiation, acting as a transcriptional switch [11, 12]. When taken up in the blood meal of a mosquito, the gametocytes mature into gametes and fuse to form a diploid zygote in the mosquito gut. This zygote differentiates, forms a motile ookinete which traverses the cell wall of the midgut and forms an oocyst. Within the oocyst haploid sporozoite parasites are formed by meiosis and migrate to the mosquito's salivary glands following oocyst rupture.

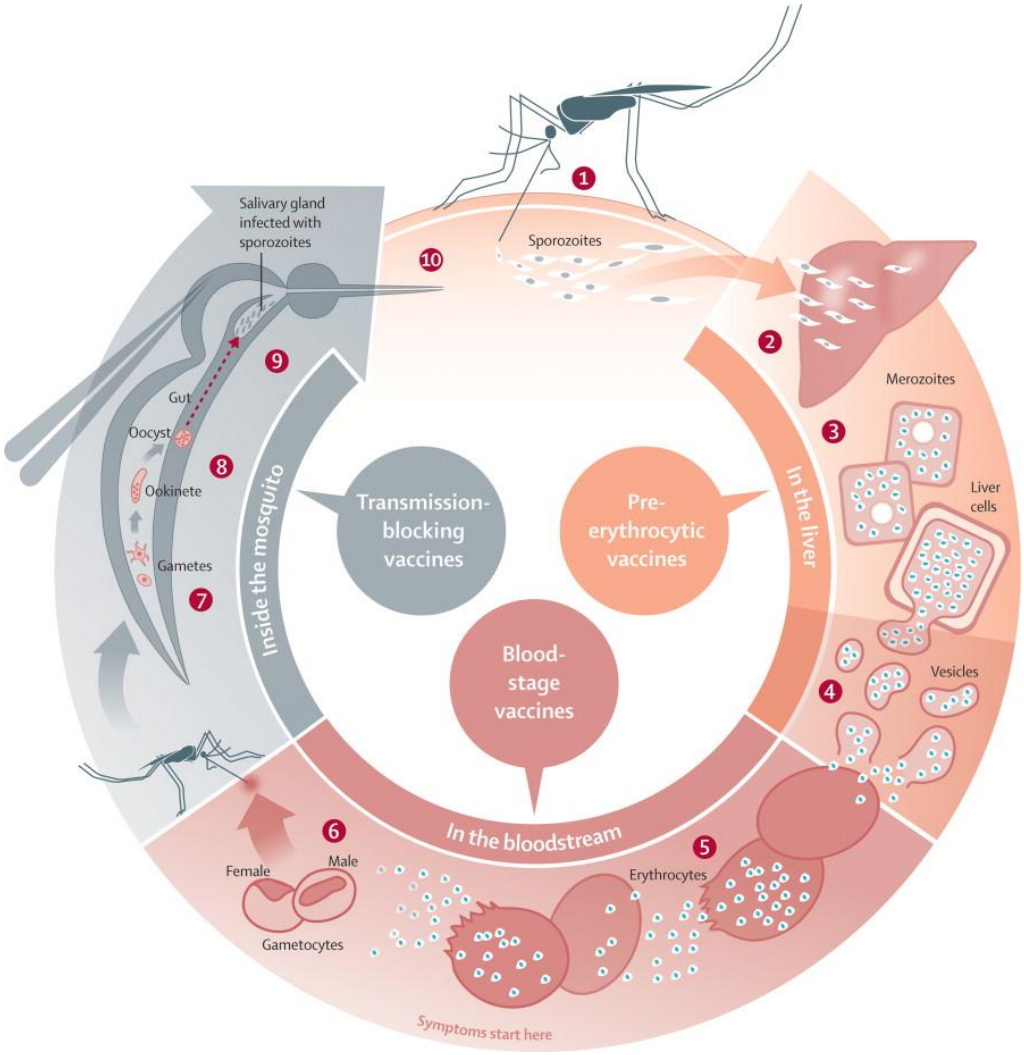


Figure 1.1: *Plasmodium falciparum* lifecycle and vaccine targets [13].

The malaria lifecycle is classically described in three stages, the liver-stage, blood-stage and mosquito-/sexual-stages. In the two human stages of the lifecycle the parasite replicates asexually in comparison to sexually at the mosquito stage. Across the different stages of parasite behaviour, preferred cellular targets and antigen expression differs. Each stage therefore offers different opportunities and challenges in the design of effective vaccines.

1.1.2. Pathology of Malaria

Whilst the liver-stage of malaria infection is typically asymptomatic, most clinical symptoms manifest during the blood-stage including headaches, fever, rigor, and joint/muscle pain. In severe malaria however a number of manifestations can lead to mortality. The rupture of erythrocytes during merozoite replication can lead to severe malarial anaemia which is a primary clinical manifestation and cause of death in children below the age of 5 years old [14]. In pregnant women, infected erythrocytes can also accumulate in the placenta leading to miscarriage, low infant birth weight, anaemia and maternal death [15].

One of the severe manifestations of malaria also associated with high mortality is cerebral malaria. This is caused primarily by sequestration of infected erythrocytes and host immune cells within the cerebral microvasculature [16]. The formation of infected erythrocyte immune complexes following repeated infection can also lead to hyper-reactive malarial splenomegaly, another condition associated with high mortality [17].

Malaria pathology has largely been linked to the select expression of parasite *var* genes, which encode variants of *P. falciparum* erythrocyte membrane protein 1 (PfEMP1) that allow for binding to different receptors of the vascular endothelium. Group A *var* genes in particular have been associated with severe cerebral [18] and childhood malaria [19], whist the conserved *var2csa* gene has been associated with placental immunopathology [15].

1.1.3. Acquisition of Naturally-Acquired Immunity

Though some studies have proposed that early protection in the first few months of life is passed from mother to infant in breast milk [20], the evidence is not conclusive [21]. It has been widely reported that naturally-acquired immunity (NAI) to human *P. falciparum* malaria is non-sterile and slow to acquire, requiring repeated infections over a number of transmission seasons and correlates strongly with age.

NAI is associated with the acquisition of a broad protective antibody repertoire against a number of often polymorphic blood-stage antigens, in particular those associated with severe disease such as PfEMP1 [22]. More recent studies have further refined this view, suggesting differences in immune repertoires acquired by individuals living in highly endemic areas, in comparison to those who live where malaria infection is less frequent [23]. In addition the traditional view that natural immunity suffers from a lack of memory has more recently been challenged [24] , with evidence accumulating for short-term and long-term memory being reported in the absence of re-infection [25, 26]. However other work has also raised concerns that in areas of high levels of intervention (bed nets, drug treatment, pesticide use), individuals may fail to develop effective natural immunity at a young age and subsequently develop more severe malaria as adults if intervention is inadequately maintained [27, 28].

1.2. Malaria Immunity

1.2.1. Innate Immunity

The purpose of the innate immune system is twofold – to provide immediate non-specific defences against invading pathogens and to facilitate induction of the adaptive immune response. The Innate response, like the adaptive response, comprises both humoral and cellular components which act immediately following infection or are rapidly induced. A number of components of the innate immune response contribute to the early induced response against malaria through mechanisms such as parasite killing, antigen presentation and induction of inflammatory cytokines such as Interferon gamma (IFN-γ) (Figure 1.2 [29]). Such mechanisms are essential for the control of blood-stage parasitaemia prior to the acquisition of protective antibody responses.

Macrophages and monocytes play an important role in the removal of infected erythrocytes in the early innate response (in the absence of opsonising antibody) through phagocytosis-mediated oxidative killing [30-32]. This has been proposed to be through binding of CD36 to PfEMP1 on the surface of the infected erythrocytes [33]. Neutrophils have also been shown to be involved in phagocytosis [34], and oxidative killing of malaria parasites [35] but typically require opsonising antibodies which allow killing through antibody-dependant respiratory burst (ADRB) activity [36]. Dendritic cells (DCs) play an important role in antigen presentation in both the innate and adaptive immune response [37]. DCs can recognise infected cells through CD36 in the same way as macrophages or through activation of Toll-like Receptors (TLR) which are important in shaping subsequent antibody responses [38]. There is also some evidence for a role of DCs in activation of other innate effector cells, such as NK cells, through production of inflammatory cytokines such as IL-12 [29]. NK cells are located in the peripheral blood, bone marrow and spleen and have been shown to play an important role in controlling early malaria infection in mice through production of cytokines, particularly IFN-γ [39]. IFN-γ, along with other cytokines such as IL-10,

induced during the innate response has also been shown to be important in determining parasitological and clinical outcomes in human infections [40]. Typically naïve individuals produce a highly pro-inflammatory response that rapidly controls parasite load, but at the cost of developing clinical symptoms. During malaria infection peripheral blood populations of innate immune cells have been characterised including NK cells and γδ T cells, with findings suggesting a protective role for the latter [41]. The complement system also plays an integral part in augmenting the innate immune response in a number of different ways, including opsonisation, inflammation and coagulation with many of these processes shown to contribute to both protection but also pathogenesis in malaria infection [42].

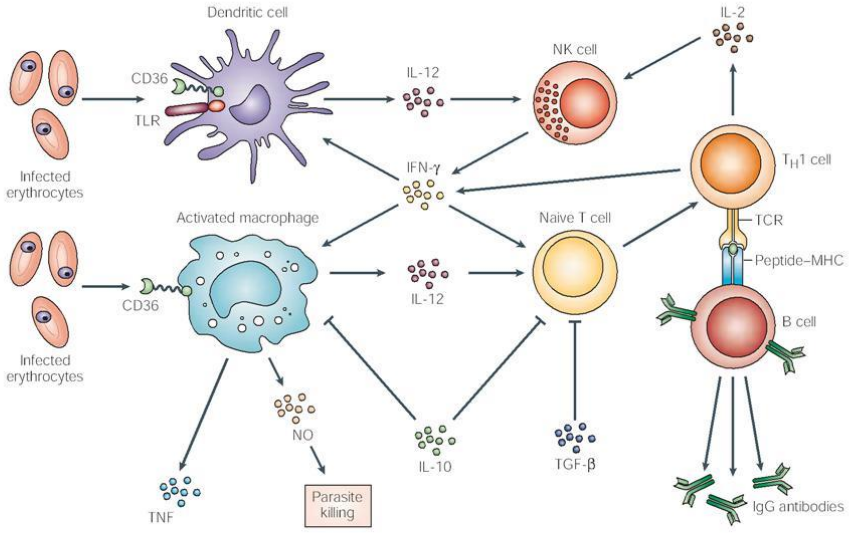


Figure 1.2: Interactions between the innate and adaptive immune system in response to malaria [29].

During malaria infection the innate immune system provides immediate, non-specific defence against parasite and facilitates induction of the adaptive immune system. Parasite killing occurs through the activity of macrophages, monocytes and neutrophils via a number of mechanisms while dendritic cells contribute to antigen presentation to the adaptive immune cells. Induction of inflammatory cytokines also plays an important role, with IFN-γ and IL-12 drivers of a Th1 directed adaptive immune response. The adaptive immune response can also provide feedback to innate cells through cytokines such as IFN-γ and IL-2

1.2.2. T cell-Mediated Immunity

The cellular adaptive immune response to malaria is primarily a Th1-type response that targets intracellular pathogens and is triggered by the cytokines IL-2 and IL-12. Activation of naïve T cells by parasite antigen in the presence of these cytokines drives their differentiation into $CD4^+$ Th1 cells that secrete IFN-γ. IFN-γ secreting $CD4^+$ Th1 cells play an important role in shaping the adaptive immune response against malaria. They contribute to activation of effector $CD8^+$ cells that target infected cells via peptides presented on their MHC class I molecules, whilst also directing appropriate antibody-mediated protection.

NAI has been mostly associated with blood-stage antibody responses indicating that effective induction of $CD4^+$ T cells is essential to provide polarising help for B cells. This likely leads to induction of cytophilic IgG isotypes that interact with innate cellular effectors such as monocytes or neutrophils [36, 43]. As most candidate blood-stage vaccines aim to induce high-titre neutralising antibodies, it has become essential to optimise the $CD4^+$ T cell response. In mouse vaccine studies using the candidate antigen merozoite surface protein 1 (MSP1), important $CD4^+$ T cell epitopes have been identified on the $MSP1_{33}$ fragment that can determine antibody induction and efficacy [44].

An increasing number of animal and human studies support a contributing role for direct cellular immunity to blood-stage malaria [45, 46], with increases observed in both $CD4^+$ and $CD8^+$ T cell subsets following natural exposure [47]. Although infected erythrocytes lack MHC molecules with which to present parasite-derived peptides, it is thought that effector $CD4^+$ T cells can enhance clearance of opsonised infected erythrocytes (IEs) by macrophages in the spleen and orchestrate the induction of parasiticidal pro-inflammatory serum cytokine responses. Vaccination with another vaccine candidate, apical membrane antigen 1(AMA1), in a *P. chabaudi* mouse model has also been shown to induce $CD4^+$ T cells that can contribute to protection independently of antibody [48]. $CD8^+$ T cells have also been

shown to be protective in the *P. yoelii* mouse model of blood-stage malaria infection [49] and can also target merozoite-derived antigens during the late stages of pre-erythrocytic parasite development within infected hepatocytes [50]. However despite strong evidence for a protective role in mice, human clinical trials have so far been disappointing despite induction of strong T cell responses to blood-stage antigens following vaccination [51, 52].

1.2.3. Antibody-Mediated Immunity

Exposure to malarial antigens, either through natural exposure or vaccination, follows a classical T cell-dependent antibody response (Figure 1.3), characterised by rapidly induced antibody secreting cells (ASC) and formation of memory B cell subsets [53, 54]. Central to this process is the formation of germinal centres (GCs) – histological structures where B cell-T cell interactions and subsequent B cell receptor (BCR) affinity selection and class switching occur. Surface bound BCR and subsequent secreted antibodies are immunoglobulins (Ig) comprised of paired heavy and light chains. In humans there are two types of light chain, kappa (κ) and lambda (λ), which are found roughly in a 2:1 ratio. Ig heavy and light chains comprise a variable region and a constant region. Variable regions are composed of a series of segments encoded by gene sequences, of which there are multiple copies, re-arranged to give high levels of diversity. The heavy chain is comprised of three: *variable* (V), *diversity* (D) and *joining* (J); whilst the light chain only comprises V and J. When translated this sequence forms a series of three loops that form the complementarity determining regions (CDRs), which are responsible for antigen recognition. In naïve B cells the BCR is based on the germ line sequence and is of the IgM or IgD isotype, however during the processes of class switch recombination (CSR), affinity maturation and somatic hypermutation (SHM) further diversity and antigen specificity is attained [55]. The constant region of an antibody also plays an important role, independent of antigen recognition. The *Fc* region at the base of the constant region is responsible for binding to a number of immune cells through their Fc receptors as well as complement, leading to downstream functionality. Ultimately all these processes require

complex interactions with a number of components of the innate and adaptive immune system to achieve a protective response.

Initiation of a T-dependant antibody response requires sufficient antigen and professional antigen presenting cells to process and present antigen on MHC class II (MHCII) molecules for activation of naïve $CD4^+$ T cells. The mechanism by which this is achieved can differ greatly according to a number of variables including site of inoculation, local inflammatory responses and in the case of intracellular pathogens such as malaria, host cell preference. In the case of vaccine antigens these mechanisms can also be modified through the use of select adjuvants [56].

Initial exposure to malaria parasites is in the skin after a mosquito bite. Specialised populations of APCs are found in the skin of humans including Langerhans cells which specialise in induction of cytotoxic T cells and CD14+ dermal dendritic cells (dDCs) which can promote antibody production by B cells [57].Mouse studies of sporozoite inoculation into the dermis have also shown that the inflammatory response to infection induces recruitment of neutrophils and inflammatory monocytes in the skin injection site and proximal draining lymph node (dLN)[58]. In humans antibody responses to sporozoite antigens contribute little to NAI. However vaccination with the sporozoite antigen circumsporozoite protein (CSP) can induce protective antibody responses, as shown with the leading candidate vaccine RTS,S (discussed in more detail in section 1.3.2). Following intramuscular vaccination including the potent liposomal-adjuvant ASO1, antigen presentation was shown to be mediated by $MHCII^{high}$ DCs [59].

As previously discussed NAI is mostly associated with acquisition of a broad protective antibody repertoire against blood-stage antigens. During blood-stage infection antigen can be obtained from both ruptured erythrocytes and accumulation of erythrocyte immune complexes in the spleen, the latter of which are a particular source of inflammation. Dendritic cells involved in presentation of blood stage antigen include populations of myeloid DCs (mDCs) found across all lymphoid tissue including the spleen

and plasmacytoid DCs (pDCs) which are found mostly in lymph nodes [37].In particular mDCs in the presence of high doses of antigen are an important source of IL-12, critical for Th1 cell development and subsequent IFN-γ production that promotes class switching to an IgG response [60, 61]. In addition to DCs macrophages also play an important role in antigen processing and presentation of blood-stage antigen particularly marginal zone macrophages through phagocytosis of infected erythrocytes (IEs) in the spleen [62]. A number of TLR ligands have been identified in *P. falciparum* that may act as endogenous adjuvants, including malarial hemozoin (a TLR9 ligand) that is abundant at the blood stage of infection[63]. Human macrophages and pDCs but not mDCs express TLR9 and activation of this receptor further promotes IL-12 secretion and a Th1 type response.

Once activated by antigen DCs upregulate costimulatory molecules including CD40, CD80, and CD86 and chemokine receptors such as CCR7, allowing relocation from sites of inflammation to the T cell areas of draining lymph nodes. Antigen primed DCs migrate to the T cell follicle of the secondary lymphoid organ where they activate naïve $CD4^+$ T cells via formation of a MHCII immune synapse [64]. Activated $CD4^+$ T helper cells (Th) proliferate and migrate towards the B cell follicle in a process proposed to be dependent on selective expression of the chemokine receptor CXCR5, countering the T cell follicle retention signal of the receptor CCR7 [65, 66].

Naïve B cells originate from primary follicles of secondary lymphoid organs and are activated following the engagement of the BCR and specific antigen. There are a number of different mechanisms by which naïve B cells can be presented with antigen, which in turn determine the type of immune response initiated [67]. In the highly vascularised spleen, blood borne antigen such as that derived from IEs, can be presented to marginal zone B cells by marginal zone resident DCs and macrophages. A large proportion of these B cells have a distinct IgM phenotype and following activation contribute to a rapid natural IgM plasma cell and IgM memory response that may be T cell dependant or Independent [68].

Lymph node resident B cells in contrast are activated by antigen derived via the lymphatic system. Migrating antigen loaded DCs entering the lymph node via high-endothelial venules can activate B cells in the paracortex. Alternatively soluble antigen, possibly associated with immune complexes, enters the subcapsular sinus of the lymph node via the afferent lymph vessel where it can be captured by subcapsular sinus macrophages and presented to naïve B cells [69]. Small soluble antigens such as low molecular weight toxins may also directly diffuse into the B cell follicles and activate B cells without presentation though this open to debate.

In a T dependant response activated B cells then migrate to the boundary of the B cell/ T cell zone where they receive T cell help from antigen primed Th cells [70]. The synapse formed between antigen experienced T and B cells is complex and involves a large number of receptors including the critical TCR-MHCII interaction [71]. During this process CSR can also occur, switching the constant region of the BCR from IgM or IgD to IgG, IgE or IgA. This process requires interaction between CD40 and CD40L, as well as selective cytokine signalling [53, 72, 73]. Following this interaction there is a split in B cell lineage commitment either into short-lived plasma cells (SLPCs) or into the germinal centre memory pathway [54]. SLPCs at this stage typically express germ line encoded BCR but can be class switched [74, 75]. B cells entering the memory lineage form GCs in B cell follicles alongside antigen presenting follicular dendritic cells (FDC), which also play an important role in maintaining an organised follicular structure [76], and specialised $CD4^+$ Th cells known as T follicular helper cells (Tfh), which express the chemokine receptor CXCR5 [77, 78]. In the dark zone of the GC, proliferation and SHM occurs, diversifying the VDJ regions of the BCR in a mechanism related in part to CSR [55]. BCRs are then selected for binding affinity against antigen presented by FDC in the light zone of the follicle [79], with the process mediated through interactions with Tfh cells and cytokine signalling [80]. The process of increased average affinity in the population over time is known as affinity maturation. GC reactions can continue whilst antigen is available and this period is extended by the antigen retaining ability of FDCs [76]. Though exact

mechanisms are still to be defined, it is predicted that intact, opsonised antigen can be retained for upwards of a year. The rationale for repeated boosting of vaccines is to extend or re-initiate these processes and increase affinity maturation over successive rounds of germinal centre selection, however it has been shown that there is a limit to this process [81]. After rounds of selection, B cells leave the GC reaction committed to one of two fates, classical memory B cells (mBC) or long-lived plasma cells (LLPCs) and induction of these populations is essential for a successful antibody-dependent immune response [54]. Plasmablast precursors of LLPCs migrate to the bone marrow via chemokine receptor signalling [82] prior to maturation in the bone marrow niche and continuous antibody secretion, contributing to maintenance of serum antibody titres [83]. In contrast, mBC enter circulation in the peripheral blood in preparation for secondary antigen exposure.

Not all B cell responses are dependent on T cell help and the formation of germinal centres to induce differentiation of antigen experienced B cell into antibody producing cells. T cell independent antigens are often bacterial, typically either polysaccharides or lipopolysaccharides. Natural IgM cells activation by TLR9 in the spleen have already been discussed as a one source of a T independent B cell response that is germinal centre independent but can induce a memory population [68]. Both DCs and macrophages have been shown to directly induce T independent activation and class switching in B cells [84]. Such responses are typically germinal centre independent with limited or no somatic hypermutation and can produce long-lived plasma cells but little to no memory response [85].

During secondary antigen exposure, mBC will differentiate rapidly into a population of antigen-specific antibody secreting plasmablasts that can contribute to pathogen clearance more effectively than in a primary response. Such cells can be classically identified 7 days post-boost following vaccination [86]. In addition, mBCs may re-enter GCs and undergo additional somatic hypermutation. Important mouse models have suggested that existing IgG memory cells are most likely to differentiate into peripheral

plasmablasts while IgM memory subsets reinitiated the GC reaction[87]. Such studies suggest that B cell memory comprises a number of overplapping layers of T-independent and T dependant subsets.

The protective role of anti-malarial antibodies was classically described though passive transfer experiments where pooled serum from immune adults was shown to confer protection in children [88]. Accumulation of high-titre antibody (Ab) responses (particularly the subclass IgG), with increasing age and exposure has been shown to be the main correlate of protective natural immunity in endemic human populations [89-91]. A number of blood-stage antigens have been associated with NAI including PfEMP1, AMA1, merozoite surface proteins (MSP) 1, 2, 3 , erythrocyte binding antigen 175 (EBA175) and glutamate rich protein (GLURP) [92]. In areas where *P. falciparum* malaria transmission is low, Ab and memory B cell (mBC) responses have been shown to be induced and long-lived [93, 94] with the breadth (but not magnitude) of the mBC response expanding with age and exposure [95]. In other studies Ab and mBC responses to these antigens have been reported to be short-lived or below detection in the peripheral blood [96-98]. It may be that both human and parasite population level differences may explain contrasting evidence for protective antibody responses [99].

The key subclass associated with protective natural immunity is IgG with evidence for different modes of action for its isotypes IgG1, IgG3 [100] and IgG2 and IgG4 [101], with dominance often depending on the target antigen, e.g. IgG1 for MSP1 and IgG3 for AMA1 [102, 103]. Similarly the mechanisms by which naturally-induced antibodies may contribute to clinical protection vary by antigen. For MSP1, for example, three mechanisms have been proposed: inhibition of MSP1 processing; direct inhibition of erythrocyte invasion; and inhibition of intracellular parasite development following red blood cell invasion [104]. However, in nearly all cases, such immunity is non-sterile and leads to asymptomatic individuals still contributing to carriage and transmission. Antibody can also act through interactions with the innate immune system. One of the best characterised, ADRB activity, utilises complement along

with neutrophils, antibody and reactive oxygen species to neutralise the merozoite parasites [105]. Another mechanism that requires interaction with innate cells is antibody-dependant cellular inhibition (ADCI), where antibody alone displays no growth inhibition *in vitro*, but can do so in the presence of monocytes [106].

The observations that antibodies to blood-stage malaria antigens are important in natural immunity led to the early development of candidate vaccines to antigens such as MSP1 and AMA1. These antigens showed promise, with high levels of protection in pre-clinical studies of mice [107, 108] and non-human primates [109, 110]. Protection is associated with high titres of IgG antibodies that provide neutralisation and growth inhibitory effects, preventing blood-stage parasite replication. Most vaccine-induced antibody responses are assessed following booster vaccination and are dominated by the IgG isotype, with IgG1/2a commonly induced in mice [111, 112], and IgG1/3 in humans [113]. However to date significant protective clinical efficacy has not been achieved in human studies despite induction of antigen-specific serum antibody up to 50-100 µg/mL [51, 114]. Another long-standing problem for these candidate vaccines is the high level of antigenic polymorphism in these antigens, with the limited protection induced by AMA1 only seen against vaccine-homologous parasite strains [115]. Newer approaches are focussing on blood-stage antigens that are not dominant targets of NAI and that display low levels of antigenic polymorphism such as the reticulocyte-binding protein homologue (RH) family of proteins. Pre-clinical work on antigens such as PfRH5 has shown promise with induction of cross-strain neutralising antibodies [116-118] which can also display synergy in combination with other blood-stage antigens [119]. Whether such observations hold true in human studies is much anticipated.

Most of our understanding of the generation of vaccine antigen-specific antibody responses comes from mouse studies where there is easy access to germinal centres and bone marrow to recover cells such as Tfh and LLPC respectively. As these are not easily obtainable in human studies due to obvious ethical

considerations, the focus of research in humans is on peripheral blood cell populations. Plasmablasts can be identified in the peripheral blood typically 7 days following vaccination, whilst mBC can be isolated weeks, months or even years after vaccination [120-122]. Despite this, correlations with serum antibody levels vary, largely dependent on vaccine antigen [121]. In recent years a number of studies have reported correlations between different peripheral blood populations of memory $CD4^+$Th cells and antibody titres [78, 123]. These cells are phenotypically related to Tfh cells through expression of CXCR5 and display similar B cell helper functions *in vitro*, yet have distinct Th1 or Th2 response profiles [124, 125]. Though further study is required to gauge the importance of these peripheral populations, it is hoped that they may help predict the ability of an individual to produce an effective, targeted antibody responses and/or can be effectively induced by vaccination to give increased efficacy.

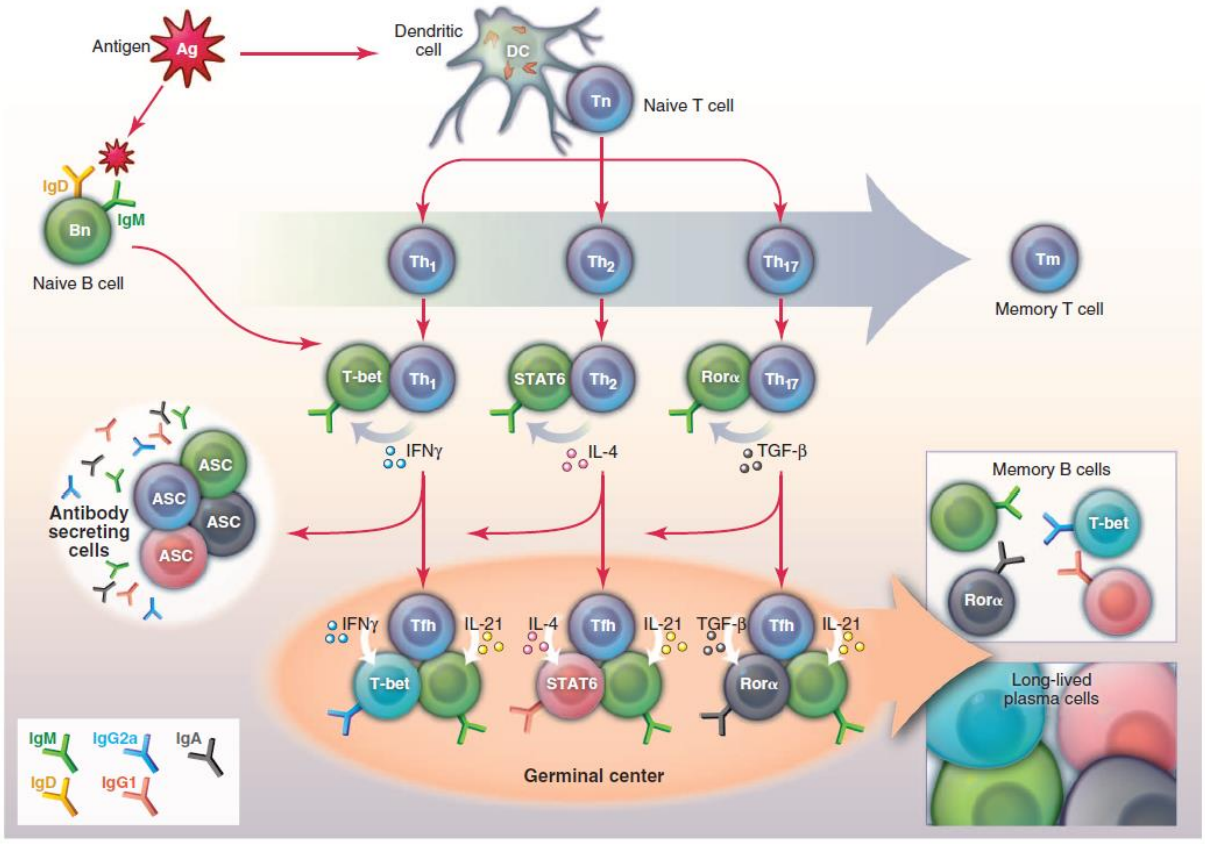


Figure 1.3: T-dependent development of B cell subsets in a primary response in mice [54].

In the presence of T cell-dependent antigen, B cells can develop along two pathways; either rapidly forming antibody secreting cells that are short-lived, or contributing towards germinal centres before undergoing somatic hypermutation and affinity selection prior to formation of memory B cells or long-lived plasma cells. During malaria, antigen priming of T cells induces a Th1 phenotype which is characterised by induction of IFN-γ. When Th1 $CD4^+$ T cells interact with antigen-primed B cells the resultant antibody response is dominated by the IgG isotype, with IgG2a commonly induced in mice and IgG1/3 in humans.

1.2.4. Parasite-Mediated Evasion of Natural Immunity

One of the proposed reasons for why natural immunity is non-sterile is that *P. falciparum* can modulate the immune system as an immune-evasion strategy. It has been observed that malaria infection in Kenyan children can lead to disturbances in peripheral B cell homeostasis [126, 127]; whilst continued exposure can lead to expansion of a so-called 'atypical mBC' subset with reduced proliferative capacity [128, 129]. These data, in conjunction with the known gradual acquisition of antibody-mediated natural immunity, have led many to propose malaria infection induces dysregulation of B cell function [130]. There are a number of possible factors that may drive such a phenomenon during both acute and chronic blood stage infection. For example dysregulation of BAFF-R expression on B cells may contribute to short-lived antibody responses to malarial antigens in children [131].Focusing more on antigen presentation, modulation of monocytes, macrophages and myeloid DC function by IEs has been shown to lead to a reduced capacity to stimulate Th cells [132, 133]. In a *P. chabaudi* model at peak parasitemia, DCs transiently lost their ability to stimulate transferred MSP1 specific $CD4^+$ T cells, recovering only as the parasitemia is controlled[134]. In fatal human cases failure to control parasitemia has been associated with breakdown of splenic architecture and loss of B cells [135].

Another mechanism adopted by malaria parasites is to utilise variant surface antigens (VSA) to avoid immune antibody binding. One of the best studied examples, PfEMP1, has been shown to have distinct differential expression of variants, with a conserved subset dominating in non-immune individuals and those with severe malaria, whilst a broader range of variants are found in individuals with NAI or uncomplicated infections [136]. Studies have shown that some variants associated with severe malaria can bind non-immune IgM at the Fc region. This can have a number of functional consequences including interference with innate clearance mechanisms, prevention of antigen presentation to B cells, blocking of neutralising antibody binding and enhanced sequestration of infected erythrocytes in the microvasculature or placenta [137].

Induction of T cell priming bias (immune interference) [138], limited effector level recall in the presence of multiple epitopes (immune antagonism) [99] and redirected recall to previously primed non-cross reactive epitopes (immune diversion) [138] have also been proposed as mechanisms which can facilitate survival and co-habitation of parasites in endemic areas. Malaria parasites have also been shown to interfere directly with DCs, via infected erythrocyte-CD36 adherence, preventing maturation and reducing their capacity to stimulate T cells [132].

1.3. Need for a Malaria Vaccine

1.3.1. Aim of Malaria Vaccines

There are currently no licensed vaccines available for *P. falciparum* or *P. vivax* malaria despite the obvious need given the high levels of morbidity and mortality associated with clinical disease. The key role of any vaccine is a reduction in mortality and this is ideally achieved through induction of sterile, protection. However given that natural immunity does not provide sterile protection, alternative immunological mechanisms are likely required to achieve this goal. A vaccine that reduces mortality by reduction of clinical symptoms, but does not afford sterile protection would also be welcome but it may possibly not contribute to prevention of transmission between hosts. Alternative vaccine approaches that prevent transmission between hosts could also be implemented to complement such a vaccine. An important consideration with any vaccination campaign is the age group with which to target. In the case of malaria the most at risk groups are children <5 years old and pregnant women. Therefore vaccination for any prospective malaria vaccines would be best delivered through the Expanded Programme of Immunisation (EPI) [139] in endemic countries. Adult vaccinations are likely to also be necessary in the absence of lifelong immunity, during pregnancy and for non-endemic tourists and military personnel. To coordinate malaria vaccine strategies, the world's leading health organisations came together to form the 'Malaria Vaccine Technology Roadmap' in 2006. This initiative aimed for licensing of a first-generation vaccine that provides 50% protection against severe disease for at least a year by 2015. A recent update in 2013 has set a new target: a licenced vaccine that affords 75% protection, can be used in most endemic settings and makes inroads towards elimination, by 2030 [140].

1.3.2. Targets for Malaria Vaccines

Vaccines against malaria have traditionally been classified according to the stage(s) of the parasite's lifecycle which they target (Figure 1.1).

Pre-erythrocytic vaccines target either migrating sporozoites or infected hepatocytes [141], while blood-stage vaccines target merozoites in the bloodstream or infected erythrocytes [142]. All these stages are within the human host and aim to arrest parasite growth entirely at their respective stage. Transmission-blocking vaccines in contrast target the sexual stages of the parasite: gametocytes in the bloodstream or gametes, zygotes and ookinetes within the gut of the mosquito host and therefore do not contribute to control of clinical disease within the vaccinated individual. At each of these stages different components of the immune response are required to target the parasite. In addition, and key for vaccine design, the antigenic targets expressed by the malaria parasite vary according to the stage of its lifecycle (Figure 1.4).

Circumsporozoite protein (CSP), the most abundant surface protein of the sporozoite parasite, is multifunctional, involved in motility within both hosts and is essential for liver cell invasion [143]. Such characteristics and its presence immediately following infection made it a prime vaccine candidate historically and the most successful to-date in the form of RTS,S. This vaccine comprises a large segment of CSP containing known B and T cell epitopes, fused with the hepatitis B surface antigen (HBsAg) [144]. Thrombospondin-Related Adhesion Protein (TRAP) is also expressed on the sporozoite parasite and is similarly involved in motility and liver-stage invasion [145], as well as salivary gland invasion in the mosquito [146]. Therefore it is seen as another key liver-stage antigen, with the leading vaccine candidate METRAP comprising the antigen preceded by a string of multiple $CD8^+$ T cell epitopes [147, 148].

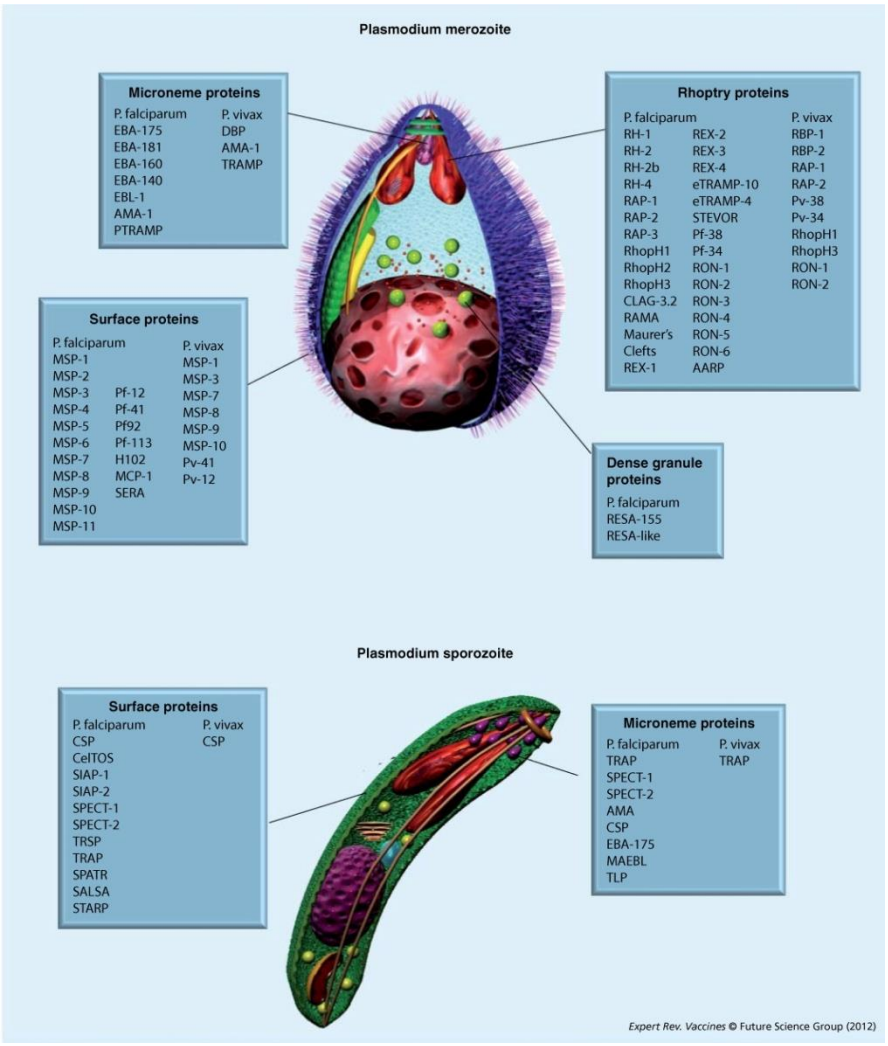


Figure 1.4: Vaccine candidates on the *Plasmodium* merozoite and sporozoite [149]

A number of candidate vaccine antigens have been identified that are differentially expressed at different stages during the lifecycle of *P. falciparum*. Many antigens such as MSP1 are found on the parasite surface and therefore are readily exposed to the immune system, whilst other antigens such as AMA1 are secreted from the micronemes during the process of erythrocyte invasion and so have more limited immune exposure. Very few antigens are expressed at both the sporozoite and merozoite stages and there are differences in antigen expression observed between *Plasmodium* species, with some antigens such as RH5 unique to *P. falciparum.* This list is not exhaustive and new vaccine candidates are being added to this list following screening programs, many of which are of unknown function or are hypothetical proteins.

Vaccines targeting the blood-stage of malaria can either target the merozoite directly or target proteins displayed on the surface of infected erythrocytes. For merozoites there are three categories of target proteins. Surface proteins tend to be highly abundant and readily exposed to the immune system but as a consequence of this, they are often highly polymorphic. Micronemal proteins and rhoptry proteins are generally less abundant and are typically located only at the apical end of the merozoite. They are commonly used in erythrocyte binding and invasion and have varying degrees of polymorphism. Many of these proteins are found in both *P. falciparum* and *P. vivax* species though some are unique. A number of blood-stage antigens are also expressed in the late stages of development in the sporozoite parasite (e.g. AMA1).

Merozoite surface protein 1 (MSP1) is the most abundant and well-studied protein found on the merozoite parasite. Synthesised as a 190 kDa protein, MSP1 forms a complex with MSP6 and 7 on the surface of the developing merozoite within the schizont. During or just prior to merozoite egress from an infected erythrocyte, the MSP1 protein undergoes primary processing and the 190 kDa protein is cleaved into four fragments (Figure 1.5). During invasion of new erythrocytes, secondary processing causes cleavage of the 42 kDa C-terminal region ($MSP1_{42}$) into two fragments of 19 kDa and 33 kDa, known as $MSP1_{19}$ and $MSP1_{33}$ respectively [150, 151]. Whilst $MSP1_{19}$ remains membrane bound and enters the erythrocyte with the parasite, $MSP1_{33}$ is shed along with other associated complex proteins. This process, along with the observation that $MSP1_{19}$ is more conserved than $MSP1_{33}$ [152], made it a key target for early vaccine studies. Natural polymorphisms in MSP1 have posed a problem to vaccine design, with contrasting observations for allele-specific responses correlating with antigen exposure in natural populations [98, 153, 154]. This has led to questions as to whether MSP1 contributes to possible mechanisms of immune evasion, particularly when more than one parasite strain is in circulation [155] and whether such problems may translate to vaccines containing multiple alleles. Recent studies using

biallelic vaccines have provided evidence calming such concerns, instead suggesting that differences in T cell responses to different alleles may be due to differences in host HLA type [156].

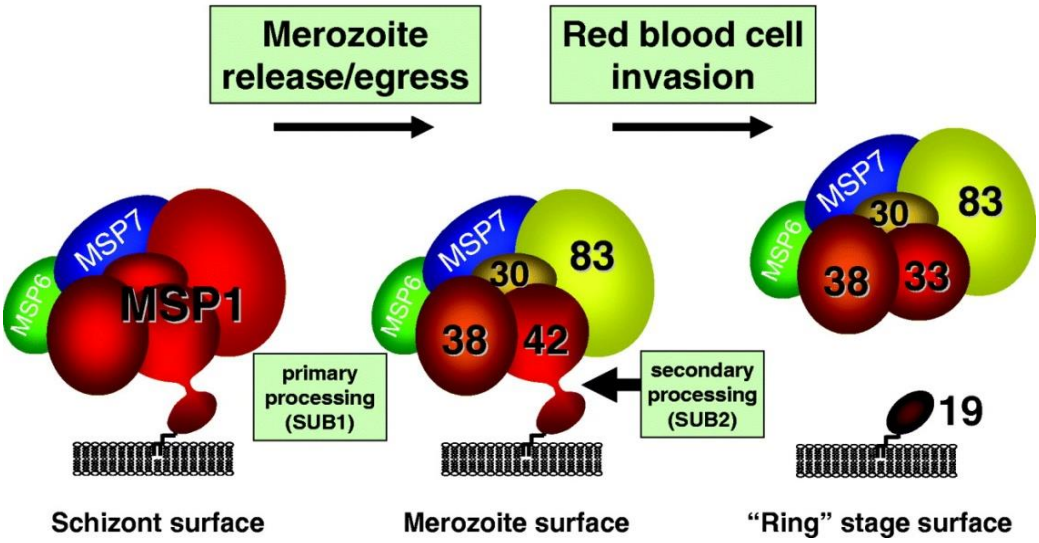


Figure 1.5: MSP1 processing on the merozoite surface during development and erythrocyte invasion [151].

MSP1 is found as part of a complex with the proteins MSP6 and 7 in the maturing schizont. Primary processing (SUB1) during merozoite release/egress from schizont cleaves MSP1 into four fragments of 30, 38, 42 and 83 kDa. During erythrocyte invasion the 42 kDa fragment undergoes secondary processing (SUB2) and is cleaved into two fragments of 33 and 19 kDa. The 33 kDa region along with the protein complex is shed, whilst the 19 kDa fragment is maintained on the parasite as it enters the erythrocyte.

Apical membrane antigen 1 (AMA1) is located within the micronemes of the merozoite as well as the sporozoite and is involved in cellular invasion of both erythrocytes and hepatocytes. Full length 83kDa AMA1 protein, located in the apical complex is cleaved to the 66 kDa fragment post-synthesis by removal of an N-terminal peptide. In mature merozoites the 66 kDa fragment translocates to the parasite surface where it is circumferentially redistributed and undergoes two C-terminal cleavages to give rise to 48- and 44-kDa soluble forms [157]. After initial merozoite binding and reorientation of the apical tip, AMA1 contributes to formation of a tight junction, following secretion of the rhoptry contents which include members of the rhoptry neck (RON) family of rhoptry proteins (Figure 1.6). A complex of RON proteins translocates the host red blood cell membrane and subsequent binding of AMA1 to this complex precedes parasite traversal through the tight junction [158, 159]. Antibodies that disrupt this process have been shown to prevent invasion validating AMA1 as a leading vaccine candidate. AMA1 is not only found in *Plasmodium* species but is common in other *apicomplexans* such as *Toxoplasma*, where it performs a similar role [160]. Despite this conservation of function, the AMA1 sequence is relatively polymorphic within malaria species [161, 162]. Though individuals have been shown to produce antibodies recognising both conserved and polymorphic regions of AMA1 [163], it has also been shown that a single amino acid change can abolish cross-strain neutralisation [164]. As a result, maximising allelic coverage is proving to be critical in the development of AMA1 vaccines [165, 166].

Rhoptry antigens such as the RH family offer other targets for blood-stage vaccine development. During invasion, the RH family of proteins exploit receptors on the erythrocyte surface [167] (Figure 1.6). These interactions have traditionally been regarded as redundant, whereby blocking of one interaction/ invasion pathway induces switching to another. In recent years, PfRH5 has emerged as a new leading candidate antigen which is not redundant (unlike all the other RH antigens) and has been shown to induce broadly neutralising antibodies in pre-clinical studies [168]. RH5 also appears a lot more conserved compared to other RH proteins, increasing the possibility for effective vaccine induced cross-

strain protection. PfRH5 binds to the receptor basigin in an interaction that is essential for parasite invasion as shown by potent inhibition using soluble basigin, basigin knockdown and antibodies [169]. Further characterisation of this receptor-ligand interaction has provided insights including monoclonal antibody (mAb) binding sites and association/dissociation binding kinetics of highly growth inhibitory mAbs [170].

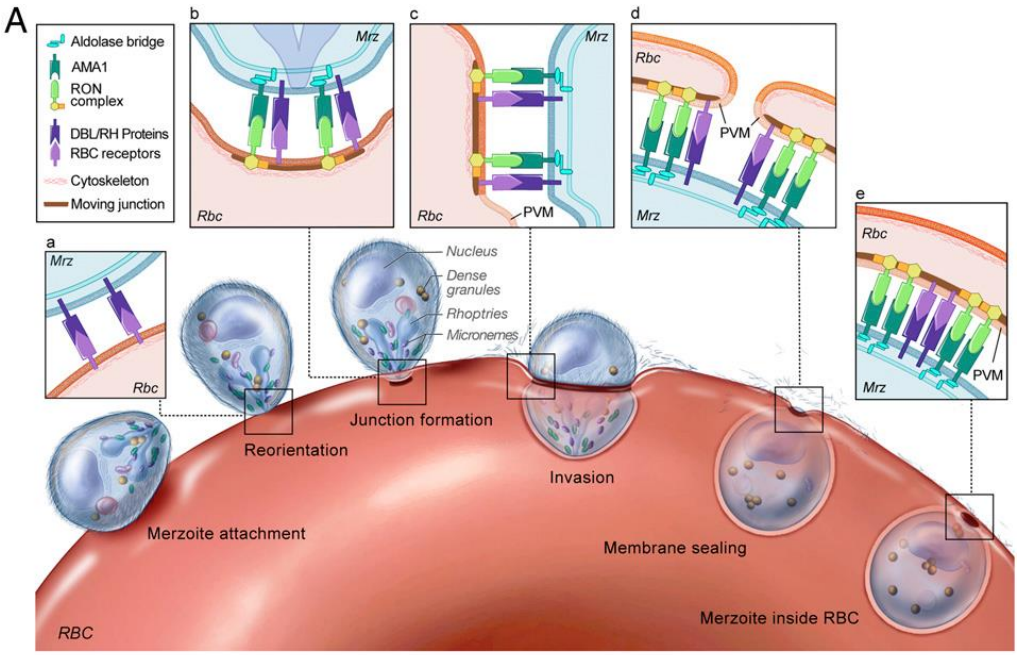


Figure 1.6: Role of AMA1 and RH proteins in erythrocyte invasion [159].

Attachment and reorientation of the merozoite is mediated in part by binding of the RH family of proteins binding to receptors on the erythrocyte surface. Following this AMA1 is released from the micronemes along with the contents of the rhoptries, including members of the RON family which translocate the erythrocyte membrane. The binding of AMA1 to the RON complex initiates formation of a tight junction. The AMA1/RON complex in turn interacts with the erythrocyte cytoskeleton, mediating parasite traversal through the tight junction into the cell before disengaging upon completion.

Transmission-blocking vaccines target antigens found on sexual-stage gametocytes or parasite forms located within the mosquito gut. The antigen Pfs25 is expressed on the zygote and ookinete stage of the parasite. Whilst Pfs25 mRNA can be found in human stage gametocytes, translation is repressed until the mosquito stage along with a number of other antigens [171]. Pfs25 is highly conserved, likely due to lack of immune pressure from the human host. Other candidates including Pfs230 and Pfs48/45 are expressed on the gametocyte stage of the parasite. Both are particularly important in male gametocytes with Pfs230 involved in the formation of exflaggelation centres in association with uninfected erythrocytes [172], whilst Pfs48/45 plays a key role in attachment and penetration of female gametes during fertilisation [173]. Production of a vaccine that targets these antigens or even the mosquito gut receptors used for traversal such as APN1, can prevent development of sporozoites in the salivary glands of the mosquito and block malaria transmission between hosts [174, 175]. This approach does not protect the vaccinated individual so would be best used as part of a combination vaccine regime with pre-erythrocytic and/or blood-stage candidates. This combined vaccine approach is considered a crucial component in future efforts to eradicate malaria [176].

1.3.3. Vaccine Delivery Platforms

The ultimate aim of any vaccine regime is to induce robust long-lived immunity against the target pathogen. Typically an initial vaccination primes the immune system whilst subsequent booster vaccinations allow formation of circulating humoral and cellular effectors in addition to adaptive immune memory. Therefore careful selection of the type of vaccine used for the prime and boost, as well as the interval is very important in maximising or tailoring the induction of both cellular and humoral elements of the immune system.

Most traditional vaccines comprise of killed organisms or attenuated live versions that can infect but not replicate within the host. Whilst this is possible for malaria, and will be discussed later, it has become

more commonplace to develop subunit vaccines for practical reasons, such as improved ease of delivery, deployment and storage. Subunit vaccines typically target a single antigen but often require adjuvants to maximise immunogenicity. There are a number of approaches to subunit vaccination delivery including DNA plasmid, recombinant protein and viral vectors.

Viruses are highly effective delivery vectors for subunit vaccines. They have a relatively large capacity for incorporation of non-viral sequences (i.e. vaccine antigens) which can be expressed via endogenous or exogenous promoters to maximise transgene expression [177-183]. Adenoviruses, which have the E1 region removed, are incapable of replication whilst removal of additional regions including E2b and E3 improve viral titres and increase insert capacity [184].This approach has been effectively used in the creation of candidate vaccines containing antigen inserts from a number of infectious diseases including malaria [51, 185], influenza [186] and HIV [187]. Modified vaccinia virus Ankara (MVA) is also non-replicating when used in human vaccinees, having lost the required genes by natural attenuation through continuous passage in chicken embryonic fibroblasts (CEFs) [188-190]. As a result both vectors have been shown to have a very favourable safety profile for vaccination, with MVA previously used as a safer alternative to wild type vaccinia virus for smallpox vaccinations [191].

The recombinant human adenovirus serotype 5 (AdHu5) has been shown to be highly effective as a priming agent for vaccination in both pre-clinical [192-196] and human studies [197-199]. Despite this, there have been concerns that pre-existing anti-vector immunity to this serotype may hamper its onward clinical development [200-202]. Therefore a lot of time and research has been invested in the development of recombinant chimpanzee adenovirus vectors, such as ChAd63, for which naturally occurring anti-vector immunity is much less prevalent in humans [203, 204]. Induction of type 1 interferon and innate immunity has been shown to be key in the adaptive response to adenovirus vectors. This proposed to be mediated by both pDCs via a TLR9 dependant mechanism and conventional

DCs and macrophages via a TLR independent mechanism [205]. Mechanisms may however vary between serotypes, possibly accounting for differences in their potency [206]. Original host specificity may also have a significant impact on vector biodistribution, persistence and gene expression in alternative species [207]. Adenoviruses can also effectively boost responses in animal studies, especially when heterologous serotypes are used [208, 209], although this has been less convincing in human studies [210]. MVA however is a much more effective boosting agent, in particular for T cells, when used post adenovirus prime. MVA having lost a number of the immunomodulatory factors, can induce rapid local immune responses that can attract innate and adaptive immune cells [211]. Induction of CD8 T cells by MVA has been shown to be mediated by phagocytic myeloid cells following antigen transport to the bone marrow by neutrophils [212]. A recent study has also shown that MVA infected APCs are able to directly transfer endogenous viral proteins into the MHCII pathway to efficiently activate CD4+ T-cells[213]. Consequently adenovirus followed by MVA has been adopted as the current regimen of choice for a number of clinical vaccine trials that aim to elicit strong T cell responses, for example liver-stage malaria, HCV and HIV [147, 214, 215]. This Adenovirus-MVA regime has also been shown to induce moderately high levels of antibody in preclinical [107, 108] and human clinical trials for blood-stage malaria antigens [51, 216, 217]. This may in part be due to the addition of the tPA leader sequence to blood-stage vaccine constructs. This was historically shown to improve response to MSP1 DNA vaccination [218] and is proposed to aid in antigen secretion from infected cells in the viral vector model.

Recombinant protein produced in eukaryotic cell lines has proved a successful route for vaccine development. Recombinant protein vaccination has proved very effective at inducing high-titre antibody responses, but typically requires three vaccinations and inclusion of potent adjuvants to maximise immunogenicity [219], however recent studies have shown that the use of recombinant adenovirus as a prime followed by a single protein boost can achieve equivalent antibody titres in mice [220].Similarly

the use of multivalent antigen in the form of virus-like particles can also improve immune antibody responses to recombinant proteins [221]. This is achieved by high density presentation of B cell epitopes that can increase crosslinking of the BCR as well as enhancing signalling and interaction with $CD4^+$ Tfh cells. Selecting appropriate adjuvants for such regimes can also have significant consequences on the effectiveness and specificity of the immune response which will be discussed in section 1.3.4.

Route of vaccination can also be important in determining the subsequent immune response. Most human vaccines are given either intramuscular or intradermal both of which target different populations of antigen presenting cells in the respective muscle [59]or skin [57]. Route of vaccination can significantly impact the success of some vaccines (e.g. rabies) [222] whilst for other it may have little impact (e.g. influenza)[223]. For some vaccines alternative routes of vaccination have been tested to try and target responses to sites of infection, for example intranasal, aerosol vaccination can induce both local mucosal responses in the lungs as well as systemic responses for influenza [224] and TB [225]. Another example, microneedle-mediated immunization, has been shown to improve antigen specific antibody immunity of an adenovirus vaccine whilst reducing vector specific responses [226]. This is proposed to be due to early, transient expression of cytokines, a reduced pro-inflammatory response only at the site of administration and reduced drainage of vectored antigen to the lymph nodes.

Another important consideration for vaccine regimes is the interval between prime and booster vaccinations. If they are too close together then there may not be enough time for an effective memory response to develop. Additionally the presence of high numbers of antigen-specific or vector-specific effector cells may interfere with recombinant viral vector invasion and antigen expression. An eight week interval between prime and boost for Ad-MVA or Ad-protein vaccines is the most commonly used in the human malaria vaccine field [51, 147, 216, 217] following on from early preclinical studies [50,

227, 228], whilst protein-protein vaccines usually have a reduced interval between vaccinations, typically around 4 weeks [219, 229].

1.3.4. Adjuvants

In the context of malaria vaccines, adjuvants have been utilised to improve and modulate both cellular and humoral responses [230]. Adjuvants can be combined with a vaccine either recombinantly or co-administered during vaccination. A leading example can be seen with the pre-erythrocytic vaccine RTS,S. In this vaccine CSP fused to HBsAg (RTS) is expressed together with unfused HBsAg (S), which forms particles which increase the immunogenicity compared to soluble circumsporozoite protein alone [231]. In a number of other vaccine studies the co-administration of molecular adjuvants and immunomodulators have been used to attempt to improve the immune response [232]. Similar approaches were used to further improve the cellular response and efficacy of RTS'S [233], with the most successful being the adjuvant systems AS01 [234] and its predecessor AS02 [235, 236]. These contain two components; the TLR agonist MPL and the *Quillaja saponaria* bark extract QS21, either in a liposome formulation (AS01) or an oil-in-water-based emulsion (AS02). Similar approaches have been utilised to attempt to improve both T cell and antibody responses to blood-stage malaria antigens, given the requirements of especially high titres of Ab for protection [237, 238]. A number of alternative adjuvant strategies also target the TLR pathways using soluble TLR agonists [38, 239, 240]. In particular targeting of TLR9 with the microbial DNA motif CpG has been shown to be an effective adjuvant of antibody and B cell responses for malaria protein vaccines in both mice [241-243] and humans [219, 244]. This approach has often been in conjunction with the classical aluminium salt adjuvant 'alum' (aluminium hydroxide).

The major limitation on clinically available adjuvants is safety. In pre-clinical studies a large number of candidate adjuvants have been tested alongside candidate malaria vaccines with success [230], however

licensure for human use requires extensive safety profiling. Even clinically licensed adjuvants have reported negative side effects. Mild to moderate adverse events, such as increased pain at the site of injection or fever are commonly associated with TLR based adjuvants, but are considered a fair trade off for increased immunogenicity [245]. Other side effects of TLR adjuvants such as production of anti-CpG antibodies have been described but have not been associated with pathology [246].Though concerns exist regarding pathological side effects such as autoimmunity resulting from adjuvants there is little evidence of this in humans to date [247].

1.4. Controlled Human Malaria Infection (CHMI)

1.4.1. CHMI Delivery

Controlled human malaria infection is an approach by which healthy human individuals can be infected with a laboratory strain of *P. falciparum* or *P. vivax* malaria. There are three methods by which *P. falciparum* parasites can be delivered for CHMI. In direct feeds, adult *Anopheles* mosquitoes are infected with a lab adapted strain of malaria [248], typically 3D7 or NF54 [249] , although alternative challenge strains are in preparation for CHMI. Volunteers are then exposed to a defined number of infectious bites (n=5 or n=3) from these mosquitoes, confirmed by subsequent dissection of the mosquito salivary glands. Direct feeding using mosquitoes more accurately mimics the natural route of infection and allows for both liver-stage and blood-stage infection to occur. However due to natural variation in sporozoite load in mosquito salivary glands, inoculation dose is impossible to standardise both inter- and intra-experimentally. The two alternative methods of CHMI both involve delivery with needle and syringe which allows for a more controlled parasite dosage. Blood-stage inoculation can be achieved by using an aliquot of infected blood that was frozen down from a volunteer under controlled conditions over 15 years ago [250]. This method has now been used in a number of studies for *P. falciparum* (clone 3D7) [114]and more recently *P. vivax* [251] CHMI. In contrast the injection of sporozoites has been restricted to *P. falciparum*. The sporozoite inoculum, developed by Sanaria Inc., is derived from cultured and cryopreserved NF54 strain parasites which are thawed from liquid nitrogen storage before injection and are well characterised following extensive safety testing [252].

1.4.2. Testing Vaccine Efficacy with CHMI

One of the most common applications of CHMI is in the study of vaccine efficacy. Following a vaccination regime, CHMI can be used to look for varying degrees of vaccine protection including sterile protection, delay to patency and a change in blood-stage parasite growth rates [249]. CHMI has been

used to test both liver-stage [185, 253] and blood-stage vaccine [51] candidates with the best efficacy in terms of sterile protection observed with liver-stage vaccines to date. In the study of antigens that are present at the blood-stage or both the liver- and blood-stage of the parasite lifecycle, CHMI using the blood-stage inoculum containing infected erythrocytes (IEs) can directly test the effect of a vaccine on blood-stage parasite multiplication rates [114]. Most of these vaccine/CHMI studies to-date have been tested in malaria-naïve, healthy, UK and US individuals in Phase IIa clinical trials. More recently CHMI studies have been performed in individuals from malaria endemic countries, including those with varying degrees of prior natural exposure [254] (Hodgson *et al* in press).

1.4.3. CHMI as a Vaccine Platform

CHMI can also be used as an effective platform for whole-organism vaccination. One approach has been to use either genetically attenuated [255] or irradiated [252] sporozoites for vaccination which arrest during development in the liver. More recent approaches have concentrated on the use of multiple exposures of viable parasites via CHMI under drug cover [256, 257]. The advantage of this approach is that parasites mature into early blood-stage parasites, increasing the number of antigens exposed to the immune system. Both approaches have yielded much higher levels of sterile efficacy compared to subunit vaccination regimes to-date, however, deployability of this approach in the field remains a critical challenge [258-260]. Data point to efficacy being mediated against pre-erythrocytic and liver-stage parasites, with little to no protection driven through responses to blood-stage parasites. This has been clearly demonstrated by using the blood-stage parasite inoculum to bypass the liver-stage of infection[52]. The same regime that afforded complete protection (5/5) against sporozoite challenge, afforded no protection (0/9) against blood-stage challenge.

1.5. Immunological Assays

A number of immunological techniques, commonly used in the study of NAI and vaccine-induced immunity to malaria and other infectious diseases, have been increasingly standardised over recent years to ensure comparability of data within and between their respective fields. Here these techniques and their prior applications will be discussed in the context of the work presented in this thesis.

1.5.1. ELISPOT

The Enzyme-Linked Immunosorbent Spot assay is routinely used in the detection of both T and B cells responses to vaccination due to its sensitivity, robustness and reproducibility. IFN-γ producing antigen-specific T cells are commonly monitored in human malaria clinical trials as an indicator of cellular immunogenicity [51, 147, 216, 217]. In such studies peripheral blood mononuclear cells (PBMC) are re-stimulated in the presence of peptide antigen for 16-18 hours to measure the antigen specific, effector re-call response, expressed as spot forming units per million PBMC (SFU/10^6 PBMC). Responses are typically characterised to pools of peptides that allow immunogenic regions of antigens to be identified or in the case of biallelic vaccines, relative immune responses to each allele. This assay has been used to study antigen-specific T cell responses to circulating parasite strains in endemic populations [261], as well as in studies of possible malaria driven T cell dysregulation in both endemic [153, 155] and vaccinated populations [156].

The memory B cell (mBC) ELISPOT is commonly used for the study of peripheral blood B cells in humans [262]. This assay allows identification of antigen-specific mBC derived antibody secreting cells by *ex-vivo* ELISPOT assay following a 6 day polyclonal culture, and has been used to measure both naturally-acquired [90, 91, 94, 95] and vaccine-induced responses [219]. The assay can also be adapted to look at populations of antibody secreting cells (ASC) induced post booster vaccination without the need for

culture [86, 263]. For blood-stage malaria studies, B cells studied are typically antigen-specific IgG^+ and are quantified in two ways, per million PBMC or as a % of total IgG^+ secreting cells [219].

1.5.2. ELISA

Given the prominent role for antibody in protection against malaria sporozoites and blood-stage merozoites, quantification and identification of antigen-specific parasite neutralising antibodies has become an essential tool in malaria research. The basic principle of the Enzyme Linked Immunosorbent Assay (ELISA) is as follows; antigen is coated onto the surface of a plate, which is in turn recognised by antibodies in serum specific for that antigen. Excess serum antibody is washed off and then an anti-species-specific antibody conjugated to an enzyme recognises the antigen-bound serum antibody. Further washing followed by addition of substrate for the enzyme will then initiate a reaction which triggers a colour change which can be detected at a specified wavelength. In a quantitative ELISA the reaction is compared to a standard curve of known anti-antigen antibody concentrations to report results in terms of µg/mL antigen-specific Ab. A number of variations of the assay exist including direct, indirect, sandwich and competition. ELISA is most commonly used to measure antibody responses to malaria antigens of interest in studies of endemic populations [264, 265] and both pre-clinical [50, 266] and clinical vaccine trials [51, 216, 217, 267]. Studies, particularly of blood-stage antigens, have also looked to see if the affinity and avidity of antibodies increased with exposure and/or vaccination [268] and whether allelic specificity has an impact on antigen recognition [163]. Following multiple booster vaccinations, natural constraints to antibody affinity maturation may provide a limiting factor [81], although this may be antigen-dependent.

ELISA has also been used to look at changes in the levels of serum cytokines and chemokines such as Granzyme A and B, IL-10, IFN-γ, and TNF-α in the peripheral blood during natural and controlled exposure in a number of malaria models [269-271]. Such profiles can also be characterised in the days

following vaccination, with these being influenced through the selective use of vaccine delivery platform or adjuvant, e.g. viral vectors [272]. Such changes can then be analysed for possible association with increases/decreases in peripheral blood cellular subsets at select time points or with positive or negative disease outcomes [270, 271, 273, 274].

1.5.3. Flow Cytometry

Flow cytometry is a powerful tool used for phenotyping different cells of the immune system. Antibodies specific for both external and internal cell markers are conjugated to fluorophores which are used to stain cell samples with or without fixation. In a flow cytometer, cells in a liquid stream are passed in single file in front of a light source comprising a series of lasers emitting different wavelengths of light. Each fluorophore has a specific excitation and emission wavelength. A detector receives signals that characterise the individual cells, including forward and side scatter (FSC and SSC) which determine size and granularity, as well as emission from fluorophores. As fluorophore emissions often overlap compensation is used to maximise specificity of detection. Subsequent analysis of the detected signals is then used to establish all the markers that were positive or negative for each cell and 'gate' groups of cells to determine subsets. Quantification of cell subsets has been utilised to characterise transient changes in frequencies of cells following vaccination and natural infection in a number of models, establishing whether or not these cell populations associate with functional responses [122, 124, 129, 275].

Flow cytometry can also be used to identify antigen-specific cells. Biotinylated target, (peptide:MHC tetramer in the case of T cells, antigen in the case of B cells) is bound by antigen-specific cells and can be detected using streptavidin conjugated to fluorophores. This technique has been used to quantify antigen-specific B and T cells for a number of infectious diseases including influenza [276] and HIV [277]. Other studies, such as those using the common blood-stage malaria antigens AMA1 and MSP1, have

been less successful, citing antigen instability and high levels of non-specific binding as problematic [278].

Isolation of bulk antigen-specific B cells (mBCs, ASCs, LLPCs) can allow study of the B cell receptor repertoire and identify specific variable gene usage and patterns of SHM common to vaccination or natural exposure [81]. Isolation of single cells, particularly antigen-specific cells allows even greater insights into specific VDJ combinations and mutations from germline sequences that may be commonly associated with protection. Specific B cell clones can also be studied over time following vaccination or natural exposure [263, 279, 280]. This allows determination of whether the response is dominated by a large number of similar clones, or is highly diverse, as well as whether this changes over time due to affinity maturation. More recent work has also sought to determine how clones behave and their longevity, for example looking to see whether clones present in the peripheral blood as plasmablasts match those in the bone marrow as LLPC that contribute to long term antibody secretion (Rafi Ahmed unpublished data). Single cell clones are also commonly used in the production of monoclonal antibodies.

1.5.4. Production of Monoclonal Antibodies

Monoclonal antibodies (mAbs), first developed in the 1980s and derived from mice were a promising enterprise but suffered initially from limited therapeutic success [281]. However advances in technology in the 1990s and early 2000s, in particular the ability to make fully human mAbs, has led to the rise of a highly successful and broadly ranging industry, with licenced treatments targeting a range of conditions including autoimmune disease, cancer and infectious disease among many others [282]. More recently there has been growing interest in the study of rare, often broadly-neutralising antibodies (bNAbs) that confer some level of protection against difficult infectious disease targets including HIV and influenza [283-285]. Isolation and production of mAbs with these rare but highly protective specificities may lead

to greater understanding of the development of these responses naturally, and importantly should help to guide vaccine design [286]. The identification of bNAbs is of similar interest in malaria, especially given the polymorphisms observed in blood-stage antigens. However to-date studies have not described such antibodies resulting from natural exposure or vaccination in humans [287], although some vaccine studies in mice do show promise [166, 170].

There are a number of sources from which human mAbs can now be derived including ASC and mBC, each with their own advantages and applications [288]. Older methods relied on immortalisation of B cells using Epstein-Barr Virus (EBV) [288] and the production of hybridomas [289], humanisation of mouse antibodies [290], chimerisation [291] or the use of phage display libraries [292]. These methods were often low throughput and low efficiency. Newer methods, using expression vector cloning of single sorted B cells of defined origin, have been shown to be much more specific and higher throughput [293, 294]. This method has been successfully used to generate influenza [263], HIV [285] and malaria [287] specific monoclonal antibodies from a number of different B cell subsets.

1.5.5. Assay of Growth Inhibitory Activity

The assay of growth inhibitory activity (GIA) was developed as a means of measuring the ability of natural or vaccine-induced antibodies to prevent merozoite growth within and/or invasion of erythrocytes. Different antigens require differing concentrations of antibody to neutralise parasites effectively. To standardise results, antibody performance is typically summarised by its IC_{50}, the median inhibitory concentration required to neutralise 50% of parasites, estimated using a number of serum dilutions and a percent inhibition curve. When comparing GIA across studies, a number of important considerations must be borne in mind when interpreting the data. Experiments can be performed using whole polyclonal sera, purified IgG or mAbs. The total antigen-specific IgG present can therefore vary hugely from mg/mL to µg/mL. Other variables include heat inactivation of complement, number of

growth cycles and possible drug contamination in serum from individuals living in endemic areas. Importantly, the assay has been standardised by the GIA Reference Laboratory led by Dr Carole Long at the NIH, USA. All studies in this thesis use this standardised methodology.

The assay of GIA critically relies on effective long term culture of human malaria parasites [295] that are synchronised as blood-stage schizonts prior to exposure to immune sera or purified immunoglobulin. The GIA assay has been used extensively in the study of blood-stage vaccine candidates such as MSP1 and AMA1, with the latter shown to be more effective [296]. It has been observed, however, that high levels of growth inhibition achieved in preclinical studies using mouse, rabbit and macaque sera [266, 297, 298] are not achievable following human vaccination [51, 216, 217]. This is possibly due to current clinical vaccine regimes being unable to reach the exceptionally high concentrations of antibody required for merozoite neutralisation when using the MSP1 and AMA1 targets. Encouragingly, newly identified antigens such as PfRH5 may be quantitatively more susceptible to vaccine-induced antibodies [116, 119]. More recent studies have observed that mixing of antibodies to different blood-stage antigens can also give additive or even synergistic GIA responses, particularly when including PfRH5 [119]. Whilst these results are promising this work now needs to be validated in future human studies.

1.6. Thesis Aims & Outlines

An efficacious blood-stage malaria vaccine requires the induction of high titre neutralising antibodies. To achieve this, vaccine regimens have been designed specifically to maximise antibody induction and maintenance. B cells are responsible for production of antibody, so understanding how these cells are generated by vaccination and correlate with antibody responses is of great importance. The ultimate test of any candidate vaccine is clinical efficacy. Controlled human malaria infection (CHMI) is a powerful tool for measuring efficacy but also allows insight into how vaccine-induced populations of cells respond to parasite exposure, providing insight to how such populations may respond following natural infection. The measurement of vaccine-induced responses to both vaccination and CHMI may therefore lead to identification of the components of the immune response that are critical for vaccine-mediated antibody driven protection. Once identified there are a number of possible applications for such data. Information gathered could be used to produce next generation vaccines, design novel adjuvants that promote specific responses, or could be applied to the production of therapeutics as supplements or alternatives to vaccination.

1.6.1. Aims

- To establish the kinetics of B cell induction in humans following prime-boost vaccination with candidate viral vectored and protein vaccines targeting the blood-stage malaria antigens MSP1 and AMA1.
- To determine induction of B cells to blood-stage antigens in malaria-naïve individuals following CHMI.
- To investigate how CHMI may impact on pre-existing populations of vaccine-induced blood-stage antigen-specific B cells and how this may impact on vaccine efficacy.

- To isolate antigen-specific B cells induced by vaccination and use them to assess the function of human monoclonal antibodies to the candidate antigen AMA1 and establish whether any display broadly neutralising activity.
- To explore the possible role and identity of peripheral blood T follicular helper cell subsets contributing to the antibody and B cell response to blood-stage malaria antigens in humans.

1.6.2. Outlines

Chapter 2: Material and Methods

Chapter 3: B cell induction following ChAd63-MVA MSP1 and AMA1 immunisation and controlled human malaria infection

Chapter 4: Phenotypic characterisation of B cell subsets during CHMI

Chapter 5: Single B cell sorting

Chapter 6: Production and characterisation of human monoclonal antibodies

Chapter 7: Association of peripheral blood T follicular helper cell populations with vaccine-induced antibody and B cell responses

Chapter 8: Discussion and Future Directions.

2. Materials and Methods

2.1. Materials

2.1.1. Reagents

Reagent	**Company**	**Cat. number**
1M Tris-HCl pH 8.0	Sigma	T2694-100ML
1M Tris-HCl pH 9.0	Sigma	T2819-100ML
3-Acetylpyridine Adenine Dinucleotide (APAD)	Sigma	A5251
5-alpha Competent E. coli (High Efficiency)	NEB	C2987H
70% ethanol	Sigma	02877-1L
Agarose	Sigma	A9539-500G
Alkaline phosphatase conjugates: Goat-anti-human IgG (γ chain specific)	Calbiochem	401442
BCIP/NBT Development Buffer	Europa Bioproducts	M0711A
BD CompBeads anti mouse Ig, K	BD Bioscience	51-90-900-1229
Benzonase >99% purity	Merck Chemicals Ltd	70664-3
Brefeldin A	Sigma Aldrich	B7651-5MG
Casyton counting buffer	Sedna Scientific	3813
CpG-2006 (TCG-TCG-TTT-TGT-CGT-TTT-GTC-GTT) (0.2mg/ml)	Invivogen (Source BioScience)	tlrl-hodnb-1
Criterion TGX Precast Gels (Any kD)	Bio-Rad	567-1125

Diaphorase from Clostridium klyiveri	Sigma	D5540-1.5KU
Diphtheria Toxoid	NIBSC	02/176
dNTPs 10nM Mix	Invitrogen	Y02256
D-sorbitol	Sigma	S1876
Dulbecco's Modified Eagle Medium (DMEM)	Sigma	D6546
EasySep Buffer	EasySep	20144
FCS	Biotest Biosera	S1810 1001/500
Flow Cytometry Fixation & Permeabilization Buffer Kit I	R&D Systems	FC009
Gene Ruler DNA ladder	Thermo Scientific	SM0312
HEK293A cell line	In House (non-commercial)	
HEK293E cell line	In House (non-commercial)	
HotStar Taq DNA Polymerase	Qiagen	203203
Human IFN-γ ELISA Ready Set Go!	eBioscience	88-7316
Human MIG Instant ELISA	eBioscience	BMS285INST
Human Pan B cell Enrichment Kit	EasySep	19554
Human Red Blood Cells	N/A	N/A
Ig's (Polyvalent), Goat Anti-Human, (Purified)	Caltag	H17000
Ionomycin	Sigma Aldrich	I0634
L-Glutamine	Gibco	25030-24

Loading Dye		
Monensin	eBioscience	00-4505-51
Nitro Blue Tetrazolium tablets	Sigma	N5514
Nuclease Free water	Qiagen	129114
One Comp eBeads	eBioscience	01-1111-42
One Step RT-PCR Kit	Qiagen	210212
Paraformaldehyde 4% in PBS	Santa Cruz Biotechnology	sc-281692
PBS	Sigma	401442
PBS with Tween-20	Sigma	P3563
Penicillin/Streptomycin	GibcoBRL / Invitrogen	15140-122
Percoll	Sigma	77237-100ML
PMA	Sigma Aldrich	P8139
Pokeweed Mitogen (PWM)	Sigma	L-9379
Polyethylenimine, Linear (MW 25,000)	Alfa Aesar	43896.03
Recombinant RNasin Ribonuclease Inhibitor	Promega	N2515
RLT Lysis Buffer	Qiagen	79216
RNase Zap	Sigma	R-2020
RPMI-1640	Sigma	R0883
Staphylococcal enterotoxin B (SEB)	Sigma	S4881
Sodium L (+)-lactate	Sigma	L7022

Staphylococcus aureus Cowans Strain Pansorbin cells (SAC)	Calbiochem	507858
Sybr Safe DNA Gel Stain	Invitrogen	S33102
Thermo Scientific 1.1X ReddyMix PCR Master Mix	Thermo Scientific	AB-0575-LD
Tris Acetate EDTA(TAE) Buffer 50x	Fisher Bio reagents	BP1332
Tris pH8 (1M)	Ambion	AM9855G
Triton-x100	Sigma	79284-100 mL
Virkon	Fisher	HYG-205-230B
β-Mercaptoethanol	Calbiochem	444203

2.1.2. Buffers and Solutions

Buffer/Solution	**Components**			
R0	RPMI media	Pen/Strep (0.1 mg/mL)	L-Glutamine (4mM)	
R10	RPMI media	Pen/Strep (0.1 mg/mL)	L-Glutamine (4mM)	FCS (10%)
H10	RPMI media	Pen/Strep (0.1 mg/mL)	L-Glutamine (4mM)	Human Serum (10%)
FACS Buffer	PBS	1% BSA	0.1% NaN3	

Modified FACS Buffer	PBS	1% BSA		
RT-PCR Catch Buffer	RNasin (1u/µL)	1M Tris pH8 (1%)	Nuclease free H_2O	
mBC Stimulation Mix	R10	SAC (0.42 µg/mL)	PWM (0.16 µg/mL)	CpG (5 µg/mL)
D0	DMEM	Pen/Strep (0.1 mg/mL)	L-Glutamine (4mM)	
D10	DMEM	Pen/Strep (0.1 mg/mL)	L-Glutamine (4mM)	FCS
LDH substrate buffer	1M Tris HCl pH 8.0 10%	H_2O	Sodium L-Lactate (2.8g)	
Nitro Blue Tetrazolium (NBT) solution	LDH buffer	NBT tablet (10mg)		
2x complete medium	Incomplete medium	7.5% sodium bicarbonate solution	heat inactivated filtered pooled human serum	Gentamicin (10mg/mL)
0.1M Glycine pH 2.7	Glycine-HCl	dH_2O		

2.1.3. Flow Cytometry Antibodies

Marker	**Clone**	**Specificity**	**Company**	**Cat. Number**
CCR6 PE	11A9	Mouse anti-human	BD Bioscience	551773
CD10 APC	Hl10a	Mouse anti-human	BD Bioscience	332777

CD154 FITC	TRAP1	Mouse anti-human	BD Bioscience	555699
CD183/CXCR3 Alexa Fluor 488	1C6/CXCR3	Mouse anti-human	BD Bioscience	558047
CD19 PE-Cy7	SJ25C1	Mouse anti-human	BD Bioscience	557835
CD20 APC eFluor780	2H7	Mouse anti-human	eBioscience	47-0209-42
CD21 eFluor450	HB5	Mouse anti-human	eBioscience	9048-0219-025
CD21 FITC	LT21	Mouse anti-human	Biolegend,	315104
CD27 Qdot 605	CLB-27/1	Mouse anti-human	Invitrogen	Q10065
CD28 Purified	CD28.2	Mouse anti-human	eBioscience	16-0289-81
CD3 PE TexasRed	S4.1	Mouse anti-human	Invitrogen	MHCD0317
CD38 PE-Cy5	HIT2	Mouse anti-human	eBioscience	15-0389-42
CD4 APC-H7	SK3	Mouse anti-human	BD Bioscience	641398
CD40 Purified	G28.5	Mouse anti-human	Biolegend	303602
CD45RO PECy7	UCHL1	Mouse anti-human	BD Bioscience	337168
CD49d Purified	9F10	Mouse anti-human	eBioscience	14-0499-80
CXCR3 APC	1C6/CXCR3	Mouse anti-human	BD Bioscience	550967
CXCR3 BV421	1C6/CXCR3	Mouse anti-human	BD Bioscience	562558
CXCR5 Alexa Fluor 488	RF8B2	Rat anti-human	BD Bioscience	558112
CXCR5 BV421	RF8B2	Rat anti-human	BD Bioscience	562747
ICOS Biotin	3D12	Mouse anti-human	BD Bioscience	552174
IgG PE	G18-145	Mouse anti-human	BD Bioscience	555787

IgM FITC	SA-DA4	Mouse anti-human	eBioscience	11-9998-42
IL-21 A647	3A3-N2	Mouse anti-human	Biolegend	513006
L/D Aqua Stain	N/A	N/A	Invitrogen	L34957
PD-1 BV421	EH12.1	Mouse anti-human	BD Bioscience	562516
SA PerCP	N/A	N/A	BD Bioscience	340130
Streptavidin APC	N/A	N/A	eBioscience	17-4317-82
Streptavidin FITC	N/A	N/A	eBioscience	11-4317-87

2.1.4. Primers

#	Name	Sequence 5' - 3'
RT-PCR primers		
1	5' L VH1	ACAGGTGCCCACTCCCAGGTGCAG
2	5' L VH3	AAGGTGTCCAGTGTGARGTGCAG
3	5' L VH4/6	CCCAGATGGGTCCTGTCCCAGGTGCAG
4	5' L VH5	CAAGGAGTCTGTTCCGAGGTGCAG
5	3' Cγ CH1	GGAAGGTGTGCACGCCGCTGGTC
6	5' L VK1/2	ATGAGGSTCCCYGCTCAGCTGCTGG
7	5' L VK3	CTCTTCCTCCTGCTACTCTGGCTCCCAG
8	5' L VK4	ATTTCTCTGTTGCTCTGGATCTCTG
9	3' CK 543	GTTTCTCGTAGTCTGCTTTGCTCA
10	5' L Vλ1	GGTCCTGGGCCCAGTCTGTGCTG
11	5' L Vλ2	GGTCCTGGGCCCAGTCTGCCCTG
12	5' L Vλ3	GCTCTGTGACCTCCTATGAGCTG
13	5' L Vλ4/5	GGTCTCTCTCSCAGCYTGTGCTG
14	5' L Vλ6	GTTCTTGGGCCAATTTTATGCTG
15	5' L Vλ7	GGTCCAATTCYCAGGCTGTGGTG
16	5' L Vλ8	GAGTGGATTCTCAGACTGTGGTG
17	3' Cλ	CACCAGTGTGGCCTTGTTGGCTTG
Nested PCR Primers		
18	5' AgeI VH1/5/7	CTGCAACCGGTGTACATTCCGAGGTGCAGCTGGTGCAG

19	5' AgeI VH3	CTGCAACCGGTGTACATTCTGAGGTGCAGCTGGTGGAG
20	5' AgeI VH4	CTGCAACCGGTGTACATTCCCAGGTGCAGCTGCAGGAG
21	5' AgeI VH3-23	CTGCAACCGGTGTACATTCTGAGGTGCAGCTGTTGGAG
22	5' AgeI VH4-34	CTGCAACCGGTGTACATTCCCAGGTGCAGCTACAGCAGTG
23	5' AgeI VH 1–18	CTGCAACCGGTGTACATTCCCAGGTTCAGCTGGTGCAG
24	5' AgeI VH 1–24	CTGCAACCGGTGTACATTCCCAGGTCCAGCTGGTACAG
25	5' AgeI VH 3–9/30/33	CTGCAACCGGTGTACATTCTGAAGTGCAGCTGGTGGAG
26	5' AgeI VH 6–1	CTGCAACCGGTGTACATTCCCAGGTACAGCTGCAGCAG
27	5′ AgeI VH4–39	CTGCAACCGGTGTACATTCCCAGCTGCAGCTGCAGGAG
28	5′ AgeI VH3–33	CTGCAACCGGTGTACATTCTCAGGTGCAGCTGGTGGAG
29	3' SalI JH1/2/4/5	TGCGAAGTCGACGCTGAGGAGACGGTGACCAG
30	3' SalI JH3	TGCGAAGTCGACGCTGAAGAGACGGTGACCATTG
31	3' SalI JH6	TGCGAAGTCGACGCTGAGGAGACGGTGACCGTG
32	5' Pan VK	ATGACCCAGWCTCCABYCWCCCTG
33	3' CK 494	GTGCTGTCCTTGCTGTCCTGCTC
34	5' AgeI VK1-5	CTGCAACCGGTGTACATTCTGACATCCAGATGACCCAGTC
35	5' AgeI VK1-9/1-13	TTGTGCTGCAACCGGTGTACATTCAGACATCCAGTTGACCCAGTCT
36	5' AgeI VK1D-43/1-8	CTGCAACCGGTGTACATTGTGCCATCCGGATGACCCAGTC
37	5' AgeI VK2-24	CTGCAACCGGTGTACATGGGGATATTGTGATGACCCAGAC
38	5' AgeI VK2-28/2-30	CTGCAACCGGTGTACATGGGGATATTGTGATGACTCAGTC
39	5' AgeI VK3-11/3D-11	TTGTGCTGCAACCGGTGTACATTCAGAAATTGTGTTGACACAGTC
40	5' AgeI VK3-15/3D-15	CTGCAACCGGTGTACATTCAGAAATAGTGATGACGCAGTC
41	5' AgeI VK3-20/3D-20	TTGTGCTGCAACCGGTGTACATTCAGAAATTGTGTTGACGCAGTCT
42	5' AgeI VK4-1	CTGCAACCGGTGTACATTCGGACATCGTGATGACCCAGTC
43	3' BsiWI JK1/2/4	GCCACCGTACGTTTGATYTCCACCTTGGTC
44	3' BsiWI JK3	GCCACCGTACGTTTGATATCCACTTTGGTC
45	3' BsiWI JK5	GCCACCGTACGTTTAATCTCCAGTCGTGTC
46	3' BsiWI JK1 50/3	GCCACCGTACGTCTGATTTCCACCTTGGTC
47	5' AgeI Vλ1	CTGCTACCGGTTCCTGGGCCCAGTCTGTGCTGACKCAG
48	5' AgeI Vλ2	CTGCTACCGGTTCCTGGGCCCAGTCTGCCCTGACTCAG
49	5' AgeI Vλ3	CTGCTACCGGTTCTGTGACCTCCTATGAGCTGACWCAG
50	5' AgeI Vλ4/5	CTGCTACCGGTTCTCTCTCSCAGCYTGTGCTGACTCA
51	5' AgeI Vλ6	CTGCTACCGGTTCTTGGGCCAATTTTATGCTGACTCAG
52	5' AgeI Vλ7/8	CTGCTACCGGTTCCAATTCYCAGRCTGTGGTGACYCAG
53	3' XhoI Cλ	CTCCTCACTCGAGGGYGGGAACAGAGTG
Sequencing Primers		
54	5’Ab sense	GCTTCGTTAGAACGCGGCTAC
55	AbVec IgG Rv	GGAAGTAGTCCTTGACCAGGC
56	AbVec Igκ Rv	GTTATTCAGCAGGCACACAACAG
57	AbVec Igλ Rv	TATCTGCCTTCCAGGCCAC

CPEC Primers		
58	CPEC VH1/5/7	CTTTTTCTAGTAGCAACTGCAACCGGTGTACATTCCGAGGTGCAGCTGGTGCAG
59	CPEC VH3	CTTTTTCTAGTAGCAACTGCAACCGGTGTACATTCTGAGGTGCAGCTGGTGGAG
60	CPEC VH4	CTTTTTCTAGTAGCAACTGCAACCGGTGTACATTCCCAGGTGCAGCTGCAGGAG
61	CPEC VH3-23	CTTTTTCTAGTAGCAACTGCAACCGGTGTACATTCTGAGGTGCAGCTGTTGGAG
62	CPEC VH4-34	CTTTTTCTAGTAGCAACTGCAACCGGTGTACATTCCCAGGTGCAGCTACAGCAGTG
63	CPEC VH1–18	CTTTTTCTAGTAGCAACTGCAACCGGTGTACATTCCCAGGTTCAGCTGGTGCAG
64	CPEC VH1–24	CTTTTTCTAGTAGCAACTGCAACCGGTGTACATTCCCAGGTCCAGCTGGTACAG
65	CPEC VH3–9/30/33	CTTTTTCTAGTAGCAACTGCAACCGGTGTACATTCTGAAGTGCAGCTGGTGGAG
66	CPEC VH6–1	CTTTTTCTAGTAGCAACTGCAACCGGTGTACATTCCCAGGTACAGCTGCAGCAG
67	CPEC VH4–39	CTTTTTCTAGTAGCAACTGCAACCGGTGTACATTCCCAGCTGCAGCTGCAGGAG
68	CPEC VH3–33	CTTTTTCTAGTAGCAACTGCAACCGGTGTACATTCTCAGGTGCAGCTGGTGGAG
69	CPEC JH1/2/4/5	GATGGGCCCTTGGTCGACGCTGAGGAGACGGTGACCAG
70	CPEC JH3	GATGGGCCCTTGGTCGACGCTGAAGAGACGGTGACCATTG
71	CPEC JH6	GATGGGCCCTTGGTCGACGCTGAGGAGACGGTGACCGTG
72	IPCR AbVec GAMMA Fw	GTCGACCAAGGGCCCA
73	CPEC VK1	CTTTTTCTAGTAGCAACTGCAACCGGTGTACATTCTGACATCCAGATGACCCAGTC
74	CPEC VK1-9/1-13	CTTTTTCTAGTAGCAACTGCAACCGGTGTACATTCAGACATCCAGTTGACCCAGTCT
75	CPEC VK1D-43/1-8	CTTTTTCTAGTAGCAACTGCAACCGGTGTACATTGTGCCATCCGGATGACCCAGTC
76	CPEC VK2	CTTTTTCTAGTAGCAACTGCAACCGGTGTACATGGGGATATTGTGATGACCCAGAC
77	CPEC VK2-28/2-30	CTTTTTCTAGTAGCAACTGCAACCGGTGTACATGGGGATATTGTGATGACTCAGTC
78	CPEC VK3-11/3D-11	CTTTTTCTAGTAGCAACTGCAACCGGTGTACATTCAGAAATTGTGTTGACACAGTC
79	CPEC VK3-15/3D-15	CTTTTTCTAGTAGCAACTGCAACCGGTGTACATTCAGAAATAGTGATGACGCAGTC
80	CPEC VK3-20/3D-20	CTTTTTCTAGTAGCAACTGCAACCGGTGTACATTCAGAAATTGTGTTGACGCAGTCT
81	CPEC VK4-1	CTTTTTCTAGTAGCAACTGCAACCGGTGTACATTCGGACATCGTGATGACCCAGTC
82	CPEC JK1/2/4	ATGGTGCAGCCACCGTACGTTTGATYTCCACCTTGGTC
83	CPEC JK3	ATGGTGCAGCCACCGTACGTTTGATATCCACTTTGGTC
84	CPEC JK5	ATGGTGCAGCCACCGTACGTTTAATCTCCAGTCGTGTC
85	CPEC JK150/3	ATGGTGCAGCCACCGTACGTCTGATTTCCACCTTGGTC
86	IPCR AbVec Kappa Fw	CGTACGGTGGCTGCAC
87	CPEC VL1	CTTTTTCTAGTAGCAACTGCAACCGGTTCCTGGGCCCAGTCTGTGCTGACKCAG
88	CPEC VL2	CTTTTTCTAGTAGCAACTGCAACCGGTTCCTGGGCCCAGTCTGCCCTGACTCAG
89	CPEC VL3	CTTTTTCTAGTAGCAACTGCAACCGGTTCTGTGACCTCCTATGAGCTGACWCAG
90	CPEC VL4/5	CTTTTTCTAGTAGCAACTGCAACCGGTTCTCTCTCSCAGCYTGTGCTGACTCA
91	CPEC VL6	CTTTTTCTAGTAGCAACTGCAACCGGTTCTTGGGCCAATTTTATGCTGACTCAG
92	CPEC VL7/8	CTTTTTCTAGTAGCAACTGCAACCGGTTCCAATTCYCAGRCTGTGGTGACYCAG
93	CPEC CL reverse	GGCTTGAAGCTCCTCACTCGAGGTGAGACAAGGGYGG
94	IPCR AbVec Lambda Fw	CTCGAGTGAGGAGCTTCAAG
95	IPCR AbVec Rv	ACCGGTTGCAGTTGCTACTA

2.1.5. Laboratory Consumables

Consumable	**Company**	**Cat. number**
12 Strip PCR Caps Domed	Star Lab	I1400-1200
25cm^2 Cell Culture flask	Corning	430639
96 Well Microtest U bottom plate	Falcon	353077
96-well cell culture Plate Flat Bottom	Costar	CLS3595
96-well PCR Plate non skirted	Star Lab	E1403-1200
Casyton tubes	Sedna Scientific	43003
EasySep Magnet (Purple)	EasySep	18000
F96 Maxisorp Nunc Immuno Plate	Nunc	442404
GE Protein G HP 1mL columns	GE Healthcare Life Sciences	29-0485-81
Hard-shell PCR plates, 96-well GRN/CLR	Bio-Rad	HSP9641
MAIP ELIspot Plates	Millipore	MAIPS4510
Microseal 'F' foil	Bio-Rad	MSF1001
MinElute PCR Purification Kit	Qiagen	28006
Multidish 24 Well Plate	Nunc	142475
Parafilm Laboratory Film	Sigma	P7793-1EA
PCR Tubes Strip Domed 12 cap	Bio-Rad	TCS1201
Qiaprep spin Miniprep kit	Qiagen	27104
QIAquick Gel Extraction Kit	Qiagen	28706
Stericup filtration units	Millipore	SCGPU10RE

2.1.6. Electronic Equipment

Equipment	**Company**	**Applicable Software**
AID ELIspot plate reader	AID	AID ELIspot Reader v5.0
AKTA start FPLC machine	Ge Healthcare Bio-Sciences	29022094
BD LSRII Flow Cytometer	BD Bioscience	BD FACsDiva + FlowJo v9.7.5
BioSpectrum AC Imaging System	UVP	Vision Works LS
Casy Counter	Schärfe System	N/A
$Cyan_{ADP}$	DakoCytomation	Summit 4.3
EL800 Microplate (ELISA) Reader	BioTek	Gen5
G Storm PCR Machine	Lab Tech	N/A
Gel tank	Bi-Rad	N/A
iBind Western Blot system	Life Technologies	SLF1000
Innova 44 Incubator	New Brunswick Scientific	N/A
MoFlo Cell Sorter	Dako Cytomation	Summit 4.3 + FlowJo v9.7.5
Nanodrop ND-1000 Spectrometer	Labtech	ND-1000

2.2. Clinical Vaccines

2.2.1. Vaccine manufacture

Recombinant ChAd63 and MVA vaccines used in the studies described in this Thesis were manufactured according to Good Manufacturing Practice and underwent extensive quality control before use in human volunteers. ChAd63 vaccines containing candidate blood-stage malaria antigen inserts were manufactured at the Clinical Biomanufacturing Facility, University of Oxford. MVA vaccines containing candidate blood-stage malaria antigen inserts were manufactured at IDT Biologika, Rosslau, Germany [216, 217].

2.2.2. MSP1

The biallelic MSP1 vaccine insert (Fig. 2.1) comprises of the naturally conserved regions of the MSP1 sequence (blocks 1, 3, 5 and 12) preceding the Wellcome and 3D7/MAD20 alleles of the dimorphic 42kDa C-terminal region ($MSP1_{42}$ / sequence blocks 16+17) fused in tandem via a glycine proline linker. Each of the $MSP1_{42}$ regions is composed of an N-terminal 33kDa region ($MSP1_{33}$, block 16) followed by a C-terminal 19kDa region ($MSP1_{19}$, block 17).The 3D7 and Wellcome sequences of $MSP1_{33}$ and $MSP1_{19}$ share 51% and 96% amino acid sequence homology respectively. Details of the insert design and construction have been previously published [298].

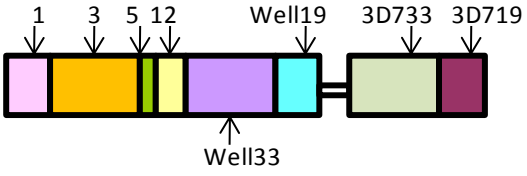


Figure 2.1: MSP1 vaccine insert

2.2.3. AMA1

The AMA1 viral vectored vaccine insert (Fig. 2.2) was designed comprising the 3D7 and FVO strain alleles fused in tandem via a glycine proline linker with the additional FVO terminus region at the end of the construct. This insert is also preceded by a tPA leader sequence with the intention of aiding in protein secretion [299] . The 3D7 and FVO ectodomain share 95% amino acid sequence homology. Details of the insert design and construction have been previously published [297].

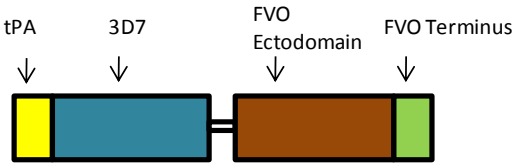


Figure 2.2: AMA1 vaccine insert

2.3. Recombinant Protein and Peptides

2.3.1. MSP1

The recombinant $MSP1_{19}$ proteins used in the ELISPOT assays in this study have been previously reported [108, 216, 298]. The proteins were produced in *Escherichia coli* and consist of the $MSP1_{19}$ region fused to glutathione *S*-transferase (GST) following minor modifications of published methods [300]. Proteins representing both alleles of $MSP1_{19}$ used in the vaccine insert, ETSR (3D7) and QKNG (Wellcome) were used in clinical assays either independently or in a 50/50 mix.

Peptides were purchased from NEO Peptide, USA. The peptides, 20 amino acids (aa) in length and overlapping by 10aa, covered the entire MSP1 insert present in the clinical vaccine insert .The complete list of peptides has been previously published ([216],Table S5). Peptides were reconstituted in 100% DMSO at 50-200mg/mL and combined into specific pools for ELISPOT and other assays.

2.3.2. AMA1

The recombinant AMA1 FVO protein used in this study has been previously reported [217], and the 3D7 AMA1 protein was a kind gift from Dr Y. Wu (NIAID, NIH, USA). Proteins representing both alleles used in the vaccine insert (3D7 and FVO) were used in clinical assays either independently or in a 50/50 mix.

Peptides were purchased from NEO Peptide, USA . The peptides, 20 amino acids (aa) in length and overlapping by 10aa, covered the entire AMA1 insert present in the clinical vaccine insert. The complete list of peptides has been previously published ([217],Table S4) . Peptides were reconstituted in 100% DMSO at 50-200mg/mL and combined into specific pools for ELISPOT and other assays.

2.4. Clinical Trials

2.4.1. VAC036

A Phase Ia clinical trial to assess the safety and immunogenicity of the candidate malaria vaccines, ChAd63 AMA1 administered alone, and with MVA AMA1, intramuscularly, in a prime-boost regime in healthy adults. 16 volunteers were enrolled across 4 groups with the vaccine regime and doses outlined in Table 2.1. The interval between vaccinations in Groups 1B and 2B was 8 weeks and volunteers were bled at key time points during the regime for routine safety tests and exploratory immunology. An outline of this bleed schedule is shown in Chapter 3, Fig. 3.1A. PBMC, plasma and serum samples were stored for further studies outside the trial's primary outcomes. The reduced MVA dosing in Group 2B compared to 1B was due to greater than expected reactogenicity during vaccination [217].

Group Number	No. of volunteers	Prime - Day 0	Boost - Day 56
1A	4	ChAd63 AMA1 5×10^9vp	-
1B	4	ChAd63 AMA1 5×10^9vp	MVA AMA1 5×10^8 pfu
2A	4	ChAd63 AMA1 5×10^{10}vp	-
2B	4	ChAd63 AMA1 5×10^{10}vp	MVA AMA1 2.5×10^8 pfu (n=1) 1.25×10^8 pfu (n=3)

Table 2.1: VAC036 Group Summary

2.4.2. VAC037

A Phase Ia clinical trial aiming to assess the safety and immunogenicity of the candidate malaria vaccines, ChAd63 MSP1 administered alone, and with MVA MSP1, intramuscularly, in a prime-boost regime in healthy adults. 16 volunteers were enrolled across 5 groups with the vaccine regime and dose outlined in Table 2.2. The interval between vaccinations in Groups 1B, 2B and 2C was 8 weeks and volunteers were bled at key time points during the regime for routine safety tests and exploratory immunology. The bleed schedule was identical to that in VAC036. PBMC, plasma and serum samples were stored for further studies outside the trials primary outcomes. Three volunteers in the trial (Group 2C) were subsequently challenged in a Phase IIa sporozoite challenge trial as a lead in study to assess safety (and efficacy) of the vaccine during CHMI [216]. An outline of this bleed schedule is shown in Chapter 3, Fig. 3.1B.

Group Number	No. of volunteers	Prime - Day 0	Boost - Day 56	CHMI
1A	2	ChAd63 MSP1 5×10^9vp	-	No
1B	4	ChAd63 MSP1 5×10^9vp	MVA MSP1 5×10^8 pfu	No
2A	2	ChAd63 MSP1 5×10^{10}vp	-	No
2B	5	ChAd63 MSP1 5×10^{10}vp	MVA MSP1 5×10^8 pfu	No
2C	3	ChAd63 MSP1 5×10^{10}vp	MVA MSP1 5×10^8 pfu	Yes

Table 2.2: VAC037 Group Summary

2.4.3. VAC039

A Phase I/IIa sporozoite challenge trial aiming to assess the immunogenicity and efficacy of the candidate blood-stage malaria vaccines MSP1 and AMA1 alone and in combination in a prime-boost regime using ChAd63 and MVA in healthy adults [51].The bleed schedule for individuals undergoing CHMI was comparable to that for VAC37 Group 3C. MSP1 was also tested in the presence of the liver-stage candidate METRAP [147]. 41 volunteers were enrolled across 5 groups with the vaccine regime and dose outlined in Table 2.3.

Group Number	No. of volunteers	Prime - Day 0	Boost - Day 56	CHMI
1	10	ChAd63 MSP1 5 x 10^{10}vp	MVA MSP1 2 x 10^{8} pfu	Yes
2	9	ChAd63 AMA1 5 x 10^{10}vp	MVA AMA1 1.25 x 10^{8} pfu	Yes
3	9	ChAd63 MSP1 5 x 10^{10}vp & ChAd63 AMA1 5 x 10^{10}vp	MVA MSP1 2 x 10^{8} pfu & MVA AMA1 1.25 x 10^{8} pfu	Yes
4	10	ChAd63 METRAP 5 x 10^{10}vp & ChAd63 MSP1 5 x 1010vp	MVA METRAP 2 x 10^{8} pfu & MVA MSP1 2 x 10^{8} pfu	Yes
5	6	-	-	Yes

Table 2.3: VAC039 Group Summary

2.4.4. VAC044

A Phase Ia clinical trial aiming to assess the immunogenicity of the candidate malaria vaccines, ChAd63 AMA1, MVA AMA1 and the protein vaccine AMA1-C1/Alhydrogel administered in a number of novel vaccine regimes in healthy adults. Variables in this trial included the presence or absence of the TLR agonist CPG 7909 with the protein-in-alum vaccine, boosting at 8 vs 16 weeks post prime and the addition of a second boost 8 weeks after the first. 31 volunteers were enrolled across 5 groups with the vaccine regime and dose outlined in Table 2.4 [301].

Group Number	No. of volunteers	Prime - Day 0	Boost - Day 56	Boost - Day 112
1	5	ChAd63 AMA1	MVA AMA1	AMA1-C1/Alhydrogel® + CPG 7909
2	6	ChAd63 AMA1	AMA1-C1/Alhydrogel® + CPG 7909	
3	7	ChAd63 AMA1	AMA1-C1/Alhydrogel®	
4	6	ChAd63 AMA1	-	AMA1-C1/Alhydrogel® + CPG 7909
5	7	ChAd63 AMA1	-	MVA AMA1

Table 2.4: VAC044 Group Summary

2.4.5. VAC049

A pilot Phase IIa study in humans examining the use of cryopreserved *Plasmodium falciparum* parasites for CHMI. The route of administration and dose was varied in order to identify the optimal regimen that achieves the greatest infection rate in volunteers with cryopreserved *Plasmodium falciparum* sporozoites. 18 volunteers were enrolled across three groups (Table 2.5). In this thesis only Group 3 was studied as it was the only group which achieved a 100% infection rate (Hodgson *et al* in press).

Group Number	No. of volunteers	Total Dose of PfSPZ	Total Volume Administered	Route of Administration	Number of injection sites
1	6	2,500 sporozoites	50µl x 2	Intradermal	Two
2	6	2,500 sporozoites	50µl x 2	Intramuscular	Two
3	6	25,000 sporozoites	50µl x 2	Intramuscular	Two

Table 2.5: VAC049 Group Summary

2.5. Clinical Immunology

2.5.1. Blood Separation

Blood was collected in both standard and heparinised 10mL tubes in clinic in volumes according to the individual trial protocol and was then transferred to the laboratory. Initiation of the separation protocol should begin within 4 hours of blood collection. Non-heparinised tubes were centrifuged at 755 xg for 5 mins to separate serum which was removed by pipette and stored in 1-2 mL aliquots. Blood from heparinised tubes was poured into pre-prepared Leucosep tubes and centrifuged at 1000 xg for 13 mins (brake off) to allow for separation of PBMC into a distinct layer. 1 mL aliquots of plasma were taken before the excess plasma containing PBMC was transferred to a new tube. This volume was then topped up and washed with R0 media twice, before PBMC were resuspended in 10 mL R10 media ready for counting. PBMC were counted, after resting for 1 h in the incubator, using a CasyCounter.

2.5.2. IFN-γ ELISPOT

IFN-γ ELISPOT was performed according to laboratory Standard Operating Procedures (SOP) for all clinical trial samples. ELISPOT can be performed on fresh or previously cryopreserved PBMC. Though detection of IFN-γ producing cell frequencies have been reported to be slightly lower in cryopreserved vs fresh samples [302], in many case concordant results have been reported [303, 304]. Such studies also consistently report concordance across different operators and laboratories. Primary data were obtained from ELISPOT performed on freshly isolated PBMC. Frozen PBMC samples were used for repeats to replace erroneous primary data or for collecting secondary investigatory data.

MAIP ELISPOT plates were coated with 50 µL of catcher antibody (1-1DK) in coating buffer at 10 µg/mL. Plates were stored at 4^{o}C overnight in cling film to prevent evaporation prior to use. Coating buffer was removed and the plate washed three times with PBS before addition of R10 media for 1 h to block the plate. At this stage peptide pools and positive controls were thawed. Blocking solution was removed and

then 50 µL of peptides or positive control was added to each well of the plate. Clinical trial peptide pools are made up so that after the addition of cells the final concentration of each peptide in each well is 5 µg/mL. The positive control contains Staphylococcal enterotoxin B (SEB) (final concentration 0.02 µg/mL) plus phytohemagglutinin (PHA) (final concentration 10 µg/mL).PBMC were resuspended to 5 million cells/mL and then 50 µL (250,000 cells) added to the wells containing peptide or controls. Plates were then incubated for 18-20 h at 37°C and 5% CO_2. After overnight culture cells were discarded, the plate washed and 50 µL detector antibody (7-B6-1-Biotin) in PBS was added at 1 µg/mL. After 2-4 h, plates were washed and 50 µL Streptavidin-alkaline phosphatase (SA-ALP) in PBS was added at 1 µg/mL. After 1-2 h, plates were then washed again and developed using development buffer (Europa Bioproducts). 50 µL substrate per well was left to develop for 3-5 mins until spots were clearly visible, at which point the plate was washed in water and left to dry. Plates were counted using an AID ELISPOT plate reader.

2.5.3. mBC ELISPOT

The mBC ELISPOT protocol was based on a widely published method [262]. As with the IFN-γ ELISPOT this assay can be performed on fresh or cryopreserved PBMC. Similarly, concordant results have been reported for fresh vs cryopreserved cells, as well as across independent assays with the same samples and for assays performed by different operators [305]. mBC ELISPOT in this thesis were all performed from cryopreserved PBMC with all time-points from a single volunteer performed in parallel. This was to reduce possible inter-assay variability, though independent tests not presented in this thesis agree with published data that this was not an issue.

Frozen PBMC were thawed, counted and resuspended to $2x10^6$/mL. 500 µL of cells were added to each well of a 24 well plate. These cells were cultured with 500 µL of a polyclonal B cell stimulation mix containing *Staphylococcus aureus* Cowans strain Pansorbin cell 'SAC' (1/2400) (Calbiochem), the human

TLR agonist CpG ODN-2006 (5 µg/mL) (Invivogen) and pokeweed mitogen 'PWM' (1/6000) (Sigma) for six days, allowing mBC to differentiate into ASC. One well per time-point was also cultured in the absence of stimulation mix as a control. On day five of the experiment, ELISPOT plates were coated with $MSP1_{19}$ or AMA1 protein to measure the antigen-specific response and polyvalent goat-anti human IgG (Caltag) to measure the total IgG response. A separate plate was coated with a non-malaria vaccine protein/antigen (diphtheria toxoid (DT), *National Institute for Biological Standards and Control* (NIBSC)). PBS coated wells were used as a negative control. mBC were also tested against recombinant GST (the tag fused to $MSP1_{19}$ protein). On day six, cultured cells were harvested and transferred to the ELISPOT plate at $2x10^5$ cells per well, with additional dilutions of 1:2 for the antigen-specific response wells and 1:100 and 1:1000 for the total IgG response wells. After overnight culture (18-20 h) cells were discarded, the plate washed and an anti-human IgG (γ-chain) antibody conjugated to alkaline phosphatase (Calbiochem) added for 4 h. The plates were then washed again and developed using development buffer (Europa Bioproducts). The substrate was left to develop for 3-5 mins until spots were clearly visible, at which point the plate was washed in water and left to dry. Plates were counted using an AID ELISPOT plate reader.

2.5.4. ASC ELISPOT

ELISPOT plates were coated with $MSP1_{19}$ or AMA1 protein to measure the antigen-specific response. PBS coated wells were used as a negative control and DT coated wells were used as a non-malaria antigen control. PBMC were freshly prepared as previously described, and plated at $2.5x10^5$ cells per well with additional dilutions of 1:2 for the antigen-specific response. After overnight culture (18-20 h) cells were discarded, and the plate developed and counted by the same method as mBC ELISPOT.

2.5.5. MSP1 and AMA1 ELISA

Standardized ELISA was performed on serum samples isolated from volunteers vaccinated with MSP1 or AMA1 in the clinical trials as previously described [216, 217]. Briefly, total human IgG ELISA responses were measured against the 3D7/MAD20 and Wellcome variants of the 19 kDa fragment of the MSP1 protein ($MSP1_{19}$) or the 3D7 and FVO variants of AMA1 protein according to clinical trial SOP. NUNC Immuno Plates (Fisher Scientific) were coated with 2 µg/mL protein in PBS and left overnight at room temperature (RT). Plates were washed with PBS/Tween and blocked with 200 µL Casein blocking buffer (Pierce). Human hyper immune serum from Kilifi, Kenya was used as reference serum for preparing the standard curve and positive control. Test serum dilutions were prepared in Casein buffer typically ranging from 1:300 to 1:40,000 depending on time point and were tested in triplicate on the plate. Plates were covered and incubated at RT for 2 h before washing as previously described. Secondary antibody; goat anti-human IgG γ-chain (Sigma) was added at a 1:1000 dilution in Casein and incubated for 1 h covered at RT. After a final wash, 100 µL development buffer (20 mL 5x diethanolamine buffer in deionised water and one 20mg 4-nitrophenylphosphate tablet) was added. ELISA plates were read at 405nm after approximately 10 mins (AMA1) to 20 mins (MSP1) using a Bio-tek ELx800 Microplate Reader with Gen5 ELISA software.

2.5.6. IFN-γ ELISA

IFN-γ ELISA was performed using 'Human IFN gamma ELISA Ready-SET-Go!' (eBioscience, UK) as per the manufacturer's instructions. The standard curve range of the kit was 4-500 pg/mL, with baseline responses in healthy human volunteers predicted to be ≈0 pg/mL. At all time-points, neat serum or a 1:5 dilution was tested, except for DoD where up to 1:100 serum dilution was required. ELISA for all time-points and all volunteers within the same experimental group were run in parallel on the same day.

2.5.7. MIG ELISA

CXCL9 (MIG) ELISA was performed using 'Human MIG Instant ELISA' (eBioscience, UK) as per the manufacturer's instructions. The standard curve range of the kit was 30-2000 pg/mL, with baseline responses in healthy human volunteers predicted to be ≈300 pg/mL. For the dC-1 time-point neat serum was used, whist for DoD up to 1:5 serum dilution was required. ELISA for all time-points and all volunteers within the same experimental group were run in parallel on the same day.

2.6. Flow Cytometry

2.6.1. B cell Phenotyping

The B cell phenotyping flow panel in this Thesis was designed considering literature for both broad characterisation of B cell subsets, but also those subsets that are likely important during either a vaccine response or CHMI. Phenotypic analysis was performed on frozen PBMC from six MSP1 vaccinated volunteers in the VAC039 clinical trial at time points d56, d63, dC-1, dC+7, day of diagnosis (DoD) and dC+35. Three out of six vaccinated volunteers were also measured at dC+11. All vaccinated volunteers received the MSP1 vaccination regime prior to CHMI. Five CHMI unvaccinated control volunteers from the VAC039 clinical trial were also analysed at the dC-1, dC+7, DoD and dC+35 time-points for direct comparison. For each experimental sample, typically 1.5 million PBMC were resuspended in 100 µL FACS buffer prior to staining. Analyses were performed using mouse anti-human fluorophore-conjugated monoclonal antibodies specific for B cell and migratory markers: CD10 APC [HI10a], CD19 PE-Cy7 [SJ25C1], IgG PE [G18-145], CXCR3 Alexa-Fluor 488 [1C6] (BD Bioscience); CD27 Qdot 605 [CLB-27/1] (Invitrogen); CD20 APC [2H7], CD21 efluor450 [HB5], CD38 PE-Cy5 [HIT2] (eBioscience). Optimal concentrations for each antibody were determined by independent titrations. The volume used per 100 µL is shown in Table 2.6. Cells were stained for 20 mins with antibody before washing and acquisition. Fluorochrome compensation samples were prepared in parallel using compensation beads stained with the individual fluorophores at the same concentrations. Acquisition was performed on a LSRII Flow Cytometer (BD Biosciences, Franklin Lakes, NJ).

Antibody	Volume (µL)
CD10 APC	0.5
CD19 PE-Cy7	1
CD20 APC	4
CD21 efluor450	1
CD27 Qdot605	0.5
CD38 PE-Cy5	2
IgG PE	2
CXCR3 Alexa-Fluor 488	4

Table 2.6: B cell flow antibody panel

This eight colour panel was used to identify B cell subsets as follows: immature B cells ($CD19^+$, $CD10^+$), naïve B cells ($CD19^+$, $CD10^-$, $CD21^+$, $CD27^-$); classical mBC ($CD19^+$, $CD10^-$, $CD21^+$, $CD27^+$); atypical mBC ($CD19^+$, $CD10^-$, $CD21^-$, $CD27^-$); activated mBC ($CD19^+$, $CD10^-$, $CD21^-$, $CD27^+$, $CD20^+$, $CD38^-$); and plasmablast/ASC ($CD19^+$, $CD10^-$, $CD21^-$, $CD27^+$, $CD20^-$, $CD38^+$)(Chapter 4, Fig. 4.1). IgG^+ staining was also quantified for classical and atypical mBC subsets. CXCR3+ staining was quantified for classical, atypical and activated mBC subsets as well as naïve B cells. In Chapter 4, Fig. 4.2 the small number of events from the following subsets were excluded from the analysis due to undefined phenotypes, ($CD19^+$, $CD10^-$, $CD21^-$, $CD27^+$, $CD20^-$, $CD38^-$; and $CD19^+$, $CD10^-$, $CD21^-$, $CD27^+$, $CD20^+$, $CD38^+$). Analysis was performed using FlowJo software. Gating strategy for fluorochromes was determined using Fluorescence-1 (F-1) analysis and unstained controls. For F-1 analysis parallel panels were run, with one different fluorochrome removed for each panel.

2.6.2. Single Cell ASC Sorting

The single cell ASC flow panel is a simplified version of the B cell phenotyping panel described above with further optimisation to allow for use with the MoFlo cell sorter (Dako Cytomation) rather than the LSRII flow cytometer. The following antibody clones were the same as those used in the previous panel; CD19, CD20, CD27, CD38 and IgG. Only CD21 was moved onto a different fluorochrome, CD21 FITC [clone LT21]. IgM FITC [clone SA-DA4] was also added to the panel on the same fluorochrome as CD21.

Single cell sorting was performed on either frozen or fresh PBMC at 7 days post-booster vaccination (D63, D119) in volunteers vaccinated with AMA1 from various trials. Typically 5 million cells were first enriched for B cells using the 'Human Pan B cell Enrichment Kit' (EasySep) and then stained with the above panel in 100 µL FACS buffer at optimal concentrations determined by titration studies. The Pan-B cell enrichment kit depletes cells expressing CD2, CD3, CD14, CD16, CD36, CD42b, CD56, CD66b, CD123 and Glycophorin A, leaving only B cells. The concentrations required for the increased number of cells and for MoFlo differ from previously and are shown in Table 2.7.

Antibody	Volume (µL)
CD19 PE-Cy7	16
CD20 APC	20
CD21 FITC	48
CD27 Qdot605	4
CD38 PE-Cy5	16
IgG PE	16
IgM FITC	16

Table 2.7: MoFlo antibody panel

This panel was used to identify the following population of IgG^+ ASC ($CD19^+$, $CD27^+$, $CD21^-/IgM^-$, $CD20^-$, $CD38^+$, IgG^+). These cells were sorted as a single cell per well into a 96 well PCR plate (total 48 cells per plate) containing 10 µL freezing buffer (RNasin, Tris pH8 and nuclease free water). Completed plates were covered with foil lids and then snap frozen on dry ice, before long term storage at -80°C. To confirm sorted cells were antigen-specific, this IgG^+ ASC population was also sorted onto a specialised ASC ELIspot and treated as previously described.

2.6.3. Antigen-Specific Cell Staining

The experimental procedures for antigen-specific cell staining were based on the previously described B cell phenotyping and single cell sorting experiments but with additional steps included. Frozen PBMC derived from volunteers vaccinated with either AMA1 or MSP1 from various trials were used in these experiments. D0 samples were used for defining baseline responses while post-boost samples (typically D84) were used for defining responses which were known to contain antigen-specific B cells. For each sample typically 1.5 million cells were stained with either no antigen, biotinylated vaccine antigen

(AMA1 or MSP1), or biotinylated non-vaccine antigen (whichever of AMA1 or MSP1 was not the vaccine antigen). 50 µL of antigen at 5 µg/mL was added to cells for 30 mins (on ice, away from light) before washing with FACS buffer. Then Streptavidin conjugated fluorophore (either FITC or APC, at 4 µL and 0.5 µL respectively) was added for another 30 mins (on ice, away from light). After another wash, antibodies were added as previously described. Acquisition, compensation and analysis was performed as previously described, with the exception of compensation for Steptavidin-conjugated fluorophores, which was done using an equivalent antibody conjugated fluorophore which could bind to compensation beads. For dual staining experiments, sub-saturating concentrations of each fluorophore were used. For vaccine antigen staining streptavidin FITC was titrated down to sub-saturating concentrations (4, 2, 0.5 and 0.1 µL for 1million cells in 100 µL), whilst streptavidin APC was used at a standard 0.5 µL volume, added after initial FITC staining and washing.

2.6.4. Tfh Cell Staining

For Tfh cell characterisation by flow cytometry, three panels were run for each sample; a phenotyping panel, CD154 panel and IL-21 panel. Frozen PBMC derived from volunteers vaccinated with AMA1 in the VAC044 clinical trial were used in these experiments, with a minimum of 2 million cells required per experimental well (14 million total, per volunteer, per time-point). For CD154 and IL-21 stimulations, staining cocktails were made up as described in Table 2.8/2.9 and 100 µL added to 90 µL of cells. For CD154 stimulations 10 µL of H10 (Unstim control), AMA1 total peptide pool (2 µg/mL final concentration) or SEB (positive control, 1 µg/mL final concentration) were added. For IL-21, 10µL of either R10 (Unstim control), AMA1 total peptide pool (2 µg/mL final concentration) or PMA/Ionomycin (positive control, 0.05 µg/mL and 1 µg/mL final concentration respectively) were added.

CD154 Stain	Volume (µL) 1x
H10	100
CD40	0.4
CD28	0.2
CXCR3 APC	5

Table 2.8: Tfh CD154 staining panel

IL-21 Stain	Volume (µL) 1x
R10	100
Brefeldin A	0.2
Monensin	0.14
CD28	0.2
CD49d	0.2
CD4 APC-H7	1
CXCR3 APC	2

Table 2.9: Tfh IL-21 staining panel

Cells were left for 6 h prior to further stepwise extracellular and intracellular staining, as described in Table 2.10. Live/Dead (L/D) staining was included to allow exclusion of dead cells. Cells were fixed and permeabilised for intracellular staining using the Fixation & Permeabilization Buffer Kit (R&D systems) and 4% paraformaldehyde. Cells were stored overnight in the fridge wrapped in foil before acquisition using a $Cyan_{ADP}$ flow cytometer (DakoCytomation).

CD154 Stain	Volume (µL) 1x	IL-21 Stain	Volume (µL) 1x	Phenotyping Stain	Volume (µL) 1x	Timings
CD45RO PECy7	2	CD45RO PECy7	2	CXCR3 APC	5	15 min
CXCR5 BV421	1	CXCR5 AF488	2	CXCR5 AF488	2	
CCR6 PE	2	CCR6 PE	2			
CD4 APC-H7	1					
CD154 FITC	5					
Wash with PBS						
L/D Aqua (1/200)	20	L/D Aqua (1/200)	20	CD3 PE Texas Red	1	10 min (L/D)
				CD4 APC-H7	1	
				CD45RO PECy7	2	15 min
				CCR6 PE	2	
				PD-1 BV421	1	
				ICOS Biotin	1	
Fix Buffer, wash with PBS, wash with Perm Buffer				Wash with PBS		10 min
CD3 PETexas Red	1	CD3 PETexas Red	1	L/D Aqua (1/200)	20	45min (CD3) 10 min (L/D)
Perm Buffer	99	IL-21 AF647	2	SA PerCP (1/10)		
		Perm Buffer	97			
4% Paraformaldehyde						Overnight

Table 2.10: Tfh extracellular and intracellular staining panel

2.7. Monoclonal Antibody Production

2.7.1. Single Cell PCR

This protocol was based on published methodology [293, 294]. 96 well plates containing 48 single sorted B cells (see section 2.6.2) were removed from storage at -80°C and placed on ice to thaw. RT-PCR master mix was made up for 56 reactions (48 cells, 4 negative controls, plus excess) as shown in Table 2.11. The forward primer mix contained a total of 14 primers (#1-4, 6-8, 10-16) whilst the reverse mix contained 3 primers (#5, 9, 17). Primers are fully detailed in section 2.1.4 and were used at a final concentration of 10 µM (from 100 µM stock). 15 µL of master mix was added to each well containing 10 µL freezing buffer (+/- cells). RT-PCR was then run using a G Storm PCR Machine and the following settings; heated lid on, Reverse Transcription (RT) - 30 min at 50°C, RT deactivation/Taq activation – 15 min at 95°C, 50 cycles (denaturation - 94°C for 30 s, annealing - 58°C for 30 s, extension - 72°C for 1 min), final extension 72 for 10 min.

Master Mix	1x (µL)
H_2O	6.5
5x One Step RT-PCR buffer	5
Forward primer mix	1
Reverse primer mix	1
dNTPs	1
One Step RT-PCR enzyme mix	0.5

Table 2.11: RT-PCR Master Mix

3 µL of RT-PCR product was used as template DNA in subsequent nested PCR reactions. Initially heavy nested PCR was performed as a screen, and heavy positive wells are subsequently followed up with Kappa (K) and Lambda (λ) nested PCR reactions. The heavy nested PCR master mix was made up for 56 reactions (48 cells, 4 negative controls, plus excess) as shown in Table 2.12. Kappa and Lambda nested PCR master mixes were adjusted according to number of positive wells. Forward primer mixes were; Heavy, 11 primers (#18-28); Kappa, 9 primers (#34-42); Lambda, 6 primers (#47-52). Reverse primer mixes were; Heavy, 3 primers (#29-31); Kappa, 4 primers (#43-46); Lambda (#53). 37 µL of master mix and 3 µL template DNA was added to a new PCR plate and run using a G Storm PCR Machine and the following settings: heated lid on, Hot Start – 15 min at 95°C, 50 cycles (denaturation - 94°C for 30 s, annealing - 58°C for 30 s, extension - 72°C for 45 s), final extension 72°C for 10 min. Nested PCR products were run on a 1% agarose gel and screened for a positive band around 400bp. Nested products were then extracted and purified using the Quiaquick gel extraction kit.

Master Mix	1x (µL)
H_2O	30.25
10x Hot Star Taq buffer	4
Forward primer mix	1
Reverse primer mix	1
dNTPs	0.5
Hot Star Taq polymerase	0.25

Table 2.12: Nested PCR Master Mix

2.7.2. Circular Polymerase Extension Cloning (CPEC)

Circular Polymerase Extension Cloning (CPEC) [306] was used to clone heavy and light chain nested PCR products into expression plasmids containing the respective heavy or light (Kappa or Lambda) chain IgG1 antibody constant region sequences. Previously published expression plasmids ([294], accession numbers FJ475055, FJ475056 and FJ517647) underwent minor modification in house prior to CPEC cloning. Restriction sites that allow traditional cloning methods were maintained in these plasmids. Two sets of primers are necessary for the initial CPEC PCR: one set for linearising the expression plasmid backbone (H:72+95, K:86+95, λ:94+95) and one for generating the insert with homology regions complementary to the backbone(H:58-71, K:73-85, λ:87-93). These can be found in Table 2.1.4. Phusion High-Fidelity PCR Master Mix (NEB) diluted to 1x with dH_2O was used with 500 nM primers and 2 µL purified nested PCR product or 0.1 ng backbone. PCR was run using a G Storm PCR Machine and the following settings: heated lid on, 98˚C for 30 s, 38 cycles, (98˚C for 15 s, 49˚C for 30 s, 72˚C for 1.5 mins) 72˚C for 5 mins, hold for 4˚C. CPEC PCR products were run on a 1% agarose gel and screened for a positive band around 400 bp for the inserts and around 5750 bp (H) and 5000 bp (K, λ) for the linearized backbone. Correct sized bands were then extracted and purified using the Quiaquick gel extraction kit. For thermal cycling the insert and linearised vector are then mixed in a 1:1 molar ratio (100-200 ng). Using a G Storm PCR Machine, the following 8-cycle program was then used 98˚C for 30 s, 8-cycles (98˚C for 10 s, 70˚C-55˚C gradient for 65 s, 55˚C for 30 s, 72˚C for 3 mins), 72˚C for 5 mins, 4˚C hold.

2.7.3. Plasmid Sequencing

Plasmid insert sequencing was performed using specific forward and reverse primer pairs for each plasmid (H: 54+55, K: 54+56, λ: 54+57) and the Source Bioscience sequencing service (Nottingham, UK). Insert nucleotide sequences were analysed using the online analysis program IGBLAST (http://www.ncbi.nlm.nih.gov/igblast/). This revealed the most closely matched VDJ and VJ sequences in heavy and light chains respectively and % similarity to germ line sequences as well as confirming the sequence was in frame and contained no premature stop codons that may ablate functionality.

2.7.4. Transformation of E. coli

Transformation of *E. coli* was performed using 2 µL of the CPEC reaction mix and 25 µL competent *E.coli* as per product specifications. Transformed cells were plated onto an agar plate containing 100 µg/mL carbenicillin and incubated over night at 37°C. 6-8 colonies were picked and screened for the presence of the plasmid using Phusion PCR master mix and the following PCR protocol; 98 for 10 min, 35 cycles (98˚C for 30 s, 68˚C for 2 mins, 72˚C for 3 mins) hold 10 ˚C, and run on a 1% agarose gel. A single positive colony was selected and bulked up before the plasmid is extracted and purified using a Qiagen Mini- or Midi-prep kit.

2.7.5. Transfection and mAb screen

Adherent HEK293A cells were seeded from stock culture in 96 well plates at $2x10^4$ cells per well so as to be at 80-90% confluency after overnight culture. In a separate 96 well plate, 50 µL of D0 media was added to each experimental well (typically 2-3 repeat wells per transfection). 0.2 µg of paired heavy and Kappa or Lambda plasmid DNA was then added to the D0. In a separate aliquot of D0, PEI transfection reagent was diluted to 60 µg/mL and then 50 µL was added slowly to the wells containing DNA. The plate was then covered and vortexed on low speed for 15 mins. The PEI/DNA mix was then added to culture plates containing cells and topped up with 50 µL of D10. Transfection cultures were then

incubated for 2-3 days at 37°C and 5% CO_2. Supernatants were harvested and screened for antigen-specific mAb production using the AMA1 ELISA method outlined in section 2.5.5. ELISA positive transfections were then repeated using suspensionHEK293E cells to maximize mAb yield for subsequent experiments. The HEK293E cultures were spun at 1000 xg for 10 mins 4 days after transfection and 0.2 µm filtered using Millipore Stericup filtration units. Antibodies were purified on separate GE Protein G HP 1mL columns at a flow rate of 4.0 mL/min using an AKTA start FPLC machine. Wash/equilibration was done with PBS and elution was carried out with 0.1M Glycine pH 2.7. The pH of the eluate was immediately neutralised with 1M Tris-HCl pH 9.0. Antibodies were desalted into PBS using a HiPrep 26/10 desalting column at a flow rate of 20 mL/min using an AKTA Pure FPLC machine.

2.7.6. Western Blot of mAbs

Western Blot was performed using the iBind system and a denaturing SDS-PAGE gel (Criterion TGX Precast Gels), and 150µg of each of 3D7 and FVO AMA1 protein was run in each lane of the blot. mAbs to be tested were diluted to a final concentration of 1 µg/mL, with the secondary antibody (Sigma goat anti-human gamma chain specific) diluted 1:2000. The iBind was left to work for 2.5 h and the blots developed for 5-8 mins.

2.7.7. Assay of Growth Inhibitory Activity (GIA)

Plasmodium falciparum parasites were grown as per laboratory protocol (ML016) in human O^+ blood. Parasitaemia is monitored by thin smears during culture. A T25 with 10 mL 2% haematocrit (Hct) culture containing >1% late trophozoite and schizont stages just before synchronization is adequate for 1-4 GIA assay plates. Parasite cultures were synchronized using 65% Percoll solution. This is a density separation to enrich late stage parasites, which are lighter than younger parasites and uninfected RBCs and therefore float on the Percoll. Approximately 24 h after Percoll synchronisation the culture will contain mostly ring stages and young trophs. Sorbitol treatment (5% solution) is then used to kill late stage

parasites, with young parasites unaffected. No later than 20 h after sorbitol treatment the GIA assay should be performed.

Assay plates include 3 replicates at each IgG dilution tested, of each of the following: test IgG, uninfected RBCs, with any IgG; infected RBCs with negative control IgG (from a rabbit immunised with non-malaria antigens);infected RBCs with positive control IgG (from a rabbit immunised with an AMA1 vaccine known to give GIA against the parasite strain to be used). Synchronised parasites and test IgG and culture medium were added to wells of a 96 well plate and incubated for around 40 h. Relative parasitaemia in test wells is quantified by measurement of parasite lactate dehydrogenase. Percent inhibition is calculated using absorbance at 630 nm (A630) using the following formula:

$$\%\ Inhibition = 100\% - [\ \frac{(A650\ Immune\ sample - A650\ RBC\ only)}{(A650\ Pre\text{–}Immune\ control - A650\ RBC\ only)}\ x100\ ]$$

2.8. Statistics

Data were analysed using GraphPad Prism version 5.03 for Windows (GraphPad Software Inc., California, USA). Wilcoxon matched-pairs signed rank tests were carried out to compare volunteer responses (paired responses) between selected time-points. Alternatively Friedman tests were used when comparing multiple time-points from the same group (paired responses). Mann Whitney tests were used to compare between two different volunteer groups at comparable time-points. Kruskal-Wallace test with Dunn's Multiple Comparison test were used to compare between multiple volunteer groups at comparable time-points. Spearman's rank was used to analyse correlations. Statistical significance was considered at $P \leq 0.05$ (*$P<0.05$, **$P<0.01$, ***$P<0.001$).

3. B cell induction following ChAd63-MVA MSP1 and AMA1 immunisation and controlled human malaria infection

3.1. Introduction

The aim of the opening chapter of this thesis is to establish how B cell responses are induced across a number of Phase I and IIa clinical vaccine trials involving the blood-stage candidate antigens MSP1 and AMA1. Whilst T cell and serum antibody immunogenicity has been previously reported in a series of three trials using the ChAd63-MVA vectors encoding MSP1 or AMA1 [51, 216, 217], B cell responses have not been previously described following this vaccine regime with these vaccine candidates. As high titres of antigen-specific IgG were induced following vaccination in these trials I will focus on the induction of IgG B cells. Characterisation of this vaccine kinetic will allow direct comparison with other regimes / delivery platforms that have previously reported B cell induction following vaccination with these antigens. In individuals that have been previously vaccinated it is also of particular interest as to whether existing B cell responses, as well as serum antibodies, are positively or negatively impacted by malaria infection. This should be particularly informative about the suitability of a candidate vaccine for use in field studies. In addition the study of clinical trials involving CHMI adds a unique opportunity to study the impact of parasite exposure on both naïve and previously vaccinated individuals, again with a focus on B cell populations. CHMI in infectivity control volunteers also allows a comparative assessment between priming malaria antigen-specific responses with vaccines versus those in individuals undergoing natural primary exposure to parasites

Although high levels of serum IgG antibody are believed to provide the protective effector mechanism against blood-stage malaria parasites, understanding how B cells contribute to these responses is highly important. LLPC in the bone marrow that are responsible for serum antibody levels are difficult to measure in humans, however it is possible to measure other B cells in the peripheral blood, including

ASC and mBC and these have been extensively characterised in humans following vaccination with other vaccine delivery platforms, but not when using recombinant adenoviral and poxviral vectors. Typically mBC responding to antigen following vaccination will follow one of two fates: localised differentiation into SLPC or re-entry into GCs to ultimately form new higher affinity mBC or LLPC. Whilst a classical B cell response kinetic is expected following prime-boost vaccination with viral vectors it is currently unknown how such antigen-specific B cell populations may respond to CHMI, a question which will be initially addressed in this chapter. An outline highlighting bleed schedule, vaccinations and CHMI in all trials covered in this thesis are shown in Figure 3.1. Volunteers were primed by recombinant ChAd63 immunisation on day 0 (d0) and boosted 56 days later with the MVA vector encoding the same antigen. Individuals undergoing controlled human malaria infection (CHMI) who had been previously vaccinated were typically infected at 17 days post vaccine boost, with malaria-naïve infectivity controls infected in parallel.

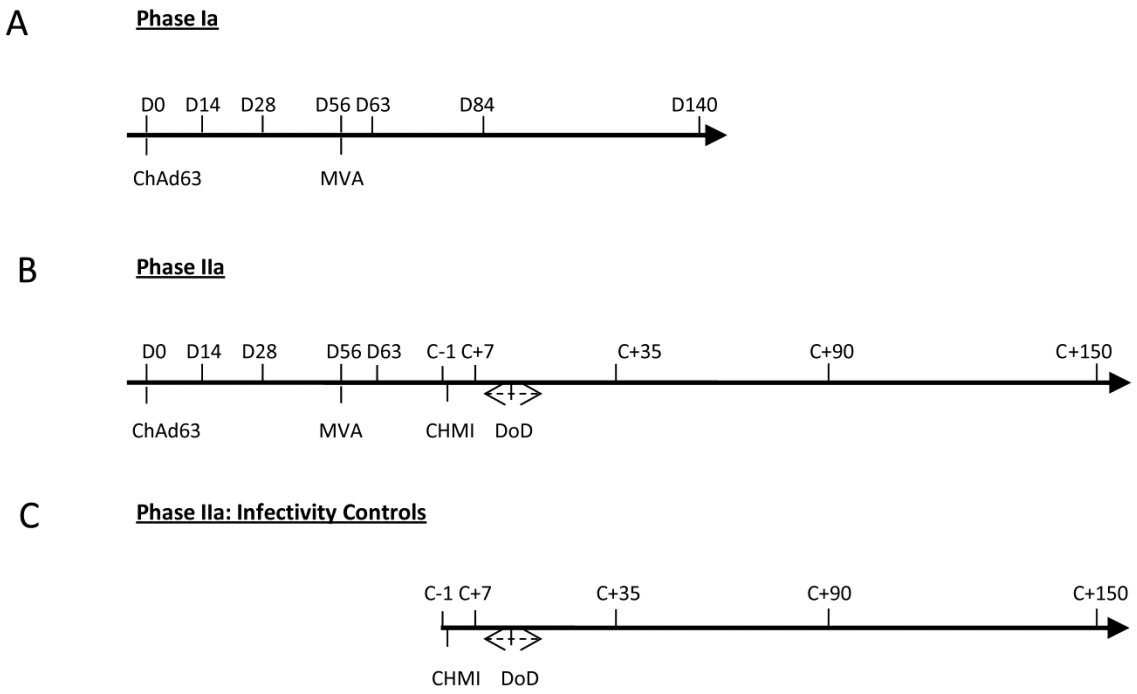


Figure 3.1: Phase I/IIa vaccine trial timelines

mBC responses from key time-points within Phase Ia (1, 2) and Phase IIa (3) clinical trials were analysed in this study. (A) In Phase Ia studies, ChAd63 priming vaccination on day 0 was followed 8 weeks later with MVA booster vaccination. (B) In Phase IIa studies, controlled human malaria infection (CHMI) followed MVA booster vaccination on average 17 days later (range 14-23). (C) Phase IIa infectivity control volunteers underwent CHMI without previous vaccination in parallel with Phase IIa vaccinated volunteers. Time-point dC-1 indicates the day before CHMI. Thereafter, time-points are referred to as the number of days post-infection, e.g. dC+35 means 35 days after CHMI. Non-protected and control volunteers were diagnosed with microscope-patent blood-stage malaria infection on average 10-11 days after challenge at which point they received anti-malarial drug treatment (3). The time window for typical day of diagnosis (DoD) is indicated. Prior to this, blood sampling occurred according to trial protocol during the period of blood-stage infection (from dC+7 until DoD). The next follow-up time-point was dC+35.

3.2. Results

3.2.1. ChAd63-MVA prime-boost vaccination induces antigen-specific mBC responses

Initially mBC ELISPOT assays were performed at each time-point (Fig. 3.1A) for volunteers vaccinated with MSP1 in a Phase I trial [216], in order to identify the kinetics of the response. As discussed in Materials and Methods, all mBC ELISPOT were performed on cryopreserved PBMC with all time-points from a single volunteer run in parallel. After ChAd63 priming (d28/56) the IgG+ mBC response was not significantly different from d0 (Fig. 3.2A). However following the MVA administration at d56, a significant boost was observed in comparison to d0, with an increase in peripheral blood mBC peaking at d84 (28 days post-boost), with a median response of 99 mBC derived ASC per million cultured. This response subsequently contracted but was maintained at a resting median level of 46 at d140. Antigen-specific IgG+ mBC derived ASC as a % of total IgG^+ mBC derived ASC is an alternative presentation of the data commonly shown in mBC studies. In this case the d84 median was 0.54%, significantly higher than d0 (Fig. 3.2D). The number of total IgG^+ mBC derived ASC detected by ELISPOT in MSP1 vaccinated volunteers did not significantly differ across the time points measured (Fig.3.2G).

In volunteers vaccinated with AMA1 [217], ChAd63 priming induced a more detectable response at d28 that was maintained up to day of boosting (d56), though was not significantly different from d0. Following the MVA boost there was a significant increase (in comparison to d0) up to a median of 122 mBC derived ASC per million cultured PBMC at d84 (Fig. 3.2B), before the response contracted to a resting level of 101 at d140 which maintained significance over baseline. When calculating antigen-specific IgG^+ mBC derived ASC as a % of total IgG^+ mBC derived ASC, a similar kinetic was observed in addition to a significant increase from pre-boost levels (d56) to post-boost peak (d84) (Fig. 3.2E). The number of total IgG^+ mBC derived ASC was found to be significantly lower in AMA1 vaccinated volunteers at d84 compared to d0 and d28 (Fig. 3.2H). This may in part be due to one volunteer having

an atypically high response at d0 and d28, however it should be noted that at d84 antigen-specific IgG^+ mBC derived ASC as a % of total IgG+ mBC derived ASC may be inflated as a result.

The resting mBC response was also measured to diphtheria toxoid (DT) as a non-malaria / bystander antigen control. Following ChAd63-MVA vaccination no bystander activation of the DT population was observed, with the median response stable at approximately 25 mBC derived ASC per million cultured PBMC (Fig. 3.2C), or 0.18% of IgG^+ mBC derived ASC (Fig. 3.2F). These data demonstrated the induction of antigen-specific mBC responses by viral vectored vaccination, with no apparent effect on pre-existing bystander responses.

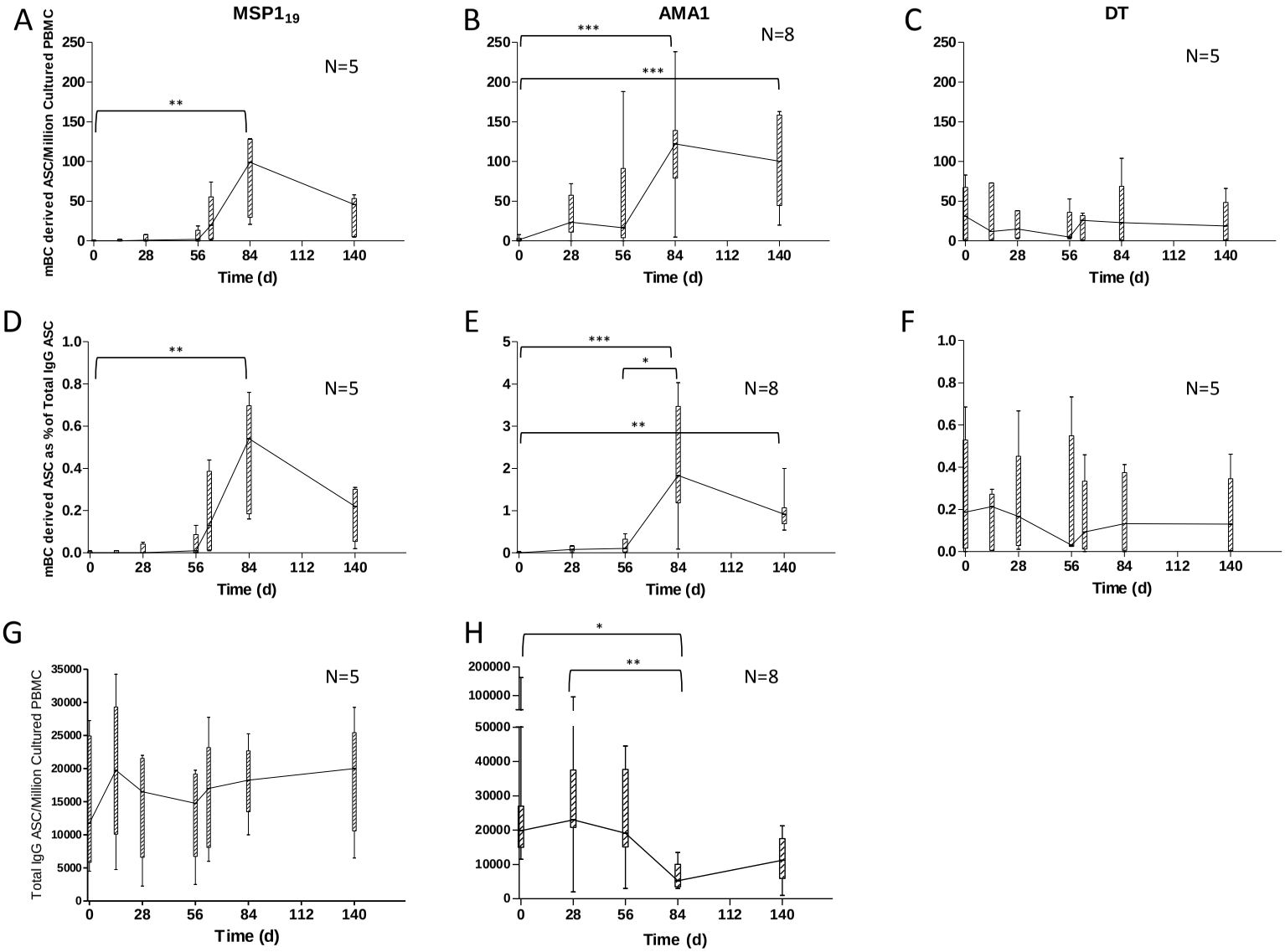

A
MSP1$_{19}$
mBC derived ASC/Million Cultured PBMC
N=5
**
Time (d)
B
AMA1
N=8
***
***
Time (d)
C
DT
N=5
Time (d)
D
mBC derived ASC as % of Total IgG ASC
N=5
**
Time (d)
E
N=8
***
*
**
Time (d)
F
N=5
Time (d)
G
Total IgG ASC/Million Cultured PBMC
N=5
Time (d)
H
N=8
*
**
Time (d)

Figure 3.2: mBC responses over time in volunteers receiving ChAd63-MVA MSP1 or AMA1 prime-boost vaccination.

Box and whisker plots show the median, range and interquartile range of antigen-specific mBC derived ASC responses measured over time using the mBC ELISPOT assay. Responses are defined as mBC derived ASC per million cultured PBMC specific for (A) $MSP1_{19}$, (B) AMA1 and (C) diphtheria toxoid (DT); or as mBC-derived ASC as a % of total IgG^+ ASC for the same antigens (D-F). Total IgG ASC responses used to calculate the latter are also shown (G-H). Assays were performed at the indicated time-points from frozen PBMC; MSP1 vaccinees (n=5), AMA1 vaccinees (n=8); DT responses are shown from MSP1 vaccinated volunteers (n=5). Assays could not be performed at the d14 and d63 time-points for AMA1 vaccinated volunteers due to limited PBMC sample availability. Friedman Test, with Dunn's post-test, **P*<0.05, ***P*<0.01 and *** *P*<0.001.

3.2.2. Controlled P. falciparum infection induces mBC to $MSP1_{19}$ but not AMA1 in unvaccinated infectivity control volunteers

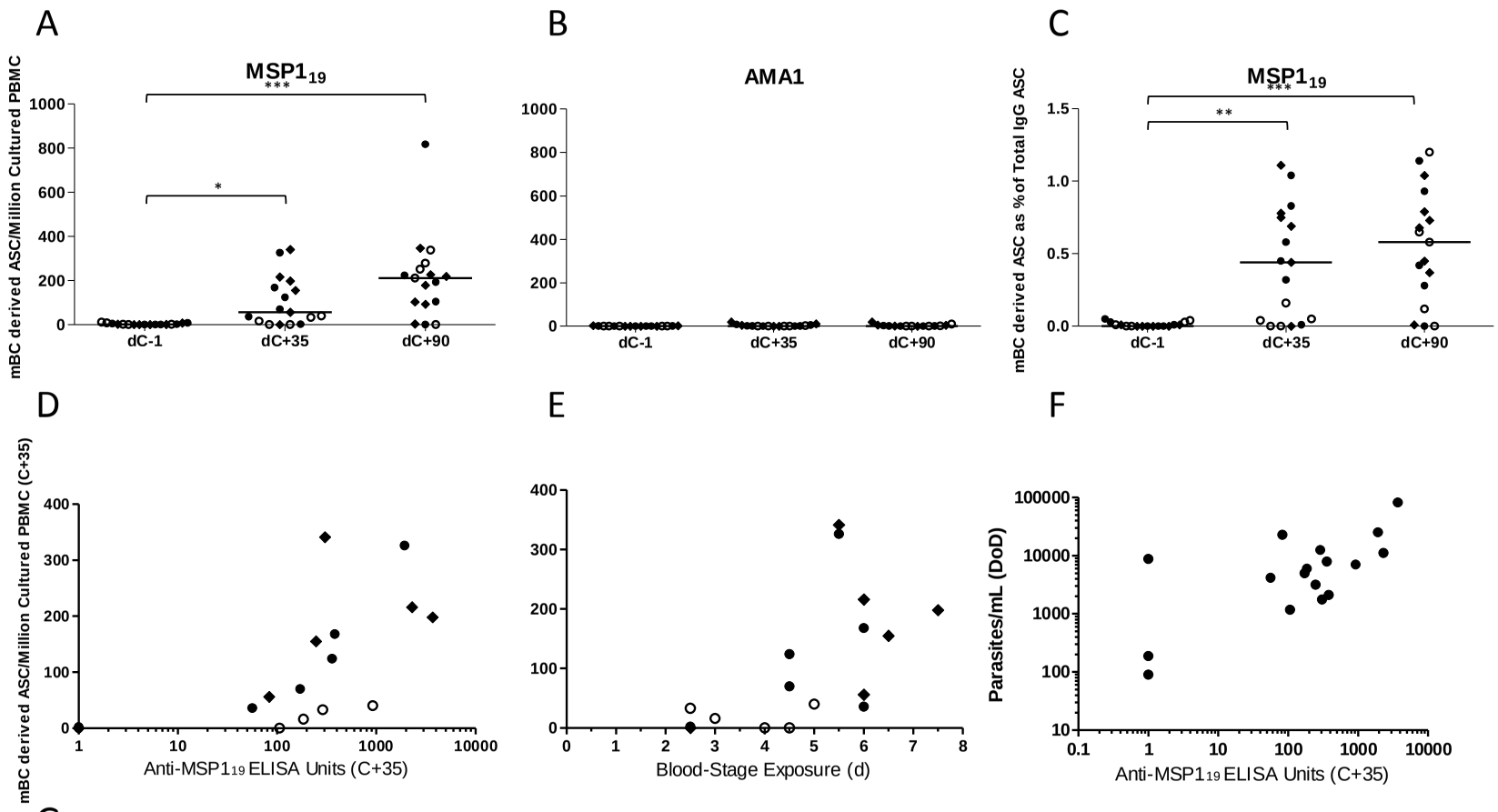
In three Phase IIa challenge trials, volunteers were vaccinated and then exposed to a controlled *P. falciparum* infection to test vaccine efficacy [51, 185] (Fig. 3.1B). Infectivity control groups (n=6 malaria-naïve individuals per study, n=17 assayed here in total, one volunteer excluded due to lack of cells) included volunteers who were exposed to controlled *P. falciparum* infection without prior vaccination (Fig. 3.1C). According to the trial protocols, volunteers were exposed to five infectious mosquito bites and then followed up to a maximum of 21 days with daily blood-films and quantitative PCR (qPCR) to measure blood parasitaemia. *P. falciparum* parasites emerge from the liver at around dC+6.5-7 and commence the blood-stage of infection which is responsible for subsequent clinical symptoms [249]. All control volunteers were diagnosed and treated with anti-malarial drugs as per protocol, with a median time to microscope-patent diagnosis of 11 days post CHMI (range 9-14 days) [51, 185]. Antigen-specific mBC ELISPOT assays for both $MSP1_{19}$ and AMA1 were subsequently performed on frozen PBMC at the dC-1 time-point (one day prior to CHMI), dC+35 and dC+90 following CHMI. 14/17 volunteers showed a

positive IgG^+ mBC response to $MSP1_{19}$ at dC+90 (Fig. 3.3A), whilst no volunteers showed a positive mBC response to AMA1 (Fig. 3.3B). Responses against $MSP1_{19}$ at dC+35 and dC+90 were significantly higher than the dC-1 baseline for both mBC derived ASC per million cultured PBMC (Fig. 3.3A) and as a % IgG+ mBC derived ASC (Fig. 3.3C). Interestingly, the $MSP1_{19}$-specific responses induced by primary parasite exposure were comparable in magnitude (if not stronger) than those induced by ChAd63-MVA MSP1 vaccination (Fig. 3.2A,D). When serum total IgG responses to these two antigens were measured, the three volunteers with no detectable mBC responses to $MSP1_{19}$ also showed no detectable antibody to $MSP1_{19}$, whilst only a minority of volunteers showed serum antibodies to AMA1 which were marginal and just above the limit of detection [113]. For the volunteers who did mount *de novo* anti-$MSP1_{19}$ Ab responses, there was a strong correlation between $MSP1_{19}$ serum total IgG as measured by ELISA and the mBC response at dC+35 (Fig. 3.3D, r_s=0.79, *P*=0.0002) which was maintained at dC+90 (*P*=0.0047, r_s=0.799; Table, Fig. 3.3G)). There was also a significant correlation between the dC+35 MSP1 mBC response (Fig. 3.3E) as well as dC+35 MSP1 serum IgG (Table, Fig. 3.3G), with the number of days volunteers were exposed to blood-stage parasitaemia. This was calculated as number of days from dC+6.5 (earliest expected time when parasites leave the liver) to the time-point of blood-film diagnosis (DoD). MSP1 serum IgG at dC+35 also correlated with peak parasitemia, defined as parasites/mL blood at day of diagnosis (DoD) as measure by qPCR (Fig3.3F).Neither of these 3 prior relationships were maintained at dC+90 (Table, Fig. 3.3G).

It should be noted that the average DoD differed across the three infectivity control groups despite individuals receiving the same number of infectious bites. Exact sporozoite inoculation rates can only be estimated and it is possible that in the group identified by open circles and diagnosed on average earlier was due to higher rates of initial infection, leading to higher liver to blood parasite inoculum and a reduced time to diagnosis by blood smear. These data suggest that in the context of natural blood-stage

infection, Ab and mBC responses against $MSP1_{19}$ dominate over those against AMA1, and at least during an acute primary infection, the magnitude of the response corresponds to the duration of infection.

To confirm whether this observation applies to other CHMI models, previously naïve unvaccinated volunteers were also studied in a trial using cryopreserved, injected sporozoites rather than mosquito vectored sporozoites [307]. The 6 volunteers studied received 25,000 sporozoites, split between two injections, delivered intramuscularly. All volunteers were diagnosed with clinical malaria in this group and parasite growth rates, seroconversion and IFN-γ T cell responses to blood stage antigens were comparable to control volunteers receiving mosquito vectored CHMI [307]. In this trial, similar observations were also made for mBC responses, with $MSP1_{19}$-specific mBC derived ASC detected in all but one volunteer by dC+90 (Fig. 3.4A, C). Responses were slightly lower compared to mosquito vectored CHMI and a significant difference was only observed between dC-1 and dC+90. Also standardised sporozoite dose did not appear to reduce variation between individuals, although the responses measured here are against the blood-stage infection, as opposed to those against the sporozoite or liver-stage. Again, in agreement with the previous data, AMA1 responses were mostly negative, although two individuals were observed to have a detectable, but low response (Fig. 3.4 B,D).



G

Correlation					Figure	P value	Significance	rs	N
MSP1 specific mBC derived ASC/million PBMC	dC+35	vs	Anti-MSP1$_{19}$ ELISA Units	dC+35	D	0.0002	***	0.788	17
MSP1 specific mBC derived ASC/million PBMC	dC+35	vs	Blood Stage Exposure (d)		E	0.0019	**	0.697	17
MSP1 specific mBC derived ASC/million PBMC	dC+35	vs	Peak Parasitemia (parasites/mL)			0.148	N/S	0.366	17
Anti-MSP1$_{19}$ ELISA Units	dC+35	vs	Blood Stage Exposure (d)			0.031	*	0.51	17
Anti-MSP1$_{19}$ ELISA Units	dC+35	vs	Peak Parasitemia (parasites/mL)		F	0.0302	*	0.526	17
MSP1 specific mBC derived ASC/million PBMC	dC+90	vs	Anti-MSP1$_{19}$ ELISA Units	dC+90		0.0047	**	0.799	11
MSP1 specific mBC derived ASC/million PBMC	dC+90	vs	Blood Stage Exposure (d)			0.817	N/S	0.061	17
MSP1 specific mBC derived ASC/million PBMC	dC+90	vs	Peak Parasitemia (parasites/mL)			0.459	N/S	0.193	17
Anti-MSP1$_{19}$ ELISA Units	dC+90	vs	Blood Stage Exposure (d)			0.903	N/S	0.044	11
Anti-MSP1$_{19}$ ELISA Units	dC+90	vs	Peak Parasitemia (parasites/mL)			0.839	N/S	0.073	11

Figure 3.3: mBC responses in control unvaccinated volunteers receiving mosquito vectored CHMI.

Antigen-specific mBC derived ASC per million cultured PBMC were quantified for the (A) $MSP1_{19}$ and (B) AMA1 antigens in malaria-naïve unvaccinated control volunteers prior to (dC-1) and following a single CHMI (dC+35 and dC+90). mBC derived ASC as a % of total IgG+ ASC for $MSP1_{19}$ are also shown (C). Data are presented as dot plots showing individual and median responses. Time-points were compared using Friedman Test, with Dunn's post-test, **P*<0.05, ***P*<0.01, and ****P*<0.001. (D) Correlation at dC+35 between $MSP1_{19}$-specific mBC derived ASC per million cultured PBMC and anti-$MSP1_{19}$ ELISA units; (E) $MSP1_{19}$-specific mBC derived ASC per million cultured PBMC at dC+35 and duration of blood-stage parasite exposure; and (F) anti-$MSP1_{19}$ ELISA units at dC+35 and parasites/mL blood at day of diagnosis (DoD), measured by qPCR. (G) Table of correlations for relationships between measure variables at C+35 and C+90. Spearman rank correlation coefficient and *P* values are shown (n=17, or N=11 where ELISA data missing for C+90). Blood-stage exposure was calculated as the number of days from dC+6.5, the predicted time-point of first blood-stage parasitaemia, to time-point of diagnosis. Data are presented and pooled from three separate CHMI trials: closed diamonds, n=6, closed circles, n=6 and open circles, n=5.

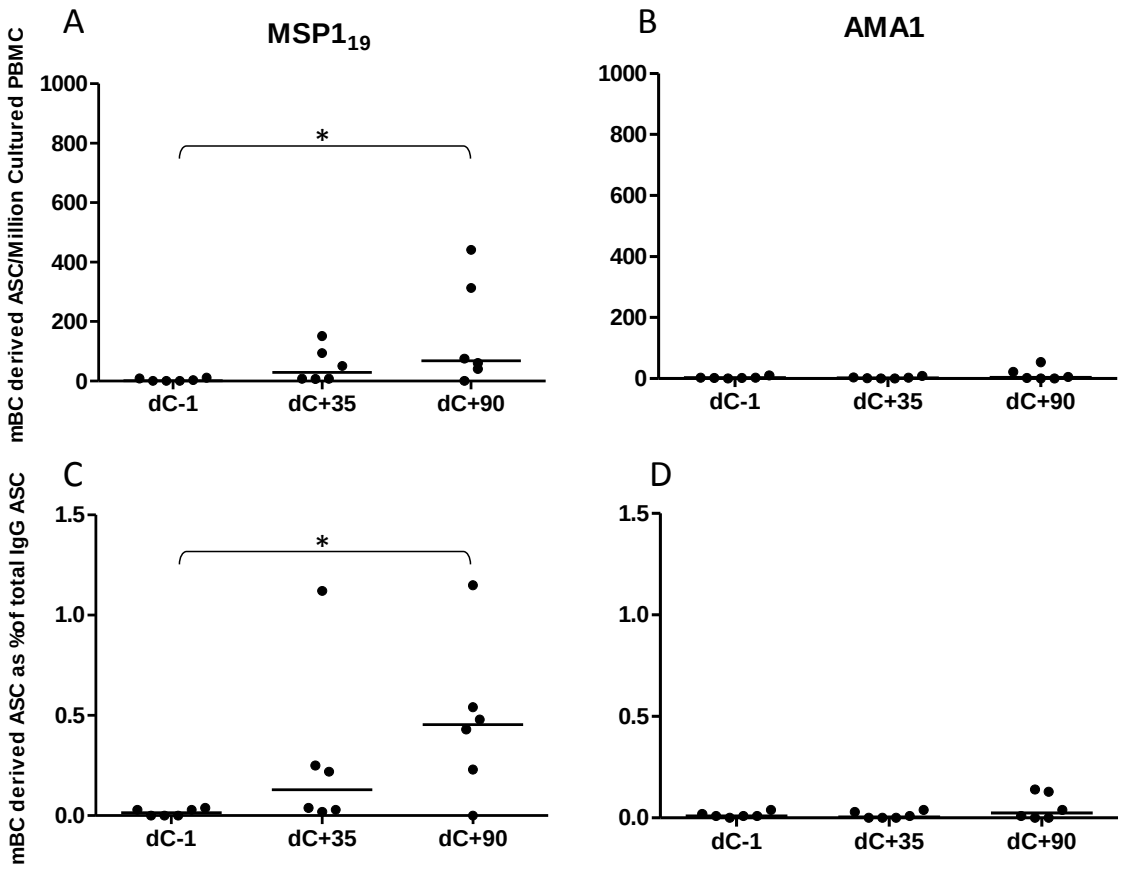


Figure 3.4: mBC responses in control unvaccinated volunteers receiving cryopreserved parasite CHMI.

Antigen-specific mBC derived ASC per million cultured PBMC were quantified for the (A) MSP1$_{19}$ and (B) AMA1 antigens in malaria-naïve unvaccinated control volunteers prior to (dC-1) and following a single CHMI (dC+35 and dC+90). mBC derived ASC as a % of total IgG+ ASC for MSP1$_{19}$ and AMA1 are also shown (C, D). Data are presented as dot plots showing individual and median responses. Time-points were compared using Friedman Test, with Dunn's post-test, **P*<0.05.

3.2.3. Controlled P. falciparum infection boosts the vaccine-induced mBC response

In two of the Phase IIa studies, volunteers were vaccinated with the MSP1 or AMA1 viral vectored vaccines and then underwent CHMI (Fig. 3.1B). Whilst no protection was observed, a subset of volunteers displayed a delay in time to diagnosis [51]. Given the conflicting evidence from immuno-epidemiological studies and rodent malaria models about the possible effect(s) of parasite exposure on B cells [130], I sought to assess the effect of CHMI on blood-stage vaccine-induced and bystander mBC populations. Volunteers vaccinated with ChAd63-MVA MSP1 showed a median response prior to CHMI (dC-1 / d72) of 142 mBC derived ASC per million cultured PBMC (Fig. 3.5A). With the exception of one high responding individual, responses were very similar to previous median results seen at d84 in the Phase Ia trial (Fig. 3.5A dashed line). Following CHMI, responses remained level during the liver-stage of infection up to dC+7 / d80, however at DoD (plotted at d84) a significant decrease (*P*=0.0059) in peripheral mBC was observed (down to a median level of 22). Following drug treatment and resolution of infection, the peripheral mBC compartment recovered and showed a boosting of the response (median of 353 measured at dC+35 / d108). This boosting did not reach significance for the measure of mBC derived ASC per million PMBC (due to the one high responder at dC-1), but was significant when comparing antigen-specific cells as a % of total IgG+ (0.61% vs 1.54%, *P*=0.016) (Fig. 3.5D). In this trial volunteers were followed up to 150 days post-CHMI (d223), thus providing an opportunity to assess the maintenance of the mBC population. In this group of vaccinated and infected volunteers, the resting level of mBC was 200 at dC+90 / d163 and this was maintained at 223 at dC+150 / d223, indicating overall that parasite exposure had boosted the $MSP1_{19}$-specific mBC compartment and that this response was maintained for the duration of the study. When compared to vaccinated only volunteers (without CHMI), there was a significant difference (*P*=0.011) in resting level responses between d140 in the Phase Ia trial and dC+90 / d163 (the closest equivalent time-point post-CHMI in the Phase IIa trial).

The same result was observed for the antigen-specific mBC response as a % of total IgG+ mBC (*P*=0.013) (Fig. 3.5D).

In a second group, volunteers were vaccinated with ChAd63-MVA AMA1 prior to CHMI. In this case, the kinetic of the mBC response differed in comparison to volunteers vaccinated with MSP1 (Fig. 3.5B). The median response prior to CHMI at dC-1 was 153, comparable to both MSP1 vaccinated volunteers and the previous AMA1 vaccinated volunteers in the Phase Ia trial (Fig. 3.5B dashed line). However, unlike for MSP1 vaccinated volunteers, there was no significant reduction of AMA1-specific peripheral blood mBC at the time of diagnosis, with the median response not significantly reduced at 106. Following drug treatment and resolution of infection the mBC compartment also expanded significantly in AMA1 vaccinated volunteers (*P*=0.02) to a peak of 342 at dC+35 in comparison to dC-1, a magnitude that was highly comparable to that observed in MSP1 vaccinees. This was also significant for mBC measured as a % of total IgG+ mBC (*P*=0.0078) (Fig. 3.5E). Subsequently, the median resting level of AMA1-specific mBC was 158 at dC+90 and 145 at dC+150. However, unlike for MSP1, this level was not significantly different from the resting level following vaccination only in the Phase Ia trial when comparing d140 and dC+90 / d163. The same observation was made with respect to antigen-specific mBC as a % of total IgG+ mBC (Fig. 3.5E). Bystander mBC responses were also measured over time against a non-malaria antigen (DT) in 17/20 vaccinees. Although there was a trend for lower peripheral DT-specific mBC derived ASC at the time of malaria diagnosis (Fig. 3.5C) this was not significantly different from the responses at all other time-points. The same result was observed for DT-specific mBC derived ASC as a % of total IgG+ (Fig. 3.5F). Otherwise responses were stable over time, at median levels comparable to those previously seen (Fig. 3.2C,F). CHMI thus appears to have minimal, if any, impact on bystander mBC populations but could boost existing malaria-specific vaccine-induced mBC responses.

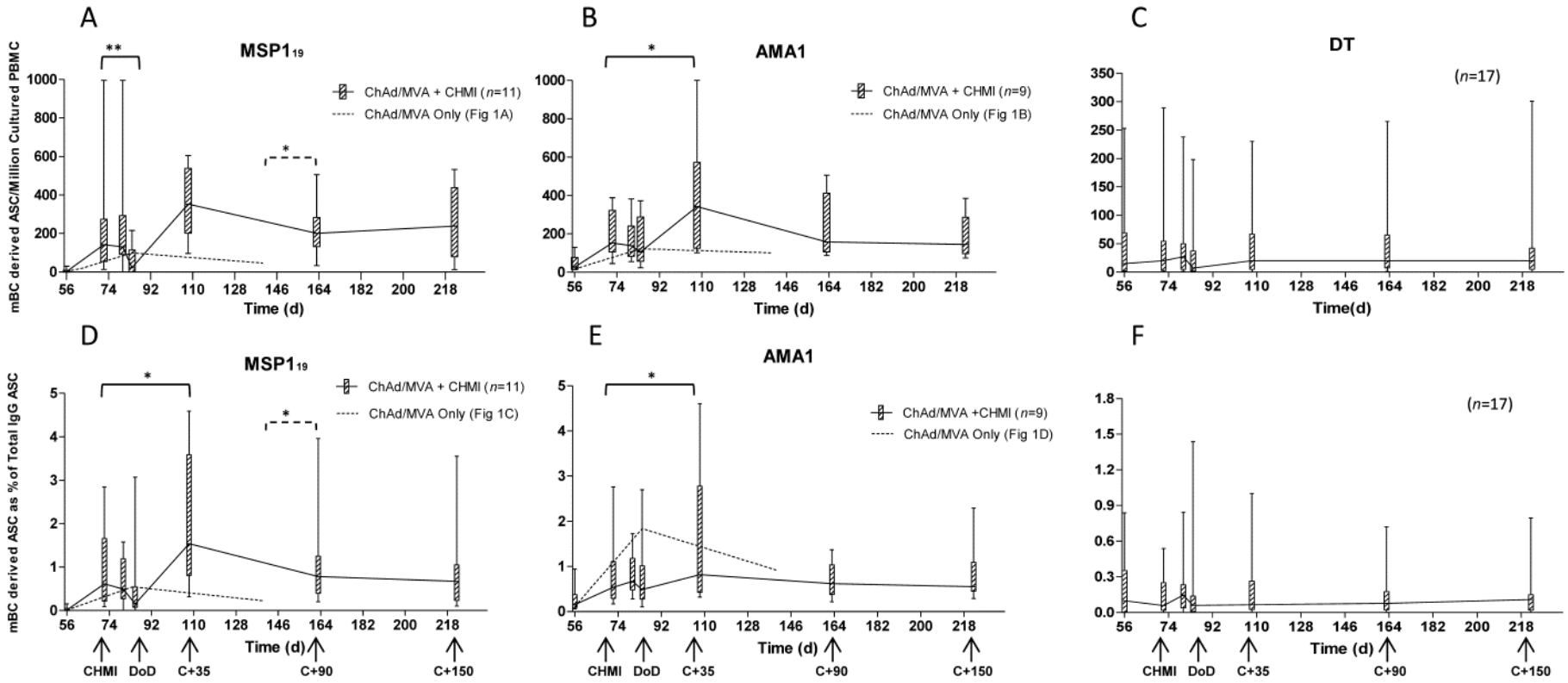

A
MSP1 19
mBC derived ASC/Million Cultured PBMC
ChAd/MVA + CHMI (n=11)
ChAd/MVA Only (Fig 1A)
Time (d)
B
AMA1
ChAd/MVA + CHMI (n=9)
ChAd/MVA Only (Fig 1B)
Time (d)
C
DT
(n=17)
Time(d)
D
MSP1 19
mBC derived ASC as % of Total IgG ASC
ChAd/MVA + CHMI (n=11)
ChAd/MVA Only (Fig 1C)
Time (d)
CHMI
DoD
C+35
C+90
C+150
E
AMA1
ChAd/MVA +CHMI (n=9)
ChAd/MVA Only (Fig 1D)
Time (d)
F
(n=17)
Time (d)

Figure 3.5: mBC responses in vaccinated volunteers receiving CHMI.

Box and whisker plots show the median, range and interquartile range of antigen-specific mBC derived ASC responses measured over time using the mBC ELISPOT assay. Responses are defined as mBC derived ASC per million cultured PBMC specific for (A) $MSP1_{19}$, (B) AMA1 and (C) DT; or as mBC derived ASC as a % of total IgG+ ASC for the same antigens (D-F). Assays were performed at the indicated time-points from frozen PBMC; MSP1 vaccinees (n=11) and AMA1 vaccinees (n=9) are shown by solid lines; DT responses are shown from vaccinated volunteers in both the MSP1 and AMA1 groups (n=17). DoD is plotted at d84 as the average diagnosis time-point. Responses from vaccinated volunteers who did not receive CHMI are shown in (A, B, D, E) from the previous Phase Ia trials (median response from Fig. 3.2A, B, D, E dashed line). Differences between time-points in the Phase IIa trial were analysed by Wilcoxon matched-pairs signed rank test (solid lines). Differences between resting levels in the Phase IIa and Phase Ia trials were analysed by Mann-Whitney test (dashed lines), **P*<0.05 and ***P*<0.01. Differences between all time-points for DT performed using Friedman test with Dunn's post-test.

3.2.4. MSP1 and AMA1 vaccine co-administration induces mBC responses to both antigens

A third group of volunteers in the Phase IIa trial received both the MSP1 and AMA1 viral vectored vaccines which were co-administered in opposite arms (but at equal doses to the first two groups of volunteers, meaning that overall the vector dose was double). It was previously reported that these volunteers showed a significant reduction in both *ex-vivo* T cell responses and ELISA antibody titres to both antigens following the MVA boost vaccination, in comparison to the single vaccine administration groups, but that responses to MSP1 appeared immuno-dominant to those against AMA1 [51]. Given that the infectivity control volunteers showed *de novo* induction of $MSP1_{19}$-specific, but not AMA1-specific mBC responses following the context of natural parasite exposure, it was of interest to also assess the effect of vaccine antigen co-administration on the induced mBC responses. The numbers of mBC derived ASC were quantified by ELISPOT assay for these volunteers at dC-1 / d72 (peak post-boost),

dC+35 / d108 (peak post-CHMI) and dC+150 / d223 (resting level) for both $MSP1_{19}$ (Fig. 3.6A) and AMA1 (Fig. 3.6B). Responses were significantly boosted by CHMI at dC+35 compared to dC-1 for MSP1 (*P*=0.039) but not for AMA1. Similar to the results for T cell and serum IgG responses [51], individual antigen-specific mBC responses in this group tended to be lower at dC+35 (MSP1: 121, AMA1: 136) compared to responses in the equivalent individual vaccine groups (MSP1: 353, AMA1: 342), but despite disparity in medians, this did not reach significance (*P*=0.224 and 0.077 respectively). No significant differences were observed at the dC-1 or dC+150 time-points, although here the medians were more comparable. When antigen-specific responses were summed in the co-administration vaccine group, the total vaccine-induced response was more comparable to the responses induced in the single vaccination groups at all time-points. (Fig. 3.6C), suggesting mBC responses were susceptible to immune interference following vaccine co-administration. However, unlike following natural parasite exposure in malaria-naïve individuals, mBC responses could be induced by vaccination against both antigens (Fig. 3.6D), although natural exposure only appeared to increase the $MSP1_{19}$-specific population in the long term, as observed with single antigen vaccination (Fig. 3.6A). mBC responses were also measured against the non-malaria antigen (DT) in the vaccine co-administration group, with results again confirming no impact of CHMI (data not shown).

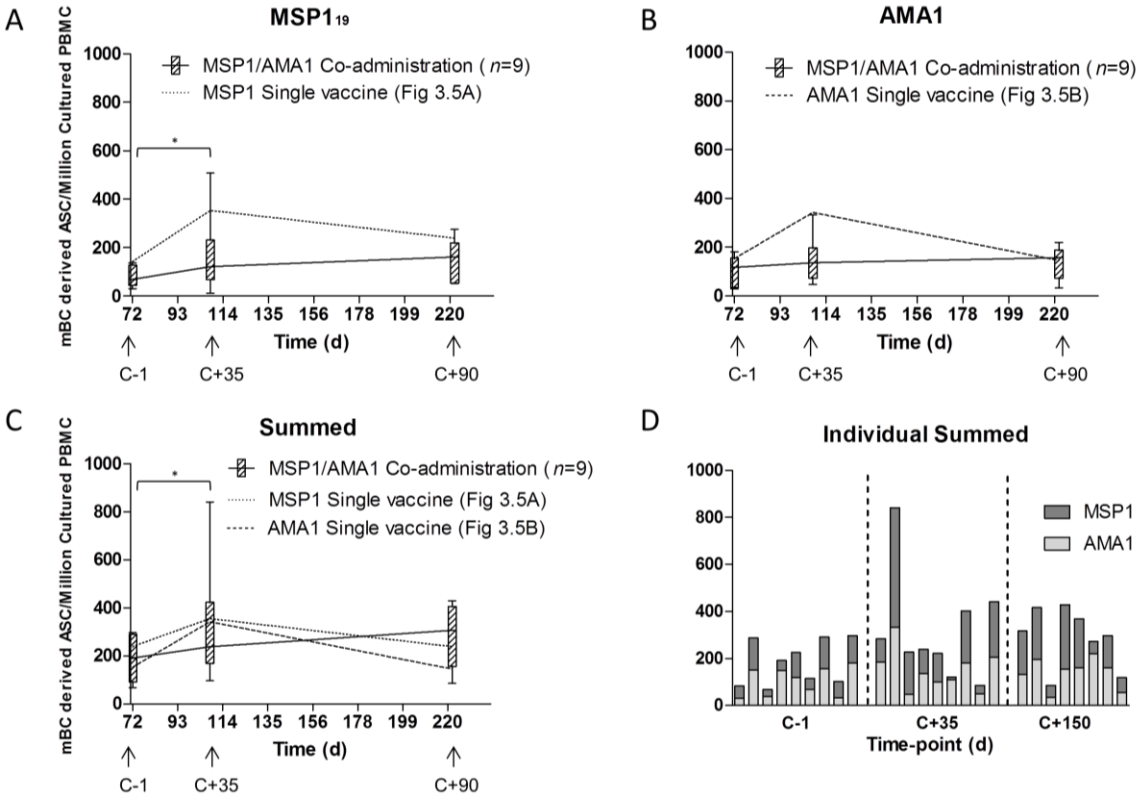


Figure 3.6: mBC responses in volunteers receiving both vaccines and CHMI.

Box and whisker plots show the median, range and interquartile range of antigen-specific mBC derived ASC responses measured over time using the mBC ELISPOT assay, in volunteers co-administered with the MSP1 and AMA1 vaccines (n=9), at the key time-points dC-1 (d72), dC+35 (d108) and dC+90 (d223). Responses are defined as mBC derived ASC per million cultured PBMC specific for (A) $MSP1_{19}$, (B) AMA1, and (C) MSP1+AMA1 summed. The dotted lines in (A) and (C) represents the median response from MSP1-only vaccinated volunteers following CHMI (Fig. 3.5A). The dashed line in (B) and (C) represents the median response from AMA1-only vaccinated volunteers following CHMI (Fig. 3.5B). Responses were compared to volunteers receiving single antigen vaccination and CHMI by Mann-Whitney test. (D) Individual breakdown of summed responses for each volunteer in the vaccine co-administration group at the three time-points. Differences between time-points in the Phase IIa trial were analysed by Wilcoxon matched-pairs signed rank test, *P<0.05 and **P<0.01.

3.2.5. $MSP1_{19}$-specific mBC responses correlate with antibodies post-MVA vaccination but not following CHMI

Having observed that serum IgG responses correlated with mBC responses in unvaccinated infectivity controls post-CHMI (Fig. 3.3D) it was of interest to investigate this relationship in vaccinees. Given that SLPCs as well as LLPCs in the bone marrow are likely to contribute to serum antibody levels, it was of interest to determine whether the mBC ELISPOT was measuring an independent attribute of the adaptive immune response in comparison to ELISA. Data were pooled following vaccination for all vaccinees in the Phase I/IIa trials. A significant positive correlation between IgG^+ mBC derived ASC and serum IgG antibodies was observed in volunteers for both $MSP1_{19}$ (r_s=0.50, *P*=0.011, n=25) (Fig. 3.7A) and AMA1 (r_s=0.49, *P*=0.010, n=26) (Fig. 3.7D). However, following CHMI in the Phase IIa trial, analysis of the dC+35 responses showed that this observed relationship for $MSP1_{19}$ (n=20) (Fig. 3.7B) was not as strongly maintained, with similar results at dC+90 (Fig. 3.7C). For AMA1 (n=18) the relationship was marginally maintained at dC+35 (Fig. 3.7E) but lost significance by dC+90 (Fig. 3.7F). Overall these data suggest that malaria exposure affects serum IgG levels and/or the circulating mBC populations leading to a more complex relationship between the two than that observed following vaccination only.

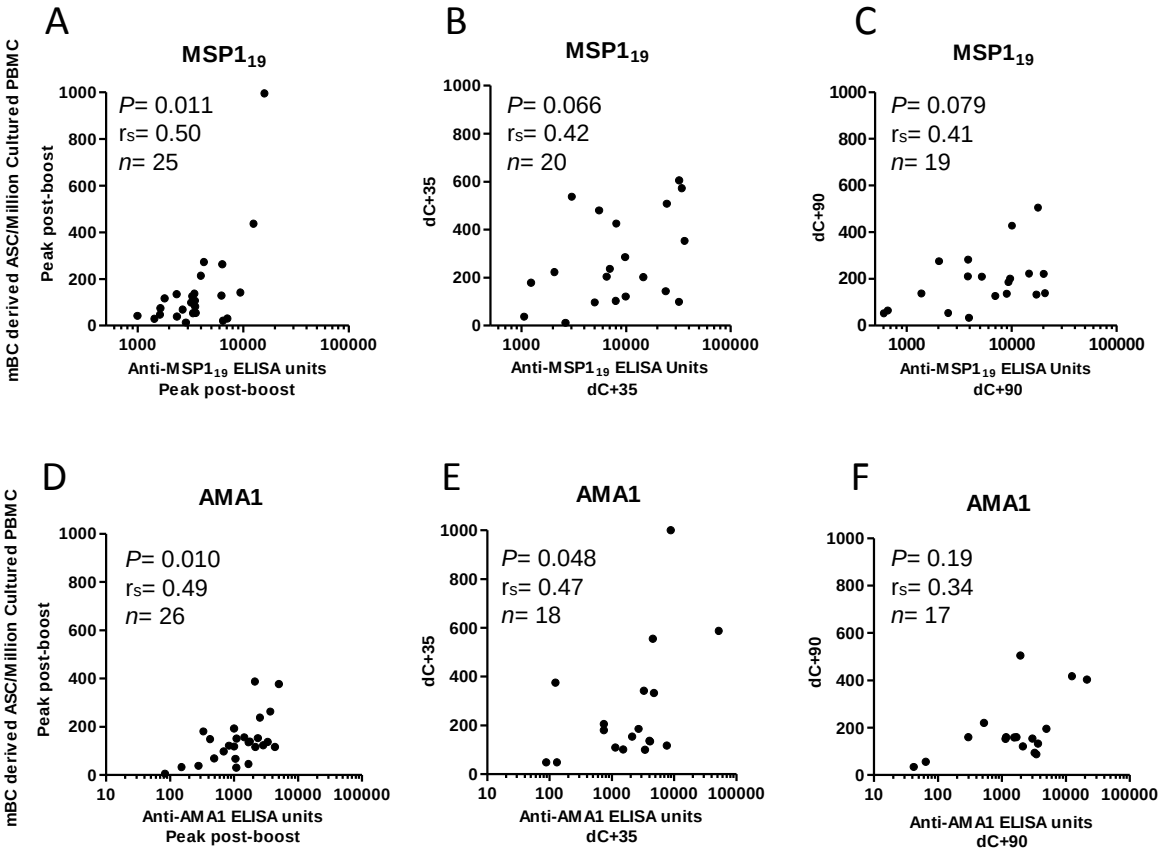


Figure 3.7: Relationship between peripheral mBC responses and serum IgG in vaccinees before and after CHMI.

Correlations between MSP1$_{19}$-specific mBC derived ASC per million cultured PBMC and levels of MSP1 specific serum IgG (reported as anti-MSP1$_{19}$ ELISA units) at set clinical time points. Results are shown (A) post ChAd63-MVA vaccination (dC-1 for volunteers later undergoing CHMI or d84 for vaccine only volunteers); (B) dC+35 post-CHMI; and (C) dC+90 post-CHMI. (D-F) show the same results for AMA1. Spearman rank correlation coefficient, *P* and n values are shown for all analyses.

3.2.6. Migratory ASC can be detected 7 days following MVA booster vaccination but were not observed at selected time-points during and post-CHMI

Parasite exposure has been shown above to perturb the relationship between serum IgG and peripheral mBC, as well as boost vaccine-induced $MSP1_{19}$-specific mBC responses and lead to their induction in control volunteers. ASC responses can be typically observed in peripheral blood seven days following a booster vaccination [86, 122, 308]. I thus sought to confirm this following MSP1 vaccination and assess whether these cell types could be observed in the peripheral blood during CHMI. *Ex-vivo* ASC ELISPOT assays were initially performed on all MSP1 immunised volunteers in the Phase IIa clinical trial, aiming to assay at the d7 time-point post-booster vaccination to confirm the induction of these cells. The ELISPOT data for each volunteer are plotted according to the exact number of days assayed following booster vaccination (given this varied for reasons such as safety monitoring, and logistical limitations relating to clinic attendance and co-coordinating vaccinations with subsequent CHMI). In agreement with studies using different types of vaccines [86, 122, 308] , $MSP1_{19}$-specific ASC responses appeared to peak in the periphery around day 7-8 following a booster vaccination with MVA MSP1 (given either alone or co-administered [51]) (Fig. 3.8), with the median response approximately 100 ASC/million PBMC. Lower responses were observed up to two days either side.

I subsequently performed the same assessment in nine volunteers vaccinated with MSP1 alone at all available time-points post-CHMI (Fig. 3.8). Responses were next measured at one day prior to CHMI (dC-1), on average 15 days after MVA vaccination. At this time-point most volunteers showed no detectable $MSP1_{19}$-specific ASC, although three volunteers still had residual responses around 40 ASC/million PBMC. Following CHMI, *ex-vivo* ASC ELISPOT assays were performed at days C+7, +11 and +35, but responses at all time-points were considered negative for detectable ASC after subtracting background. Day of diagnosis (DoD) was not included due to lack of cells, however it should be noted C+11 coincided with DoD for some volunteers. In CHMI control volunteers receiving no prior vaccines, ASC responses

were also negative at these time-points (data not shown). Thus despite the noted boosting of $MSP1_{19}$-specific mBC responses, I was unable to detect a migratory ASC population during infection at the limited number of time-points for which PBMC were available. As with mBC ELISPOT, DT controls were run alongside the vaccine antigen. No DT-specific ASC were detected at any time-point in the study suggesting no bystander responses or LLPC displacement from the bone marrow (data not shown).

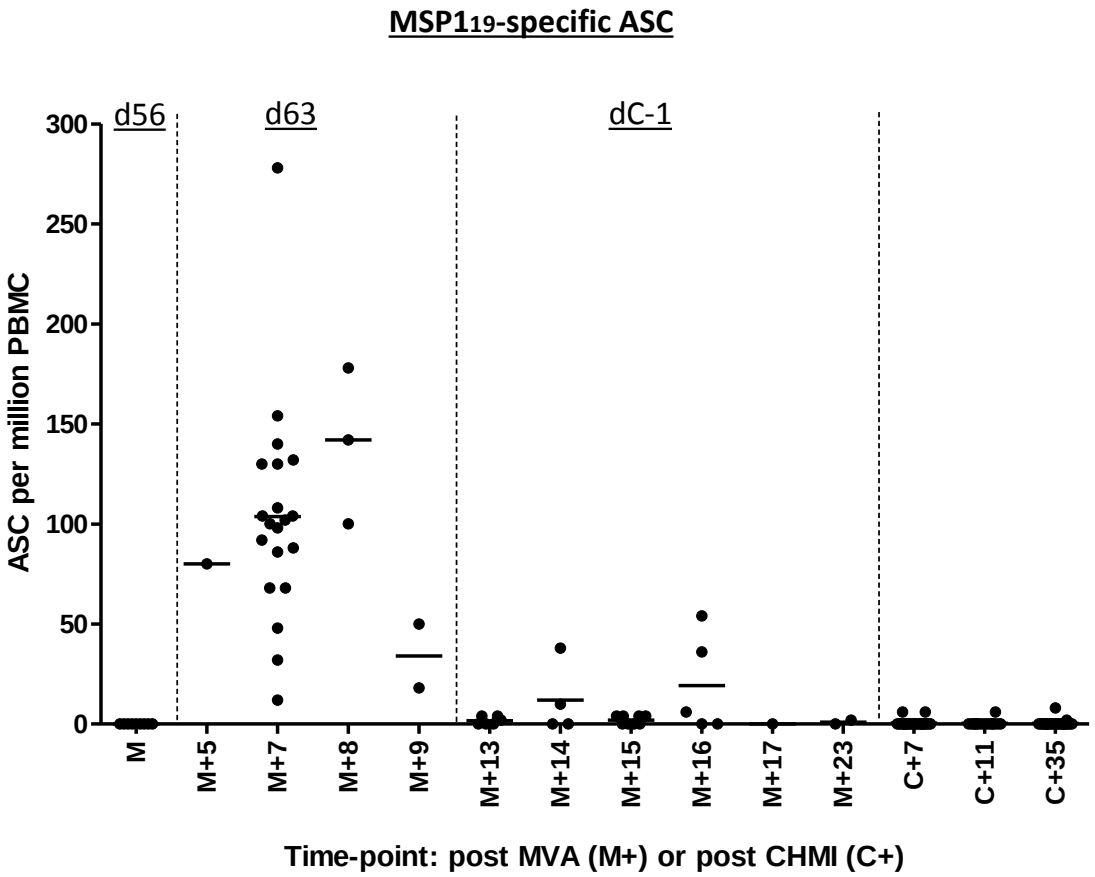


Figure 3.8: Measurement of $MSP1_{19}$-specific peripheral blood ASC post MVA vaccination and CHMI.

$MSP1_{19}$-specific ASC responses (per million PMBC) were assessed by *ex-vivo* ELISPOT at the stated time-points after MVA-MSP1 booster vaccination. At d56 volunteers all received MVA-MSP1 booster vaccination, either alone (n=9) or co-administered with another MVA (n=18). The responses are reported as the exact number of days post MVA booster vaccination (M+), taken at two windows post-boost (d63 and dC-1). ASC were also measured post CHMI (C+) at dC+7, dC+11 and dC+35. Data are presented as dot plots showing individual and median responses.

3.3. Discussion

In this chapter I describe for the first time the induction of IgG mBC in healthy adult volunteers immunised with ChAd63-MVA viral vectored vaccines encoding the blood-stage merozoite antigens MSP1 and AMA1. This highly immunogenic subunit vaccine delivery platform has undergone recent clinical development for a range of difficult infectious disease targets [238, 309], and these vaccine candidates were previously reported to induce high levels of antigen-specific T cells as well as substantial serum IgG Ab responses in healthy adult UK volunteers [216, 217]. Here it is shown that antigen-specific mBC responses were primed and boosted against both antigens following ChAd63-MVA MSP1 or AMA1 vaccination. The levels of antigen-specific mBC were higher than those reported in healthy US adults following three immunisations of MSP1 or AMA1 protein vaccine formulated with the aluminium-based adjuvant Alhydrogel, although slightly lower than when the TLR9 agonist CPG7909 was also included in the formulation [219]. In contrast, the same Alhydrogel-CPG7909 adjuvant failed to show improved mBC responses over Alhydrogel alone in a Malian adult cohort [310]. It remains to be seen how viral vectored vaccines would perform for mBC induction in an endemic population, although they appear to generate comparable T cell immunogenicity in endemic adults [148].

Unlike many human pathogens which induce high levels of protective immunological memory after a single infection [311], the acquisition of NAI against *P. falciparum* malaria requires repeated exposure over significant periods of time [23]. Such NAI is largely Ab-mediated against the blood-stage parasite forms, but is non-sterilising – leading to asymptomatic carriage of parasites in older individuals living in endemic areas. Although many potential hypotheses could be proposed as to why such immunity arises, in recent years a number of rodent malaria and immuno-epidemiological studies have argued that the inefficient acquisition of protective Abs is linked to parasite-related dysregulation of B cell function [130]. An alternative approach to address these important questions is provided by access to established CHMI models [250, 312], however, to-date these highly valuable opportunities have not been utilised to

assess the impact of experimental infection on human B cells. A series of Phase IIa studies aimed at assessing the vaccine efficacy of viral vectored MSP1 and AMA1 using the CHMI model have recently been completed [51]. Overall all vaccinated volunteers (bar one co-immunised with MSP1 and AMA1) developed blood-stage infection, and there was no measurable impact of the vaccines on blood-stage parasite multiplication rates [30]. However, these studies provided a unique opportunity to assess the possible effects of CHMI on B cells in both vaccinated individuals as well as non-immunised infectivity control volunteers.

Cohorts of controls were assessed from three separate studies where infection was initiated by the bites of five infected *Anopheles stephensi* mosquitoes harbouring 3D7 clone sporozoites. Following liver-stage infection, merozoites rupture out of infected hepatocytes thus initiating blood-stage infection. The peak of the first wave of parasitaemia is typically detected by sensitive qPCR monitoring on day seven, and on average blood-stage infection is detected by thick-film microscopy on days 10-11 in controls (typically at qPCR levels of ~5,000 parasites/mL blood), at which point drug treatment is initiated to clear the infection [51, 249]. It was observed that 14/17 malaria-naïve control volunteers subjected to mosquito-bite CHMI developed mBC and serum IgG responses to $MSP1_{19}$ after a single controlled infection, in contrast to AMA1 where responses were largely undetectable. Identical results were observed in a separate trial where cryopreserved sporozoites were delivered by needle-and-syringe. The $MSP1_{19}$-specific mBC response appeared comparable, if not stronger, than that observed following ChAd63-MVA MSP1 vaccination alone. These immune responses positively correlated with each other, and also the duration of blood-stage parasite exposure. In contrast, responses to both antigens have been reported in the field [90, 93, 95, 96, 278, 313], but in agreement with the data here, results from low transmission areas have shown $MSP1_{19}$ to generate more robust Ab responses than AMA1, as well as mBC responses after a single reported infection [94]. mBC induction following co-administration of the ChAd63-MVA vaccines encoding MSP1 and AMA1 was also assessed in the work in this chapter. In this case, responses

to both antigens were on average lower in comparison to single vaccine administration; however, these data confirm it is possible to mount responses against both antigens at the same time. These data thus suggest that in the context of primary acute human *P. falciparum* infection, Ab and mBC induction occurs more consistently and effectively for $MSP1_{19}$ than AMA1. Moreover, *in vitro* functional assays measuring the ability of purified IgG to neutralise red blood cell invasion by merozoites have shown anti-AMA1 IgG to be quantitatively more effective than anti-$MSP1_{42}$ [296]. It therefore seems possible the parasite may have evolved to evoke primary immune responses against less susceptible antigenic targets – a possible reflection of exposure time [314] or antigen abundance within the blood-stage merozoite. Alternatively, such responses may be a simple consequence of immuno-dominance hierarchies that inevitably arise when the immune system is exposed to so many antigens in the context of a highly complex pathogen. Route of antigen presentation must also be considered when comparing natural parasite and vaccine antigen presentation. During CHMI antigen is most likely derived from infected erythrocytes and dead parasites in the peripheral blood and so is most likely processed in the spleen. In contrast intramuscular vaccination would lead to antigen processing in draining lymph nodes which contain different resident APC populations. In the spleen APCs are also likely to encounter both antigens at once and so immuno-dominance hierarchies play a significant role. In contrast in the co-vaccination regimen vaccines were given in separate arms and so it is possible antigen could drain to alternative lymph nodes, reducing such competition. Although not tested here, repeated or prolonged exposure may therefore be required before responses develop to AMA1, as noted in the field where the mBC repertoire expands with increased exposure [95].

In the case of immunised volunteers, mBC responses for both $MSP1_{19}$ and AMA1 were clearly boosted following CHMI and drug clearance. However the resting mBC level approximately three months post-drug treatment was significantly higher only for MSP1 vaccinated volunteers, in comparison to vaccination only responses at the most similar time-point. A 'division in labour' of the mBC response can

also be seen in natural infection whereby responses increase in antigen breadth, but not overall magnitude [95], which would agree with the AMA1 data here, although in this study I did not assess *de novo* responses against other antigens in these vaccinees. A field study in Mali, a high transmission area, has shown similar boosting of MSP1- and AMA1-specific mBC responses following an acute episode, with only a marginal increase in long-term mBC resting levels [91] – again very similar to the data shown here following a single CHMI. Data suggests that pre-exisiting, vaccine induced MSP1 and AMA1 mBC respond similarly to CHMI, despite the suggestion previously that MSP1 is significantly more abundant. Studies in mice have also shown P. falciparum $MSP1_{19}$-vaccine-induced mBC are re-stimulated to produce ASC and Abs following challenge with transgenic *P. berghei* parasite expressing P falciparum $MSP1_{19}$ [315]. The key difference may be that parasite exposure from CHMI also induces formation of a population of MSP1-specific mBC that are derived from a primary immune response as seen in naïve individuals that can supplement vaccine induced populations in MSP1 vaccinated volunteers. Importantly, and in contrast to data from the *P. yoelii* mouse model [316], these data confirm that vaccine-induced mBC responses are neither reduced nor ablated following a single exposure to blood-stage malaria parasites. Although mBC responses were only assessed after a single CHMI, these data are encouraging for malaria vaccine development and provide impetus for similar studies in the future to address the impact of natural and repeated malaria exposure on vaccine-induced mBC.

Previous studies using the same antigens have also suggested relationships between antigen specific IgG serum antibody titres and mBC responses post vaccination. In a study using the antigens MSP1 and AMA1 as proteins formulated $^{+/-}$CpG, mBC present at the time-point of boosting predicted antibody 14 days later [219].Observations for a proportional increase in mBC and serum antibody post vaccination has also been reported following influenza vaccination [280]. mBC also correlated with Ab responses at steady state in this trial. In contrast this relationship was less well maintained after CHMI, in agreement with some studies of natural exposure [93, 95], but not others [96]. It is possible that polyclonal

stimulation could drive B cell responses influencing this relationship and it has been suggested that parasite derived products of blood-stage infection such as hemozoin may also act as endogenous adjuvants to drive this process [63]. Two field studies have also noted possible polyclonal activation of DT and tetanus toxoid (TT)-specific bystander mBC responses following episodes of clinical malaria [91, 95]. In contrast, TT-specific mBC responses were reported to be stable following asymptomatic or persistent infection of Kenyan children [90]. No obvious detrimental impact of either vaccination or malaria exposure on bystander mBC responses to DT were observed in this study. Another possibility is that post-CHMI the mBC pool is comprised of populations of different origins compared to that after vaccination. After vaccination mBC and LLPC that contribute to serum antibody responses are likely derived from lymph node GCs whilst after CHMI they may additionally be of splenic GC origin, and each population may contribute differently to the peripheral mBC population or serum antibody production.

A peak of migratory antigen-specific IgG^+ ASC was detected in the peripheral blood 7-8 days following the MVA booster vaccination. These observations are typical of an antigen-specific secondary immune response [53] with similar observations in humans seen with seasonal influenza vaccination [263], pneumococcal conjugate vaccines [317] and TT [279]. These ASC populations observed at days 7-8 in the peripheral blood are referred to as plasmablasts (PB), and likely reflect cells that have arisen from mBC re-stimulation in the lymphoid system and now en route to their niche within the bone marrow where they will remain as plasma cells. However, following CHMI, I was unable to detect $MSP1_{19}$-specific PB responses, although PBMC samples were available from a limited number of time-points, and none between drug treatment and 35 days post-challenge. Expanded total PB populations have been seen after infection in the field [94], and in the *P. chabaudi* mouse model, $MSP1_{19}$-specific ASC were also observed in the blood 10-25 days following a primary infection [318]. In other disease models such as dengue fever, PB populations have been shown to be dramatically expanded 4-7 days after first sign of symptoms, a high proportion of which are antigen specific but non-neutralising and contribute to

pathology [319]. A more detailed kinetic analysis of ASC responses is required in future CHMI studies to assess this in more detail. One particular question, whether some cells can be observed earlier than 7 days post-boost is addressed in chapter 7.

During these studies, I also noted a significant decrease in the number of $MSP1_{19}$-specific mBC in the peripheral blood at the time-point of diagnosis. Decreases in absolute numbers of peripheral lymphocytes have been previously reported following CHMI, although % $CD19^{+}$ cells within the lymphocyte population remained stable [41]. During active infection, inflammation at sites such as the spleen is likely to drive a generalised migration of peripheral blood cells including mBC. MSP1 as an abundant or possibly immuno-dominant antigen is more likely to be presented by APCs at such sites and therefore the chances of interactions between these and MSP1-specific mBC is increased. Subsequent activation and differentiation of this MSP1-specific mBC population results in removal of such cells from the peripheral blood population at this point in time. AMA1-specific cells are less likely to encounter APCs presenting AMA1 and so a greater proportion is more likely to re-enter the peripheral blood. This would account for the small but not significant decrease in this population.

In summary, NAI to blood-stage malaria arises over multiple exposures and there remains a need to better understand whether this is due to dysregulated B cell responses. In this Chapter, I have investigated this for the first time in the CHMI model. Whilst data compare favourably with those from low transmission areas, it remains impossible to study higher levels of parasitaemia, more frequent exposure, or chronic infection in the CHMI model, conditions more comparable to those observed in high transmission areas. Nevertheless, data generated in this Chapter is encouraging for vaccines and suggest vaccine-induced mBC responses can be effectively boosted by low-level blood-stage parasite exposure, with no evidence of B cell ablation of malaria-specific or bystander responses. The next Chapter will continue this work by exploring the impact of CHMI on specific B cell subsets. It is of

particular interest to establish whether the decrease in antigen specific mBC observed at DoD is restricted to certain subsets or is part of a broader picture. If specific subsets are temporarily disappearing from the periphery as predicted then finding what is driving this change may allow us to better understand how vaccine induced immune cells respond to infection.

4. Phenotypic characterisation of B cell subsets during CHMI

4.1. Introduction

In the previous Chapter it was shown that ChAd63-MVA prime-boost vaccination can induce mBC responses to candidate blood-stage malaria antigens that can be boosted by CHMI, significantly in the case of the antigen MSP1. Whilst responses following booster vaccination with MVA followed a classical secondary response kinetic, responses following CHMI appeared notably different. There are many factors that may have contributed to such differences. Firstly CHMI is an active infection with blood-stage parasites and, therefore, antigen dose is likely to increase steadily as the infection progresses, with the accumulation of infected erythrocytes and dead parasites at sights such as the spleen. Secondly live parasites exhibit differential expression levels of candidate vaccine antigens, in some cases possibly as a mechanism of immune-evasion. This means antigen dosage / exposure to the immune system may differ vastly from vaccination, depending on relative abundance or antigen expression levels. The timing of diagnosis (and thus cumulative parasite burden within the infected host) is also likely to have a significant impact on antigen load / exposure to the immune system prior to treatment. The longer the infection progresses, the more live parasites are exposed to the immune system and following drug treatment there are a greater number of killed parasites in those individuals who progressed furthest, providing more potential antigen for processing. The observation in naïve controls that longer exposure correlates with mBC responses goes some way to supporting this. However, in vaccinated individuals this is further complicated by pre-existing vaccine-induced immune responses, re-stimulation of memory cells as opposed to de novo priming of responses in controls, and the possibility that parasites could be killed by pre-existing vaccine-induced immunity. The observation of reduced liver-to-blood inocula in these challenged individuals [51], clearly shows a minor impact of vaccine-induced immunity (albeit likely at the liver-stage). In particular the observation that MSP1-specific mBC responses

significantly decreased in the peripheral blood of vaccinees at DoD during CHMI (Fig. 3.4A,D), indicates possible mBC activation/recruitment and so warranted further investigation. In particular, the proportions of phenotypically distinct B cell populations in the peripheral blood were of interest, given the apparent link between malaria exposure in the field and the development of so-called 'atypical' memory B cell populations [129]. Work undertaken in this Chapter therefore sought to establish whether this observed decrease was part of a generalised loss of B cells or just a particular subset.

In this Chapter, six B cell subsets will be characterised using differential expression of surface markers as defined by previous studies (Table 4.1).

- Immature B cells are the earliest stage B cells that have left the bone marrow to migrate to peripheral lymphoid organs. They express CD10 which is subsequently downregulated during maturity alongside upregulation of surface IgM and IgD.
- Naïve B cells comprise a population of mature B cells that are non-antigen experienced non-switched (IgM or IgD) and express germ line encoded BCRs. During a primary immune response naïve B cells respond to T cell-dependent or -independent antigen to form the initial antigen-specific B cell response.
- Classical mBC are antigen experienced B cells that are typically class switched (IgG, IgA, IgE) and express mutated BCRs following somatic hypermutation in GCs following a T-dependent response. Classical mBC can respond rapidly to antigen re-exposure either forming SLPC or re-entering GCs. Such cells expressing IgG are the focus of this study as they are the most likely induced by the vaccine regimen presented here, though other antigen experienced memory populations do exist. IgM memory cells [68] are an independent mBC population that are GC independent, respond to polyclonal TLR9 stimulation that can differentiate rapidly to produce

plasma cells secreting somatically hypermutated IgM. mBC may also derive from GC-independent, T-independent reactions where neither somatic hypermutation nor class switching is observed. Recent evidence also suggests there can be GC-independent, T-dependent responses that can generate mBC with germ line sequences but that are class switched [54].

- Activated mBC comprise a transitional population of mostly activated classical mBC that are undergoing differentiation into SLPC via plasmablast intermediates. CD21 is down-regulated in this population but CD20 is still expressed and CD38 is not yet expressed.
- In this Chapter the subset described as 'Plasma Cells' is used to broadly encompass all cells that are both $CD38^{+}$ and $CD20^{-}$ and that all secrete antibody. This population contains non-terminally differentiated plasmablasts as well as terminally differentiated SLPC or LLPCs. These cells can originate from GC-dependent or -independent reactions and from existing classical mBC or newly antigen experienced naïve B cell populations. Typically frequencies of these cells are low in the peripheral blood under normal conditions.
- Atypical mBC were first described as an 'exhausted' mBC population in HIV patients [320] and a similar population has subsequently been observed in individuals from highly endemic malaria areas [129]. This subset, broadly defined as $CD27^{-}$, $CD21^{-}$ B cells contains a heterogeneous population which previous literature has yet to fully define, but may possibly contribute to secretion of functional serum antibody [287].

Using flow cytometry these B cell subsets can be identified and quantified over time and this may provide an insight as to what is happening during CHMI, particularly at DoD. The antigen-specific population would be expected to be within the IgG^{+} classical mBC population but it is important to consider other subsets such as activated mBC and, given their association with natural exposure,

atypical mBC. Additionally if the hypothesis that mBC are migrating out of the peripheral blood is correct there must be a stimulus. Malaria infection induces an inflammatory response and changes in expression levels of a number of cytokines including IFN-γ, IL-10, TGF-α and TGF-β have been associated with disease severity and resolution in both natural and experimental infections [270, 321]. Viral vectored vaccine regimens are known for their induction of high levels of IFN-γ-producing antigen-specific T cells and such vectors containing the antigens MSP1 and AMA1 are no exception [51, 216, 217]. It is therefore possible that IFN-γ could be involved with the orchestration of inflammation driven cell migration. Signalling molecules downstream of IFN-γ and associated cell surface receptors involved in migration were therefore investigated.

4.2. Results

4.2.1. Relative populations of different B cell subsets do not significantly change during CHMI

Initially PBMC at selected time-points from six individuals vaccinated with MSP1 from the Phase IIa trial were stained with B cell phenotypic markers, described in Table 4.1, and gated as shown in Figure 4.1 to identify key B cell subsets. $CD19^+$ B cells typically comprise about 5% of PBMC, a proportion which was confirmed in this study and was maintained across all time-points (data not shown). Within the $CD19^+$ population the subsets of B cells characterised through this staining strategy remained stable over time in most individuals (Fig. 4.2) with no significant differences observed between time points. Plasma cells were seen to be increased in one volunteer at d63 but no increase was observed during CHMI (Fig. 4.2D) in agreement with the ASC data (Fig. 3.7B). Though frozen cells were used for flow cytometry analysis in comparison to fresh PBMC used for the *ex-vivo* ELISPOT, studies have shown evidence that this should not significantly affect sensitivity [322]. Similar observations were noted in unvaccinated infectivity control volunteers (data not shown).

Marker	Function	Immature B Cell	Naïve B cell	Classical mBC	Atypical mBC	Activated mBC	Plasma Cell
CD10	Down-regulated during B cell maturity	+	-	-	-	-	-
CD19	Major B cell lineage marker	+	+	+	+	+	+
CD20	Absence marks Early/Late stage B cell subsets	-	+	+	(+/-)*	+	-
CD21	Mature B cell marker, complexes with CD19	-	+	+	-	-	-
CD27	B cell activation marker	-	-	+	-	+	+
CD38	Plasma Cell marker	-	-	-	(+/-)*	-	+
IgG	IgG Isotype Switched B cell marker	-	-	+/-	+/-	+/-	+/-
CXCR3	Migratory receptor for inflammatory chemokines	-	+/-	+/-	+/-	+/-	+/-

Table 4.1: B cell phenotypic markers and relative expression on B cell subsets.

B cells express a number of identifiable surface markers that can be used to identify B cell subset and phenotype using flow cytometry analysis. All B cells express CD19 whilst many other markers are up or down-regulated depending on factors such as cell maturity, activation status and stage of differentiation. In most cases a single subset has defined homologous expression of a particular CD antigen across all cells within that population. Some heterologous populations are grouped either because literature has yet to define the population in more detail (atypical) or multiple additional markers would be required for accurate definition (plasma cells). The proportion of cells expressing IgG and CXCR3 differs across B cell subsets, but are typically higher in subsets that contain antigen experienced cells. *Not used in defining subset.

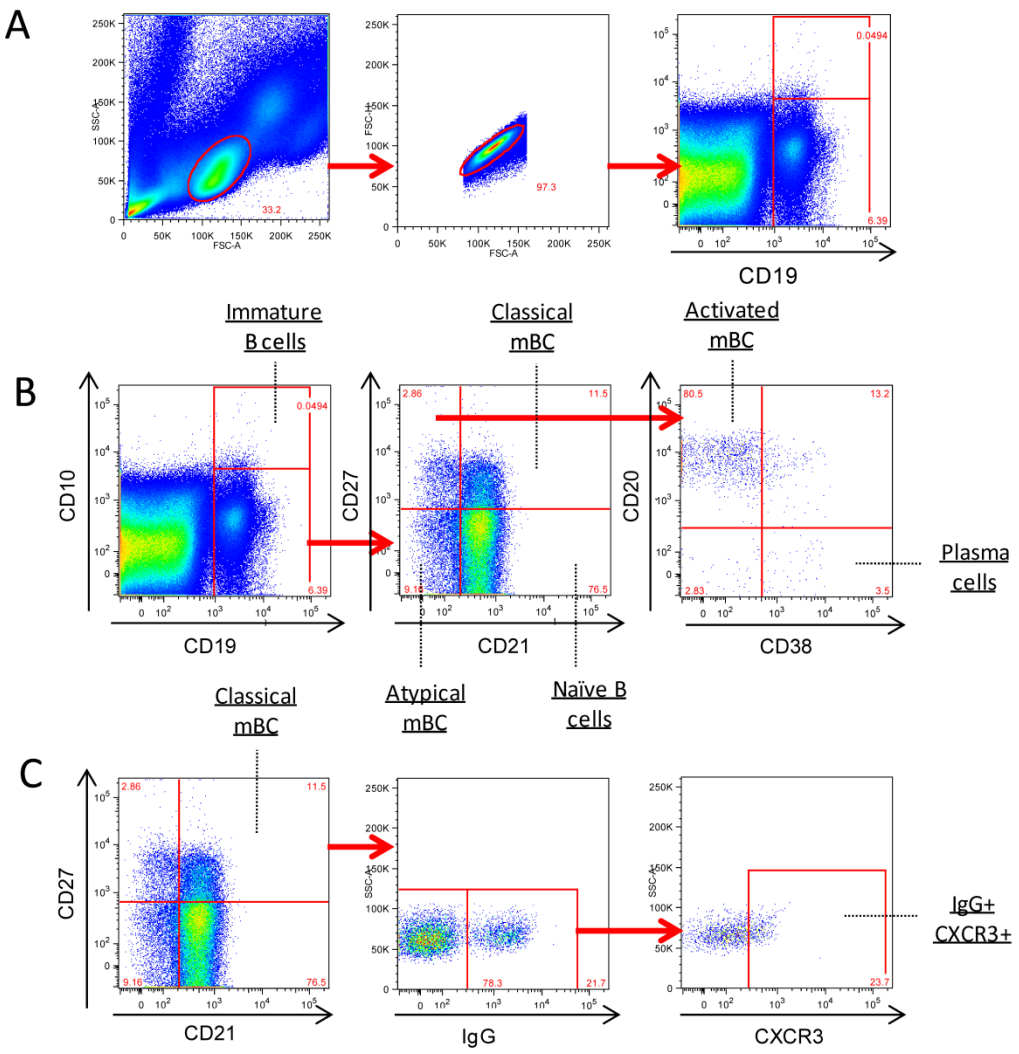


Figure 4.1: B cell gating strategy.

(A) Whole PBMC were gated first by lymphocytes (left) and then singlets (centre) before gating on $CD19^+$ to identify B cells (right). (B) Immature B cells were gated as $CD19^+$ $CD10^+$ (left), whilst $CD19^+$ $CD10^-$ cells were further gated using CD21 and CD27 (centre) to distinguish naïve B cells, classical mBC and atypical mBC. The $CD21^-$ $CD27^+$ population was further gated using CD20 and CD38 (right) to distinguish activated mBC and plasma cells. (C) Classical mBC populations were gated using $IgG^{+/-}$ (centre) and then CXCR3 (right) to identify further subsets of interest.

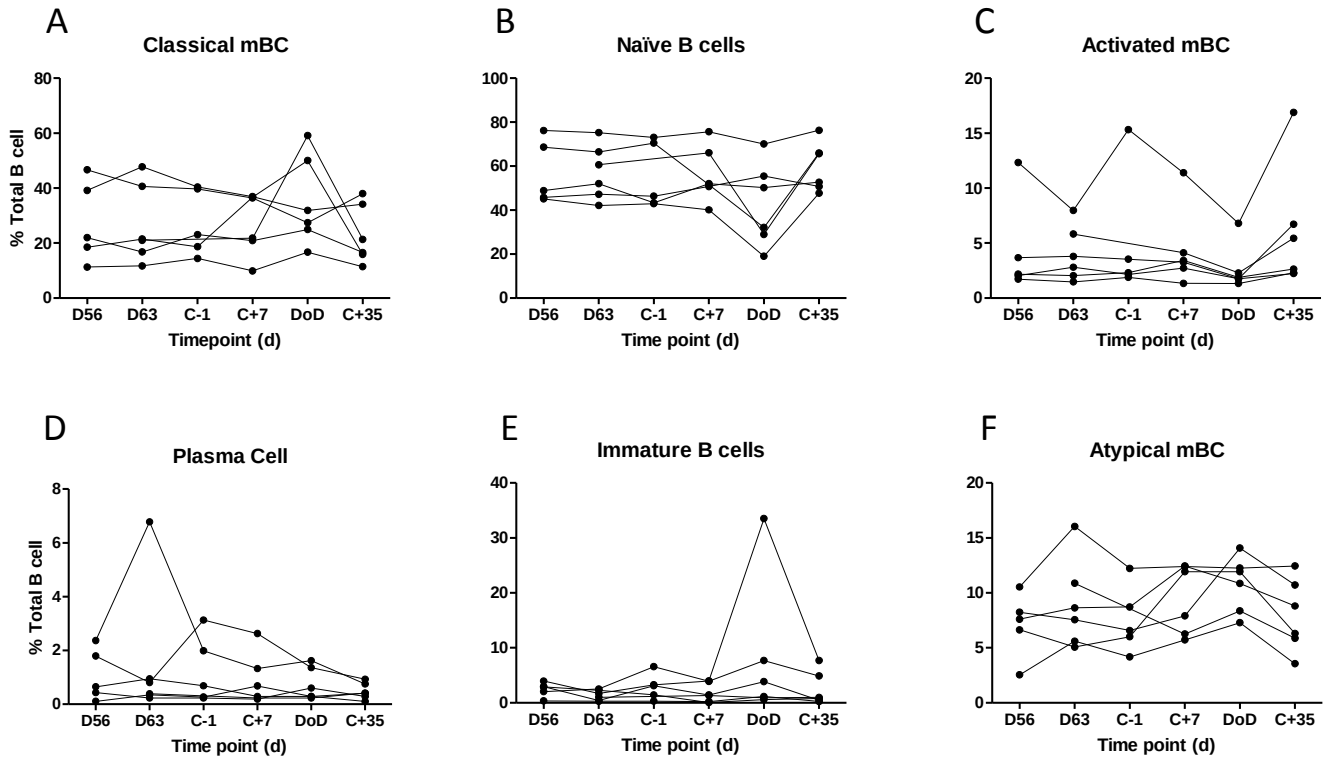


Figure 4.2: B cell subset composition of total B cell pool over time.

Flow cytometry was used to identify relative changes to B cell subsets over time in 6 volunteers receiving the MSP1 vaccine regime followed by CHMI. Subsets are expressed as a % of total B cells, defined as number of gated events for each subset out of total $CD19^{+}$ events (after subtraction of undefined subsets as described in Chapter 2: Methods). Subsets % are plotted for individuals over time for (A) classical mBC, (B) naïve B cells, (C) activated mBC, (D) plasma cells, (E) immature B cells, and (F) atypical mBC. Differences between time-points assessed by Wilcoxon matched-pairs signed rank test, with no significant difference observed.

4.2.2. A decrease in CXCR3$^+$ B cells in the peripheral blood was observed at the point of diagnosis

Given there was no generalised loss of peripheral mBC populations at DoD, subsequent analysis assessed the CXC chemokine receptor 3 positive (CXCR3$^+$) populations within each subset. CXCR3 is a marker associated with migration to areas of inflammation via the ligand CXC chemokine ligand 9 (CXCL9), also known as Monokine induced by gamma interferon (MIG) [323]. This marker is commonly expressed on mature B cells (CD19$^+$, CD10$^-$), particularly those that express CD27 and are class switched [324]. In agreement with this, the majority of CXCR3$^+$ CD19$^+$ CD10$^-$ B cells were found to be CD27$^+$ at the dC-1 time-point (Fig. 4.3A). Interestingly, the total number of CXCR3$^+$, CD19$^+$, CD10$^-$ B cells was observed to decrease at DoD in comparison to dC-1, and then recover by dC+35 (Fig. 4.3A). CXCR3$^+$ cells comprised approximately 20% of the IgG$^+$ classical mBC population at most time-points measured, however this dropped to a median level of 5.2% at DoD (Fig. 4.3B). A significant difference was observed between the % CXCR3$^+$ cells at DoD and dC+35 (P=0.0313), whilst the same trend was observed between dC-1 and DoD (P=0.065). Typically individuals with a high % of CXCR3$^+$ cells prior to DoD showed the greatest reduction at DoD. Similarly, CXCR3$^+$, IgG$^-$ cells (which comprise approximately 10% of the classical mBC population at most time-points) decreased at DoD (median 4%) again significantly from dC+35 (P=0.0313) (Fig.4.3C). Similar observations to that observed with IgG$^+$ classical mBC were also apparent for the activated mBC (Fig. 4.4A) and atypical mBC (Fig. 4.4B) populations. Naïve B cells in which CXCR3 is expressed on a much lower proportion of the population and which are not expected to contain antigen experienced cells were not significantly effected at DoD though a slight trend for a decrease was observed (Fig. 4.4 C). In contrast to the MSP1 vaccinated volunteers, in unvaccinated infectivity control volunteers the % of cells expressing CXCR3 was stable over time for both IgG$^{+/-}$ classical mBC (Fig. 4.3D, E) and all other B cell subsets (Fig. 4.4D-F).

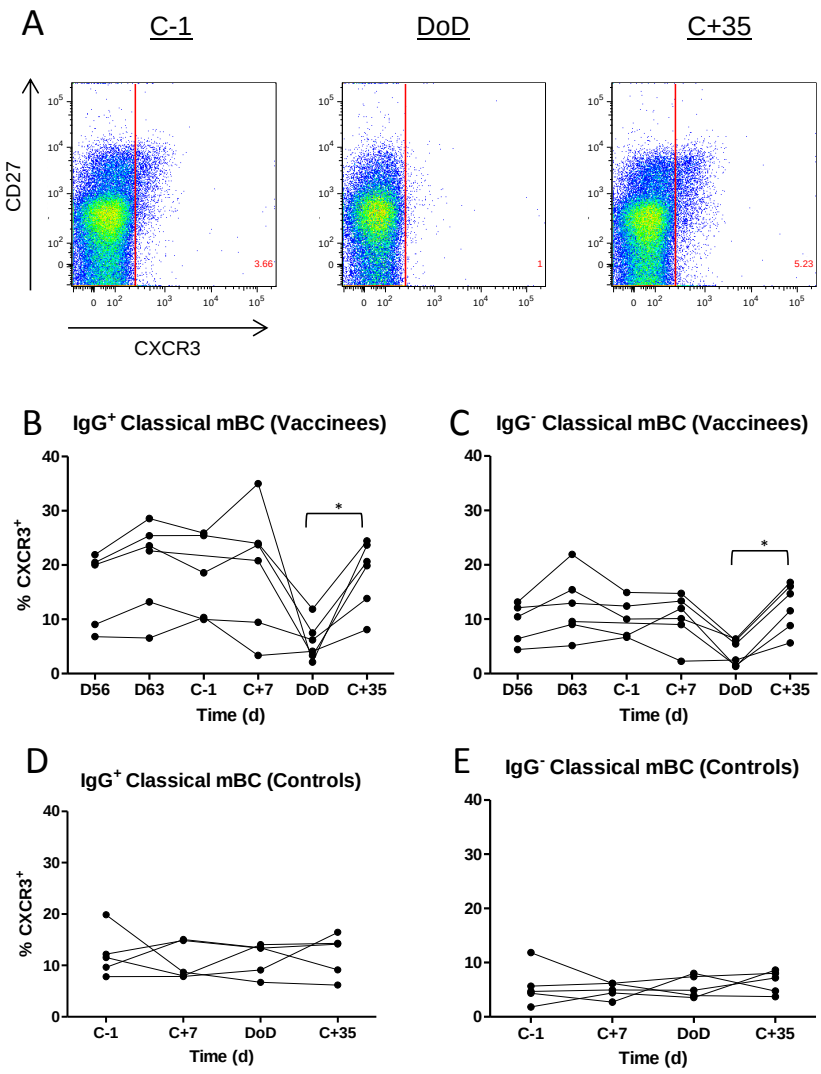


Figure 4.3: CXCR3$^+$ mBC in peripheral blood during blood-stage infection.

Flow cytometry was used to identify CXCR3$^+$ B cells before, during and after CHMI. (A) CXCR3 expression on 'mature' B cells, gated as lymphocytes, singlets, CD19$^+$ and CD10$^-$. Representative flow plots are shown for the dC-1, DoD and dC+35 time-points. (B) % of IgG$^+$ classical mBC expressing CXCR3 and (C) % of IgG$^-$ classical mBC expressing CXCR3 in 6 volunteers vaccinated with MSP1. (D) % of IgG$^+$ classical mBC expressing CXCR3 and (E) % of IgG$^-$ classical mBC expressing CXCR3 in 5 control volunteers. Individual data points at each time point are plotted and connected. Differences between time-points were analysed by Wilcoxon matched-pairs signed rank test (solid lines), *P<0.05.

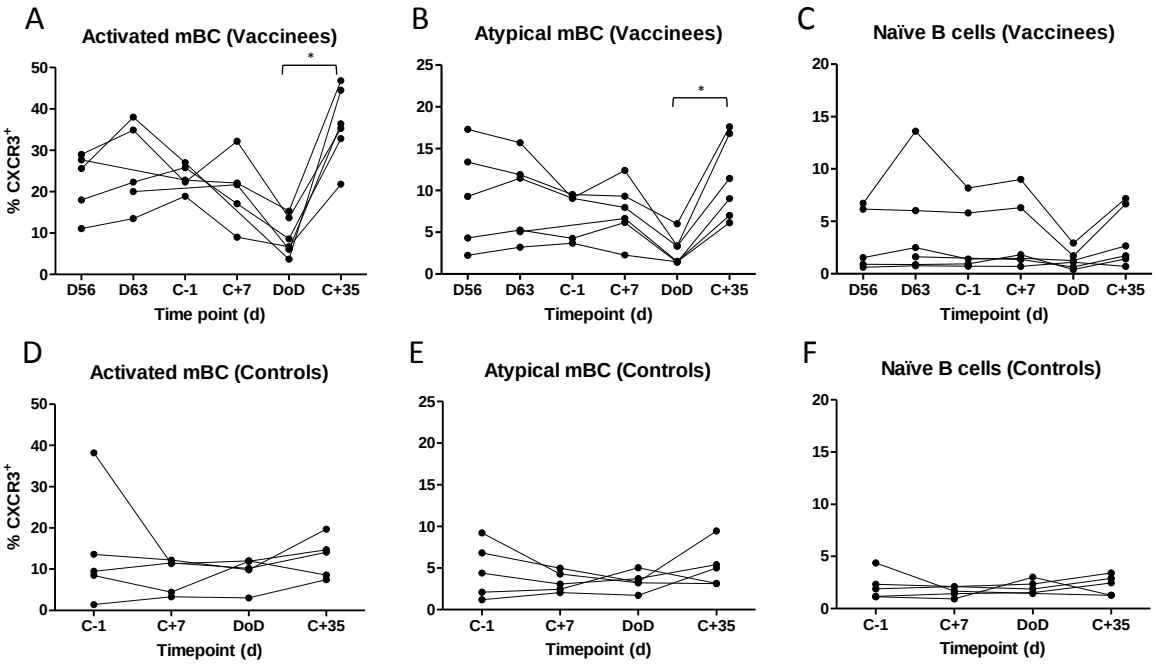


Figure 4.4: CXCR3 expression on other B cell subsets.

Flow cytometry was used to identify $CXCR3^+$ B cells before, during and after CHMI. (A) % of activated mBC expressing CXCR3, (B) % of atypical mBC expressing CXCR3 and (C) % of naïve B cells expressing CXCR3 in 6 volunteers vaccinated with MSP1 prior to CHMI. (D) % of activated mBC expressing CXCR3, (E) % of atypical mBC expressing CXCR3 and (F) % of naïve B cells expressing CXCR3 in 5 unvaccinated infectivity control volunteers. Individual data points at each time point are plotted and connected. Differences between time-points were analysed by Wilcoxon matched-pairs signed rank test (solid lines), *P<0.05.

4.2.3. The inflammatory cytokines IFN-γ and CXCL9 may contribute to possible migration of CXCR3⁺ B cells away from the periphery.

Following the observation that fewer $CXCR3^+$ B cells were observed in the peripheral blood of vaccinees at DoD, it was determined that the next step should be to assess for up-regulation of the inflammatory serum cytokines IFN-γ and CXCL9 that may be driving migration. In both vaccinated and naïve individuals expected physiological levels were observed for both IFN-γ (≈0 pg/mL) and CXCL9 (150-500 pg/mL) at dC-1 (baseline/~2 weeks post final immunisation). Serum ELISA showed significant up-regulation of IFN-γ and CXCL9 in both MSP1 ($P=0.0313$ for both) and AMA1 ($P=0.0078$ for both) vaccinated volunteers but not in controls at DoD as compared to dC-1 (Fig. 4.5A, B). At DoD there was also a significant difference in the serum levels of both IFN-γ and CXCL9 between MSP1 vaccinated volunteers and control volunteers, but not between AMA1 volunteers and control volunteers (likely a reflection of the relatively small numbers of volunteers per group). Although a significant difference was not noted between plasma IFN-γ levels in MSP1 and AMA1 volunteers most volunteers were notably higher for MSP1. IFN-γ and CXCL9 responses by ELISA strongly correlated with one another (Fig. 4.5C). An increase in serum IFN-γ was also observed during the period of blood-stage infection (prior to diagnosis) in individuals vaccinated with MSP1 (Fig. 4.5D) and AMA1 (Fig. 4.5E), but to a much lesser extent in control volunteers (Fig. 4.5F). Typically individuals diagnosed at earlier time-points showed earlier raised levels of IFN-γ but this had no impact on peak cytokine response. Overall, these higher levels of IFN-γ and CXCL9 could account for an increased level of $CXCR3^+$ B cell migration out of the periphery in MSP1 vaccinees.

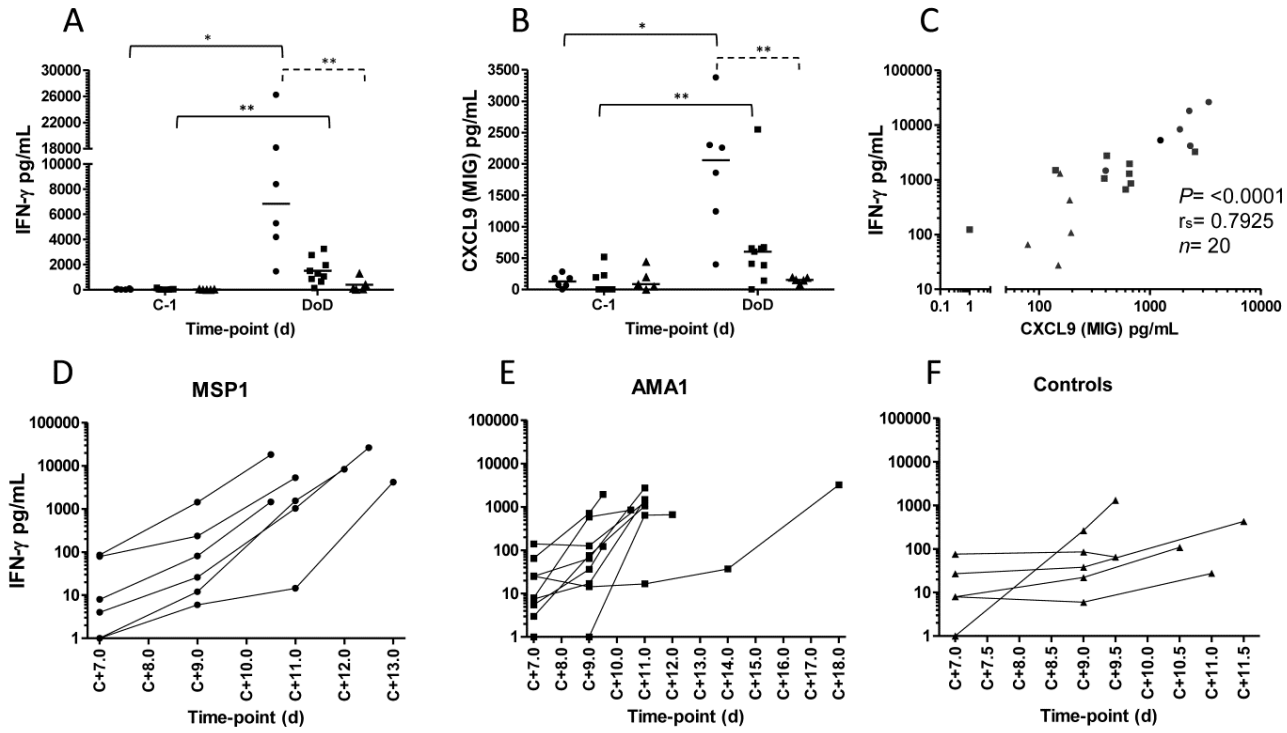


Figure 4.5: Serum levels of IFN-γ and CXCL9 before and during CHMI.

Serum levels of (A) IFN-γ and (B) CXCL9 were assessed by ELISA in volunteers that received MSP1 vaccination (circles), AMA1 vaccination (squares) and unvaccinated control volunteers (triangles) prior to CHMI and at DoD. Individual responses and medians are shown. (C) Correlation between IFN-γ and CXCL9 with Spearman's rank correlation analysis. The individual serum IFN-γ levels following CHMI and during blood-stage infection are shown for (D) MSP1 vaccinees, (E) AMA1 vaccinees and (F) unvaccinated controls. Differences between time-points were analysed by Wilcoxon matched-pairs signed rank test (solid lines); differences between vaccinated volunteers and CHMI controls were analysed by Kruskal-Wallis test (dashed lines); *P<0.05 and **P<0.01.

4.2.4. Functional response to blood-stage parasite antigen likely drives production of IFN-γ.

The observation that MSP1 vaccinated volunteers produce large amounts of IFN-γ in response to CHMI likely indicates an antigen-specific functional Th1 response to parasites at the blood-stage of infection. To address this question, serum IFN-γ in volunteers who were vaccinated with the pre-erythrocytic vaccine candidates CS and METRAP was also measured (in a separate Phase IIa CHMI study). Despite high levels of antigen-specific IFN-γ producing T cells present at dC-1 (up to 2000 SFU/million PBMC by ELISPOT (Hodgson *et al* in press) serum IFN-γ levels at DoD were comparable to controls in both groups (Figure 4.6A), confirming induction of IFN-γ is likely associated with blood-stage antigen restimulation of vaccine-induced responses. Additionally serum IFN-γ responses were also measured in volunteers receiving co-administration of AMA1 and MSP1 in the VAC039 trial [51]. In contrast to individuals receiving single vaccinations, particularly MSP1, the serum IFN-γ response was no different from control volunteers (Figure 4.6A). In comparison to the MSP1 and AMA1 only groups, these three new groups tested each contained individuals who were sterilely protected from malaria. These volunteers (Figure 4.6A, red shapes) showed amongst the lowest levels of serum IFN-γ, essentially negative. Given 3/4 sterilely protected individuals were protected by pre-erythrocytic vaccines it can be assumed that the absence in serum IFN-γ is due to the absence of parasites in the blood. However, high levels of serum IFN-γ may also be due to high numbers of parasite in the peripheral blood. In support of this, parasite load at DoD was correlated with serum IFN-γ (Figure 4.6B) with very high significance ($P<0.0001$, r_s 0.58). Data therefore suggests a more complex model where prior blood-stage immunisation in vaccinees results in increased IFN-γ, a delay to diagnosis, but ultimately higher levels of parasitemia at diagnosis, which in turn drive late production of IFN-γ.

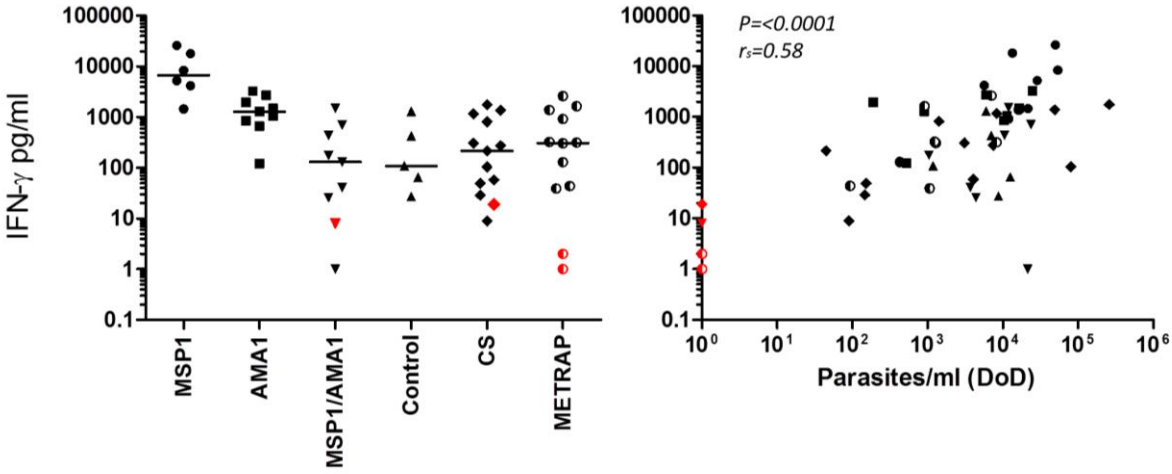


Figure 4.6: Serum IFN-γ at DoD differs across groups receiving pre-erythrocytic or blood-stage viral vectored vaccines.

(A) Serum IFN-γ at DoD was assessed by ELISA in individuals who had been vaccinated with MSP1/AMA1 co-administered (inverted triangles), CS (diamonds) and METRAP (half shaded circles). Individual responses and medians are shown, including those from Fig. 4.5 for comparison with AMA1 and MSP1. Individuals who were sterilely protected against CHMI are shown in red. (B) Correlation between serum IFN-γ and number of parasites per millilitre of blood detected at DoD by qPCR. Spearman's rank correlation is shown.

4.3. Discussion

In the previous Chapter it was reported that there was a significant decrease in the number of $MSP1_{19}$-specific mBC in the peripheral blood at the time-point of diagnosis. Decreases in absolute numbers of peripheral lymphocytes have been previously reported following CHMI, although % $CD19^{+}$ cells within the lymphocyte population remained stable [41]. Interestingly, the classical mBC population, within which the $MSP1_{19}$-specific population would be located, remained stable during this period

All other subsets measured were similarly not significantly affected by CHMI at DoD. A minor decrease in naïve B cells was theoretically possible at this time point through activation of B cells in a primary response to new antigens presented during CHMI but wasn't observed. This lack of significance possibly confirms the previous observation that a single CHMI does not induce responses to a broad range of antigens, as noted by the lack of AMA1 responses in naïve individuals after CHMI. This is supported by previous reports of the antibody responses in these individuals which show that previous vaccination with MSP1 does not enhance acquisition of antibody to AMA1 following CHMI [113]. Given no significant reduction in AMA1-specific or bystander DT-specific mBC was observed, it was concluded that reduced levels of $MSP1_{19}$-specific mBC is likely driven by migration as a result of inflammation at sites such as the spleen, in combination with MSP1-specific differentiation. As discussed in Chapter 3, MSP1 due to abundance or immuno-dominance is likely to be preferentially presented by APCs at such sites. In addition the presence of pre-exisiting antibodies to MSP1 in vaccinees may enhance phagocytosis by macrophages further driving this process. Innate cells would contribute to early IFN-γ production and attraction of adaptive immune cells. Increased antigen presentation of MSP1 would lead to increased activation of vaccine induced antigen-specific B cells and T cells at such site. The latter population would further drive IFN-γ production which increases inflammation, further attracting peripheral blood populations non-specifically, whilst also possibly contributing to some control of early parasitemia. MSP1-specific mBCs encountering cognate antigen presented on APCs that drive differentiation into

antibody secreting cells, removing them from the peripheral mBC pool. Other subsets which don't encounter specific antigen re-enter the peripheral blood without activation. Given that prior to CHMI the antigen-specific $MSP1_{19}$-specific mBC population only comprised around 1% of the total IgG pool (and therefore only a small proportion of the total classical mBC pool), it is not surprising that such a decrease did not impact the total classical mBC pool, especially during an ongoing primary response.

To further investigate this hypothesis, expression of the migratory chemokine receptor marker CXCR3 was assessed. Consistent with the literature, CXCR3 was expressed predominantly on $CD27^+$ cells and those cells expressing IgG. These populations were significantly decreased at DoD in MSP1 vaccinees as predicted. CXCL9 (MIG) is induced by IFN-γ and plays an important role in the recruitment of $CXCR3^+$ cells to sights of inflammation [325, 326]. The up-regulation of CXCL9 by antigen-specific T cells has been previously demonstrated [327] and CXCL9 and IFN-γ have been shown to correlate following immunisation with another viral vectored malaria vaccine regime [272]. The original ChAd63-MVA vaccine candidates for MSP1 and AMA1 were developed to assess the possibility that strong cellular immunity, in conjunction with antibodies, may better impact on blood-stage parasite growth than antibodies alone [216, 217]. Although the Phase IIa efficacy trial showed this not to be the case [51], significant levels of serum IFN-γ were observed during blood-stage infection in vaccinees, in contrast to the unvaccinated controls, with prior MSP1 vaccination again leading to higher levels than AMA1. In agreement with this observation, immune recognition of blood-stage antigens has been reported in a blood-stage challenge model, accompanied by a reduction in peripheral blood lymphocytes [52]. In contrast, control volunteers lacking pre-existing malaria-specific T cells showed lower levels of serum IFN-γ, similar to those previously reported in other studies [270, 271], and thus less marked migration of $CXCR3^+$ B cells away from the periphery.

Notably, not only $CXCR3^+$ classical mBC appear to migrate away from the periphery at DoD. Both activated and atypical mBC populations were also shown to be significantly reduced at this time-point in

MSP1 vaccinees but not in controls, whilst naïve B cells remained relatively stable possibly due to lower expression of CXCR3 in this subset. This fits with the previous observation that the relative ratio of B cell subsets remains stable at DoD. In particular, the migration of $CXCR3^+$ atypical mBC opens up the debate as to the functionality of these cells. Original studies in both HIV-1 and malaria describe such a population as exhausted and non-functional [129, 320] whilst more recent studies suggest they may contribute to production of functional antibodies against malaria [287]. The lack of clinical protection afforded by the MSP1 vaccine candidate does not help answer this question, but in future studies where protection is achieved further investigation of such populations may be warranted.

An alternative possibility is that by the time of diagnosis there is induction of apoptosis in activated $MSP1_{19}$-specific $CXCR3^+$ B cells. However, given that these malaria-specific responses are significantly boosted following CHMI and that B cell populations appeared stable in controls, it seemed unlikely that high levels of cell death would have led to the observed decrease in $MSP1_{19}$-specific mBC at these levels of parasitemia.

The proposed model of $CXCR3^+$ mBC recruitment away from the periphery to areas of inflammation could also shed light on the observations that ASC were not observed in the peripheral blood during CHMI. Once upregulated, CXCR3 expression is maintained on $CXCR3^+$ mBC following activation and is increasingly expressed on $CXCR3^-$ mBC upon differentiation into ASC in the presence of IFN-γ. CXCR3 and its ligands including CXCL9 have also been shown to be important in plasma cell migration to both bone marrow and/or inflamed tissues [82], with reports indicating possible migration to sites of liver inflammation (specifically in chronic hepatitis C infection [328]). An inflammatory environment has also been shown to promote differentiation of mBC into SLPC, particularly in a chronic setting such as multiple sclerosis [329]. In mouse studies of acute *P. chabaudi* malaria, infection has been associated with splenic inflammation and increased population of the spleen with B cells up to peak of infection, which then rapidly disappear afterwards suggesting a short-lived phenotype [330]. Despite this, LLPC

populations are induced normally post infection in this model. Given the high levels of inflammatory cytokines induced in MSP1 vaccinated volunteers and the abundance of antigen, it is possible that during infection mBC are primarily differentiating into SLPC but their frequency in the peripheral blood is below the limit of detection. Only after treatment, in the absence of inflammation and in the presence of abundant antigen from dead parasites, mBC can enter GCs, differentiate into affinity matured LLPC and mBC and would enter a more traditional migratory pattern to the bone marrow or peripheral blood respectively, through alternative ligands for CXCR4 and to a lesser extent CXCR3. If this is the case, then it would not have been possible to detect a migratory ASC population given the time-point sampling in this clinical trial (only up to DoD and then about 20 days later at dC+35). This would also imply that the LLPC population and peripheral mBC population is not supplemented by new cells until post-CHMI, which would fit data presented so far in this thesis.

An important question raised by the data in this Chapter and the previous, is whether or not the MSP1 response induced by vaccination and/or CHMI actually has any positive input towards protective efficacy or whether in fact it plays a negative role through immune diversion. Here it has been shown that a vaccine-induced response to MSP1 can respond to parasite exposure with both T cells and B cells clearly activated during infection. However this response appears to afford little or no protective efficacy suggesting a lack of neutralising antibody. However it is possible that MSP1-specific antibody is contributing to the innate response to parasite, perhaps through formation of immune complexes and enhanced phagocytosis by APCs. In NAI, antibodies to MSP1 have been shown to be functional so it may be that more rounds of exposure to the antigen and more affinity maturation of B cells is required to induce efficacy. If this is true then the fact the vaccine-induced B cell response was boosted by CHMI may be a positive outcome. However, it has been shown that avidity of anti-$MSP1_{19}$ antibodies is not improved following CHMI in these volunteers [113]. If multiple additional vaccinations or rounds of

CHMI are therefore needed to gain any sort of efficacy, MSP1 loses attractiveness as a vaccine candidate.

It is also possible to view much of these data from the point of view that MSP1 is actually performing an immune diversionary role. By being highly abundant and immunogenic the host immune response is directed towards it rather than more important antigens, i.e. those susceptible to host immune attack. In the previous Chapter this was clearly shown for mBC responses in naïve individuals following CHMI, and to a lesser extent in vaccinees receiving both MSP1 and AMA1 co-administered at the same time. It has also been previously reported for T cells and antibodies [51]. The way in which MSP1 is processed and presented by different APCs may also contribute to immune diversion. The $MSP1_{33}$ fragment of MSP1, shed during erythrocyte invasion but contains a high concentration of T cell epitopes. In studies using mice and rabbits the induction of helper T cells to some of these epitopes enhanced induction of antibody against the $MSP1_{19}$ fragment [44]. However other epitopes induced high titres of non-inhibitory antibodies that interfered with neutralising antibodies. In those previously vaccinated with MSP1 the highly inflammatory response to antigen may in fact also contribute to immune diversion through misdirection of B cell responses. mBC attracted to sites of inflammation may offer only a minimal functional role at disrupting parasite growth rates though differentiation into SLPCs and, whilst the mBC response was boosted overall, serum IgG titre was only boosted in the short term and neither was antibody avidity improved. It is possible that instead of delaying the LLPC response as previously proposed, high levels of inflammation prevent or severely hamper production of new LLPC. It would be interesting to see if similar observations were made in naïve controls upon a second CHMI given the induction of comparable levels of $MSP1_{19}$-specific mBC to vaccinees.

In this Chapter the focus has been on characterising total B cell subsets using flow cytometry with a particular focus on mBC. I was able to show clearly that IgG^+, $CXCR3^+$ mBC were significantly reduced in the peripheral blood at DoD. One limitation of this study was that I was unable to prove definitively that

this population contained the antigen-specific cells predicted. The ability to identify antigen-specific B cells by flow cytometry would have obvious benefits and as such was assessed in the work detailed in Chapter 5. An alternative approach to identifying antigen-specific cells is to phenotype, sort and plate out specific B cells on an ELISPOT plate before quantification. This technique will also be explored in the next Chapter, particularly for isolating ASC/plasma cells.

5. Single B cell sorting

5.1. Introduction

In Chapter 3 it was shown that priming with ChAd63 followed by boosting with MVA induced a classical secondary B cell response, whereby antigen-specific ASC could be identified in the peripheral blood at 7 days post-boost by *ex-vivo* ELISPOT and mBC peaked around 4 weeks post-boost as measured by cultured ELISPOT. Whilst highly sensitive, the *ex-vivo* ELISPOT detects all cells capable of secreting antibody, meaning the population may be phenotypically heterogeneous. In Chapter 4 it was shown how B cells subsets could be defined and quantified using flow cytometry. Whilst the focus here was on mBC populations, an increased number of plasma cells (defined as $CD10^-$, $CD19^+$, $CD27^+$, $CD21^-$, $CD20^-$, $CD38^+$, Table 4.1) was observed by flow cytometry in a few individuals at d63 (Fig. 4.2D), coinciding with the peak detected by *ex-vivo* ASC ELISPOT, although not consistently representative. It is possible that other phenotypes present in whole PBMC, including activated mBC and atypical 'plasma cell-like' cells, may contribute to secreted serum antibody. Whilst freeze thawing of B cells has been shown to have minimal impact on effective detection of antigen-specific ASC cells by *ex-vivo* ELISPOT, specific detection of ASC by flow cytometry was shown to be notably reduced [322], offering another possible explanation for this observation. This all suggests that further investigation is required to more accurately link together the work presented in Chapters 3 and 4, taking into account fresh vs frozen and cultured vs non-cultured cells.

In addition to quantification, B cells that have been phenotyped using flow cytometry can also be isolated from other subsets using MoFlo sorting techniques. Typically cells are sorted either onto an ELISPOT plate to identify frequency of antigen-specific cells, or into a nucleic acid stabilising buffer that allows for subsequent amplification of cDNA from cellular RNA [294]. Sequencing of B cell receptor genes from bulk plasma cells can allow broad study of the B cell receptor repertoire and identify specific

variable gene usage and patterns of SHM common to vaccination or natural exposure [81, 331]. However whilst this gives a broad overview of the repertoire at a snap shot in time, traditional sequencing of bulk cells does not allow for identification of cognate heavy and light chain pairs or tell you specifically which sequences can recognise antigen. B cells can however be sorted as single cells which retain the heavy light chain pairing following sequencing [332]. This has the advantage of being able to identify specific VDJ combinations and mutations from germline sequences within single clones as well as their presence and frequency at different time-points following infection or vaccination.

Single isolated B cells can also be used to generate monoclonal antibodies through cloning into eukaryotic expression vectors and transfection of stable cell lines [293, 294]. This importantly allows characterisation of functional attributes of the immunoglobulin sequence. Monoclonal antibodies can be screened for antigen-specificity, affinity, functional neutralisation of pathogens and additive or synergistic effects with other monoclonal antibodies. Crystallography can also be used to characterise binding sites of antibody/antigen and whether these epitopes are conformational or not [333, 334]. Much of the information that can be gleamed from the study of monoclonal antibodies can be fed back into next-generation vaccine development. This will be discussed in greater detail in the next Chapter of this thesis.

In this Chapter I will discuss the techniques involved in the isolation of single B cells from PBMC, with a particular focus on ASC observed at 7 days post boost in volunteers vaccinated in our clinical trials, which are predicted to be plasmablasts derived from antigen-specific GC-dependent reactions. Experiments here were performed on volunteers vaccinated with MSP1 and AMA1 antigens, although ultimately the focus on monoclonal antibodies in the next Chapter will be on AMA1 alone. Many of the experiments discussed here were aimed at optimising the process to maximise isolation of antigen-specific cells.

One method to improve isolation of target B cells is the use of antigen-specific reagents for the detection of B cells via the BCR. Such regents include small molecules, linear epitopes or native antigen in the form of whole proteins or virions [335]. The most commonly used method is to use biotinylated antigen that can then be detected using streptavidin fused fluorophores using flow cytometry. This method has been effectively utilised for a number of HIV-1 antigens such as gp140 [277] and influenza antigens such as hemagglutinin [276, 336] . However, previous efforts using the blood-stage antigens MSP1 and AMA1 have reported a lack of success [278]. Despite this previous report, here antigen-specific staining was attempted for both MSP1 and AMA1 using various published methodologies, with the ultimate goal of maximising the isolation of antigen-specific plasma cells at 7 days post-boost to reduce screening time and costs on irrelevant cells.

The basic principle behind antigen-specific staining is that the BCR of B cells specific for vaccine antigen will bind and retain tagged antigen during the staining process, thus enabling detection by flow cytometry. One important consideration is that the tagging of the antigen should not obscure any epitopes that BCRs may recognise. Whilst for some antigens the crystal structure has been resolved and antibody binding sights defined others have not. Biotinylation can therefore be targeted to specific sites on the antigen or done randomly to target a number of sites. In this study biotinylated antigen was produced using in-house AMA1 and MSP1 protein and a commercially available biotinylation kit (Pierce biotechnology, Sulf-NHS-LC-Biotin). Using recommended conditions of a 20-fold molar excess of biotin this would be predicted to give 4-6 biotin groups per antigen molecule.

mBC display BCR on their surface which are internalised upon antigen cross linking, prior to antigen presentation to $CD4^+$ cells in a T-dependent response. *In vitro* mBC can be surface stained for antigen-binding (in theory relatively easily), even for very rare populations [337], therefore initial attempts to isolate antigen-specific B cells focused on the mBC population. Staining antigen-specific plasma cells,

however, is likely more difficult than mBC. Plasma cells are classically described as terminally differentiated, secrete large amounts of antibody and lack expression of BCR on their surface. It has recently been suggested that active BCR can be found on IgA and IgM plasma cells but there is no evidence for this on IgG plasma cells [338]. As a result, detection of antigen-specific IgG plasma cells typically requires intracellular staining for IgG [339]or the use of methods that trap secreted molecules in an affinity matrix [340], however both methods limit subsequent detection of secreted IgG by ELISPOT. It has been suggested that surface staining for membrane bound IgG may be sufficient for staining for non-terminally differentiated plasmablasts, though this is still open to debate.

5.2. Results

5.2.1. Optimisation of single B cell MoFlo sorting of ASC at 7 days post-boost

Previous phenotyping experiments had all been done using frozen PBMC, thawed on the day of the experiment and run on an LSRII flow cytometer. Whilst all individuals showed a peak antigen-specific ASC population at d63 by *ex-vivo* ELISPOT, only one volunteer showed a notably large increase in plasma cells at the same time-point, as detected by flow cytometry. It is possible that the freeze/thawing process has a detrimental impact on the staining of plasma cell surface markers as previously reported [322].

To assess whether using fresh cells increases the sensitivity of detection of this subset, the phenotyping panel from Chapter 4 (Fig. 4.1 and Table 4.1) was run on fresh cells from volunteers vaccinated with AMA1 in a subsequent Phase Ia clinical trial [301] at 7 days post-boost. In some volunteers tested, a large increase in the number of plasma cells was detectable by flow cytometry, in a distinct $CD27^{high}$ population (Fig. 5.1A-C). There was a trend for this population to correlate with ASC responses detected by *ex-vivo* ELISPOT, most notably with high responders (Fig. 5.1D). Other subsets were consistent with previous observations at this time-point using the same flow panel. The lack of a strong significant correlation between *ex-vivo* ASC and plasma cells detected by flow may suggest additional antibody secreting phenotypes are detected by ELISPOT.

In the mBC ELISPOT assay, ASC are derived from cultured, polyclonally stimulated mBC. Given that plasmablasts and plasma cells derived from mBC contribute to the secondary B cell response, I wanted to confirm that the cells derived in culture are phenotypically the same as ASC observed in fresh blood (i.e. those detected in the ASC ELISPOT). Fig. 5.2A-C shows that following culture most of the cells plated on the mBC ELISPOT are phenotypically $CD38^{+}$ plasma cells. A proportion of cells remaining after culture are activated mBC (Fig 5.2B) and atypical mBC (Fig 5.2A,D,E). These may also contribute to secretion of

antigen-specific antibody that would be picked up by ELISPOT (independent of the $CD38^+$ plasma cell population). If similar populations are present in fresh PBMC derived from *in vivo* responses, then this could also explain the discrepancy between fresh ELISPOT and plasma cell responses seen in Fig. 5.1D.

To study these observations further the next step was to sort B cells of defined phenotypes, using MoFlo onto ELISPOT plates, in order to determine their relative contribution to the total production of antigen-specific antibody. The staining panel needed to be adapted to take into account the differences between the MoFlo and LSRII machines, in particular regarding lasers and ability to detect certain fluorophores. In brief, the panel was reduced to 6 markers, CD19, CD20, CD21, CD27, CD38 and IgG, with CD21 changed to the fluorophore FITC. This new panel was initially tested using the LSRII machine to confirm accuracy and then subsequently transferred to the MoFlo machine.

To confirm that plasma cells identified using this new staining panel contained the antigen-specific population of interest; different subsets of previously cultured cells were sorted using MoFlo, onto an ASC ELISPOT plate coated with AMA1. Five subset populations were sorted at 1000 cells per well; total lymphocytes, $CD19^+$ (total B cells), $CD19^+/CD27^+/CD20^-/CD21^-/CD38^+$ (plasma cells), $CD19^+/CD27^+/CD20^-/CD21^-$ ('plasma cells', $CD38^+/^-$) and $CD19^+/CD27^+/CD20^+/CD21^-$ (activated mBC). As expected the greatest concentration of IgG^+ and $AMA1^+$ cells were found in the '…$CD38^+$' defined population, with over 14% of cells IgG^+ (Fig. 5.3A) and 1% $AMA1^+$ (Fig. 5.3B). It appears that the addition of $CD38^+$ staining doesn't largely increase the proportion of positive cells and that the activated mBC population contains a large proportion of antigen-specific antibody secreting cells. It is also possible that during the overnight ELISPOT culture many activated mBC or $CD38^-$ 'plasma cells' have differentiated into $CD38^+$ plasma cells. In this MoFlo sort, cells were not sorted using stains for IgG^+, which could have helped to enrich the IgG^+ population. However using the data obtained we can estimate that the proportion on AMA1+ cells within the '…$CD38^+$' IgG^+ population to be around 7% (Fig. 5.3C).

Another step added early on in the optimisation of the single cell ASC sorting protocol was the inclusion of a B cell enrichment step prior to cell staining. The Easy Sep human Pan-B cell enrichment immunomagnetic kit depletes cells expressing CD2, CD3, CD14, CD16, CD36, CD42b, CD56, CD66b, CD123 and Glycophorin A, leaving only B cells. This was found to improve staining efficiency and made it easier to define clear populations when MoFlo sorting fresh samples that contained more background populations compared to cultured cells (Fig. 5.4). In particular CD27 staining is improved and the majority of $CD20^-/CD21^-$ cells are $CD38^+$ which is itself a more defined population. Steps to further improve gating were the inclusion of IgM and IgG to the panel. IgM was included on the same fluorophore as CD21 to additionally remove these cells in the $CD21^+$, IgM^+ dump population. IgG was used to further gate $CD38^+$ plasma cells to attempt to enrich the final population of interest.

The finalised protocol used to sort plasma cells including all the above components has been subsequently used to sort cells at 7 days post-boost for subsequent production of monoclonal antibodies (see Chapter 6). This has successfully been done from both fresh and frozen PBMC. An example of antigen-specific and IgG^+ ELISPOT wells and the typical % positive rates for AMA1 and IgG can be seen in Fig. 5.5. The example shown suggests that the majority of IgG^+ cells are likely to be also $AMA1^+$ at this time-point. Although cells were sorted as IgG^+, detection for IgG by ELISPOT averaged only 15%. It is possible that some cells were dead or stressed, preventing IgG secretion after plating. Also, although frequencies are lower on average here compared to similar experiments using influenza $CD38^+$ plasma cells, this is consistent with comparisons between ASC ELISPOT which suggest influenza vaccination induces a significantly larger response 7 days after boost [263].

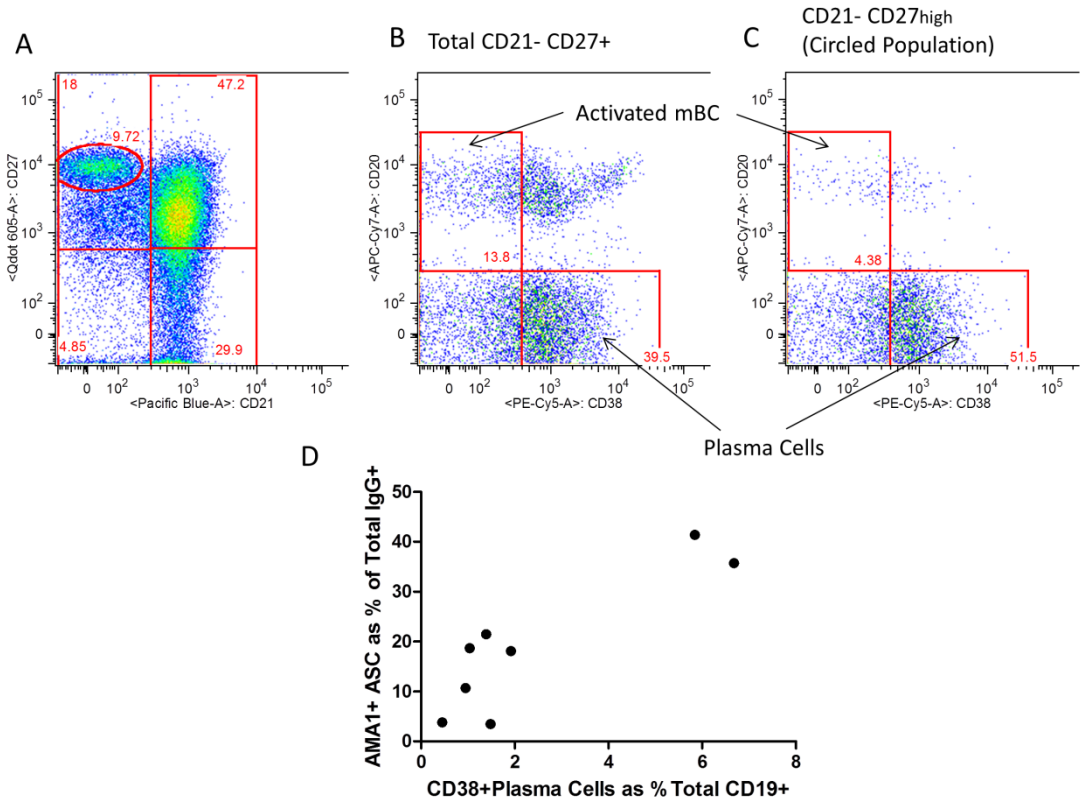


Figure 5.1: Phenotypic identification of ASC at 7 days post-boost from fresh blood.

ASC identified in the peripheral blood at 7 days post-boost by ASC ELISPOT co-inside with an increase in plasma cells as measured by flow cytometry. (A) At day 7 post-boost, the CD21-, CD27high population (circled) is notably distinct within the total CD21-, CD27+ population. (B) Within the total CD21-, CD27+ population activated mBC (CD20+, CD38-) are detectable along with other intermediate phenotypes (CD20-, CD38- & CD20+, CD38+) and plasma cells (CD20-, CD38+). (C) Within the circled CD21-, CD27high population, plasma cells are the dominant phenotype with reduced numbers of activated mBC. (D) Individuals with larger numbers of flow detectable plasma cells (defined by CD38+ cells as a % of total CD19) trend to also have a higher proportion of AMA1 specific ASC (as a % of total IgG ASC) as detected by ASC ELISPOT.

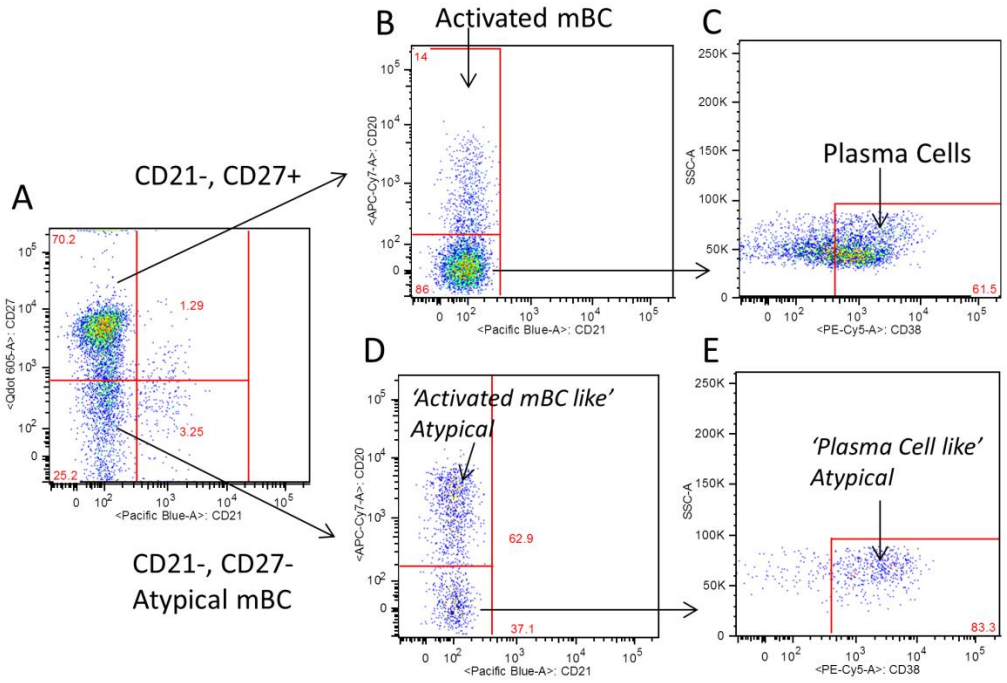


Figure 5.2: Phenotypic characterisation of ASC derived from culture of mBC.

The ratio of B cell subsets present in PBMC differs significantly in comparison to those cells present following the 6 day polyclonal stimulation used to derive ASC from mBC for the mBC ELISPOT. (A) Gating of $CD19^{+}$, $CD10^{-}$ cells using CD21 and CD27 shows an almost complete absence of both classical mBC ($CD21^{+}$,$CD27^{+}$) and naïve B cells ($CD21^{+}$, $CD27^{-}$). Within the $CD21^{-}$, $CD27^{+}$ population a small number of $CD20^{+}$ activated mBC (B) and a large number of $CD20^{-}$, $CD38^{+}$ plasma cells (C) are identified. Within the $CD21^{-}$, $CD27^{-}$ atypical mBC gate cells can be identified with similar phenotypic profiles to the $CD21^{-}$, $CD27^{+}$ population including 'activated mBC' like atypical cells (D) and 'plasma cell-like' atypical cells (E).

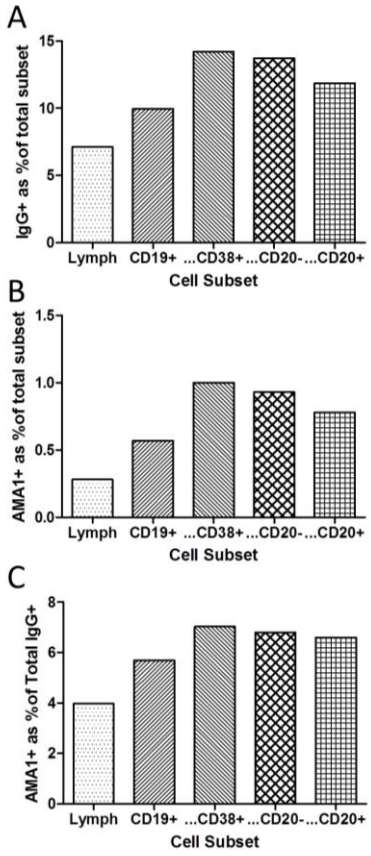


Figure 5.3: Proportions of IgG^+ and antigen-specific cells within cultured B cell populations.

PBMC were cultured for 6 days with polyclonal stimulation before B cell populations were identified and independently sorted onto an ELISPOT plate detecting either IgG^+ (A) or $AMA1^+$ (B) cells at 1000 cells per well. Results are expressed as a % of total subset. The proportion of IgG^+ cells that would be predicted to be also $AMA1^+$ was estimated from proportions of total subsets (C). Subsets from left to right:

- Total lymphocytes (Lymph): defined by side scatter (SSC) vs forward scatter (FSC
- Total B cells ($CD19^+$).
- Plasma cells (…$CD38^+$): $CD19^+$, $CD10^-$, $CD21^-$, $CD27^+$, $CD20^-$, $CD38^+$
- 'Plasma cells' (…$CD20^-$): $CD19^+$, $CD10^-$, $CD21^-$, $CD27^+$, $CD20^-$, $CD38^{+/-}$
- Activated mBC (…$CD20^+$): $CD19^+$, $CD10^-$, $CD21^-$, $CD27^+$, $CD20^+$

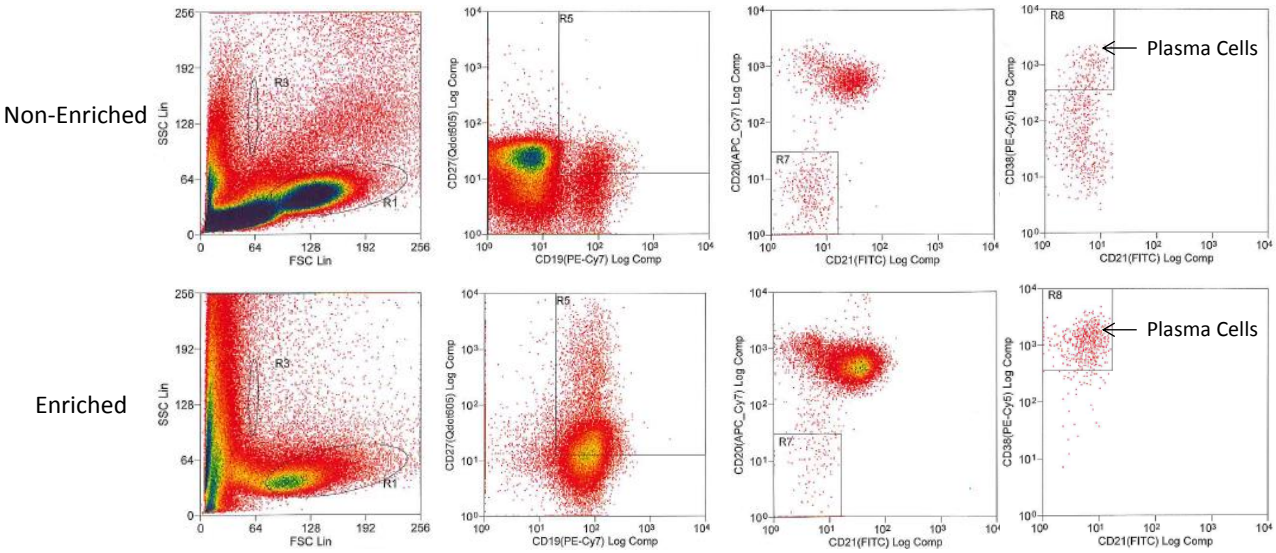


Figure 5.4: Effect of B cell enrichment on MoFlo gating of B cell subsets.

The effect of B cell enrichment was compared by staining of fresh PBMC at 7 days post-boost. Enriched cells were immuno-magnetically depleted of non-B cells prior to staining with anti CD19, CD20, CD21, CD27 and CD38 antibodies. Differences in staining and population distinctiveness are compared above at sequential gating stages, total lymphocytes, CD27/CD19, CD20/CD21 and CD38 as the final population of interest.

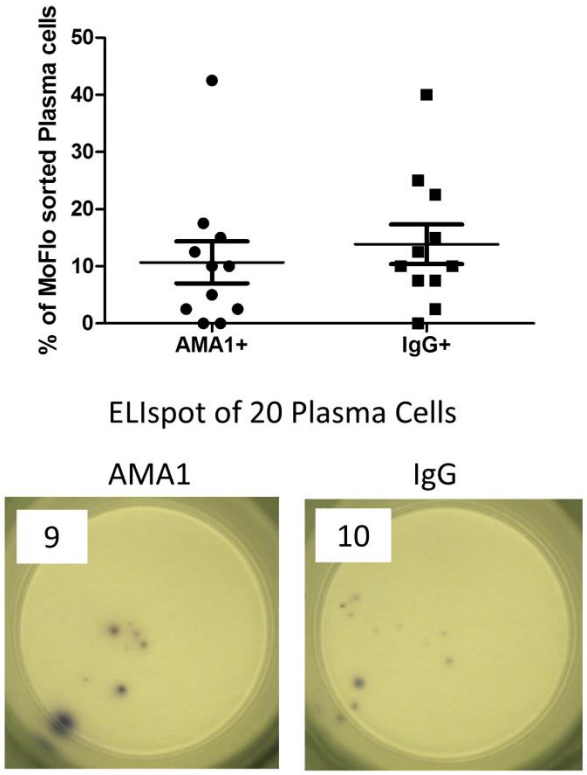


Figure 5.5: Ratio of AMA1^{+} and IgG^{+} plasma cells detected by ASC ELISPOT post MoFlo sort.

Fresh PBMC from volunteers vaccinated with an AMA1 protein vaccine were obtained at 7 days post boost after either second or third vaccination in an on-going clinical trial (VAC054). 20 plasma cells (CD19^{+}, CD20^{-}, CD21^{-}, CD27^{+}, CD38^{+}, IgG^{+}, IgM^{-}) were MoFlo sorted onto wells of an ASC ELISPOT in duplicates, coated with either AMA1 protein or polyvalent goat anti human IgG. Spots were counted, averaged across duplicates and the proportions that were AMA1^{+} or IgG^{+} recorded.

5.2.2. Antigen-specific B cell staining for the blood-stage antigens MSP1 and AMA1

Given the previous report of antigen-specific staining for AMA1 and MSP1 being difficult due to non-specific binding of antigen, an initial experiment was designed to maximise the positive signal and minimise (or at least gauge) the background. To begin with, antigen-specific staining was focused on mBC rather than plasma cells due to greater success with rare populations reported in the literature for the former. Multi-biotinylated, 'homemade' AMA1 and MSP1 were used along with two separate streptavidin conjugated fluorophores (FITC and APC) to compare relative signal strength. PBMC samples from d0 (pre-vaccination) and d84 (post-vaccination) from two volunteers, one vaccinated with AMA1 and one with MSP1, were used in this experiment. For each sample three conditions were tested: no antigen, vaccine antigen (AMA1 or MSP1), non-specific antigen (AMA1 or MSP1, alternate of vaccine antigen). Cells were first stained with antigen before addition of streptavidin-conjugated fluorophores. For the no antigen control, streptavidin-conjugated fluorophores were added to rule out non-specific binding at this step. Following this step, normal B cell staining was performed as previously described. Day 84 samples were chosen as this was the peak of the antigen-specific mBC response as assessed by cultured ELISPOT (Chapter 3), and this was the population targeted for staining initially. In the no antigen controls there was little to no background for both fluorophores at all time-points, suggesting non-specific binding of streptavidin to cells is not an issue (Fig. 5.6A). However when looking at vaccine antigen and non-specific antigen staining, highly variable results were observed. For AMA1 vaccinated volunteers detection by streptavidin FITC gave low background at d0 and weak detection of AMA1 at d84, but high background staining with non-specific MSP1 (Fig. 5.6B). In contrast, detection by streptavidin APC gave high AMA1 background at d0 but very little background with non-specific MSP1 (Fig. 5.6C). Observations for MSP1 vaccinated volunteers showed similar problems. With Streptavidin FITC, MSP1 background was high and non-specific AMA1 staining was minimal (Fig. 5.6D), whilst for streptavidin APC MSP1 background was low at d0, minimal signal at d84 and high background with non-

specific AMA1 (Fig. 5.6E). From this experiment it was not possible to accurately identify an antigen-specific population from background or controls.

It has previously been described how B cell enrichment improved efficiency of staining of B cells used in MoFlo. Therefore it was tested as to whether addition of this step may also improve antigen-specific staining. The previous experimental conditions using PBMC from AMA1 vaccinated individuals and streptavidin APC were used, and antigen-specific staining compared between enriched and non-enriched PBMC. Enrichment unfortunately showed no improvement to antigen-specific staining and did not reduce background at d0 or reduce staining of non-specific antigen (Fig. 5.7).

The next step was to utilise both fluorophores in a dual staining protocol [341]. Here sub-saturating concentrations of each fluorophore are used and only cells positive for both signals are considered antigen-specific. As with the initial antigen staining experiment, both AMA1 and MSP1 staining was attempted on d84 PBMC from individuals previously vaccinated with a single antigen. For vaccine antigen staining, streptavidin FITC was titrated down to sub-saturating concentrations (4, 2, 0.5 and 0.1 µL for 1million cells in 100 µL), whilst streptavidin APC was used at a standard 0.5 µL volume, added after initial FITC staining and washing. It must be considered that saturation of the biotinylated antigen may vary between antigens depending on the efficiency of the biotinylation step and size of antigen. Once antigen-specific staining had been performed a simplified phenotyping panel including CD19, CD21 and CD27 was used to identify the classical mBC population and double stained populations were compared to single stained ones. Double stained populations were observed before gating, with best results at 4 µL FITC / 0.5 µL APC, however very few of these were within the classical mBC gate ($CD21^+$, $CD27^+$) (Fig. 5.8). Follow up experiments were performed to include d0 and non-specific antigen controls but, as previously seen, these showed background levels of staining that suggested these observed populations are not likely real.

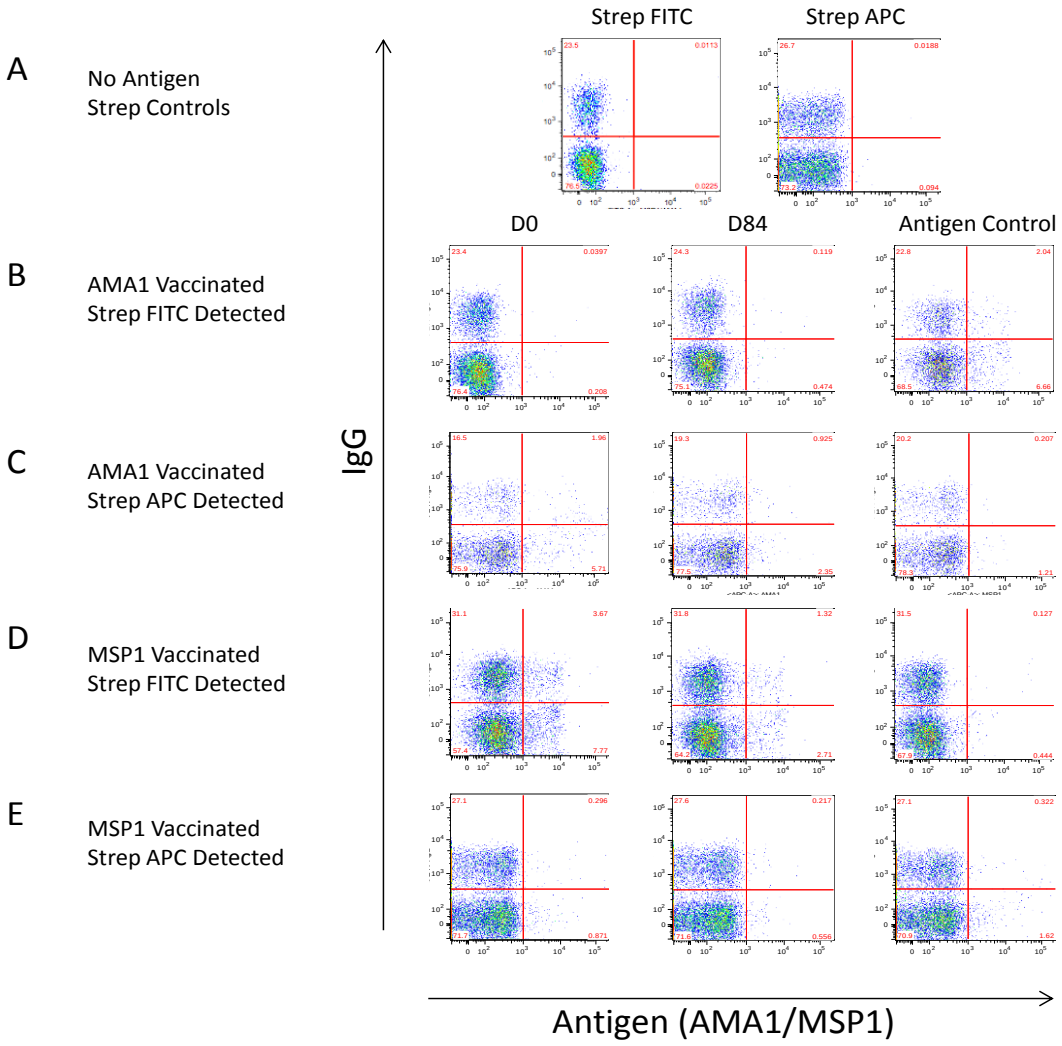


Figure 5.6: Comparison of different fluorochromes in the detection of antigen-specific classical mBC.

Frozen PBMC from D0 (baseline) and D84 (peak of antigen-specific mBC response) were stained using the B cell phenotyping flow panel and multi-biotinylated antigen detected by use of streptavidin conjugated fluorophores (either FITC or APC). (A) PBMC was stained with streptavidin conjugated fluorophore in the absence of multi-biotinylated antigen to ensure absence of non-specific binding. PMBC from AMA1 vaccinated volunteers were stained with multi-biotinylated AMA1 at D0 and D84 or antigen control (MSP1) and detected using either streptavidin conjugated to FITC (B) or APC (C). PMBC from MSP1 vaccinated volunteers was stained with multi-biotinylated MSP1 at D0 and D84 or antigen control (AMA1) and detected using either streptavidin conjugated to FITC (D) or APC (E).

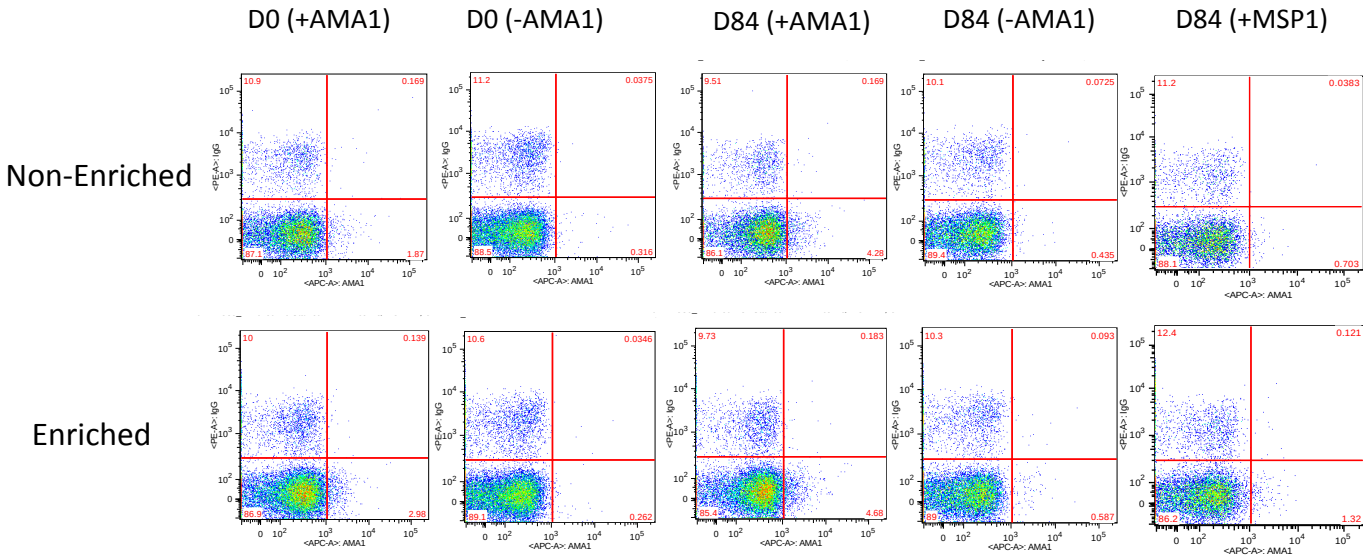


Figure 5.7: Effect of B cell enrichment on antigen-specific staining of classical mBC.

The effect of B cell enrichment on antigen-specific staining was compared on frozen cells at D0 and D84 from individuals vaccinated with AMA1 antigen. Enriched cells were immuno-magnetically depleted of non-B cells prior to staining with multi-biotinylated AMA1 and subsequently with anti CD10, CD19, CD20, CD21, CD27, CD38 and IgG antibodies. Biotin was detected with streptavidin conjugated to the APC fluorochrome. Control samples received either no antigen (-AMA1) or non-exposed control antigen (MSP1).

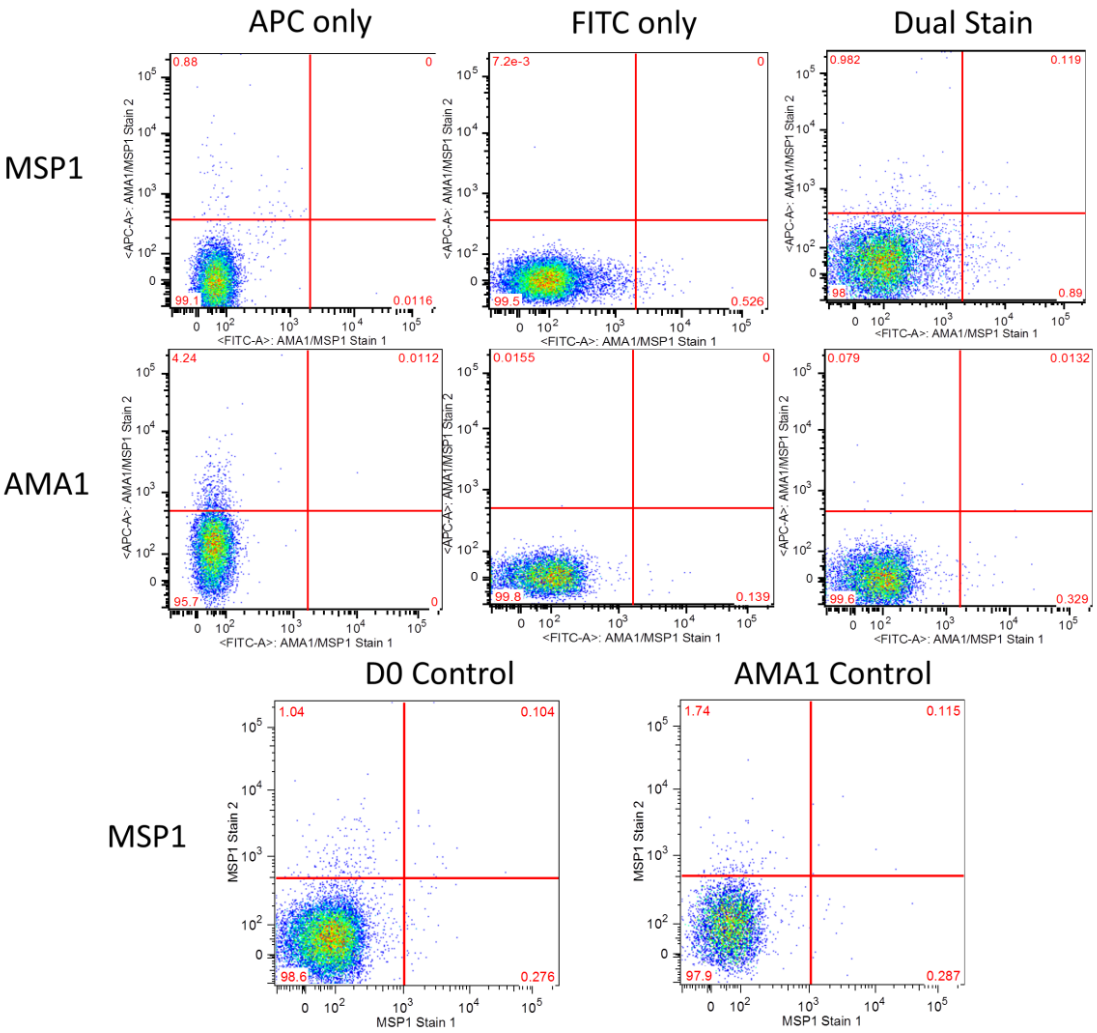


Figure 5.8: Use of dual staining in the detection of antigen-specific classical mBC.

Frozen PBMC from individuals vaccinated with either MSP1 or AMA1 were stained with their respective multi-biotinylated antigen prior to staining using anti CD19, CD21, CD27 antibodies to detect classical mBC. Biotin was detected by dual staining, using titrated concentrations of Streptavidin FITC (Stain 1) and a standardised concentration of Streptavidin APC (Stain 2). Dual stain plots displayed are for 4 µL FITC, 0.5 µL APC. Single stain controls were also run, stained at the highest concentrations used. D0 baseline samples and non-vaccine antigen controls for MSP1 vaccinated volunteers were subsequently run using optimised stain ratios.

5.3. Discussion

In this Chapter there were a number of key aims: to more accurately characterise the plasma cell response using flow cytometry; to identify antigen-specific cells within this population of cells; and to effectively sort this population using MoFlo techniques. This work would not only validate work from previous Chapters, but would also provide the framework for future work producing monoclonal Antibodies (mAbs).

Initially it was shown that the sensitivity of detection for plasma cells using flow cytometry was improved by using fresh rather than frozen PBMC. Previous reports had shown that whilst sensitivity of detection by *ex-vivo* ELISPOT of plasma cells was not reduced by freezing, detection by flow cytometry was, although this was a limited study with only three individuals tested [322]. Previous work in this thesis had used a similar *ex-vivo* ELISPOT and my data supported the view that use of frozen cells had minimal impact on sensitivity (data not shown). Here detection of plasma cells from fresh PBMC also trended with detection by ELISPOT, more accurately than when frozen cells were used. Also consistent with other studies, the increased plasma cell population detected is distinctly visualised as a $CD27^{hi}$ population within the $CD21^{-}$, $CD27^{+}$ gate. This same $CD27^{hi}$ population is also identified by flow cytometry when it is performed on B cells that have been cultured for 6 days from mBC. This validates that the cells detected in the *ex-vivo* ASC and mBC ELISPOT are phenotypically identical in the context of this flow panel, even if derived from distinct populations. This experiment also showed that following culture, a population of atypical B cells ($CD21^{-}$, $CD27^{-}$) are expanded that also appear to have 'plasma cell-like' phenotype ($CD20^{-}$, $CD38^{+}$). Although the majority of mBC-derived ASC plated on the *ex-vivo* mBC ELISPOT have been shown to be plasma cells, other subsets present could also contribute to antibody detected in this assay, in particular the activated mBC population that might subsequently mature during overnight incubation. Whilst this is not a fundamental problem, before selecting the plasma cell population ($CD19^{+}$/$CD27^{+}$/$CD20^{-}$/$CD21^{-}$/$CD38^{+}$) for single cell sorting, I wanted to confirm

that the majority of the antigen-specific B cells were within this population at the d63 time-point. As expected, when gating cells using the complete gating strategy including CD38 the greatest proportion of antigen-specific cells was achieved, as detected by an adapted *ex-vivo* ASC ELISPOT. Interestingly, the activated mBC population also contained a proportion of cells capable of secreting antigen-specific IgG and not selecting on $CD38^+$ didn't greatly reduce numbers. This may be an artefact of the polyclonal stimulation and may not apply to fresh cells, although this has not been looked into further. These cell subsets may also be maturing to $CD38^+$ plasma cells during the overnight incubation in the ASC ELISPOT and it must be noted that when sorting single cells into 96 well plates (rather than ELISPOT plates) they will be flash frozen. Therefore despite the presence of antigen-specific cells in other populations, the final single sort protocol includes CD38 staining to ensure maximal yield from fresh cells immediately after sorting.

During the process of adapting the flow panel to be used for MoFlo rather than on the LSRII, a number of additional steps were added to the protocol to try and increase the number of antigen-specific, IgG^+ cells that are selected. Firstly, concentrations of antibody used for staining were increased, followed by the enrichment of B cells using the Pan B cell kit. This maximised the staining of target populations, removed background and allowed for more accurate gating of cells. On top of this, the addition of IgM and IgG to the panel also appeared to possibly increase gating efficiency. Whilst it has been previously shown that plasma cells can be stained for surface IgM [338] there is little to show the same for IgG. However, data here show IgG^+ cells can be identified in the plasma cell pool after sorting by ELISPOT, although not with 100% effectiveness. It is however possible that stress from MoFlo sorting reduces IgG secretion in sorted cells, backed up by the observation of reduced spot size and number in these ELISPOTs. Typically 5 million enriched and stained PBMC were selected for their IgG^+ plasma cell population and sorted into half a 96 well plate. As will be shown in the next Chapter, this population did

contain antigen-specific IgG^+ cells, although there is still room for improvement regarding their frequency.

One possible way of improving the sorting frequency of antigen-specific cells is to include biotinylated antigen in the staining procedure that when bound to cells can be detected by using a fluorophore conjugated to streptavidin. This method has been effectively used for both flu and HIV antigens for mBC and plasma cells, but has been previously reported to be problematic for the malaria antigens MSP1 and AMA1 [278]. It was claimed that the reason for this was that these antigens are extremely 'sticky', and gave very high levels of background due to non-specific binding. Unfortunately the same problem was encountered here when using basic staining methods to test for antigen-specific B cell populations. In some cases there was positive staining at d0 when there should be no antigen-specific cells present, in others, cells stained strongly with antigen the person had not been previously vaccinated with, often more so than when using the antigen they had been. Strangely there were also problems with different antigens and different fluorochrome combinations, although reassuringly there was no problem with non-specific binding of the streptavidin conjugated fluorophore itself. Following this it was decided to attempt a dual staining protocol. Whilst it is possible that antigen-specific populations are of low frequency, the previous literature for this technique claims high sensitivity. Similarly it is claimed that the likelihood of double stained background populations is low. Whilst strong single stained populations were observed these were dismissed as background, and whilst there were little to no background staining in the double positive gates, any real double staining is not convincing enough to incorporate into any single cell sorting panel, especially when the panel is limited to 6 colours and mBC populations should be easier to stain than plasma cells.

Whilst antigen-specific staining has failed for the antigens MSP1 and AMA1 in this set of experiments, the techniques here may be more successful for other malaria antigens, perhaps those that are smaller

or less ‘sticky’. The fact most success in antigen-specific staining has been achieved for small viral antigens may support this observation. Newer techniques for antigen-specific staining are currently under development which may be able to help overcome many of the problems observed here with these blood-stage antigens. These involve the use of antigen tetramers, targeted biotinylation to specific sites and inclusion of steps to remove unbound/loosely bound antigen from cell populations before detection. Therefore it may be just a matter of revisiting this problem at a later date. In the meantime the protocol I have is sufficient for the required task of sorting at least a small number of single antigen-specific plasma cells into a plate ready for production of monoclonal antibodies. How this is achieved in the topic of the next Chapter.

6. Production and Characterisation of Human Monoclonal Antibodies

6.1. Authorship Statement

The work presented in this chapter is part of a collaborative effort to set in place the framework for the generation and analysis of human monoclonal antibodies at the Jenner Institute, University of Oxford.

RT-PCR and nested PCR were performed by Sean Elias.

Daniel Alanine developed the CPEC BCR cloning method, performed modifications to the expression plasmids and designed the CPEC primers described in this chapter.

Transformations, screening and transfections were performed by Sean Elias and Daniel Alanine.

Daniel Alanine performed the ELISA and Western blot analyses.

Rebecca Brown performed the GIA experiments.

6.2. Introduction

In the previous Chapter it was discussed how it was possible to isolate and sort single plasma cells into 96 well plates using MoFlo. At 7 days post-booster vaccination a large proportion of plasma cells found in the peripheral blood would be expected to be antigen-specific, and data previously presented in this Thesis have shown this to be true following vaccination with blood-stage malaria antigens. It was hoped that antigen-specific staining could be utilised to maximise the proportion of antigen-specific plasma cells isolated during MoFlo sorting (Chapter 5). Whilst this unfortunately wasn't possible, MoFlo sorting of plasma cells defined as $CD19^{+}/CD27^{+}/CD20^{-}/CD21^{-}/CD38^{+}/IgG^{+}$, yielded on average >10% of cells that are capable of secreting antigen-specific antibody post-sorting as shown by ELISPOT. MoFlo sorted cells were sorted into 48 wells (half a plate) of a 96 well plate (Fig.5.5). Each well contained catch buffer containing RNasin – an RNase inhibitor that functions to preserve the RNA transcripts coding for the

antigen-specific BCR within the plasma cell. Using RT-PCR (and relatively well-established methodologies), these transcripts can be transcribed and amplified for a number of purposes, including characterisation of BCR gene usage, studying somatic hypermutation and for the production of functional human monoclonal antibodies (mAbs)[81, 263, 331, 342]. In this Chapter the primary aim of the work was to identify, express and characterise functional AMA1-specific human mAbs from plasma cells identified from the peripheral blood of volunteers 7 days post-boost, as proof of principle. Notably these techniques have not yet been applied or reported in the malaria vaccine field.

There are a number of reasons for identifying and producing antigen-specific human monoclonal antibodies. The ability to identify antibodies with high neutralising activity on target pathogens has an obvious application as a therapeutic or prophylactic agent. In particular the development of Adeno-associated virus (AAV) vectored immune-prophylaxis (VIP) allows for high-dose delivery of mAbs over a prolonged period [343, 344]. However many antibodies have been shown to be highly strain-specific, and so would be less useful in the broad treatment of disease. Therefor one area of particular interest is the identification of broadly-neutralising mAbs (bNAbs). These antibodies have been shown to be cross-strain neutralising in a number of difficult-to-target viral pathogens, such as HIV and Influenza, and their presence in exposed individuals often correlates with better prognosis [283-285]. Isolation and production of mAbs with these rare, but highly protective specificities, may offer promise in the field of therapeutics, but understanding what conditions lead to their induction can also be applied to vaccine production. Understanding the antigenic targets and fine specificities of antibody binding is also of particular relevance in vaccine development. Crystallography can also be used to characterise binding sites of antibody/antigen and whether these epitopes are conformational or not [333, 334]. Looking at competition or synergy between antibodies can also inform about the breadth of the response and factors that contribute positively or negatively to pathogen neutralisation [119]. When fed back into vaccine design and production, such understanding can help in selection of specific antigen variants or

immunogen design; or selection of epitope-rich regions within an antigen as vaccine candidates. These strategies seek to maximise induction of antibodies of interest, whilst avoiding induction of diversionary antibody specificities (e.g. possibly MSP1 as previously discussed); original antigenic sin (e.g. dengue [319]); production of antibodies against non-neutralising epitopes (e.g. HIV [345]); or induction of non-cytophylic antibody subtypes (e.g. malaria [346]).

A number of different methods have been utilised over the years in the production of mAbs. Older methods relied on immortalisation of B cells using Epstein-Barr virus (EBV) [288] and the production of hybridomas [289]; humanisation of mouse antibodies[290]; chimerisation [291]; or the use of phage display libraries [292]. Such methods are often low throughput and low efficiency and have more recently been replaced with expression vector cloning methods which have been shown to be much more specific and higher throughput [293, 294]. To summarise, this more recent methodology involves using RT-PCR and nested PCR to amplify the VDJ heavy genes and VJ light genes from single sorted B cells, followed by cloning into specific vectors containing human IgG1 heavy and light (Kappa or Lambda) backbones. Plasmids encoding the heavy and light chain pairs are then transiently transfected into mammalian cell lines that will secrete Ab, which can be screened for antigen specificity. It has been quoted that this method can provide large quantities of mAb in as little as 28 days[294]. Here this method was utilised with some small adjustments to further save time and reduce costs. For each AMA1-specific human mAb produced, data are provided for the V(D)J usage, distance from germ line sequence, yield and ability to neutralise parasite growth using the assay of Growth Inhibitory Activity (GIA). Although the focus here is on AMA1 mAbs, this method can be applied to any vaccine antigen of interest and in future studies mAbs will be of particular interest in regimes where protective efficacy is observed.

It is also important to note that the work described in the Chapter was seeking to establish this methodology in our laboratory for the first time, and despite published protocols [293, 294], a number of steps have required a significant amount of optimisation. The Results below describe these preliminary studies followed by a Discussion of on-going optimisation.

6.3. Results

6.3.1. RT-PCR, Nested PCR and identification of heavy and light chains genes of the BCR

I initially sought to establish these methods in the lab with available PBMC samples from the AMA1 clinical trials. In Chapter 5 it was shown how single $CD38^+$ 'plasma cells' could be MoFlo sorted as single cells into either individual wells of a 96 well plate containing RNA stabilisation buffer, or onto an ELISPOT plate to quantify the frequency of IgG and antigen-specific cells. Sorting of fresh PBMC typically resulted in a positive hit rate of around 10% for AMA1 and 12% IgG by ASC ELISPOT, as shown previously in Figure 5.5. This process was also performed on PBMC that have previously been frozen, however this appeared to reduce the positive hit rate to around 5% and 10% respectively for AMA1 and IgG. These numbers are important to note, especially when assessing the proportion of AMA1-specific and IgG mAbs detected during screening however it is possible that the stress of the sorting process causes cells to stop secreting IgG, which would influence detection by ELISPOT but not by PCR screening.

For the initial experimental run frozen PBMC were thawed from two time-points from one volunteer in VAC044 G1 (volunteer #1017), at d63 and d119. Fresh *ex-vivo* ASC ELISPOT had previously been performed on this volunteer at both d63 and d119 and suggested that up to 20% of IgG^+ ASC at these time points are $AMA1^+$ (Table 6.1). Cells from these two time points were sorted into PCR plates as described in Chapter 5. Post-MoFlo ASC ELISPOT was not performed on these cells.

Initially one plate of each of d63 and d119 single cells underwent RT-PCR followed by nested PCR as described in Materials and Methods (2.7.1). For the d63 plate, 13 out of 48 (27%) wells were positive for heavy chain initially. When these 13 wells were screened for kappa and lambda light chains, 5 were positive for kappa and 1 for lambda giving a final complete IgG^+ hit rate of 6/48 (12.5%).Figure 6.1 shows nested PCR products for these 6 positive wells. For the d119 plate, only 6 out of 48 (12.5%) wells were

positive for heavy chain initially with 4 subsequently positive for kappa and 0 for lambda, giving a final complete IgG^+ hit rate of 4/48 (8.33%). Although these hit rates are relatively low I continued to produce human mAbs with the available gene sequences. PCR optimisation has since been undertaken (see Discussion) and suggests that in this initial experiment the number of heavy and light chain positive wells was likely underestimated.

#1017	ASC ELISPOT	
	AMA1+ ASC/million PBMC	AMA1+ ASC as % total IgG
d63	102	13.8
d119	132	20.3

Table 6.1: Volunteer #1017 ASC ELISPOT responses

Ex-vivo ASC ELISPOT was performed on volunteer #1017 at d63 and d119 using fresh PBMC (as described in materials and methods 2.5.4). #1017 was selected from Group 1 of the VAC044 clinical trial. Further characterisation of ASC responses in VAC044 can be found in Chapter 7 (7.3.1).

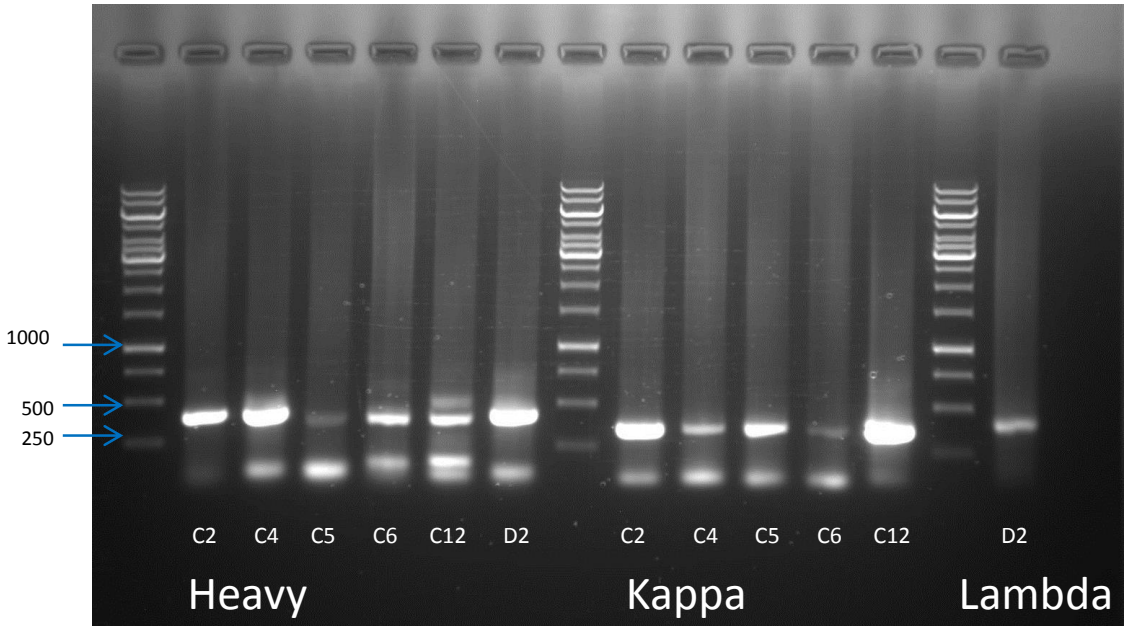


Figure 6.1: Positive nested PCR products from screen of volunteer #1017 at d63.

Nested PCR was performed independently on RT-PCR product for heavy, kappa and lambda chain sequences using specific forward and reverse primer mixes. PCR product was run on a 1% agarose gel for 40 min at 100 V. 1 kbp smart ladder run as reference DNA with positive PCR products identified as a 400 bp band.

6.3.2. Circular Polymerase Extension Cloning (CPEC) of heavy and light chain genes into expression vectors

Published methodology uses labour-intensive restriction enzyme cloning of the Ab chain PCR products [293, 294]. In parallel to my work on the above PCR, a novel restriction enzyme-independent cloning system was being established by Daniel Alanine using CPEC methodology [306], which should allow for more rapid and high-throughput cloning of these genes into the expression plasmids by PCR. In order to test this method for the first time using genes isolated from human B cells, CPEC PCR was performed on 5 of the initial 10 IgG matching heavy and light chain pair nested PCR products, in order to produce insert fragments with homology regions matching the expression plasmid backbones (Fig.6.2A). Plasmids independently underwent PCR for linearisation (Fig. 6.2B). Insert and linearised plasmid subsequently underwent CPEC at a 1:1 molar ratio. Cloned plasmids were then transformed into *E. coli* and screened for colonies containing correctly sized inserts (Fig. 6.2C-E). Single correct sized plasmids were selected for each heavy and light chain pair. Plasmids were then sent off for sequencing (Source Bioscience) to confirm the heavy and light chain inserts were cloned in frame and could theoretically produce viable antibody. Of the initial 10 IgG pairs, 5 were successfully cloned by this method and pairs of plasmids were subsequently bulked up by midi-prep. The five plasmid pairs were named: C2(H1K4), D2(H3L8), and D10(H3L7) [from volunteer #1017 d63]; and B8(H3K6) and B9(H1K3) [from #1017 d119]. Numbers in brackets refer to the colonies screened.

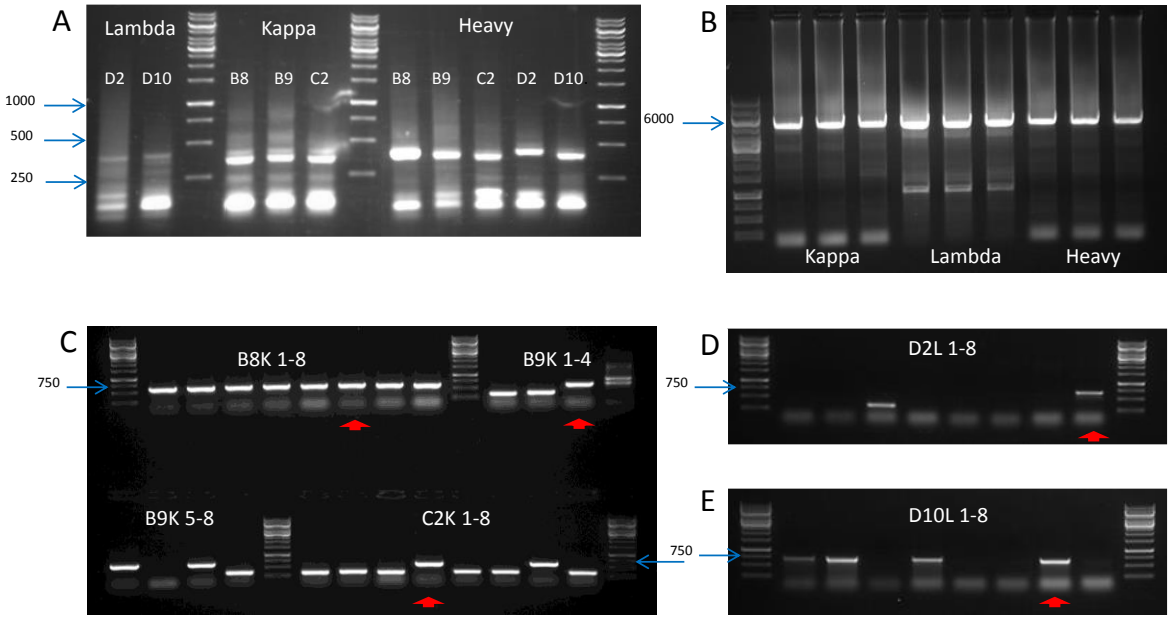


Figure 6.2: Circular Polymerase Extension Cloning

A) Purified nested PCR product underwent PCR to generate an insert of around 440 bp with homology regions complementary to the backbone. B) The expression plasmid backbones for Heavy, Kappa and Lambda were linearised to give a band at around 4000 bp. Insert and backbone are gel extracted, purified and annealed via CPEC. Heavy and light chain pairs were then independently transformed into *E. coli* and screened for positive colonies. Typically 8 colonies were screened per transformation for Heavy (not shown), Kappa (C) and Lambda (D-E) prospective candidates. Correct sized bands were roughly 600-700bp, with this dependent on individual VDJ or VD sequence lengths. Red arrows indicate colonies selected for subsequent gel purification, mini-prep and sequencing. 1 kbp smart ladder was run as reference DNA. Bands of incorrect size were not acknowledged for insert or backbone PCR. A select number of the smaller bands were sequenced from the colony screens to confirm they were not complete VDJ or VD sequences.

6.3.3. HEK293 transfection and screening for antigen-specific IgG

Adherent HEK293A cells were transfected with the 5 paired heavy and light chain IgG plasmids, C2(H1K4), D2(H3L8), D10(H3L7), B8(H3K6) and B9(H1K3), initially in a 96 well plate format to allow screening. After 2-3 days supernatant was harvested and screened by ELISA for IgG and AMA1 specificity. Both conditioned HEK293 supernatant and mock transfection controls were also run by ELISA. All five supernatants screened positive for human IgG by ELISA, but only C2(H1K4) and D2(H3L8) were positive for AMA1 protein recognition, including both the 3D7 and FVO allelic versions (Fig. 6.3). Western blot was also performed on these two ELISA positive mAbs (Fig. 6.4). Using a denatured SDS-PAGE gel, both C2(H1K4) and D2(H3L8) mAbs were shown to recognise both 3D7 and FVO protein. These two AMA1 positive transfections were then repeated on a larger scale in HEK293E suspension cells, with IgG yield around 60 μg/mL for both mAbs.

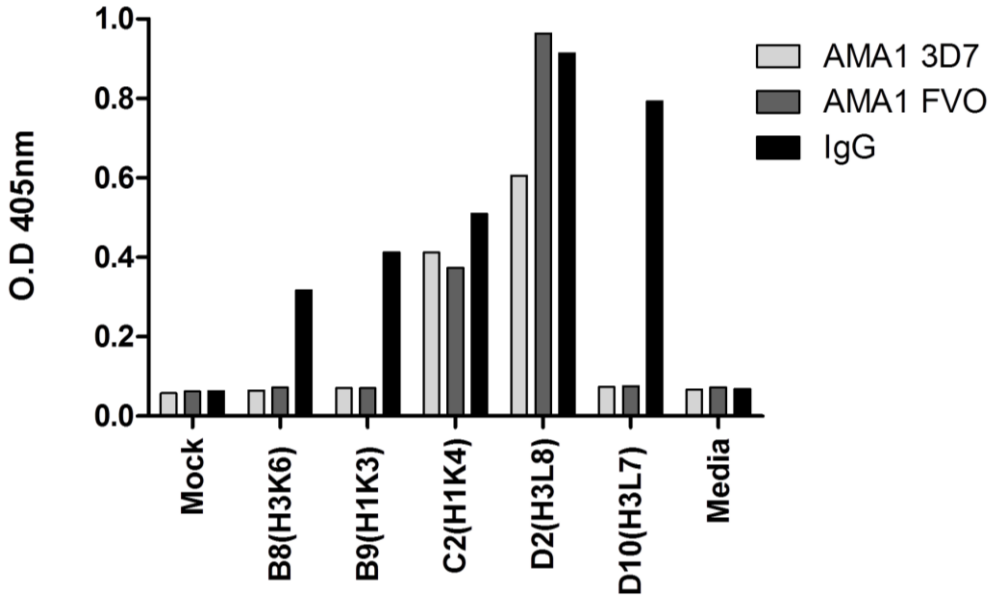


Figure 6.3: mAb ELISA Screen

96 well plate transfection supernatant was run on a standardised ELISA for human IgG and both AMA1 3D7 and FVO protein. Five mAbs B8(H3K6), B9(H1K3), C2(H1K4), D2(H3L8) and D10(H3L7) were tested alongside negative controls in the form of a mock transfection with PEI and H_20 (Mock) and conditioned media in which HEK293 cells have previously been grown (Media).

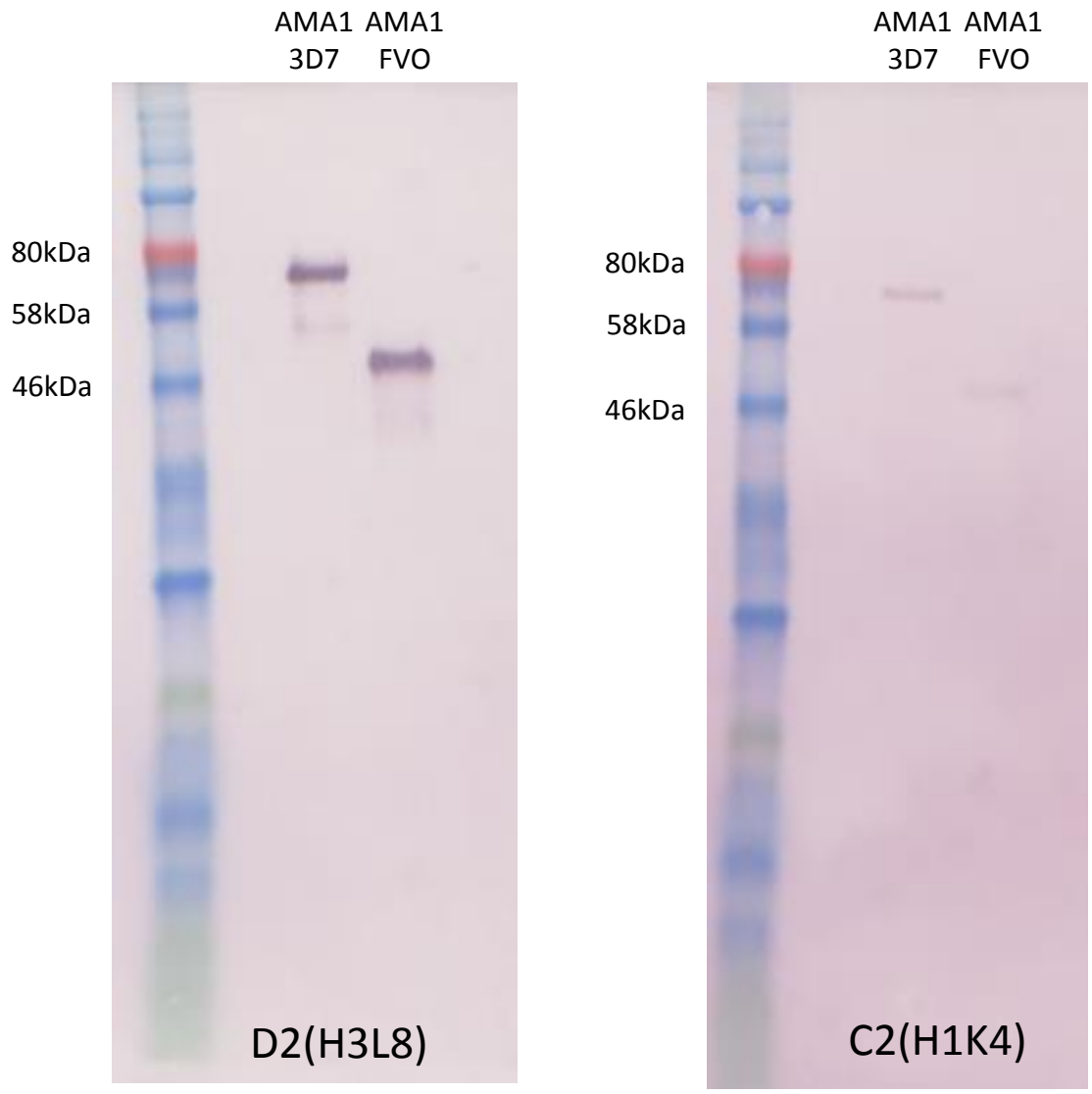


Figure 6.4: Western Blot of the mAbs C2(H1K4) and D2(H3L8)

150 µg of each of 3D7 (66 kDa fragment) and FVO (48 kDa fragment) AMA1 protein was run on lanes of a denaturing SDS-PAGE gel. Full length 83kDa AMA1 protein, located in the apical complex is cleaved to the 66 kDa fragment post-synthesis by removal of an N-terminal peptide. In mature merozoites the 66 kDa fragment translocates to the parasite surface where it is circumferentially redistributed and undergoes two C-terminal cleavages to give rise to 48- and 44-kDa soluble forms. 1 µg/mL C2(H1K4) and D2(H3L8) mAbs bound both proteins fragments and were detected by use of goat anti-human gamma chain specific secondary antibody.

6.3.4. Sequence analysis of AMA1-specific human mAbs

A summary of the IgG gene sequencing data for the two AMA1-specific human mAbs C2(H1K4) and D2(H3L8) is shown in Table 6.2. Overall only small deviations from germline sequences are observed for both mAbs in both their heavy and light chains. When this is refined to look at the three CDR loops in the V regions of the heavy and light chains, there is little to no somatic hypermutation of the heavy chains, but there is in both the kappa and lambda chains, particularly in the hypervariable CDR3 region.

mAb	Chain	Top V gene match	Top D gene match	Top J gene match	Total similarity to germline sequence	Mismatches
C2	Heavy	IGHV4-39*07	IGHD3-10*02, IGHD1-7*01 ,IGHD3-10*01	IGHJ4*02	96.9%	9
	Kappa	IGKV1-5*03		IGKJ3*01	97.9%	6
D2	Heavy	IGHV1-8*01	IGHD2-2*02	IGHJ6*02	99.3%	2
	Lambda	IGLV3-25*02		IGLJ2*01,IGLJ3*01	96.9%	9

mAb	Chain	(V)CDR1 Length	% similarity to germline sequence	(V) CDR2 Length	% similarity to germline sequence	(V) CDR3 Length	% similarity to germline sequence
C2	Heavy	30	100.0%	21	95.2%	5	100.0%
	Kappa	18	94.4%	9	100.0%	23	82.6%
D2	Heavy	24	100.0%	24	100.0%	8	100.0%
	Lambda	18	100.0%	9	100.0%	27	88.9%

Table 6.2: Sequencing information of AMA1-specific human mAbs

IgG heavy and light chain sequence identification generated through the online analysis programme IGBLAST. Each Heavy and Light (Kappa or Lambda) chain sequence has its respective VDJ or VJ sequence compared to a library of germ line sequences and the closest match identified. In some cases, top matches may be quoted. Total similarity to germline sequence is the % value of combined top matched VDJ sequences. The length of the CDR loops 1, 2 and 3 within each V region are given in base pairs, and similarity to germline sequence given as a % value.

6.3.5. Assay of Growth Inhibitory Activity (GIA)

The two AMA1-specific mAbs C2(H1K4) and D2(H3L8) were subsequently tested for *in vitro* growth inhibitory activity against *P. falciparum* using the GIA assay. mAbs were diluted to test concentrations of 1 mg/mL, 0.5 mg/mL, 0.25 mg/mL, 0.125 mg/mL, 0.0625 mg/mL, 0.03 mg/mL, 0.016 mg/mL and 0.008 mg/mL. GIA assay results are shown in Figure 6.5. For both the 3D7 and FVO strains of the parasite C2(H1K4) gave significant levels of growth inhibition (3D7: >95% down to 0.25 mg/mL, FVO: >90% down to 0.5 mg/mL), whilst D2(H3L8)showed no inhibition for either strain at any concentration (Fig. 6.5A/B). The IC_{50} for C2(H1K4) was determined in these experiments as 0.09 mg/mL for 3D7 and 0.15 mg/mL for FVO (Fig.6.5C/D).

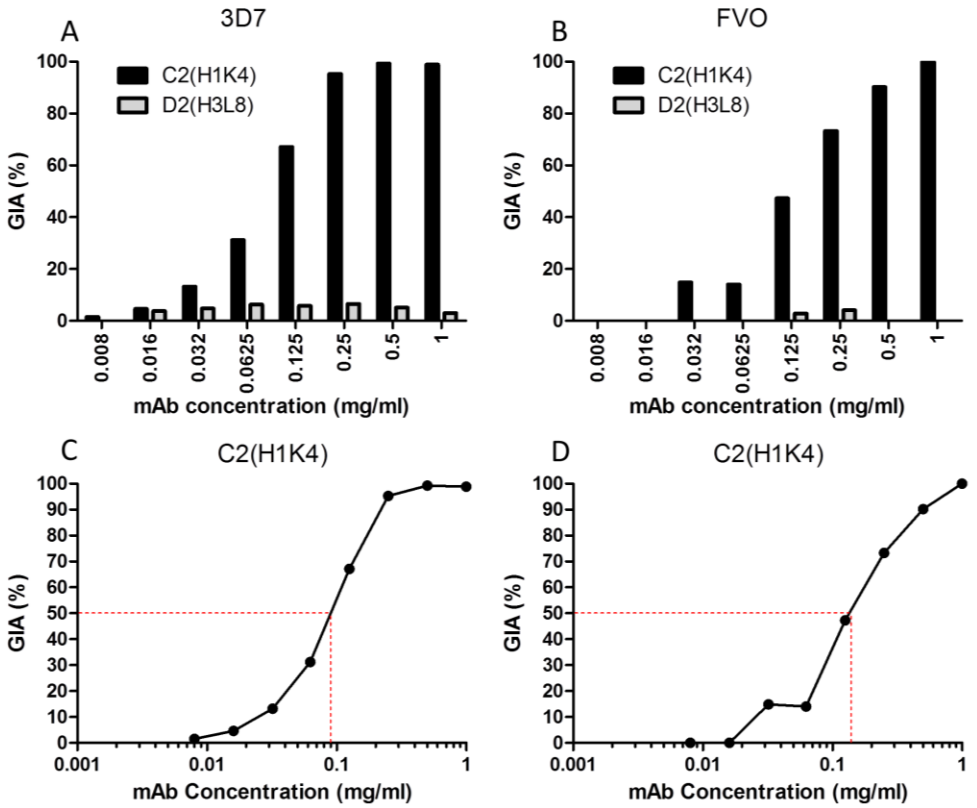


Figure 6.5: Assay of Growth Inhibitory Activity (GIA)

The % growth inhibitory activity of the mAbs C2(H1K4) and D2(H3L8) against 3D7 clone parasites (A) and FVO strain parasites (B) at concentrations titrated from 1 mg/mL – 0.008 mg/mL. The IC_{50} of C2(H1K4), the mAb concentration required to give 50% GIA against 3D7 (C) and FVO (D) parasite strains.

6.4. Discussion

In this Chapter I have provided proof of principle for the production of AMA1-specific human mAbs, from IgG^+ ASC isolated at d7 post-boost. The preliminary results described were generated using established methods [293, 294], with alterations such as the use of CPEC described in Results. Using this method, despite ultimately isolating two AMA1-specific mAbs, I found the ratio of heavy and light chain pairs detected by nested PCR disappointing compared to reported literature. Since completing the work in this Chapter, on-going studies have sought to optimise the RT-PCR and nested PCR. I have assessed temperature gradients, new reagents, MgCl2 concentration and reaction volumes. These studies have shown that the nested PCR efficiency is greatly improved by using reduced template volumes in each reaction. A typical plate of 48 single sorted B cells now yields on average a 50% success rate more in line with reported literature. In subsequent studies this should allow screening of a larger panel of candidate mAbs from each plate.

The two AMA1-specific mAbs generated here are the first fully human mAbs generated against this antigen. Previously, the only AMA1-specific mAbs described in the literature are derived from mice or rats. Two of these are well characterised, 4G2 [347, 348] and 1F9 [164, 349, 350]. 4G2 has been shown to bind the D2 loop of AMA1 and displays broad strain specificity, while 1F9 binds the hydrophobic trough and is highly vaccine strain-specific (3D7). In both cases, binding of both the heavy and light chains has been shown to be important, with CDR2 and CDR3 from the light chain and CDR3 from the heavy chain key for 1F9. Both antibodies are quoted to give a modest 20% growth inhibition at 1 mg/mL with the mechanism of action proposed to be through preventing AMA1 binding to its ligand RON2 [159]. More recently, a new panel of mouse AMA1-specific mAbs have been described [166]. Of these, the most potent (≈65% growth inhibition at 1 mg/mL, IC_{50} 0.25-0.35 mg/mL) were shown to target the D1 region of AMA1 (particularly the 1e loop), were broadly neutralising and blocked RON2 binding. While many other mAbs were non-neutralising, one other showed low level growth inhibition by a

different mechanism, preventing proteolytic processing of AMA1 and leaving increased levels of an anomalous 53 kDa product. This mAb was also broadly neutralising, recognised the D3 loop and showed synergy with 4G2.

Though such in depth analysis has not yet been performed on the mAbs C2(H1K4) and D2(H3L8), there are a number of comparisons, conclusions and hypotheses that can be drawn from the available data. Firstly all the described binding sights for the above mouse mAbs can be found in the vaccine construct used to vaccinate the individual from whom these human mAbs were isolated, so in theory C2(H1K4) and D2(H3L8) could bind to a previously described site. The vaccine constructs used in the VAC044 clinical trial was also biallelic (3D7 and FVO), with the aim of generating broadly neutralising antibodies, much in the way a tetravalent vaccine was used to successfully generate the new mouse mAbs mentioned above [166]. It should be noted that since the time of the design of the vaccines tested in VAC044, consensus in the field has suggested at least three (and preferably four or five) alleles of AMA1 are required to induce broadly-reactive IgG responses [165, 351]. ELISA and Western blot analysis show that both human mAbs recognise the 3D7 and FVO alleles of AMA1, with D2(H3L8) possibly having stronger affinity for FVO. In the Western blot, the FVO protein used was the 48 kDa fragment (a processing product of the parasite, shed during red blood cell invasion), whilst the 3D7 protein used was the full-length 66 kDa ectodomain (lacking the N-terminal pro-domain). The observation that both human mAbs recognise both fragments implies that the binding site of these mAbs is found in the 48 kDa fragment. Another conclusion from the Western blot is that the strong binding and fast development of D2(H3L8) may suggest that this mAb recognises a linear (or at least, not entirely conformational) epitope and that the affinity is likely to be reasonably strong. The C2(H1K4) blot was slower to develop and weaker, possibly suggesting this antibody recognises a conformational epitope or that the affinity of this antibody is generally lower than D2(H3L8).

The most potent of the previously described mouse mAbs recognised the D1 1e loop region of AMA1 and blocked RON2 binding, with growth inhibition of between 50-80% across 5-6 different strains at 1 mg/mL and an IC_{50} of around 0.25-0.35 mg/mL[166]. Alternatively 1F9 recognises the hydrophobic trough of D1, similarly blocking RON2 binding but with growth inhibition of around 20% only to 3D7 and an IC_{50} exceeding 2 mg/mL. C2(H1K4) outperforms these mouse mAbs with >95% growth inhibition down to 0.25 mg/mL and a predicted IC_{50} or around 0.09 mg/mL. Confirmation is required, however, as to the exact binding site of C2(H1K4), and to the extent of its GIA against non-vaccine strains of *P. falciparum*. In contrast to the inhibitory mouse mAbs that recognise the D1 region, a number of mAbs were previously described that recognise both the D2 and D3 loops of AMA1 with broad cross-strain specificity, but which had no growth inhibitory activity. The human mAb D2(H3L8) appears to fall into this category, but again, its binding site currently remains undetermined.

Previous characterisation of the mouse mAb 1F9 showed that CDR2 and CDR3 from the light chain and CDR3 from the heavy chain were key to functionality [350]. The human mAb C2(H1K4) sequence is very different to 1F9 ([350] supplemental data), but it has a similarly short heavy CD3 region. For C2(H1K4), the Kappa CDR3 loop displays the most significant somatic hypermutation, whilst the CDR2 loop is short and of germline origin, implying Kappa CDR3 may be important for function. Further investigation is clearly required to confirm this speculation.

Whilst the discovery of a broadly neutralising, strongly inhibitory human mAb is greatly encouraging it is important to place it in context of the larger picture. The two mAbs, C2(H1K4) and D2(H3L8), were isolated from one volunteer (#1017) post-MVA-boost (d63). At the peak of this individual's antibody response (d84), their AMA1-specific antibody titre was around the group median, with AMA1-specific IgG calculated to be 38 μg/mL. Growth inhibition of polyclonal IgG at 10 mg/mL against 3D7 was only 12%. After the second protein-in-adjuvant (+CPG 7909) vaccination this individual's antibody titre did

not boost and growth inhibition remained the same in contrast to most other individuals in the same group. There are a number of possible interpretations of this, although most is just speculation at this stage. It is likely that the C2(H1K4) antibody comprises a very minor component of the total IgG responses and therefore is not at a sufficient concentration to effect parasite growth at serum concentrations of total IgG. Even if C2(H1K4) comprised 100% of the 38 μg/mL predicted AMA1-specific antibody in this volunteer, we would expect at best 20% GIA. It is also possible that there are other antibodies with higher affinity for the same binding site as C2(H1K4) that out-compete it yet provide no protection. As for the lack of improvement in either AMA1-specific antibody titre or growth inhibition in this individual after the second boost, it is possible that the epitope for C2(H1K4) (or other inhibitory antibodies) is not as well presented in the context of protein-in-adjuvant (+CPG 7909) vaccination compared to MVA vaccination. Clearly it is difficult to draw definitive conclusions from such a small sample of only two mAbs isolated on day 7 post-boost. Future studies will aim to expand this work and characterise a large number of mAbs from different individuals after different vaccination regimens, to get a better feel for the repertoire of antibodies induced. Notably, the process of mAb isolation is still time-consuming and expensive and requires further optimisation (see below). Given that AMA1-based vaccines have yet to be shown to be efficacious in clinical trials, it may be that such detailed analyses would be better suited to characterising mAbs against alternative antigen candidates. Indeed, the PfRH5 antigen is now the leading candidate antigen in clinical development by our group [116, 119]. A mouse mAb raised against this antigen has the most potent IC_{50} yet reported against the blood-stage malaria parasite (15 μg/mL)[170], which bodes well for the human studies (initiated in August 2014), given the first human mAb isolated here against AMA1 is more potent than any mAb reported from mice.

7. Association of peripheral blood T follicular helper cell populations with vaccine induced antibody and B cell responses

7.1. Authorship Statement

This chapter was conceived as collaboration between Sean Elias, Simon Draper (Jenner institute, University of Oxford), Persephone Borrow and Cecilia Chui (Nuffield Dept. Medicine, University of Oxford).

Flow panels used to characterise T follicular helper cells were developed by Cecilia Chui.

Sean Elias and Cecilia Chui performed the flow cytometry experiments.

Flow cytometry data were analysed by Sean Elias.

B cell data presented in this chapter were the work of Sean Elias. Data are also published in a manuscript in *Molecular Therapy* 2014 [301].

7.2. Introduction

T follicular helper cells (Tfh) play critical role in the T-dependent antibody response. This $CD4^+$ T cell population was initially described in humans in the tonsils as defined by the expression of the Germinal Centre (GC) migratory marker CXC Chemokine Receptor 5 (CXCR5) and the ability to induce antibody production by providing help to B cells [352]. Work on mouse models has yielded more information into the exact role of these cells in the GC, with knockouts of Tfh markers often key to our understanding of their role. Whilst mouse Tfh do differ slightly from human populations [78], the inaccessibility of lymphoid organs in humans other than tonsils (due to ethical considerations) has limited the in-depth replication of such mouse work. However, the studies that have managed to look at human GC Tfh

populations found expected levels of up-regulation in the key markers and high levels of helper activity for B cells [353], reflecting, to an extent, observations seen in mouse studies.

The interactions of Tfh cells with the other cells of the secondary lymphoid organs and the key molecules involved in these interactions are shown in Figure 7.1 [354]. A number of models have historically been proposed for Tfh differentiation and interaction with such cells but recent evidence seems to promote a multistage, multifactorial model [78]. During antigen exposure from either vaccination or infection, DCs will present antigen via MHC class II to naïve $CD4^+$ Th cells in the T cell zone of secondary lymphoid organs and induce proliferation to an effector Th (pre-Tfh) population [64]. Activated Th cells migrate towards the B cell follicle in a process proposed to be dependent on selective expression of the chemokine receptors CXCR5 and CCR7 [65, 66]. Whilst CXCR5 up-regulation allows increased migration towards the chemokine CXCL13, found in GCs, CCR7 is down-regulated, with high expression blocking this migration [355]. At the boundary of the T cell zone and B cell follicle these antigen primed effector Tfh cells form a synapse with antigen-specific B cells which involves a large number of receptors and cytokines [71] and provides an important step for the differentiation of both subsets . This effector Tfh population is also that which was first observed in human tonsils [352] and mouse GC [356]. Important interactions at this point include CD40 and CD40L (CD154), ICOSL and ICOS, PD-1 and PDL-1 as well as SA and SLAM family receptors. The CD40-CD40L interaction in particular is critical for class switch recombination (CSR) during this interaction [357] whilst IL-21 also plays an important role. CSR is strongly influenced by the polarisation (Th1, Th2, Th17) of the T cells providing help at this stage [54] (Figure 1.3). It has been discussed at great length as to exactly when Th cells obtain such polarisation and whether it is independent of Tfh differentiation or not [78]. Either way, these polarised subsets can be identified by differential cytokine expression (IFN-γ, IL-4, and TGF-β, Fig.1.3).

Following these interactions there is a split in B cell lineage commitment either into extra follicular plasmablasts, which go on to form short lived plasma cells (SLPCs) or into the germinal centre memory pathway, of which some are proposed to form early memory populations. Tfh also undergo lineage commitment, with those cells with the highest expression of key Tfh markers, particularly CXCR5, PD-1 and Bcl6 [65] contributing to GC formation alongside memory lineage B cells and follicular dendritic cells (FDC). During initiation of the GC, GC Tfh cells induce B cell differentiation through stimulation of Bcl6 expression in combination with survival signals including CD40L [357], IL-4 [80] and BAFF [358]. In addition GC Tfh cells also provide proliferation signals to B cells including PD-1 [359] and IL-21 [360, 361], which are expressed at higher levels in GC Tfh compared to earlier Tfh populations. In the absence of these signals, GC Tfh cells will induce apoptosis in GC B cells via competing Fas-FasL interactions [362]. B cells also provide return signals for GC Tfh cells that are important for their development and for GC formation such as ICOSL through ICOS, although this requirement has been shown to less critical in the presence of abundant antigen [363].During the germinal centre reaction SHM occurs, diversifying the VDJ regions of the BCR by selecting for binding affinity against antigen presented by FDC, with the process mediated through competitive interactions with GC Tfh cells and cytokine signalling [80].

After rounds of selection, B cells leave the GC reaction committed to one of two fates, classical memory B cells (mBC) or long lived plasma cells (LLPCs). Whilst the key roles of PD-1 and IL-21 signalling from GC Tfh are well established in the control of commitment to a plasma cell fate, less is currently known about the commitment signals leading to the classical memory B cell fate lineage. There is also much debate as to what happens to GC Tfh post GC reaction, with some studies suggesting formation of a GC Tfh memory population [364]. Such cells can survive in lymphoid tissue in the absence of antigen, downregulating key markers such as CXCR5 and PD-1. They can however rapidly readopt a GC Tfh phenotype following secondary antigen exposure.

Recently it has been discovered that Tfh-like populations can be found in the peripheral blood in humans, whilst an equivalent population is absent from mice [78]. These cells are $CXCR5^+$ $CD4^+$ T cells from the memory compartment as characterised by the expression of $CD45RO^+$ [352]. Whilst these cells have been shown to be typically less effective secretors of the classical Tfh cytokines as compared to Tfh or GC Tfh populations, they have been shown to be able to provide help to B cells *in vitro* following co-culture, although again less effectively compared to GC Tfh cells [353]. They also show distinct polarisation into Th1, Th2 and Th17 subsets similar to classical Tfh, with differential cytokine secretion in addition to different migratory markers including CXCR3 and CCR6 [365].

This field has opened much debate as to the origin and function of these cells as well as their relationship with classical Tfh populations. It may be that these populations are derived from GC reactions [364], or that they are an independent extra follicular-derived population [366]. Either way they provide distinct Th1, Th2 and Th17 roles much in the same way as other Tfh populations and so are likely derived from specific T-dependent responses. To address such questions, studies have looked into the presence of this population of cells both as baseline predictors of effective antibody responses or as an induced population following antigen exposure. In one HIV study, circulating $PD\text{-}1^+$, $CXCR3^-$, $CXCR5^+$, memory Tfh cells of Th2 delineation were found to correlate with the presence of broadly neutralising antibodies in infected individuals [124]. These cells were highly functional, secreting high levels of IL-21 and IL-4 and showed superior activation of mBC *in vitro* compared to other $CXCR5^+$ subsets. In a study of Tfh responses following trivalent split-virus influenza vaccination, it was observed that a distinct $ICOS^+$, $CXCR3^+$, $CXCR5^+$, $CD4^+$ population was observed to increase at 7 days post vaccination and correlated with antibody induction [125]. Typical of a Th1-type response, these cells secreted high amounts of IFN-γ whilst also secreting high levels of IL-21. Much like the memory Tfh population induced in the HIV study, these cells were also effective at helping mBC in comparison to other $CXCR5^+$ subsets. Helper

function however is not limited to $CXCR5^+$ cells, with a recent influenza study showing a functional role for $CXCR5^-$, $ICOS1^+$, $CD4^+$ T cells in the production of functional antibodies to H5N1 [367].

What such studies seem to broadly suggest is that peripheral blood $CD4^+$ 'Tfh' populations are highly flexible, with different antigens or infectious pathogens inducing or requiring different phenotypes of Tfh population, which in turn provide qualitatively different helper functions [368]. To date no-one has looked at what populations of peripheral blood Tfh are induced following vaccination with malaria vaccine antigens or exposure to malaria or whether the baseline presence of certain subsets may correlate with antibody responses. Given that most responses to malaria antigens are Th1 (typically IFN-γ dependent), and that it has been shown in Chapter 4 that $CXCR3^+$ B cells are influenced by malaria exposure, one might predict that $CXCR3^+$ T cells play an important role, perhaps in a similar way to that seen in influenza vaccine studies. Additionally the use of viral vectored and/or protein-in-adjuvant vaccine platforms may induce different phenotypes of Tfh response. Given the apparent flexibility of peripheral blood Tfh populations all subsets will be therefore be considered. An improved understanding of these responses could help to guide the design of appropriate vaccination regimens.

In the VAC044 vaccine study [301] a variety of promising 'mixed-modality' regimens were tested for the blood-stage antigen AMA1, with the aim of establishing whether different regimens improved the antibody response quantitatively or qualitatively. Three regimens in this study used the standard 8 week intervals previously described; Adenovirus-MVA-Protein/Alhydrogel + CPG 7909 (AMP^+), Adenovirus-Protein/Alhydrogel + CPG 7909 (AP+), Adenovirus- Protein/Alhydrogel (AP-). Two other regimens utilised a 16 week interval between vaccinations; Adenovirus-Protein/Alhydrogel + CPG 7909 (A_P+) and Adenovirus-MVA (A_M). The rationale for these regimens comes from a number of preclinical studies [220]. The immunological responses to these regimens have been extensively studied including T cell and antibody responses [301]. Here B cell responses are initially characterised in the manner previously

reported in Chapter 3. Then using a series of flow panels to characterise the Tfh responses in different groups, a series of key questions were addressed aiming to link these cells with quantitative and qualitative aspects of the B cell and antibody responses. In particular it is of interest whether certain baseline Tfh subsets can be observed as predictors of subsequent immune responses, or whether the induction of Tfh subsets during vaccination correlates with other aspects of functional cellular and humoral immunity.

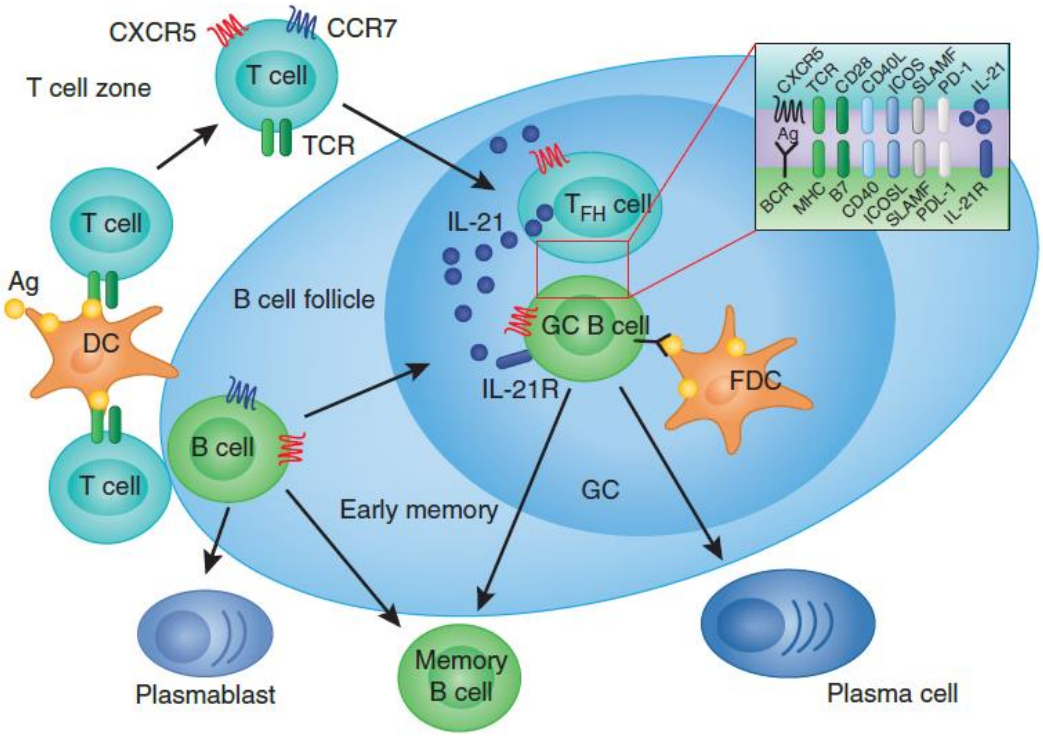


Figure 7.1: Interactions and signalling between Tfh cells and B cells during a T cell-dependent antibody response [354].

During the early stages of a T cell-dependent antibody response, T cells and B cells interact at the boundary of the T cell zone and B cell follicle. Early interactions define early B cell differentiation into plasmablasts (subsequently SLPC), early memory populations or entry into the GC reaction. At this stage class switch recombination also occurs. Migration of both T and B cells into the GC involves up-regulation of CXCR5 and down-regulation of CCR7. In the GC, interactions between Tfh, GC B cells and FDC mediate somatic hypermutation and affinity selection. A number of key surface and soluble molecules and their receptors (as displayed in the magnified inset box) are involved in all these processes. Whilst the subsequent fate of GC B cells is well defined following this interaction, less is known about Tfh cells and whether they persist in the presence of antigen or enter the peripheral blood and circulation.

7.3. Results

7.3.1. B cell responses induced by 'mixed-modality' regimens

Initially B cell responses, including mBC and ASC were characterised for these mixed modality regimens using the same methods previously described for other clinical trials (Chapter 3). This would allow characterisation of the response kinetics of the different groups and establish whether there were notable differences compared to one another or previously described AMA1 vaccine regimens.

Firstly ASC responses were characterised following booster vaccinations using *ex-vivo* ASC ELISPOT at day of vaccination and then at +1, 4, 7 and 28 days. All volunteers had a detectable peak ASC response at 7 days post boost which contracted by 4 weeks post-boost (Fig.7.2 A-E). In volunteers receiving Protein/Alhydrogel + CPG 7909 (Groups 1, 2, 4, Fig.7.2 A, B, D) ASC were first detectable at 4 days post-boost, most notably in those boosted 8 weeks after their previous vaccination (Groups 1, 2, Fig. 7.2 A, B). This observation was not made in any individuals following vaccination with MVA or Protein/Alhydrogel in the absence of CPG 7909 and all volunteers were negative for ASC at day of vaccination and one day later. In terms of the magnitude of the ASC response, the greatest number of $AMA1^+$ ASC observed by ELISPOT were in Group 4 which was significantly higher than Groups 3 and 5 (Fig.7.2 F). However when AMA1+ ASC were analysed as a proportion of IgG^+ ASC, Group 1 after second vaccination showed the largest median, although there was a broad range of responses (Fig. 7.2 G). For both measurements, Groups 3 and 5 appear to show the weakest ASC responses. In Chapter 3, only $MSP1_{19}$-specific ASC responses were reported. Group 1 d63 responses suggest that following the commonly used Ad-MVA, 8 week vaccination regimen, induction of ASC to AMA1 is higher than to $MSP1_{19}$ (median 230 vs 100 ASC per million PBMC). Peak ASC responses at d63/d119 correlated with antibody responses, strongly at the equivalent time-point (P= 0.001) but also with peak antibody

responses at d84/d140 (*P*=0.01) (Fig. 7.3 A, B). This was not previously observed in individuals vaccinated with MSP1 (data not shown in Chapter 3).

Next mBC response kinetics were characterised for the 5 vaccine groups. mBC responses showed similar kinetics across all the groups with peak response typically at 4 weeks post-boost (Fig. 7.4 A-E). Peak mBC responses were comparable between groups with around 200-250 mBC derived ASC per million cultured PBMC. In Group 1 the mBC response following MVA is notably the lowest responding group, significantly lower than Group 4 (Fig. 7.4F), however this response is comparable to previously measured AMA1 mBC responses following Ad-MVA 8 weeks apart. At the late time point d140/d190 mBC responses had contracted, but were still detectable and no significant differences were observed between groups (Fig. 7.4 G). It is worth noting that in individuals receiving proteins boosts (with or without CPG 7909) there was an increase in the number of mBC observed at d63 as compared to those receiving MVA (Groups 1-5, Fig. 7.4A-E). Additionally in Groups 1 and 4, receiving Protein/Alhydrogel + CPG 7909 there appear to be a greater range of responses across individuals at d63 and d84 (Fig 7.4 A, D). Consistent with previously reported data, there was no change to diphtheria mBC responses over time in any of the VAC044 Groups following vaccination (data not shown). mBC responses measured alternatively as mBC derived ASC as a % of total IgG+ ASC were previously shown in Chapter 3 to strongly mirror results shown as mBC derived ASC per million cultured PBMC. This was also true of responses in these regimens (data not shown).

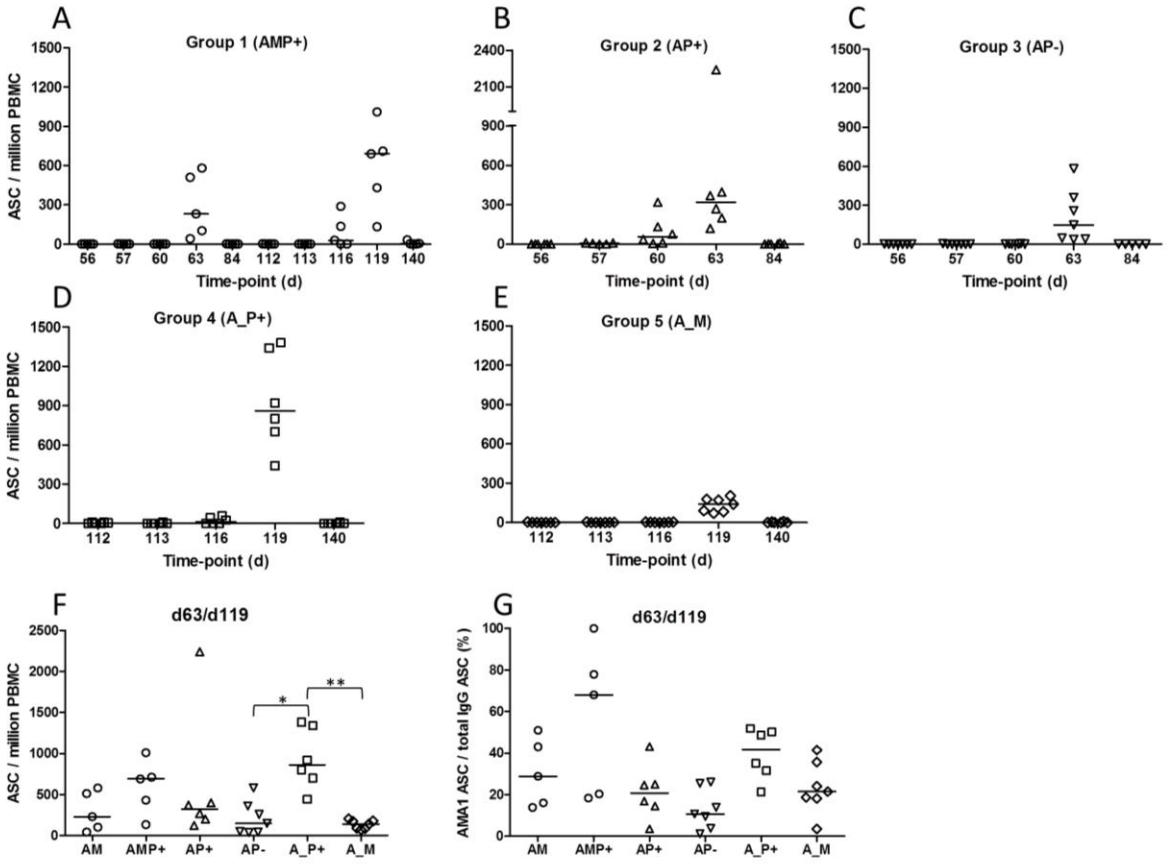


Figure 7.2: Measurement of AMA1-specific peripheral blood ASC, post- boost in mixed modality vaccine regimens.

AMA1-specific ASC responses (per million PMBC) were assessed by *ex-vivo* ELISPOT at the stated time-points after a variety of different AMA1 booster vaccinations, as part of a mixed-modality vaccine regimen. All volunteers received the same ChAd63 adenovirus prime vaccination. Vaccine regimen denoted as follows; (A) Group 1 Adenovirus-MVA-Protein/Alhydrogel + CPG 7909 (AMP+); (B) Group 2 Adenovirus- Protein/Alhydrogel + CPG 7909 (AP+); (C) Group 3 Adenovirus- Protein/Alhydrogel (AP-); (D) Group 4 Adenovirus-Protein/Alhydrogel + CPG 7909 with 16 week interval (A_P+); and (E) Group 5 Adenovirus-MVA with 16 week interval (A_M). (F) Comparison of peak ASC per million PBMC between groups, 7 days post-boost. (G) Comparison of peak AMA1 ASC as a proportion of total IgG+ ASC between groups, 7 days post-boost. Differences between groups analysed by Kruskal-Wallis test.*P<0.05 and **P<0.01.Data are presented as dot plots showing individual and median responses.

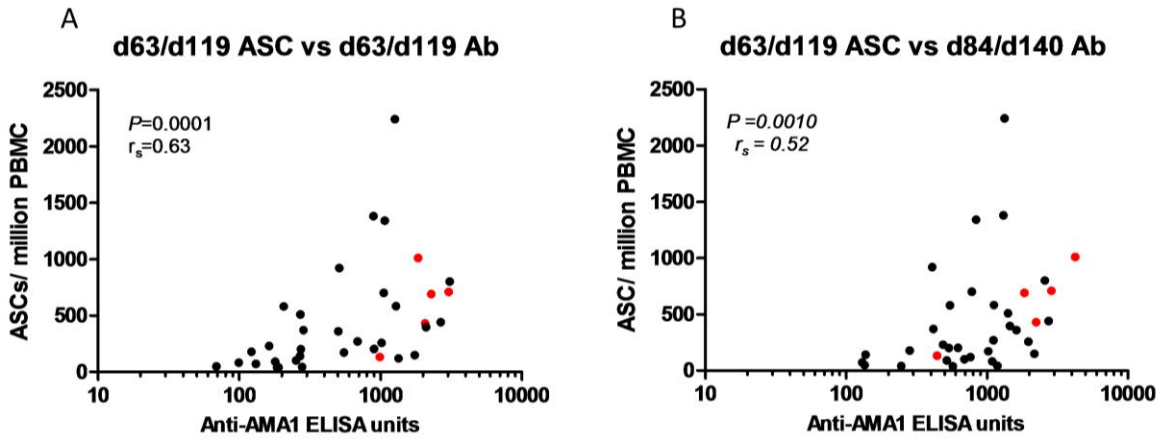


Figure 7.3: Relationship between peripheral ASC responses and serum IgG following AMA1 vaccination.

Correlation of AMA1-specific ASC per million cultured PBMC and levels of serum IgG reported as anti-AMA1 ELISA units. Results are shown (A) d63/d119 ASC vs d63/d119 Ab and (B) d63/d119 ASC vs d84/d140 (peak) Ab. Spearman rank correlation coefficient and P values are shown for all analyses. Red data points denote responses of Group 1 individuals after their 2nd booster vaccination.

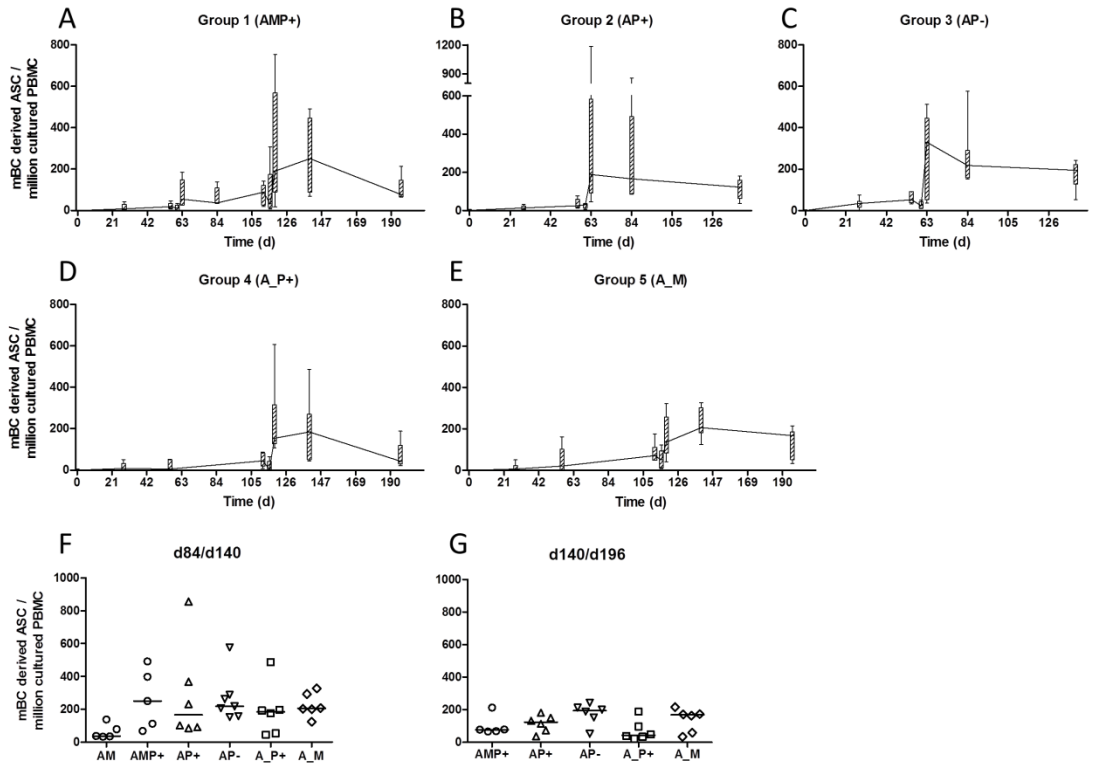


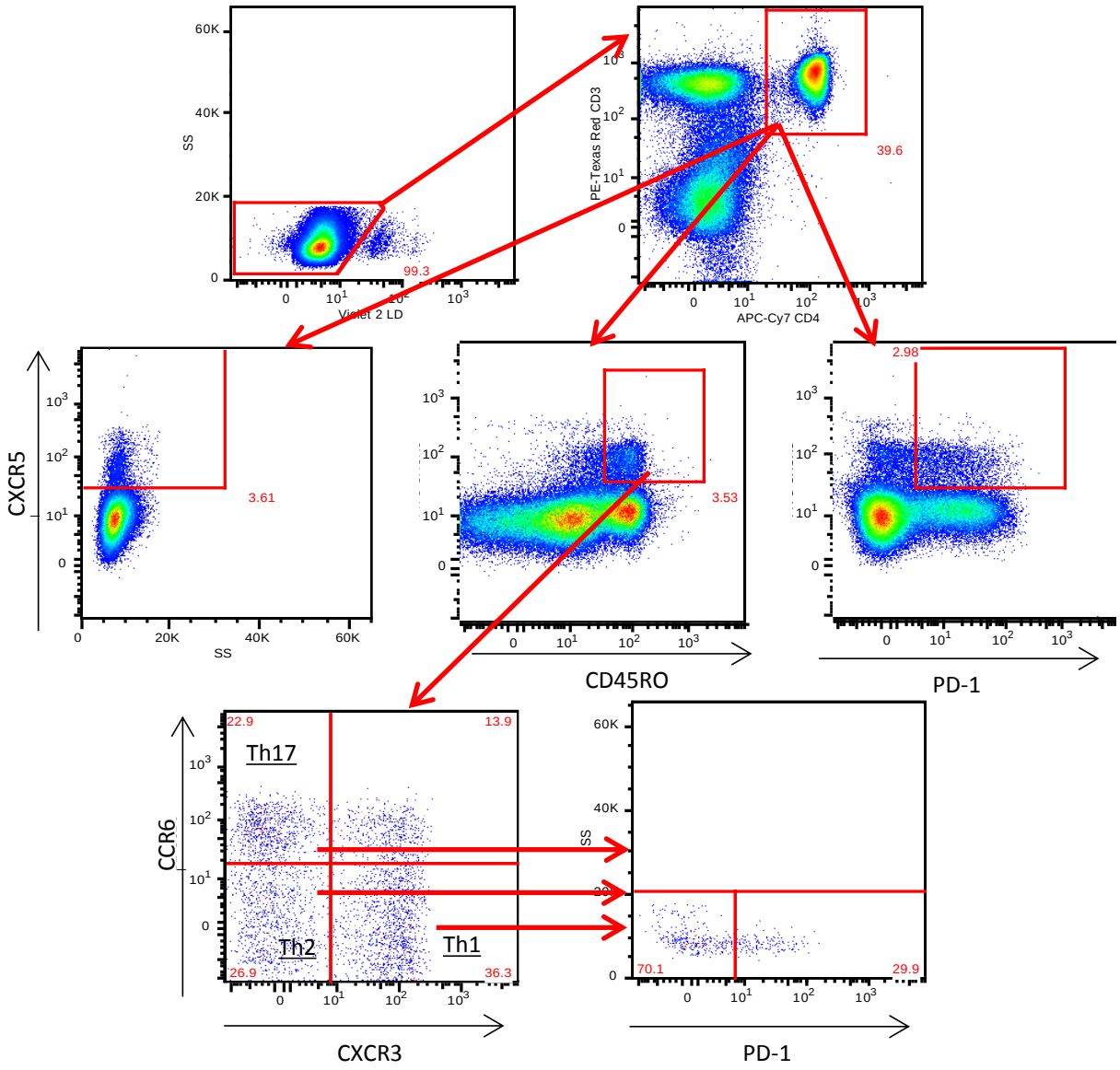
Figure 7.4: Measurement of AMA1-specific peripheral blood mBC in mixed-modality vaccine regimens.

AMA1-specific mBC responses (measured as mBC derived ASC per million cultured PBMC) were assessed by *ex-vivo* ELISPOT at the stated time-points after a variety of different AMA1 booster vaccinations, as part of a mixed-modality vaccine regimen. All volunteers received equal dose Adenovirus prime vaccines. Vaccine regimen denoted as follows; (A) Group 1-Adenovirus-MVA-Protein/Alhydrogel + CPG 7909 [AMP+], (B) Group 2 Adenovirus- Protein/Alhydrogel + CPG 7909 [AP+], (C) Group 3 Adenovirus- Protein/Alhydrogel [AP-], (D) Group 4 Adenovirus-Protein/Alhydrogel + CPG 7909 with 16 week interval [A_P+], (E) Group 5 Adenovirus-MVA with 16 week interval [A_M]. (F) Comparison of peak mBC responses between groups, 4 weeks post boost. (G) Comparison of resting level mBC responses between groups, 11 weeks post boost. Differences between groups analysed by Kruskal-Wallis test with Dunns multiple comparison test.*P<0.05. Data are presented as box and whisker plots showing the median, range and interquartile range of antigen-specific mBC, or as dot plots showing individual and median responses.

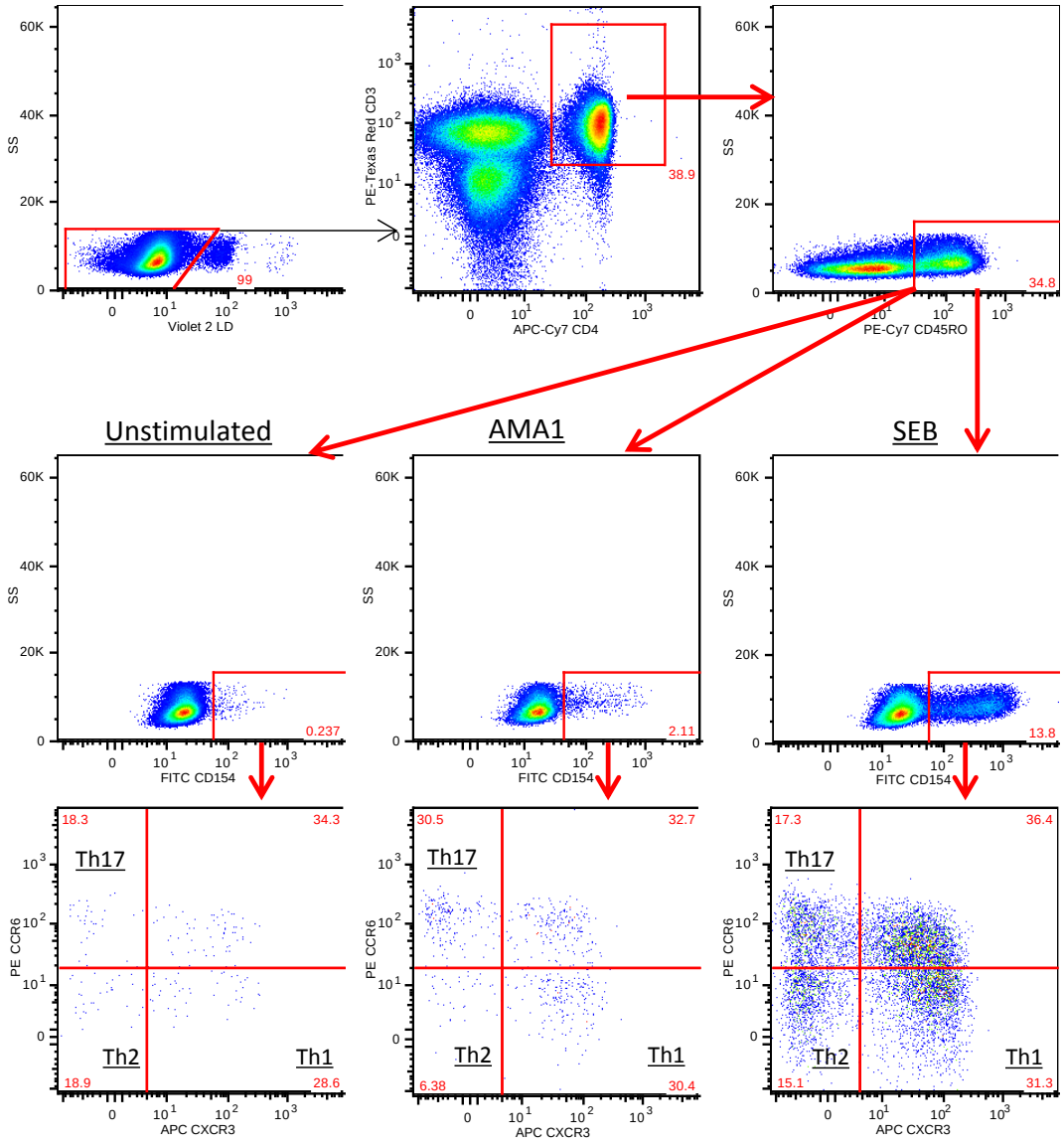
7.3.2. Baseline Tfh responses do not predict immune response post-prime.

The observation in the HIV field that the baseline presence of a particular peripheral memory Tfh population can correlate with an individual's ability to produce a functional antibody responses (e.g. broadly neutralising antibodies) [124] opened the question as to whether the presence of particular Tfh populations prior to vaccination may predict subsequent responses. In the VAC044 study all volunteers across the 5 groups received the same dose of ChAd63 AMA1 vaccine prime (n=31), with post-prime peak antibody and mBC responses observed at d28 .To investigate whether baseline (d0) Tfh populations could predict the functional response to adenoviral vaccine priming, a number of phenotypically distinct Tfh populations described in the literature were quantified using flow cytometry (Fig. 7.5A) on frozen PBMC from available volunteer samples (n=26). Given this was an open hypothesis a broad range of phenotypic populations of different sizes were considered, from total $CXCR5^+$ to lineage specific Th1/2/17, $PD\text{-}1^+$ cells with previous populations of interest used as a guide. For example in the HIV study the baseline population that correlated with broadly neutralising antibody production was $CXCR5^+$, $CXCR3^-$, $PD\text{-}1^+$ while it may also be predicted that Th1 lineage cells would likely play more of a role in the response to adenoviral vectors, than Th2 or Th17 lineage cells. All relationships were assessed between the proportional representation of different defined Tfh lineage subsets in individuals at baseline before vaccination (d0) and either peak post-prime antibody responses (defined as Anti-AMA1 FVO ELISA units at d28), or peak-post prime mBC (defined as AMA1 specific mBC derived ASC/Million cultured PBMC at d28) are shown in Table 7.1. No significant relationships were observed.

A. Phenotyping



B. CD154


SS
Violet 2 LD
99
PE-Texas Red CD3
APC-Cy7 CD4
38.9
PE-Cy7 CD45RO
34.8
Unstimulated
AMA1
SEB
FITC CD154
0.237
2.11
13.8
PE CCR6
APC CXCR3
Th17
Th2
Th1
18.3
34.3
18.9
28.6
30.5
32.7
6.38
30.4
17.3
36.4
15.1
31.3

C. IL-21

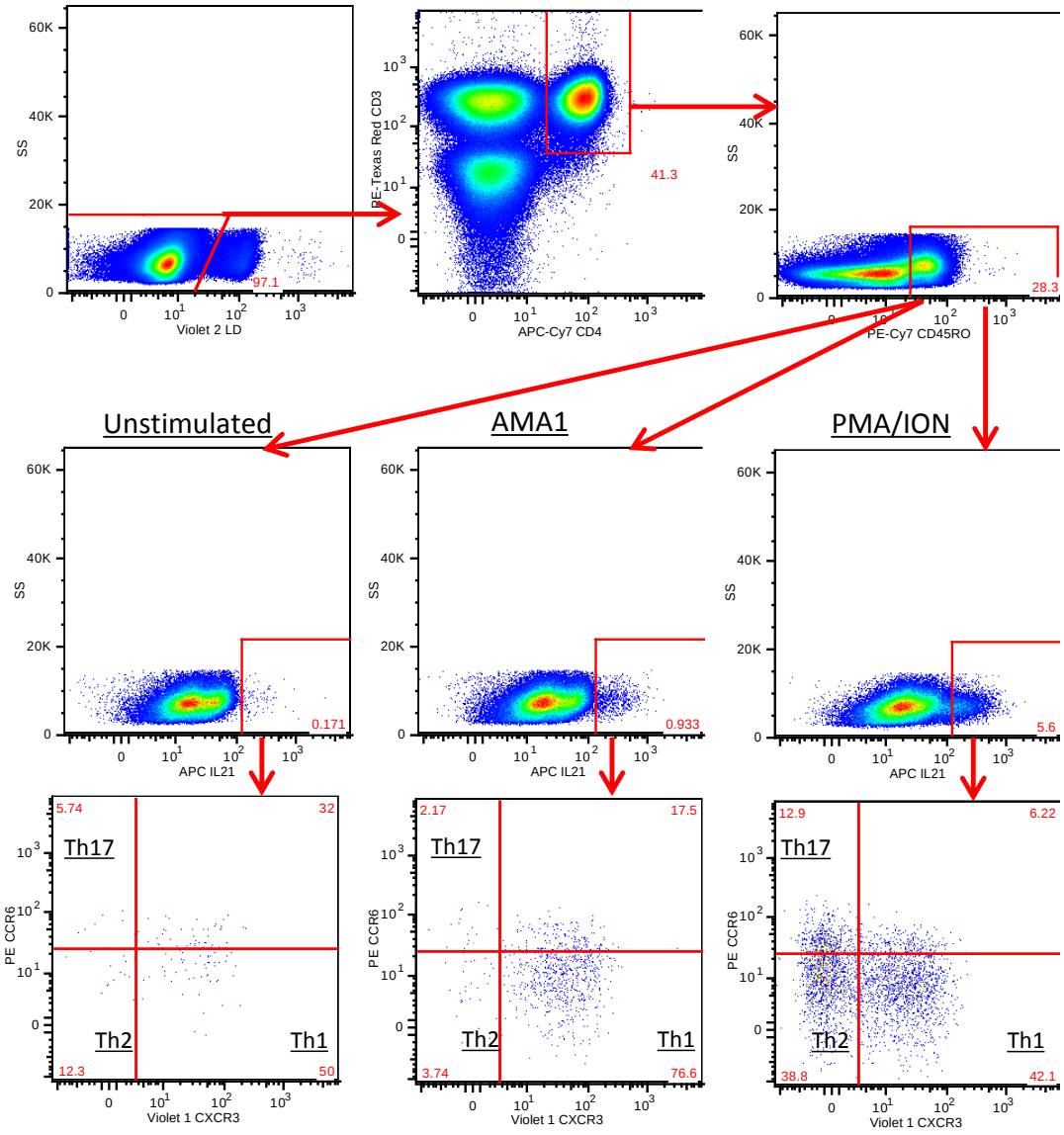

SS
Violet 2 LD
97.1
PE-Texas Red CD3
APC-Cy7 CD4
41.3
PE-Cy7 CD45RO
28.3
Unstimulated
AMA1
PMA/ION
APC IL21
0.171
0.933
5.6
PE CCR6
Violet 1 CXCR3
Th17
Th2
Th1
5.74
32
12.3
50
2.17
17.5
3.74
76.6
12.9
6.22
38.8
42.1

Figure 7.5: Peripheral blood Tfh gating strategy.

Three flow cytometry panels were run in parallel to characterise Tfh cells. In the 'Phenotyping' panel (A) whole PBMC were gated first by lymphocytes and then singlets before gating on Live/Dead and $CD3^+/CD4^+$ (top row). $CD3^+/CD4^+$ cells were then gated as $CXCR5^+$, or as $CXCR5^+/CD45RO^+$ or $CXCR5^+/PD\text{-}1^+$ (centre row). $CXCR5^+/CD45RO^+$ cells were further gated according to expression of CCR6 and CXCR3 to identify Th1, Th2 and Th17 subsets and then subsequently by expression of PD-1 (bottom row). In the 'CD154' panel (B) whole PBMC were gated first by lymphocytes and then singlets before gating on Live/Dead and $CD3^+/CD4^+$ and then $CD45RO^+$ (top row). $CD45RO^+$ cells were then gated as $CD154^+$ (middle row) before further gating according to expression of CCR6 and CXCR3 to identify Th1, Th2 and Th17 subsets (bottom row). In the 'IL-21' panel (C) PBMC were gated in the same way as the 'CD154' panel with CD154 gating substituted for IL-21 (middle row). CD154 and IL-21 positive cells were gated from the total $CD4^+$ memory ($CD45RO^+$) population. CXCR5 was removed from the gating strategy for this population to maximise the total number of antigen-specific cells detected.

Correlation					P value	Significance	rs	N
% CXCR5+ (of total CD4+)	d0	vs	Anti-AMA1 FVO ELISA units	d28	0.334	N/S	-0.211	23
% CXCR5+, PD1+ (of total CD4+)	d0	vs	Anti-AMA1 FVO ELISA units	d28	0.295	N/S	-0.2283	23
% CXCR5+, CD45RO+ (of total CD4+)	d0	vs	Anti-AMA1 FVO ELISA units	d28	0.246	N/S	-0.252	23
% Th1, PD-1+ (of total CXCR5+, CD45RO+)	d0	vs	Anti-AMA1 FVO ELISA units	d28	0.907	N/S	-0.0257	23
% Th2, PD-1+ (of total CXCR5+, CD45RO+)	d0	vs	Anti-AMA1 FVO ELISA units	d28	0.699	N/S	-0.0879	23
% Th17, PD-1+ (of total CXCR5+, CD45RO+)	d0	vs	Anti-AMA1 FVO ELISA units	d28	0.727	N/S	0.0771	23
% CXCR3-, PD-1+ (of total CXCR5+, CD45RO+)	d0	vs	Anti-AMA1 FVO ELISA units	d28	0.744	N/S	-0.0721	23
% CXCR5+ (of total CD4+)	d0	vs	AMA1 mBC derived ASC/million cultured PBMC	d28	0.803	N/S	-0.0563	22
% CXCR5+, PD1+ (of total CD4+)	d0	vs	AMA1 mBC derived ASC/million cultured PBMC	d28	0.562	N/S	-0.1307	22
% CXCR5+, CD45RO+ (of total CD4+)	d0	vs	AMA1 mBC derived ASC/million cultured PBMC	d28	0.725	N/S	0.0795	22
% Th1, PD-1+ (of total CXCR5+, CD45RO+)	d0	vs	AMA1 mBC derived ASC/million cultured PBMC	d28	0.668	N/S	-0.0966	22
% Th2, PD-1+ (of total CXCR5+, CD45RO+)	d0	vs	AMA1 mBC derived ASC/million cultured PBMC	d28	0.0889	N/S	-0.363	22
% Th17, PD-1+ (of total CXCR5+, CD45RO+)	d0	vs	AMA1 mBC derived ASC/million cultured PBMC	d28	0.4789	N/S	-0.155	22
% CXCR3-, PD-1+ (of total CXCR5+, CD45RO+)	d0	vs	AMA1 mBC derived ASC/million cultured PBMC	d28	0.126	N/S	-0.3361	22

Table 7.1: Correlations between baseline Tfh subsets and post adenoviral prime antibody/ mBC responses.

Relationships were assessed between the proportional representation of different defined Tfh lineage subsets in individuals at baseline before vaccination (d0) and either peak post-prime antibody responses (defined as Anti-AMA1 FVO ELISA units at d28), or peak-post prime mBC (defined as AMA1 specific mBC derived ASC/Million cultured PBMC at d28). Spearman rank correlation coefficient, P and n values are shown for all analyses.

7.3.3. Tfh populations induced following booster vaccination correlate with peak post-boost immune responses.

In addition to baseline (d0), populations of Tfh cells were also measured by flow cytometry at 7 days post-booster vaccination (d63/d119) in volunteers for which PBMC were available. This time-point contained the peak of the antigen specific T cell response as measured by IFN-γ ELISPOT and also contained the greatest proportion of antigen specific CD4+ memory cells in an initial screening experiment when compared to other time-points. Gating of these populations was performed as with d0 populations (Fig. 7.5A). Here volunteers will be displayed either as a total population or subdivided by group. Consideration must be made to the fact that post-boost volunteers all receive different booster vaccines, some at different time intervals. A broad range of phenotypic populations of different sizes were considered, from total $CXCR5^+$ to lineage specific Th1/2/17, PD-1+/- cells. In this experiment some of these populations were directly comparable to those described in previous studies and are noted where relevant.

Initially differences between the two time-points were investigated for the expression of key Tfh markers across $CD4^+$ populations. The % of$CXCR5^+$ cells in the total $CD3^+/CD4^+$ population did not differ between baseline and post-boost time-points when all volunteers were grouped (Fig.7.6a). This observation appears to also be true when volunteers are split by group, although there appears to be a trend for a reduction in the $\%CXCR5^+$ cells post-boost following vaccination with MVA (G1 d63 and G5 d119), but there is a lack of power to confirm this. Similar observations were made when looking at the $\%CXCR5^+/PD\text{-}1^+$ (Fig. 7.6B) and $CXCR5^+/CD45RO^+$ (Fig.7.6C) populations. The $CXCR5^+/ICOS^+$ population was also investigated but given no positive populations were detected at either baseline or post-boost (data not shown) this population was omitted from subsequent analyses.

Next the composition of the $CXCR5^+/CD45RO^+$ population was characterised based on expression of CCR6, CXCR3 into Th1 ($CCR6^-/CXCR3^+$), Th2 ($CCR6^-/CXCR3^-$)and Th17 ($CCR6^+/CXCR3^-$)lineage subsets. These populations can be further subdivided according to expression of PD-1. Such subsets have been independently associated with a variety of functional responses in different models and are attributed with differing degrees of helper ability [368]. When these subsets are measured as a % of the $CXCR5^+/CD45RO^+$ population they all individually appear to be relatively stable both over time and between vaccine groups (Fig. 7.7). Therefore the possible reduction in $CXCR5^+$ cells seen in Group 1 and 5 after MVA (Fig.7.6) would appear to affect all subsets equally. Next it was investigated as to whether the relative abundance of these subsets present at d63/d119 post-boost in individuals correlated with peak immune responses post-boost. Table 7.2 shows the relationship between the proportional representation of defined Tfh lineage subsets in individuals at 7 days post-boost (d63/d119) and either peak antibody responses (defined as Anti-AMA1 FVO ELISA units at d84/d140), ASC (defined as AMA1 specific ASC/Million PBMC at d63/d119) or peak mBC (defined as AMA1 specific mBC derived ASC/Million cultured PBMC at d84/d140). The ASC response was previously shown to correlate with antibody responses (Fig. 7.3). Notably both ASC and antibody positively correlated with the % of total Th1 cells ($CCR6^-/CXCR3^+$) within the $CXCR5^+/CD45RO^+$ population post-boost (d63/d119) and most notably those which were $PD\text{-}1^+$. ASC and antibody responses negatively correlated with Th2 and Th17, $PD\text{-}1^-$ populations. ASC and antibody responses did not correlate with mBC responses in this trial, and it was observed that the % of total Th1 cells ($CCR6^-/CXCR3^+$) that correlated with ASC and antibody negatively correlated with mBC response. In contrast the % of total $CXCR3^-$, $PD\text{-}1^+$ cells (including both Th2 and Th17 cells) within the $CXCR5^+/CD45RO^+$ population post-boost did correlate with the peak mBC response. When focusing on the Th17 lineage subsets, the % of total Th17 cells ($CCR6^+/CXCR3^-$, $PD\text{-}1^{+/-}$) were found to strongly correlate with peak mBC responses. Within both Th2 and Th17 lineages $PD\text{-}1^+$ subsets correlated with mBC while $PD\text{-}1^-$ subsets did not.

In addition to this 'phenotyping' panel, two additional panels were performed to study antigen-specific cell populations, a 'CD154' panel and an 'IL-21' panel, with gating for these populations described in Fig. 7.5B and 7.5C respectively. In these panels, pools of cells from baseline or post-boost were either left unstimulated, or stimulated with AMA1 or control antigen (SEB or PMA/Ionomycin) for 6 hours before staining for Tfh markers. To calculate the proportion of $CD154^+$ or $IL\text{-}21^+$ cells, the unstimulated response was subtracted from the antigen-specific response. The % of $CD154^+$ cells within the $CD4^+$, $CD45RO^+$ population was found to be significantly higher post-boost compared to baseline (P=0.0058), with average responses notably lower than control SEB responses (Fig. 7.9A). The % of $IL\text{-}21^+$ cells within the $CD4^+$, $CD45RO^+$ population cells trended to be higher post-boost compared to baseline, but the lack of data points at baseline (due to limited PBMC) meant this analysis lacked the power to detect possible significance in a paired comparison (Fig7.9B). $IL\text{-}21^+$ responses were also notably lower than control PMA/ION responses. Neither % $CD154^+$ or $IL\text{-}21^+$ at d63/d119 correlated with ASC, antibody or mBC responses post-boost (data not shown). In volunteers with a positive antigen-specific CD154 or IL-21 response at d63/d119 (defined as >0.1% after subtracting unstimulated response) the Th lineage profiles were characterised within this population using CCR6/CXCR3 gating (Fig. 7.9C). In the AMA1-stimulated $CD154^+$ population, Th17 and Th1 cells were dominant in comparison to Th2 cells in the SEB-stimulated $CD154^+$ population. In the AMA1 stimulated $IL\text{-}21^+$ population, Th1 cells alone were dominant in comparison to Th2 cells in the PMA/ION stimulated $IL\text{-}21^+$ populations. Th17 cells comprised a minor population in both $IL\text{-}21^+$ populations.

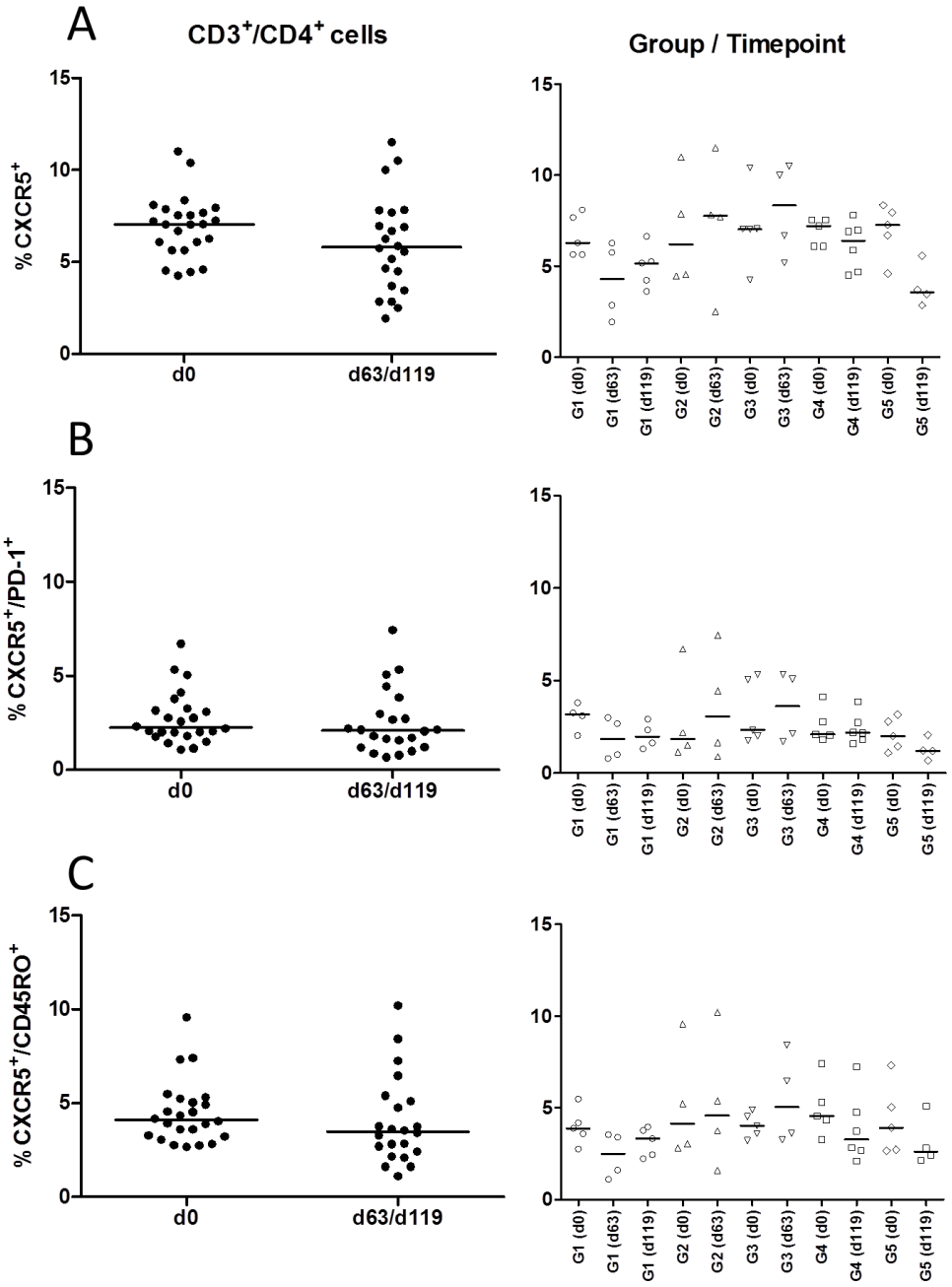

A
CD3+/CD4+ cells
Group / Timepoint
% CXCR5+
15
10
5
0
d0
d63/d119
G1 (d0)
G1 (d63)
G1 (d119)
G2 (d0)
G2 (d63)
G3 (d0)
G3 (d63)
G4 (d0)
G4 (d119)
G5 (d0)
G5 (d119)
B
% CXCR5+/PD-1+
C
% CXCR5+/CD45RO+

Figure 7.6: Comparing $CD4^+$ Tfh cell populations at baseline and post-boost.

(A) Comparison between the % of $CXCR5^+$ cells within the $CD3^+/CD4^+$ population at both baseline and post-boost and across vaccine groups. (B) Comparison between the % of $CXCR5^+/PD\text{-}1^+$ cells within the $CD3^+/CD4^+$ population at both baseline and post-boost and across vaccine groups. (C) Comparison between the % of $CXCR5^+/CD45RO^+$ cells within the $CD3^+/CD4^+$ population at both baseline and post-boost and across vaccine groups. No significant differences were observed for total datasets. Wilcoxon matched-pairs signed rank test used for combined group analysis. Medians are shown for group/time-point.

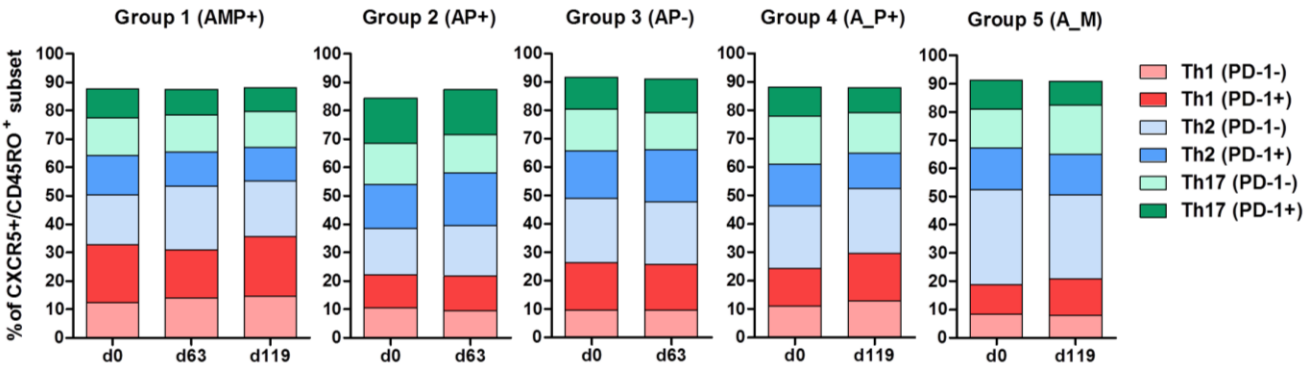


Figure 7.7: Comparison of the composition of the $CXCR5^{+}/CD45RO^{+}$subset pre-/post-vaccination. $CXCR5^{+}/CD45RO^{+}$ cells were sub-divided using CCR6 and CXCR3 into Th1 ($CCR6^{-}/CXCR3^{+}$), Th2 ($CCR6^{-}/CXCR3^{-}$), and Th17 ($CCR6^{+}/CXCR3^{-}$). These were further divided into $PD\text{-}1^{+}$ and $PD\text{-}1^{-}$ populations. Proportions of these cells as a % of the $CXCR5^{+}/CD45RO^{+}$ population are shown for baseline (d0) and post-boost (d63/d119) for the 5 vaccine groups.

Correlation					P value	Significance	rs	N
% CXCR5+ (of total CD4+)	d63/d119	vs	Anti-AMA1 FVO ELISA units	d84/d140	0.457	N/S	0.15	26
% CXCR5+, PD1+ (of total CD4+)	d63/d119	vs	Anti-AMA1 FVO ELISA units	d84/d140	0.237	N/S	0.24	26
% CXCR5+, CD45RO+ (of total CD4+)	d63/d119	vs	Anti-AMA1 FVO ELISA units	d84/d140	0.0092	**	0.492	26
% Th1 (of total CXCR5+, CD45RO+)	d63/d119	vs	Anti-AMA1 FVO ELISA units	d84/d140	0.0216	*	0.44	26
% Th1, PD-1+ (of total CXCR5+, CD45RO+)	d63/d119	vs	Anti-AMA1 FVO ELISA units	d84/d140	0.0302	*	0.418	26
% Th1, PD-1- (of total CXCR5+, CD45RO+)	d63/d119	vs	Anti-AMA1 FVO ELISA units	d84/d140	0.0912	N/S	0.332	26
% Th2 (of total CXCR5+, CD45RO+)	d63/d119	vs	Anti-AMA1 FVO ELISA units	d84/d140	0.0602	N/S	-0.366	26
% Th2, PD-1+ (of total CXCR5+, CD45RO+)	d63/d119	vs	Anti-AMA1 FVO ELISA units	d84/d140	0.447	N/S	-0.153	26
% Th2, PD-1- (of total CXCR5+, CD45RO+)	d63/d119	vs	Anti-AMA1 FVO ELISA units	d84/d140	0.0029	**	-0.551	26
% Th17 (of total CXCR5+, CD45RO+)	d63/d119	vs	Anti-AMA1 FVO ELISA units	d84/d140	0.3944	*	-0.394	26
% Th17, PD-1+ (of total CXCR5+, CD45RO+)	d63/d119	vs	Anti-AMA1 FVO ELISA units	d84/d140	0.1476	N/S	-0.286	26
% Th17, PD-1- (of total CXCR5+, CD45RO+)	d63/d119	vs	Anti-AMA1 FVO ELISA units	d84/d140	0.0461	*	-0.387	26
% CXCR3-, PD-1+ (of total CXCR5+, CD45RO+)	d63/d119	vs	Anti-AMA1 FVO ELISA units	d84/d140	0.891	N/S	-0.0311	26
% CXCR5+ (of total CD4+)	d63/d119	vs	AMA1 ASC/millionPBMC	d63/d119	0.112	N/S	0.0319	26
% CXCR5+, PD1+ (of total CD4+)	d63/d119	vs	AMA1 ASC/millionPBMC	d63/d119	0.022	*	0.455	26
% CXCR5+, CD45RO+ (of total CD4+)	d63/d119	vs	AMA1 ASC/millionPBMC	d63/d119	0.065	NS	0.367	26
% Th1 (of total CXCR5+, CD45RO+)	d63/d119	vs	AMA1 ASC/millionPBMC	d63/d119	0.013	*	0.483	26
% Th1, PD-1+ (of total CXCR5+, CD45RO+)	d63/d119	vs	AMA1 ASC/millionPBMC	d63/d119	0.0006	***	0.628	26
% Th1, PD-1- (of total CXCR5+, CD45RO+)	d63/d119	vs	AMA1 ASC/millionPBMC	d63/d119	0.158	N/S	0.286	26
% Th2 (of total CXCR5+, CD45RO+)	d63/d119	vs	AMA1 ASC/millionPBMC	d63/d119	0.006	**	-0.524	26
% Th2, PD-1+ (of total CXCR5+, CD45RO+)	d63/d119	vs	AMA1 ASC/millionPBMC	d63/d119	0.353	N/S	-0.19	26
% Th2, PD-1- (of total CXCR5+, CD45RO+)	d63/d119	vs	AMA1 ASC/millionPBMC	d63/d119	0.224	N/S	-0.247	26
% Th17 (of total CXCR5+, CD45RO+)	d63/d119	vs	AMA1 ASC/millionPBMC	d63/d119	0.024	*	-0.441	26
% Th17, PD-1+ (of total CXCR5+, CD45RO+)	d63/d119	vs	AMA1 ASC/millionPBMC	d63/d119	0.336	N/S	-0.197	26
% Th17, PD-1- (of total CXCR5+, CD45RO+)	d63/d119	vs	AMA1 ASC/millionPBMC	d63/d119	0.013	*	-0.48	26
% CXCR3-, PD-1+ (of total CXCR5+, CD45RO+)	d63/d119	vs	AMA1 ASC/millionPBMC	d63/d119	0.255	N/S	-0.023	26
% CXCR5+ (of total CD4+)	d63/d119	vs	AMA1 mBC derived ASC/million cultured PBMC	d84/d140	0.816	N/S	0.055	20
% CXCR5+, PD1+ (of total CD4+)	d63/d119	vs	AMA1 mBC derived ASC/million cultured PBMC	d84/d140	0.687	N/S	0.096	20
% CXCR5+, CD45RO+ (of total CD4+)	d63/d119	vs	AMA1 mBC derived ASC/million cultured PBMC	d84/d140	0.885	N/S	0.035	20
% Th1 (of total CXCR5+, CD45RO+)	d63/d119	vs	AMA1 mBC derived ASC/million cultured PBMC	d84/d140	0.0037	**	-0.618	20
% Th1, PD-1+ (of total CXCR5+, CD45RO+)	d63/d119	vs	AMA1 mBC derived ASC/million cultured PBMC	d84/d140	0.202	N/S	-0.298	20
% Th1, PD-1- (of total CXCR5+, CD45RO+)	d63/d119	vs	AMA1 mBC derived ASC/million cultured PBMC	d84/d140	0.0012	**	-0.671	20
% Th2 (of total CXCR5+, CD45RO+)	d63/d119	vs	AMA1 mBC derived ASC/million cultured PBMC	d84/d140	0.222	N/S	0.286	20
% Th2, PD-1+ (of total CXCR5+, CD45RO+)	d63/d119	vs	AMA1 mBC derived ASC/million cultured PBMC	d84/d140	0.0096	**	0.564	20
% Th2, PD-1- (of total CXCR5+, CD45RO+)	d63/d119	vs	AMA1 mBC derived ASC/million cultured PBMC	d84/d140	0.677	N/S	-0.099	20
% Th17 (of total CXCR5+, CD45RO+)	d63/d119	vs	AMA1 mBC derived ASC/million cultured PBMC	d84/d140	0.0004	***	0.714	20
% Th17, PD-1+ (of total CXCR5+, CD45RO+)	d63/d119	vs	AMA1 mBC derived ASC/million cultured PBMC	d84/d140	0.0205	*	0.514	20
% Th17, PD-1- (of total CXCR5+, CD45RO+)	d63/d119	vs	AMA1 mBC derived ASC/million cultured PBMC	d84/d140	0.277	N/S	0.256	20
% CXCR3-, PD-1+ (of total CXCR5+, CD45RO+)	d63/d119	vs	AMA1 mBC derived ASC/million cultured PBMC	d84/d140	0.0058	**	0.594	20

Table 7.2: Correlations between Th lineage subsets and antibody/B cell responses post-boost. Relationships were assessed between the proportional representation of defined Tfh lineage subsets in individuals at 7 days post-boost (d63/d119) and either peak antibody responses (defined as Anti-AMA1 FVO ELISA units at d84/d140), ASC (defined as AMA1 specific ASC/Million PBMC at d63/d119) or peak mBC (defined as AMA1 specific mBC derived ASC/Million cultured PBMC at d84/d140). Spearman rank correlation coefficient, P and n values are shown for all analyses. Red highlighting indicates positive correlations, blue indicates negative correlations. *P<0.05, **P<0.01, and ***P<0.001

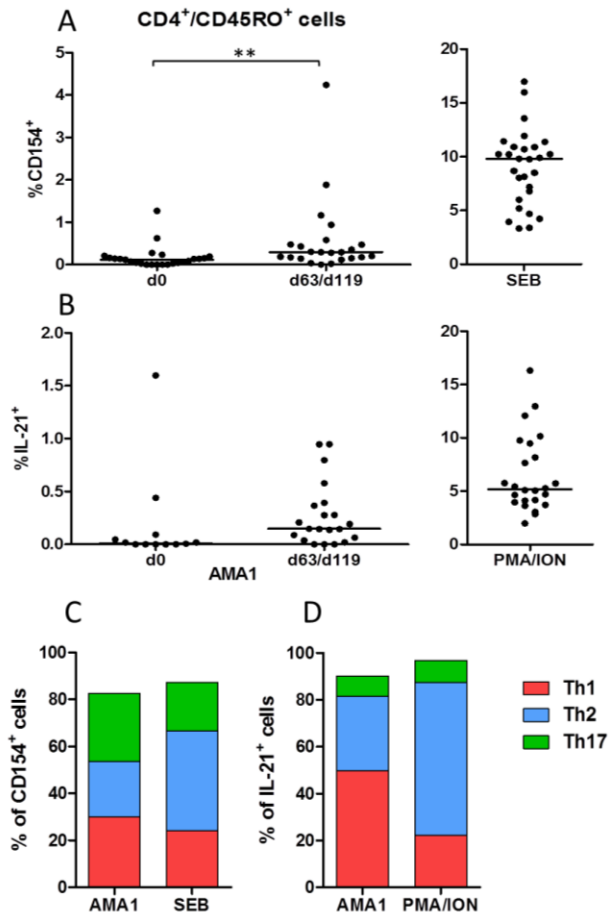


Figure 7.8: Quantification and phenotypic characterisation of antigen-specific CD154$^+$ and IL-21$^+$ cells.

CD154$^+$ (A) and IL-21$^+$ (B) cells as a % of total CD4$^+$/CD45RO$^+$ cells following antigenic peptide stimulation. For AMA1 stimulated cells, baseline (d0) and post-boost (d63/d119) responses are shown, with unstimulated responses from the same time-point subtracted. SEB and PMA/ION responses shown are from post-boost stimulated cells, with unstimulated responses subtracted. Medians plotted for each group. CD154$^+$ (C) and IL-21$^+$ (D) cells were sub-divided using CCR6 and CXCR3 into Th1 (CCR6$^-$/CXCR3$^+$), Th2 (CCR6$^-$/CXCR3$^-$) , and Th17 (CCR6$^+$/CXCR3$^-$) subsets to characterise the antigen-specific profiles of AMA1 and SEB or PMA/ION stimulated cells post-boost (d63/d119). Profiles averaged across all volunteers who had an antigen-specific CD154$^+$ or IL-21 response >0.1% after subtraction of unstimulated response. See figure 7.5B-C for example plots.

7.4. Discussion

In previous chapters I have discussed the relationships between antibody responses, ASC responses and mBC responses following vaccination and CHMI (Chapter 3) and how $CXCR3^+$ B cells in particular appear to respond functionally to cytokine responses derived most likely from Th1, IFN-γ producing, vaccine induced T cells activated during CHMI (Chapter 4). In this chapter the aim was to try and link together the B and T cell populations that contribute to a functional humoral response. One of the major limitations in human studies of B cell/helper T cell interactions is the difficulty of studying germinal centre reactions in lymphoid organs due to ethical considerations, especially in healthy individuals. The discovery in recent years of peripheral blood Tfh populations and their functionality in providing help to B cells have allowed an opportunity to study additional parameters and interactions using readily available peripheral blood PBMC. Interestingly the peripheral blood Tfh cell populations appear to be highly variable, antigen-specific and may be modulated by factors such as dose, repeated exposure or accompanying adjuvants [80, 369-371]. The VAC044 AMA1 vaccine trial [301] encompasses a number of these variables and so provided an ideal opportunity to study the relationships between peripheral blood Tfh populations and antibody, ASC and mBC responses.

Initially I looked to see whether baseline populations of different Tfh cells could be used to predict antibody or mBC responses following vaccination. In VAC044 all individuals, irrespective of group, received the same dose of ChAd63 as a vaccine prime and so provided good power for detecting a relationship. No significant correlations were observed between baseline Tfh responses and either antibody or mBC responses at d28. There are a number of possible reasons for this. Firstly antibody and mBC responses are relatively weak after adenovirus prime so the signal may not be strong enough to detect a relationship across individuals. Unfortunately in this trial all volunteers had different vaccine boost regimens (n=5-7 per group) so the relationship between baseline populations and peak antibody/mBC was not assessed. Therefore looking at a larger number of volunteers all receiving the

same prime-boost regimen in the future would more definitively answer this question. Alternatively this observation may be real and the observations that baseline Tfh predict antibody functionality may only be true when the baseline measured is in a chronic state such a HIV [124] or in individuals with autoimmune predisposition [365] where time is a key variable. Whether or not baseline Tfh populations can be used to predict the potential vaccine-induced response in an individual clearly requires more investigation.

Judging from the literature it would appear that peripheral Tfh cells induced following vaccination and located within the peak of the $CD4^+$ T cell response may more accurately represent those populations involved in production of functional antibody and B cell responses. Initially I looked at broad populations expressing key Tfh associated markers including CXCR5, PD-1, CD45RO and ICOS. There were no significant differences in the overall proportions of cells expressing these markers between baseline and post-boost (d63/d119), with no detection of any significant population expressing ICOS at any time-point. The lack of any ICOS expressing cells post-boost suggests that previously reported observations following influenza vaccination may be specific to that regime/antigen and not widely applicable following vaccination with Th1 biased immunogens [125]. It may be, however, that this population was absent in the 'phenotyping' panel due to a lack of antigenic stimulation. The next step was to establish whether there were any changes to the proportions of Th1, Th2 and Th17 cells in the memory ($CXCR5^+$, $CD45RO^+$) population following vaccination. Despite the lack of an $ICOS^+$ population, these populations can still be subdivided into 6 different functional populations using a 3D analysis model as proposed by Schmitt *et al* [368] based on expression of CCR6, CXCR3 and PD-1. These populations also showed very little change over time when volunteers were divided up into groups suggesting that none of the regimens had a significant impact on the homeostasis of these populations. It was however noted that between individuals within groups there was natural variation in the proportions of the 6 subsets post-boost. Therefore the proportions of these subsets at d63/d119 were

measured against an individual's ability to produce an ASC, antibody and mBC response. Individuals who had a higher proportion of Th1 cells at d63/d119, particularly in the PD-1$^+$ pool, produced a larger ASC response at the same time-point and had a greater peak antibody response at d84/d140. Th1 subsets were expected to be induced following vaccination with ChAd63, given the induction of IFN-γ producing T cells by viral vectors. However it has been suggested that Th1 cells are non-efficient helpers compared to those in the Th2 and Th17 pools [368], and are unable to provide help to naïve B cells [365]. Therefore any direct role for these cells would likely have to be through interaction with existing mBC. To date the only example of such help was from the ICOS$^+$ influenza induced population (that I have already shown the equivalent to be absent here). In contrast individuals with higher proportions of Th2 and Th17 PD-1$^+$ cells in the memory pool have the highest peak mBC response. Given that peak mBC did not correlate with ASC or antibody in this trial it is plausible that different populations of Tfh cells are independently responsible for helping each cell population. Of the 6 subsets defined by the 3D analysis, Th2 and Th17 PD-1$^+$ cells are proposed to be the best helpers of B cells. In contrast to Th1 these cells can help both naïve and memory B cells and actively promote class switching [365]. This supports the notion that these populations may be involved in determining the number of IgG$^+$, antigen-specific mBC in circulation post-boost. In this analysis negative correlations were also observed, between Th1 subsets and mBC and Th2/17 subsets and ASC/antibody. Whilst these observations may support the idea that Tfh subset composition may determine an individual's preference for production of an mBC or ASC/antibody response, they could be a consequence of analysing multiple % subsets and so should not be considered definitive.

To further characterise the functionality of Tfh cells following vaccination, cells were stimulated with AMA1 peptides and the CD154$^+$ and IL-21$^+$ populations characterised. CD154 is expressed on activated antigen-specific T cells in the presence of antigen and provides survival signals to CD40$^+$ B cells. Expression was significantly higher at d63/d119 compared to baseline which would be expected and

there was a trend for CD154^{+} cells to be more biased to Th1 and Th17 cells following AMA1 restimulation, at least in comparison to SEB stimulation which is Th2 biased. In contrast, only low numbers of cells produced IL-21^{+} and only a trend for an increased number of these cells at d63/d119 compared to baseline was observed, although the power to observe a significant difference was limited by a lack of data at baseline. In those individuals with a reasonable number of IL-21 producing cells at d63/d119 there was a strong bias towards Th1 subsets. Given IL-21 is crucial for B cell survival and the differentiation of B cells into plasma cells, but has less impact on the formation of early memory [360], such data support the suggestion of a role for these Th1 subsets in production of the ASC response. IL-21 has also been shown to be important for memory formation following secondary antigen exposure [372], given the supposedly poor help provided by Th1 subsets it would be reasonable to assume that other IL-21 producing subsets, likely within the Th2 and Th17 populations provide a more significant role in this process. Without access to GCs this cannot be definitively proven here but the correlation between increased numbers of Th2/Th17 cells (in the phenotyping panel) and the mBC response offers limited support for such a hypothesis.

Clearly further work is required to characterise functionality of the Tfh subsets quantified here. Many studies have looked at the ability of Tfh subsets to induce naïve B cell and mBC differentiation *in vitro* and such experiments would supplement these data. Of particular interest would be determining the helper capacity of the Th1 subsets that are supposedly poor helpers. Previously in Chapters 3 and 4 I speculated that early on during CHMI, vaccine-induced helper T cells may be driving CXCR3^{+} mBC to differentiate into short lived plasma cells. It is possible that it is the Th1 PD-1^{+} cells that are driving this response which may be extrafollicular in nature. It is possible this type of response is detrimental to memory acquisition in cases of prolonged exposure more akin to natural infection. It may be that the immunological properties of antigens such as MSP1 and AMA1 promote acquisition of T cells that drive such a response as an immune evasion strategy. For example a particular T cell epitope on the MSP1$_{33}$

fragment has been shown in preclinical studies to induce a skewed Th2 response and induction of non-neutralising antibodies that interfered with neutralising antibodies [44].This may explain why it takes multiple natural exposures to build up a broad memory response. I also speculated that after drug treatment, when inflammation has subsided and antigen is abundant, a more typical GC reaction occurs which drives mBC generation as observed in Chapter 3. This may in turn be driven by cells within the Th2 or Th17 Tfh subsets, which data here suggests to be involved in mBC generation following vaccination. Further study of different Tfh subsets and their role in inducing B cell differentiation may provide support for such notions and allow direct comparison between immune responses following vaccination or CHMI in context of boosting an immune response. The interactions between B cell and Tfh cells are as much about the survival and differentiation of Tfh cells as B cells. Given that populations of Tfh cells at baseline in this study do not appear to predict B cell or antibody responses, it may be important instead to look at how vaccination induces bias in Tfh populations, which are subsequently responsible for the B cell and antibody responses. Given the power of adjuvants to direct the immune response it may be possible to induce the relevant proportions of Tfh cells to give greater memory, antibody or both. How such vaccine- induced populations respond during secondary antigen exposure, be it vaccination or CHMI, may provide clues as to how vaccine induced responses may respond to natural infection and such understanding may be useful for maximising the potential for vaccines that may enter field trials in the future.

8. Discussion and Future Directions

8.1. Summary

The ultimate aim for candidate *Plasmodium falciparum* blood-stage malaria vaccines is to induce high titre neutralising antibodies which target the parasite and provide sterile protection. The antigens MSP1 and AMA1 were originally selected as promising candidates due to the presence of antibodies against these antigens in individuals with naturally acquired immunity (NAI). To date a number of candidate vaccines containing these two antigens have been tested in humans, encompassing a range of delivery methods and vaccine regimens [51, 114, 216, 217, 219, 301, 373, 374]. Many of these trials have induced high levels of serum antibody against these target antigens, yet efficacy has so far not been convincingly observed in Phase II clinical trials. Further understanding the quality of the antibody response and the context in which such antibody is produced is essential for the progression towards a more efficacious vaccine. In this Thesis I have investigated the induction and behaviour of the B cell populations that are responsible for producing antibody both in the short and long term in humans, as well as other populations that may aid them (i.e. peripheral blood T follicular helper (Tfh) cells). In addition to studying these populations after vaccination I was in the unique position to study these cells following controlled human malaria infection, a powerful tool for testing vaccine efficacy, but also capable of at least partly mimicking the effect(s) of natural parasite exposure on a vaccine-induced immune response. Data presented in this Thesis have shown that B cell responses, both memory B cell (mBC) and antibody secreting cells (ASC), as well as Tfh cells are important correlates of the antibody response to blood-stage malaria antigen vaccination. However due to a lack of efficacy so far with these vaccines, clearly more work is required to identify improved antigenic targets within the parasite. Nevertheless, it is likely the study of these key cellular subsets will inform immuno-monitoring of other vaccines targeting other antigens, and these data can inform vaccine developers as to which cellular

responses are important in the context of second-generation vaccines or alternative delivery regimens. It is likely future antigen targets will need to achieve an even better quantity or quality of antibody response.

8.2. Conclusions

8.2.1. B cell responses to candidate blood-stage malaria antigens mostly follow classical kinetics following vaccination.

In Chapter 3 and 7, I showed that both ASC and mBC responses follow mostly classical response kinetics following vaccination with MSP1 and AMA1 candidate blood-stage malaria vaccines in a number of different regimens. ASC peaked at 7 days post-boost, while mBC peaked around 4 weeks post-boost – as seen previously with other antigens including those from Influenza and rabies virus [122, 263]. Interestingly slight variations to this classical response were observed. In Chapter 7 I described how inclusion of the TLR9 agonist CPG7909 with a protein-in-Alhydrogel adjuvant vaccine caused earlier ASC and mBC responses to be observed following booster vaccination after an adenovirus prime. Such an effect on the mBC response has been previously reported (in another trial using the same antigen in a three shot protein-in-adjuvant regime) when CPG7909 was included in the formulation, but not in its absence [219]. In this study, the authors claimed that inclusion of CPG7909 increases the magnitude and longevity of the mBC response. However my results suggest that following adenovirus priming, other regimens perform comparably to protein-in-adjuvant + CPG7909 in terms of magnitude and longevity. This effect of adenovirus priming has been previously reported in preclinical studies preceding a number of potent adjuvants [220]. CPG7909 vaccination typically induces higher reactogenicity and more systemic adverse events [301] and has also been shown to be ineffective in a Malian population for boosting B cell memory [310]. Therefor alternative regimens that are comparatively immunogenic are likely to be welcomed. Clearly more can be done to further improve the B cell response to blood-stage malaria antigens, with ASC responses reportedly far higher following influenza vaccination [263]. However this may be as much about the antigen as the vaccine regimen and newer candidate antigens may achieve higher magnitude, longer-lived responses using existing regimens or variations on a theme.

8.2.2. CHMI provides a unique insight into the differences between how B cells respond to live parasite antigen compared to vaccine antigen.

Whilst CHMI is a powerful tool for studying vaccine efficacy it can also be used to study how vaccine induced antigen-specific components of the immune system respond to native antigen exposure in the context of parasitic infection. Whilst the duration and intensity of infection in CHMI is greatly reduced compared to natural infection (due to the requirement of treatment at defined end-points), this model still provides acute exposure to an increasing level of antigen, at doses relative to parasite expression rather than vaccine dose. Malaria-naïve individuals are a good starting point for comparing how closely CHMI represents natural infection. In Chapter 3, I showed how naïve volunteers in these clinical trials induced antibody and mBC to MSP1 but not AMA1. This could be expected given the relative abundance of MSP1 compared to AMA1 on the parasite. However, in naturally-exposed African populations, mBC and antibody to both antigens are routinely reported, although dominance of an MSP1 response has been associated with a low-level single exposure in at least one other study [94]. The suggestion that low-level parasite exposure dominantly promotes expansion of an MSP1-specific response is also supported by the observation in Chapter 3 that after CHMI, vaccine-induced MSP1-specific mBC resting levels are boosted significantly whilst AMA1-specific mBC are not. Similarly the observation of a migration away from the peripheral blood of MSP1-specific mBC during CHMI suggests particular activation of MSP1-specific cells. Further investigation into this population suggested these cells were likely $CXCR3^{+}$ mBC, responding to inflammatory cytokines induced during CHMI and likely produced by vaccine-induced, antigen-specific T cells. It was also suggested that pre-existing antibody could enhance both activation of T and B cell populations by enhancing antigen uptake by APCs. One of the main questions posed from these data is whether this immediate response to CHMI is fully representative of what might happen in the field. For example, I observed that mBC responses were boosted after

antimalarial treatment, and it is unknown what would happen if the infection continued unchecked. In some studies of natural infection in areas of high malaria burden, mBC development has been shown to be limited and antibody responses short-lived [96, 97]. In contrast, in areas of low malaria burden antibody and memory responses have been shown to be long lived [93, 94]. It may be that factors such as intensity of individual infections, accessibility of treatment, type of treatment or parasite strain, may contribute to such observations. One way to test this, in theory, would be to allow CHMI volunteers to progress to higher parasitaemia, but this is not possible due to ethical restrictions, or to look at alternative methods of drug clearance (such as sub-curative dosing with antimalarial drugs, which is currently being explored as one means to induce gametocytaemia to allow for testing of transmission-blocking vaccines in the CHMI model). Such a model could allow the infection to impact on vaccine-induced B cell responses in a manner that more closely mirrors natural infection, or at least in a manner that narrows down the list confounding variables.

8.2.3. Peripheral blood Tfh cells have been described for the first time following malaria vaccination and distinct populations correlate with different aspects of the antibody and B cell response.

The study of peripheral blood Tfh cells is relatively new [78] but has already become of particular interest to those studying HIV [124], Influenza [125] and autoimmune diseases [365]. In this Thesis I characterise, for the first time, the peripheral blood Tfh response following vaccination with a malaria antigen, in this case AMA1. Recently the field has sought to consolidate available data on Tfh populations from the available studies and a 3D model has been proposed that accounts for lineage specificity and helper ability [368]. This model was utilised in Chapter 7 to look at whether specific baseline or induced populations of Tfh cells were predictors of vaccine-induced antibody or B cell

responses. No baseline populations were found to correlate with antibody titre, B cell populations or functionality after priming vaccination. Previous studies in HIV have suggested that the frequency of total circulating memory Tfh ($CD4^+$ $CXCR5^+$,$CXCR3^-$, $PD1^+$) cells are predictive of an individual's ability to produce broadly-neutralising antibodies, but these individuals were at the extremes of a spectrum [124]. Although measures of antibody functionality such as GIA and antibody affinity were measured in the volunteers presented in Chapter 7, very little variation exists after priming, and the different prime-boost regimens offered too many confounding variables to study this in depth [113, 301]. However, strong correlations were observed between different Tfh populations post-boost, and antibody, ASC and mBC responses. The observation of a correlation between Th1 lineage cells, particularly in the $PD\text{-}1^+$ subset and ASC and antibody responses, was not unexpected following vaccination with ChAd63, given the induction of IFN-γ producing T cells by viral vectors. Th1 Tfh cells express the inflammatory migratory marker $CXCR3^+$ and in Chapter 4 I suggested that vaccine-induced B cells are also likely $CXCR3^+$. It is therefore logical to assume that during an inflammatory event, such as viral vector vaccination, these populations are likely to come into contact. Further to this, Th1 Tfh populations are reported to be poor helpers and can only provide help to some memory populations and not naïve cells [368]. This may suggest that this population favours induction of a fast acting extra-follicular response. However, in the studies shown here both ASC and mBC responses are increased post-boost. The second observation that Th2/Th17 $PD\text{-}1^+$ Tfh cells correlate with mBC responses but not ASC or antibody responses explains this observation. It appears there is a division of labour in terms of helping the B cell response, with this latter population perhaps being linked or derived from GC Tfh populations that have higher helper capacity and can promote class switching and formation of new IgG^+ mBC.

8.2.4. Functional human mAbs can be isolated from volunteers vaccinated with candidate blood-stage malaria antigens

In this Thesis I have also isolated and characterised the first fully human mAbs against AMA1. In the absence of antigen-specific staining of ASC at 7 days post-boost, this process has been less efficient than previously reported for other antigens, for example from Influenza [263]. However, given how few AMA1 mAbs have been characterised which are derived from mice [166], this is a good start from a single, vaccinated individual. One of the two mAbs generated, C2(H1K4), showed high growth inhibitory activity, much greater than any AMA1-specific mouse mAbs described in the literature. As a proof of principle this result shows there is potential for using this method to generate a panel of effective and useful mAbs. Identification of a panel of broadly-neutralising, synergistic AMA1 mAbs may have potential as a therapeutic either alone, or in combination with mAbs against other candidate antigens. Approaches to deliver mAbs in a prophylactic manner using viral vectors are also now being reported [343], and such technologies could hold significant promise for the future if highly effective human mAbs can be identified. To date, despite induction of high titres of AMA1-specific antibody following vaccination no convincing efficacy has been observed. The problem may be that a large proportion of the vaccine-induced polyclonal antibody response is antigen-specific but non-neutralising, much like the mAb D2(H3L8) and such antibodies may out-compete neutralising antibodies. If AMA1 is to be further considered as a viable blood-stage malaria vaccine candidate then such problems must be addressed. It may be that other blood-stage antigens candidates such as MSP1 would have suffered from a similar problem, which given their exposure to the immune system is a distinct possibility. However, new generation vaccine candidate antigens such as PfRH5 [116] are partly selected on the basis that they are not under selection pressure, implying that the immune response may be highly directed, broadly neutralising and non-diversionary. Analysis of mAbs from such vaccine trials will hopefully yield such information and more.

8.3. Future Directions

8.3.1. The role of B cell ELISPOT in future clinical trial immuno-monitoring

The B cell ELISPOT remains a robust, sensitive and informative assay for studying vaccine-induced ASC and mBC responses. Such responses have now been reported across a range of trials, and the assay is being used to study other candidate blood-stage antigens including PfRH5 and the *Plasmodium vivax* candidate antigen DBP in Phase Ia safety and immunogenicity trials. Given that high titres of neutralising antibody will be required for efficacy, future trials of these antigens will likely include testing mixed-modality regimens to establish optimal antibody induction. In such studies measuring B cell responses is likely to be highly important for establishing correlates of antibody magnitude and longevity, as well as (hopefully) efficacy in the future.

8.3.2. Maximising the investigative potential of CHMI

In this Thesis I have looked at B cell responses following mosquito bite CHMI and established that vaccine-induced B cells can respond to such an infection. I have also characterised the induction of mBC responses in naïve British volunteers following both mosquito bite and needle and syringe CHMI. However there are still a number of questions for which CHMI studies may be a powerful tool to help answer. Firstly no-one has yet looked to see how vaccine-induced B cell populations respond to blood-stage CHMI in comparison to mosquito bite CHMI. The recently completed VAC054 clinical trial (Payne *et al.,* in preparation) may provide an opportunity to test this. Preliminary data suggest that this form of CHMI results in less systemic adverse events, which may be indicative of reduced inflammation and may be as a result of bypassing liver infection. In Chapter 4 I proposed that inflammatory cytokines (IFN-γ and CXCL9) drove migration of $CXCR3^+$ B cells away from the peripheral blood and possibly promoted proliferation of short-lived rather than long-lived plasma cells. It would be interesting to see if data from

a blood-stage CHMI supported such a model. I also proposed that following drug treatment the B cell response follows a more classical kinetic. In future it would therefore be interesting to look for ASC responses around 7 days post treatment. In both CHMI models it would be interesting to look at different cell populations in addition to $CXCR3^+$ B cells. These could include B cells expressing other migration markers such as CXCR4 or CXCR5. Given the data presented in Chapter 7 it would also be of great interest to study Tfh cells expressing these markers and how they behave during CHMI. There also remains interest in the malaria field in the 'atypical mBC' subset, particularly in the context of natural infection [128, 129] and as to whether these cells are functional [287]. While they were discussed in Chapter 4 in the context of CHMI, there is scope for further investigation as to whether this is a useful tool for studying this subset. Finally it is important to note that the CHMI model has now been used in studies in African populations including both naïve and naturally-exposed individuals [254] (Hodgson *et al.*, submitted). In future this will allow for comparison between these populations and the now existing datasets from Caucasian populations.

8.3.3. Relationships and interactions between B cell and Tfh populations

In Chapter 7 I presented the first data on the peripheral blood Tfh response following vaccination with malaria antigen. This was a preliminary investigation and as such there are numerous questions still to be answered. One of the key questions asked in this study was whether baseline populations of Tfh cells can predict antibody responses after vaccination. The VAC044 study was not powered to answer such a question due to the range of different booster vaccinations across the groups. To definitively answer this question, baseline responses will be characterised from numerous individuals all receiving the same prime and boost vaccines (ChAd63-MVA), with baseline compared to peak boost responses, where magnitude and therefore power to detect differences, is increased. Although correlations were shown

between Tfh subsets and antibody, ASC and mBC, I have not yet proved the capacity of these subsets to provide help for B cells *in vitro*. Such experiments have been performed in other studies and recently a predictive 3D model of helper capacity has been proposed based on phenotype [368]. It would therefore be of interest to determine whether the populations I identified fit such a model. A final area of interest regarding Tfh cells is whether or not the vaccine developer can manipulate these populations using selective vaccines or adjuvants. This has been discussed in the context of influenza vaccination [369], but to date there is little definitive data supporting this idea. I believe more basic scientific understanding of these subsets across more vaccine targeted diseases is required before this is a reality.

8.3.4. The future of MSP1 and AMA1 as candidate malaria vaccine candidates

In this Thesis, data have been obtained from a number of Phase Ia and IIa clinical trials testing the immunogenicity and efficacy of candidate vaccines for the blood-stage antigens MSP1 and AMA1 [51, 114, 216, 217, 301]. While the immunogenicity reported has been robust, efficacy has so far been poor: with sterile protection only described in one volunteer in VAC039 who received both AMA1 and MSP1 [51], and this is likely attributed to a liver-stage effect. In the most recent Phase IIa trial VAC054 (Payne *et al.*, in preparation) the AMA1 vaccine tested was reported to have shown strain-specific efficacy in a Malian population [375], yet showed no efficacy following strain-specific blood-stage CHMI. The outstanding question is now whether these two candidates have a future.

Firstly MSP1 has shown no protection in human clinical trials despite promise in pre-clinical studies. When included with either AMA1 or the liver-stage candidate ME-TRAP in co-vaccination regimens, reductions in antibody and T cells responses were observed for the second antigen but not MSP1, suggesting immuno-dominance of MSP1 [51]. As discussed in Chapter 4, I believe MSP1 provides an immune-diversionary role in infection with strong responses towards it induced at the expense of other

more critical antigens. The fact that it is highly abundant and the $MSP1_{33}$ fragment is shed during invasion likely contribute to this. My results also suggest that vaccine-induced MSP1-specific T cells may contribute negatively to efficacy by drawing B cells away from the periphery and promoting a short-lived response. One other problem with MSP1 as a candidate is that the predicted amount of MSP1-specific IgG required to give a 50% GIA is around 0.6-1 mg/mL [296]. Whilst this can be achieved in mice and *Aotus* monkeys with Freund's adjuvant such levels are physiologically unattainable in humans through vaccination. These data in combination lead me to believe that MSP1 is no longer a viable candidate for trying to achieve protection by means of a 'non-natural' vaccine-induced response.

AMA1 has shown more potential as a protective antigen in humans but ultimately appears to fall short of the mark for a number of reasons. AMA1 performs well in assays such as the GIA assay but the titres of antibody required for protection appear to be at a level that is not consistently achievable by vaccination in humans. However unlike MSP1 the predicted level of antibody required to give 50% GIA (100-200 µg/mL AMA1-specific IgG) may be achievable with the right regimen or technology. On top of this, polymorphisms across different strains are a major challenge [376], requiring induction of broadly neutralising antibody [351] that may only comprise a small proportion of the total response. In the VAC054 study there was no efficacy or no delay to parasitaemia following blood-stage CHMI (Payne *et al.*, in preparation). To date the only (marginal) efficacy attributable in humans to AMA1 is likely through T cells acting on liver-stage parasites expressing AMA1 at a late-stage of hepatic development [51, 267]. Recently there have also been studies questioning whether AMA1 is actually essential for parasite invasion of erythrocytes [377]. AMA1 was selected as a candidate based on its role in invasion, but such studies may provide explanations for failures of AMA1 in trials so far. Personally while I believe antibodies against AMA1 can provide some level of protection against *P. falciparum* infection, I believe this may only be achieved through a non-vaccine induced route which will allow for artificially high titres

of antibody and in combination with other blood-stage target antigens such as in a mAb cocktail (see section 8.3.6).

8.3.5. Improving the identification and isolation of antigen-specific B cells

One of the major conclusions from Chapter 5 was that antigen-specific staining of B cell populations using MSP1 and AMA1 was not possible using traditional techniques, a result that mirrors previously published data [278]. The techniques here may be more successful for other malaria antigens, perhaps those that are smaller or less 'sticky'. Newer techniques for antigen-specific staining are currently under development which will attempt to overcome such problems as non-specific binding. A working method for antigen-specific staining would allow not only more efficient identification of antigen-specific ASC at 7 days post-boost, but also mBC and other phenotypically distinct populations to be identified in order to more accurately characterise their behaviour, rather than looking at bulk subsets as in Chapter 4. The use of antigen tetramer techniques in particular can also be adapted to pull out antigen-specific $CD4^+$ peripheral Tfh cells as well as B cells, and may be of use to allow study of interactions between these antigen-specific populations.

8.3.6. Production of mAb targeting alternative blood-stage malaria antigens

The lack of efficacy afforded by AMA1 vaccination in the recent VAC054 clinical trial makes the generation of a large panel and in-depth study of AMA1-specific mAbs less of a priority. However given that the AMA1-specific mAb C2(H1K4) had significant growth inhibitory activity it would be of interest to characterise its binding sites on the AMA1 protein in the context of the previous work published using mouse mAbs [166]. It would also be worth characterising the non-neutralising mAb D2(H3L8) in more detail to observe whether it could contribute to competitive exclusion of other neutralising mAbs,

possibly in the context of an immune evasion strategy. Future work will therefore focus on production of mAbs against other candidate antigens including PfRH5 and PvDBP. Recently the crystal structure of PfRH5 in complex with its receptor basigin has been solved and the binding sites of inhibitory mouse mAbs identified [378]. Repeating this study with human derived inhibitory mAbs would be of great interest, particularly if in the future, efficacy was to be achieved with this vaccine. Similarly identifying and characterising human mAbs that inhibit the interaction between the DBP antigen and Duffy antigen receptor for chemokines (DARC) on red blood cells would be of significant interest [379]. A major challenge facing the blood-stage malaria vaccine field is generating high enough titres of antibody using current regimens. If such titres cannot be achieved through vaccination then alternative approaches may be explored. The successful use of therapeutic mAbs in the treatment of disease has been growing in the last two decades [282].Recently the experimental mAb cocktail ZMapp for the treatment of Ebola virus has been fast tracked from non-human primates [380] to humans with reported success. A similar approach with production of a cocktail of synergistic, fully human mAbs against blood-stage malaria targets is one approach that will be looked into in future. One limitation with this approach is that such therapeutics are often required at a high dose which results in a high production costs, a problem that has arisen with ZMapp. One alternative approach which bypasses such problems is vectored immunoprophylaxis [343]. Adeno-associated virus (AAV) can be used to deliver mAbs, which are expressed *in situ* from virally-transduced cells following intramuscular immunisation. In mice this approach has been shown to induce circulating serum levels of > 1000 μg/mL mAb that persist for up to 1 year, and protection against numerous mouse infectious disease challenge models [381, 382] including malaria sporozoites [344]. Utilising such an approach to induce high titres of neutralising blood-stage specific antibody is therefore an attractive prospect.

8.4. Final Remarks

An efficacious blood-stage malaria vaccine requires the induction of high titre neutralising antibodies. In this Thesis I have sought to characterise quantitative and qualitative aspects of the B cell response in humans that are responsible for both induction and maintenance of these antibodies. The blood-stage antigens MSP1 and AMA1 are the focus of clinical trials in this Thesis. Although these vaccines showed promise in pre-clinical trials and are strongly immunogenic in human trials, they have ultimately been disappointing in terms of human efficacy. In this Thesis I have attempted to provide explanations on a cellular level as to why there is such disparity between pre-clinical and human data and ultimately why these candidates may have failed to provide efficacy. Such work will provide a strong basis for analysing future clinical trials of alternative candidate blood-stage vaccines and allow accurate characterisation of immune correlates and clinical efficacy when it is achieved.

References

1. WHO, *World Malaria Report 2012.* 2012.
2. Guerra, C.A., et al., *The international limits and population at risk of Plasmodium vivax transmission in 2009.* PLoS Negl Trop Dis, 2010. **4**(8): p. e774.
3. World Health Organization., *Guidelines for the treatment of malaria*. 2nd ed. 2010, Geneva: World Health Organization. xi, 194 p.
4. Galinski, M.R. and J.W. Barnwell, *Monkey malaria kills four humans.* Trends Parasitol, 2009. **25**(5): p. 200-4.
5. Singh, B., et al., *A large focus of naturally acquired Plasmodium knowlesi infections in human beings.* Lancet, 2004. **363**(9414): p. 1017-24.
6. Sachs, J. and P. Malaney, *The economic and social burden of malaria.* Nature, 2002. **415**(6872): p. 680-5.
7. Baum, J., et al., *Host-cell invasion by malaria parasites: insights from Plasmodium and Toxoplasma.* Trends in Parasitology, 2008. **24**(12): p. 557-563.
8. Beier, J.C., *Malaria parasite development in mosquitoes.* Annu Rev Entomol, 1998. **43**: p. 519-43.
9. Stark, K.R. and A.A. James, *Salivary gland anticoagulants in culicine and anopheline mosquitoes (Diptera:Culicidae).* J Med Entomol, 1996. **33**(4): p. 645-50.
10. Hulden, L., *Activation of the hypnozoite: a part of Plasmodium vivax life cycle and survival.* Malar J. **10**: p. 90.
11. Kafsack, B.F., et al., *A transcriptional switch underlies commitment to sexual development in malaria parasites.* Nature, 2014. **507**(7491): p. 248-52.
12. Sinha, A., et al., *A cascade of DNA-binding proteins for sexual commitment and development in Plasmodium.* Nature, 2014. **507**(7491): p. 253-7.
13. Crawley, J., et al., *Malaria in children.* Lancet, 2010. **375**(9724): p. 1468-81.
14. Perkins, D.J., et al., *Severe malarial anemia: innate immunity and pathogenesis.* Int J Biol Sci. **7**(9): p. 1427-42.
15. Rogerson, S.J., et al., *Malaria in pregnancy: pathogenesis and immunity.* Lancet Infect Dis, 2007. **7**(2): p. 105-17.
16. Hunt, N.H., et al., *Immunopathogenesis of cerebral malaria.* Int J Parasitol, 2006. **36**(5): p. 569-82.
17. Alkadarou, T., et al., *Immunological characteristics of hyperreactive malarial splenomegaly syndrome in sudanese patients.* J Trop Med, 2013. **2013**: p. 961051.
18. Claessens, A., et al., *A subset of group A-like var genes encodes the malaria parasite ligands for binding to human brain endothelial cells.* Proc Natl Acad Sci U S A, 2012. **109**(26): p. E1772-81.
19. Jensen, A.T., et al., *Plasmodium falciparum associated with severe childhood malaria preferentially expresses PfEMP1 encoded by group A var genes.* J Exp Med, 2004. **199**(9): p. 1179-90.
20. Kassim, O.O., et al., *Inhibitory factors in breastmilk, maternal and infant sera against in vitro growth of Plasmodium falciparum malaria parasite.* J Trop Pediatr, 2000. **46**(2): p. 92-6.
21. Riley, E.M., et al., *Lack of association between maternal antibody and protection of African infants from malaria infection.* Infect Immun, 2000. **68**(10): p. 5856-63.
22. Bull, P.C., et al., *Parasite antigens on the infected red cell surface are targets for naturally acquired immunity to malaria.* Nat Med, 1998. **4**(3): p. 358-60.
23. Langhorne, J., et al., *Immunity to malaria: more questions than answers.* Nat Immunol, 2008. **9**(7): p. 725-32.

24. Struik, S.S. and E.M. Riley, *Does malaria suffer from lack of memory?* Immunol Rev, 2004. **201**: p. 268-90.
25. Ayieko, C., et al., *Changes in B Cell Populations and Merozoite Surface Protein-1-Specific Memory B Cell Responses after Prolonged Absence of Detectable Infection.* PLoS One, 2013. **8**(6): p. e67230.
26. Ndungu, F.M., et al., *Long-lived Plasmodium falciparum-specific memory B cells in naturally exposed Swedish Travellers.* Eur J Immunol, 2013.
27. Ghani, A.C., et al., *Loss of population levels of immunity to malaria as a result of exposure-reducing interventions: consequences for interpretation of disease trends.* PLoS One, 2009. **4**(2): p. e4383.
28. Aponte, J.J., et al., *Age interactions in the development of naturally acquired immunity to Plasmodium falciparum and its clinical presentation.* PLoS Med, 2007. **4**(7): p. e242.
29. Stevenson, M.M. and E.M. Riley, *Innate immunity to malaria.* Nat Rev Immunol, 2004. **4**(3): p. 169-80.
30. Ockenhouse, C.F., S. Schulman, and H.L. Shear, *Induction of crisis forms in the human malaria parasite Plasmodium falciparum by gamma-interferon-activated, monocyte-derived macrophages.* J Immunol, 1984. **133**(3): p. 1601-8.
31. Ockenhouse, C.F. and H.L. Shear, *Oxidative killing of the intraerythrocytic malaria parasite Plasmodium yoelii by activated macrophages.* J Immunol, 1984. **132**(1): p. 424-31.
32. Ockenhouse, C.F., S. Schulman, and H.L. Shear, *Oxidative killing of malaria parasites by mononuclear phagocytes.* Prog Clin Biol Res, 1984. **155**: p. 93-108.
33. Serghides, L., et al., *CD36 and malaria: friends or foes?* Trends Parasitol, 2003. **19**(10): p. 461-9.
34. Sun, T. and C. Chakrabarti, *Schizonts, merozoites, and phagocytosis in falciparum malaria.* Ann Clin Lab Sci, 1985. **15**(6): p. 465-9.
35. Greve, B., et al., *High oxygen radical production is associated with fast parasite clearance in children with Plasmodium falciparum malaria.* J Infect Dis, 1999. **179**(6): p. 1584-6.
36. Joos, C., et al., *Clinical protection from falciparum malaria correlates with neutrophil respiratory bursts induced by merozoites opsonized with human serum antibodies.* PLoS One, 2010. **5**(3): p. e9871.
37. Stevenson, M.M. and B.C. Urban, *Antigen presentation and dendritic cell biology in malaria.* Parasite Immunol, 2006. **28**(1-2): p. 5-14.
38. Kasturi, S.P., et al., *Programming the magnitude and persistence of antibody responses with innate immunity.* Nature, 2011. **470**(7335): p. 543-7.
39. Mohan, K., P. Moulin, and M.M. Stevenson, *Natural killer cell cytokine production, not cytotoxicity, contributes to resistance against blood-stage Plasmodium chabaudi AS infection.* J Immunol, 1997. **159**(10): p. 4990-8.
40. Walther, M., et al., *Innate immune responses to human malaria: heterogeneous cytokine responses to blood-stage Plasmodium falciparum correlate with parasitological and clinical outcomes.* J Immunol, 2006. **177**(8): p. 5736-45.
41. Rzepczyk, C.M., et al., *Experimental human Plasmodium falciparum infections: longitudinal analysis of lymphocyte responses with particular reference to gamma delta T cells.* Scand J Immunol, 1996. **43**(2): p. 219-27.
42. Silver, K.L., et al., *Complement driven innate immune response to malaria: fuelling severe malarial diseases.* Cell Microbiol, 2010. **12**(8): p. 1036-45.
43. Bouharoun-Tayoun, H., et al., *Mechanisms underlying the monocyte-mediated antibody-dependent killing of Plasmodium falciparum asexual blood stages.* J Exp Med, 1995. **182**(2): p. 409-18.

44. Pusic, K.M., et al., *T cell epitope regions of the P. falciparum MSP1-33 critically influence immune responses and in vitro efficacy of MSP1-42 vaccines.* PLoS One, 2011. **6**(9): p. e24782.
45. Good, M.F., et al., *Development and regulation of cell-mediated immune responses to the blood stages of malaria: implications for vaccine research.* Annu Rev Immunol, 2005. **23**: p. 69-99.
46. Good, M.F. and C. Engwerda, *Defying malaria: Arming T cells to halt malaria.* Nat Med, 2011. **17**(1): p. 49-51.
47. Ramharter, M., et al., *Age-dependency of Plasmodium falciparum-specific and non-specific T cell cytokine responses in individuals from a malaria-endemic area.* Eur Cytokine Netw, 2005. **16**(2): p. 135-43.
48. Xu, H., et al., *CD4+ T cells acting independently of antibody contribute to protective immunity to Plasmodium chabaudi infection after apical membrane antigen 1 immunization.* J Immunol, 2000. **165**(1): p. 389-96.
49. Imai, T., et al., *Involvement of CD8+ T cells in protective immunity against murine blood-stage infection with Plasmodium yoelii 17XL strain.* Eur J Immunol, 2010. **40**(4): p. 1053-61.
50. Draper, S.J., et al., *Recombinant viral vaccines expressing merozoite surface protein-1 induce antibody- and T cell-mediated multistage protection against malaria.* Cell Host Microbe, 2009. **5**(1): p. 95-105.
51. Sheehy, S.H., et al., *ChAd63-MVA-vectored Blood-stage Malaria Vaccines Targeting MSP1 and AMA1: Assessment of Efficacy Against Mosquito Bite Challenge in Humans.* Mol Ther, 2012. **20**(12): p. 2355-68.
52. Bijker, E.M., et al., *Protection against malaria after immunization by chloroquine prophylaxis and sporozoites is mediated by preerythrocytic immunity.* Proc Natl Acad Sci U S A, 2013. **110**(19): p. 7862-7.
53. McHeyzer-Williams, L.J. and M.G. McHeyzer-Williams, *Antigen-specific memory B cell development.* Annu Rev Immunol, 2005. **23**: p. 487-513.
54. Tarlinton, D. and K. Good-Jacobson, *Diversity among memory B cells: origin, consequences, and utility.* Science, 2013. **341**(6151): p. 1205-11.
55. Papavasiliou, F.N. and D.G. Schatz, *Somatic hypermutation of immunoglobulin genes: merging mechanisms for genetic diversity.* Cell, 2002. **109 Suppl**: p. S35-44.
56. Pulendran, B., *Modulating vaccine responses with dendritic cells and Toll-like receptors.* Immunol Rev, 2004. **199**: p. 227-50.
57. Romani, N., et al., *Targeting skin dendritic cells to improve intradermal vaccination.* Curr Top Microbiol Immunol, 2012. **351**: p. 113-38.
58. Mac-Daniel, L., et al., *Local immune response to injection of Plasmodium sporozoites into the skin.* J Immunol, 2014. **193**(3): p. 1246-57.
59. Didierlaurent, A.M., et al., *Enhancement of adaptive immunity by the human vaccine adjuvant AS01 depends on activated dendritic cells.* J Immunol, 2014. **193**(4): p. 1920-30.
60. Heufler, C., et al., *Interleukin-12 is produced by dendritic cells and mediates T helper 1 development as well as interferon-gamma production by T helper 1 cells.* Eur J Immunol, 1996. **26**(3): p. 659-68.
61. Langenkamp, A., et al., *Kinetics of dendritic cell activation: impact on priming of TH1, TH2 and nonpolarized T cells.* Nat Immunol, 2000. **1**(4): p. 311-6.
62. Chua, C.L., et al., *Monocytes and macrophages in malaria: protection or pathology?* Trends Parasitol, 2013. **29**(1): p. 26-34.
63. Coban, C., et al., *TLR9 and endogenous adjuvants of the whole blood-stage malaria vaccine.* Expert Rev Vaccines, 2010. **9**(7): p. 775-84.
64. Grakoui, A., et al., *The immunological synapse: a molecular machine controlling T cell activation.* Science, 1999. **285**(5425): p. 221-7.

65. Haynes, N.M., et al., *Role of CXCR5 and CCR7 in follicular Th cell positioning and appearance of a programmed cell death gene-1high germinal center-associated subpopulation.* J Immunol, 2007. **179**(8): p. 5099-108.
66. Hardtke, S., L. Ohl, and R. Forster, *Balanced expression of CXCR5 and CCR7 on follicular T helper cells determines their transient positioning to lymph node follicles and is essential for efficient B-cell help.* Blood, 2005. **106**(6): p. 1924-31.
67. Batista, F.D. and N.E. Harwood, *The who, how and where of antigen presentation to B cells.* Nat Rev Immunol, 2009. **9**(1): p. 15-27.
68. Capolunghi, F., et al., *Why do we need IgM memory B cells?* Immunol Lett, 2013. **152**(2): p. 114-20.
69. Gordon, S., A. Pluddemann, and S. Mukhopadhyay, *Sinusoidal Immunity: Macrophages at the Lymphohematopoietic Interface.* Cold Spring Harb Perspect Biol, 2014.
70. Pereira, J.P., L.M. Kelly, and J.G. Cyster, *Finding the right niche: B-cell migration in the early phases of T-dependent antibody responses.* Int Immunol, 2010. **22**(6): p. 413-9.
71. Bishop, G.A. and B.S. Hostager, *B lymphocyte activation by contact-mediated interactions with T lymphocytes.* Curr Opin Immunol, 2001. **13**(3): p. 278-85.
72. Stavnezer, J., J.E. Guikema, and C.E. Schrader, *Mechanism and regulation of class switch recombination.* Annu Rev Immunol, 2008. **26**: p. 261-92.
73. McAdam, A.J., et al., *ICOS is critical for CD40-mediated antibody class switching.* Nature, 2001. **409**(6816): p. 102-5.
74. Jacob, J., et al., *Intraclonal generation of antibody mutants in germinal centres.* Nature, 1991. **354**(6352): p. 389-92.
75. Smith, K.G., et al., *The phenotype and fate of the antibody-forming cells of the splenic foci.* Eur J Immunol, 1996. **26**(2): p. 444-8.
76. Heesters, B.A., R.C. Myers, and M.C. Carroll, *Follicular dendritic cells: dynamic antigen libraries.* Nat Rev Immunol, 2014. **14**(7): p. 495-504.
77. McHeyzer-Williams, L.J., et al., *Follicular helper T cells as cognate regulators of B cell immunity.* Curr Opin Immunol, 2009. **21**(3): p. 266-73.
78. Crotty, S., *Follicular helper CD4 T cells (TFH).* Annu Rev Immunol, 2011. **29**: p. 621-63.
79. Allen, C.D. and J.G. Cyster, *Follicular dendritic cell networks of primary follicles and germinal centers: phenotype and function.* Semin Immunol, 2008. **20**(1): p. 14-25.
80. Reinhardt, R.L., H.E. Liang, and R.M. Locksley, *Cytokine-secreting follicular T cells shape the antibody repertoire.* Nat Immunol, 2009. **10**(4): p. 385-93.
81. Poulsen, T.R., et al., *Limits for antibody affinity maturation and repertoire diversification in hypervaccinated humans.* J Immunol, 2011. **187**(8): p. 4229-35.
82. Hauser, A.E., et al., *Chemotactic responsiveness toward ligands for CXCR3 and CXCR4 is regulated on plasma blasts during the time course of a memory immune response.* J Immunol, 2002. **169**(3): p. 1277-82.
83. Slifka, M.K., et al., *Humoral immunity due to long-lived plasma cells.* Immunity, 1998. **8**(3): p. 363-72.
84. Xu, W. and J. Banchereau, *The antigen presenting cells instruct plasma cell differentiation.* Front Immunol, 2014. **4**: p. 504.
85. Bortnick, A. and D. Allman, *What is and what should always have been: long-lived plasma cells induced by T cell-independent antigens.* J Immunol, 2013. **190**(12): p. 5913-8.
86. Odendahl, M., et al., *Generation of migratory antigen-specific plasma blasts and mobilization of resident plasma cells in a secondary immune response.* Blood, 2005. **105**(4): p. 1614-21.
87. Dogan, I., et al., *Multiple layers of B cell memory with different effector functions.* Nat Immunol, 2009. **10**(12): p. 1292-9.

88. Cohen, S., I.A. McGregor, and S. Carrington, *Gamma-globulin and acquired immunity to human malaria.* Nature, 1961. **192**: p. 733-7.
89. Crompton, P.D., et al., *A prospective analysis of the Ab response to Plasmodium falciparum before and after a malaria season by protein microarray.* Proc Natl Acad Sci U S A, 2010. **107**(15): p. 6958-63.
90. Ndungu, F.M., et al., *Memory B cells are a more reliable archive for historical antimalarial responses than plasma antibodies in no-longer exposed children.* Proc Natl Acad Sci U S A, 2012. **109**(21): p. 8247-52.
91. Weiss, G.E., et al., *The Plasmodium falciparum-specific human memory B cell compartment expands gradually with repeated malaria infections.* PLoS Pathog, 2010. **6**(5): p. e1000912.
92. Fowkes, F.J., et al., *The relationship between anti-merozoite antibodies and incidence of Plasmodium falciparum malaria: A systematic review and meta-analysis.* PLoS Med, 2010. **7**(1): p. e1000218.
93. Wipasa, J., et al., *Long-lived antibody and B Cell memory responses to the human malaria parasites, Plasmodium falciparum and Plasmodium vivax.* PLoS Pathog, 2010. **6**(2): p. e1000770.
94. Clark, E.H., et al., *Plasmodium falciparum malaria in the Peruvian Amazon, a region of low transmission, is associated with immunologic memory.* Infect Immun, 2012. **80**(4): p. 1583-92.
95. Nogaro, S.I., et al., *The breadth, but not the magnitude, of circulating memory B cell responses to P. falciparum increases with age/exposure in an area of low transmission.* PLoS One, 2011. **6**(10): p. e25582.
96. Dorfman, J.R., et al., *B cell memory to 3 Plasmodium falciparum blood-stage antigens in a malaria-endemic area.* J Infect Dis, 2005. **191**(10): p. 1623-30.
97. Kinyanjui, S.M., et al., *IgG antibody responses to Plasmodium falciparum merozoite antigens in Kenyan children have a short half-life.* Malar J, 2007. **6**: p. 82.
98. Murhandarwati, E.E., et al., *Inhibitory antibodies specific for the 19-kilodalton fragment of merozoite surface protein 1 do not correlate with delayed appearance of infection with Plasmodium falciparum in semi-immune individuals in Vietnam.* Infect Immun, 2009. **77**(10): p. 4510-7.
99. Gilbert, S.C., et al., *Association of malaria parasite population structure, HLA, and immunological antagonism.* Science, 1998. **279**(5354): p. 1173-7.
100. Aribot, G., et al., *Pattern of immunoglobulin isotype response to Plasmodium falciparum blood-stage antigens in individuals living in a holoendemic area of Senegal (Dielmo, west Africa).* Am J Trop Med Hyg, 1996. **54**(5): p. 449-57.
101. Aucan, C., et al., *High immunoglobulin G2 (IgG2) and low IgG4 levels are associated with human resistance to Plasmodium falciparum malaria.* Infect Immun, 2000. **68**(3): p. 1252-8.
102. Nguer, C.M., et al., *Plasmodium falciparum- and merozoite surface protein 1-specific antibody isotype balance in immune Senegalese adults.* Infect Immun, 1997. **65**(11): p. 4873-6.
103. Stanisic, D.I., et al., *Immunoglobulin G subclass-specific responses against Plasmodium falciparum merozoite antigens are associated with control of parasitemia and protection from symptomatic illness.* Infect Immun, 2009. **77**(3): p. 1165-74.
104. Moss, D.K., et al., *Plasmodium falciparum merozoite surface protein (MSP) 119-specific antibodies that interfere with parasite growth in vitro can inhibit MSP1 processing, merozoite invasion and intracellular parasite development.* Infect Immun, 2011.
105. Kumaratilake, L.M., et al., *Effects of cytokines, complement, and antibody on the neutrophil respiratory burst and phagocytic response to Plasmodium falciparum merozoites.* Infect Immun, 1992. **60**(9): p. 3731-8.

106. Bouharoun-Tayoun, H., et al., *Antibodies that protect humans against Plasmodium falciparum blood stages do not on their own inhibit parasite growth and invasion in vitro, but act in cooperation with monocytes.* J Exp Med, 1990. **172**(6): p. 1633-41.
107. Biswas, S., et al., *Recombinant Viral-Vectored Vaccines Expressing Plasmodium chabaudi AS Apical Membrane Antigen 1: Mechanisms of Vaccine-Induced Blood-Stage Protection.* J Immunol, 2012. **188**(10): p. 5041-53.
108. Draper, S.J., et al., *Effective induction of high-titer antibodies by viral vector vaccines.* Nat Med, 2008. **14**(8): p. 819-21.
109. Darko, C.A., et al., *The clinical-grade 42-kilodalton fragment of merozoite surface protein 1 of Plasmodium falciparum strain FVO expressed in Escherichia coli protects Aotus nancymai against challenge with homologous erythrocytic-stage parasites.* Infect Immun, 2005. **73**(1): p. 287-97.
110. Dutta, S., et al., *High antibody titer against apical membrane antigen-1 is required to protect against malaria in the Aotus model.* PLoS One, 2009. **4**(12): p. e8138.
111. Ahlborg, N., et al., *Linkage of exogenous T-cell epitopes to the 19-kilodalton region of Plasmodium yoelii merozoite surface protein 1 (MSP1(19)) can enhance protective immunity against malaria and modulate the immunoglobulin subclass response to MSP1(19).* Infect Immun, 2000. **68**(4): p. 2102-9.
112. Miao, J., et al., *Immune responses in mice induced by prime-boost schemes of the Plasmodium falciparum apical membrane antigen 1 (PfAMA1)-based DNA, protein and recombinant modified vaccinia Ankara vaccines.* Vaccine, 2006. **24**(37-39): p. 6187-98.
113. Biswas, S., et al., *Assessment of Humoral Immune Responses to Blood-Stage Malaria Antigens following ChAd63-MVA Immunization, Controlled Human Malaria Infection and Natural Exposure.* PLoS One, 2014. **9**(9): p. e107903.
114. Duncan, C.J., et al., *Impact on Malaria Parasite Multiplication Rates in Infected Volunteers of the Protein-in-Adjuvant Vaccine AMA1-C1/Alhydrogel+CPG 7909.* PLoS One, 2011. **6**(7): p. e22271.
115. Ouattara, A., et al., *Molecular basis of allele-specific efficacy of a blood-stage malaria vaccine: vaccine development implications.* J Infect Dis, 2013. **207**(3): p. 511-9.
116. Douglas, A.D., et al., *The blood-stage malaria antigen PfRH5 is susceptible to vaccine-inducible cross-strain neutralizing antibody.* Nat Commun, 2011. **2**: p. 601.
117. Bustamante, L.Y., et al., *A full-length recombinant Plasmodium falciparum PfRH5 protein induces inhibitory antibodies that are effective across common PfRH5 genetic variants.* Vaccine, 2013. **31**(2): p. 373-9.
118. Reddy, K.S., et al., *Bacterially Expressed Full-Length Recombinant Plasmodium falciparum RH5 Protein Binds Erythrocytes and Elicits Potent Strain-Transcending Parasite-Neutralizing Antibodies.* Infect Immun, 2013. **82**(1): p. 152-64.
119. Williams, A.R., et al., *Enhancing Blockade of Plasmodium falciparum Erythrocyte Invasion: Assessing Combinations of Antibodies against PfRH5 and Other Merozoite Antigens.* PLoS Pathog, 2012. **8**(11): p. e1002991.
120. Crotty, S., et al., *Cutting edge: long-term B cell memory in humans after smallpox vaccination.* J Immunol, 2003. **171**(10): p. 4969-73.
121. Amanna, I.J., N.E. Carlson, and M.K. Slifka, *Duration of humoral immunity to common viral and vaccine antigens.* N Engl J Med, 2007. **357**(19): p. 1903-15.
122. Blanchard-Rohner, G., et al., *Appearance of peripheral blood plasma cells and memory B cells in a primary and secondary immune response in humans.* Blood, 2009. **114**(24): p. 4998-5002.
123. Chevalier, N., et al., *CXCR5 expressing human central memory CD4 T cells and their relevance for humoral immune responses.* J Immunol, 2011. **186**(10): p. 5556-68.

124. Locci, M., et al., *Human Circulating PD-1(+)CXCR3(-)CXCR5(+) Memory Tfh Cells Are Highly Functional and Correlate with Broadly Neutralizing HIV Antibody Responses.* Immunity, 2013. **39**(4): p. 758-69.
125. Bentebibel, S.E., et al., *Induction of ICOS+CXCR3+CXCR5+ TH cells correlates with antibody responses to influenza vaccination.* Sci Transl Med, 2013. **5**(176): p. 176ra32.
126. Asito, A.S., et al., *Alterations on peripheral B cell subsets following an acute uncomplicated clinical malaria infection in children.* Malar J, 2008. **7**: p. 238.
127. Asito, A.S., et al., *Suppression of circulating IgD+CD27+ memory B cells in infants living in a malaria-endemic region of Kenya.* Malar J, 2011. **10**: p. 362.
128. Weiss, G.E., et al., *A positive correlation between atypical memory B cells and Plasmodium falciparum transmission intensity in cross-sectional studies in Peru and Mali.* PLoS One, 2011. **6**(1): p. e15983.
129. Weiss, G.E., et al., *Atypical memory B cells are greatly expanded in individuals living in a malaria-endemic area.* J Immunol, 2009. **183**(3): p. 2176-82.
130. Portugal, S., S.K. Pierce, and P.D. Crompton, *Young lives lost as B cells falter: what we are learning about antibody responses in malaria.* J Immunol, 2013. **190**(7): p. 3039-46.
131. Nduati, E., et al., *The plasma concentration of the B cell activating factor is increased in children with acute malaria.* J Infect Dis, 2011. **204**(6): p. 962-70.
132. Urban, B.C., et al., *Plasmodium falciparum-infected erythrocytes modulate the maturation of dendritic cells.* Nature, 1999. **400**(6739): p. 73-7.
133. Urban, B.C. and D.J. Roberts, *Malaria, monocytes, macrophages and myeloid dendritic cells: sticking of infected erythrocytes switches off host cells.* Curr Opin Immunol, 2002. **14**(4): p. 458-65.
134. Sponaas, A.M., et al., *Transient deficiency of dendritic cells results in lack of a merozoite surface protein 1-specific CD4 T cell response during peak Plasmodium chabaudi blood-stage infection.* Infect Immun, 2012. **80**(12): p. 4248-56.
135. Urban, B.C., et al., *Fatal Plasmodium falciparum malaria causes specific patterns of splenic architectural disorganization.* Infect Immun, 2005. **73**(4): p. 1986-94.
136. van Noort, S.P., et al., *Immune selection and within-host competition can structure the repertoire of variant surface antigens in Plasmodium falciparum--a mathematical model.* Plos One, 2010. **5**(3): p. e9778.
137. Czajkowsky, D.M., et al., *IgM, Fc mu Rs, and malarial immune evasion.* J Immunol, 2010. **184**(9): p. 4597-603.
138. Plebanski, M., et al., *Altered peptide ligands narrow the repertoire of cellular immune responses by interfering with T-cell priming.* Nat Med, 1999. **5**(5): p. 565-71.
139. Keja, K., et al., *Expanded programme on immunization.* World Health Stat Q, 1988. **41**(2): p. 59-63.
140. Moorthy, V.S., R.D. Newman, and J.M. Okwo-Bele, *Malaria vaccine technology roadmap.* Lancet, 2013. **382**(9906): p. 1700-1.
141. Hill, A.V., *Pre-erythrocytic malaria vaccines: towards greater efficacy.* Nat Rev Immunol, 2006. **6**(1): p. 21-32.
142. Richards, J.S. and J.G. Beeson, *The future for blood-stage vaccines against malaria.* Immunol.Cell Biol., 2009. **87**(5): p. 377-390.
143. Coppi, A., et al., *The malaria circumsporozoite protein has two functional domains, each with distinct roles as sporozoites journey from mosquito to mammalian host.* J Exp Med, 2011. **208**(2): p. 341-56.
144. Cohen, J., et al., *From the circumsporozoite protein to the RTS, S/AS candidate vaccine.* Hum Vaccin, 2010. **6**(1): p. 90-6.

145. Baum, J., et al., *A conserved molecular motor drives cell invasion and gliding motility across malaria life cycle stages and other apicomplexan parasites.* J Biol Chem, 2006. **281**(8): p. 5197-208.
146. Wengelnik, K., et al., *The A-domain and the thrombospondin-related motif of Plasmodium falciparum TRAP are implicated in the invasion process of mosquito salivary glands.* Embo J, 1999. **18**(19): p. 5195-204.
147. O'Hara, G.A., et al., *Clinical Assessment of a Recombinant Simian Adenovirus ChAd63: A Potent New Vaccine Vector.* J Infect Dis, 2012. **205**(5): p. 772-81.
148. Ogwang, C., et al., *Safety and Immunogenicity of Heterologous Prime-Boost Immunisation with Plasmodium falciparum Malaria Candidate Vaccines, ChAd63 ME-TRAP and MVA ME-TRAP, in Healthy Gambian and Kenyan Adults.* PLoS One, 2013. **8**(3): p. e57726.
149. Patarroyo, M.A., D. Calderon, and D.A. Moreno-Perez, *Vaccines against Plasmodium vivax: a research challenge.* Expert Rev Vaccines, 2012. **11**(10): p. 1249-60.
150. Holder, A.A., et al., *A malaria merozoite surface protein (MSP1)-structure, processing and function.* Mem Inst Oswaldo Cruz, 1992. **87 Suppl 3**: p. 37-42.
151. Holder, A.A., *The carboxy-terminus of merozoite surface protein 1: structure, specific antibodies and immunity to malaria.* Parasitology, 2009. **136**(12): p. 1445-56.
152. O'Donnell, R.A., et al., *Functional conservation of the malaria vaccine antigen MSP-119across distantly related Plasmodium species.* Nat Med, 2000. **6**(1): p. 91-5.
153. Lee, E.A., et al., *Identification of frequently recognized dimorphic T-cell epitopes in plasmodium falciparum merozoite surface protein-1 in West and East Africans: lack of correlation of immune recognition and allelic prevalence.* Am J Trop Med Hyg, 2001. **64**(3-4): p. 194-203.
154. Riley, E.M., et al., *Naturally acquired cellular and humoral immune responses to the major merozoite surface antigen (PfMSP1) of Plasmodium falciparum are associated with reduced malaria morbidity.* Parasite Immunol, 1992. **14**(3): p. 321-37.
155. Lee, E.A., et al., *Dimorphic Plasmodium falciparum merozoite surface protein-1 epitopes turn off memory T cells and interfere with T cell priming.* Eur J Immunol, 2006. **36**(5): p. 1168-78.
156. Elias, S.C., et al., *Assessment of immune interference, antagonism, and diversion following human immunization with biallelic blood-stage malaria viral-vectored vaccines and controlled malaria infection.* J Immunol, 2013. **190**(3): p. 1135-47.
157. Howell, S.A., et al., *Proteolytic processing and primary structure of Plasmodium falciparum apical membrane antigen-1.* J Biol Chem, 2001. **276**(33): p. 31311-20.
158. Richard, D., et al., *Interaction between Plasmodium falciparum Apical Membrane Antigen 1 and the Rhoptry Neck Protein Complex Defines a Key Step in the Erythrocyte Invasion Process of Malaria Parasites.* Journal of Biological Chemistry, 2010. **285**(19): p. 14815-14822.
159. Srinivasan, P., et al., *Binding of Plasmodium merozoite proteins RON2 and AMA1 triggers commitment to invasion.* Proc Natl Acad Sci U S A, 2011. **108**(32): p. 13275-80.
160. Tyler, J.S., M. Treeck, and J.C. Boothroyd, *Focus on the ringleader: the role of AMA1 in apicomplexan invasion and replication.* Trends Parasitol, 2011. **27**(9): p. 410-20.
161. Escalante, A.A., et al., *Polymorphism in the gene encoding the apical membrane antigen-1 (AMA-1) of Plasmodium falciparum. X. Asembo Bay Cohort Project.* Mol Biochem Parasitol, 2001. **113**(2): p. 279-87.
162. Grynberg, P., et al., *Polymorphism at the apical membrane antigen 1 locus reflects the world population history of Plasmodium vivax.* BMC Evol Biol, 2008. **8**: p. 123.
163. Cortes, A., et al., *Allele specificity of naturally acquired antibody responses against Plasmodium falciparum apical membrane antigen 1.* Infect Immun, 2005. **73**(1): p. 422-30.

164. Coley, A.M., et al., *The most polymorphic residue on Plasmodium falciparum apical membrane antigen 1 determines binding of an invasion-inhibitory antibody.* Infect Immun, 2006. **74**(5): p. 2628-36.
165. Kusi, K.A., et al., *Immunization with different PfAMA1 alleles in sequence induces clonal imprint humoral responses that are similar to responses induced by the same alleles as a vaccine cocktail in rabbits.* Malar J, 2011. **10**: p. 40.
166. Dutta, S., et al., *Overcoming antigenic diversity by enhancing the immunogenicity of conserved epitopes on the malaria vaccine candidate apical membrane antigen-1.* PLoS Pathog, 2013. **9**(12): p. e1003840.
167. Duraisingh, M.T., et al., *Phenotypic variation of Plasmodium falciparum merozoite proteins directs receptor targeting for invasion of human erythrocytes.* Embo J, 2003. **22**(5): p. 1047-57.
168. Baum, J., et al., *Reticulocyte-binding protein homologue 5 - an essential adhesin involved in invasion of human erythrocytes by Plasmodium falciparum.* Int J Parasitol, 2009. **39**(3): p. 371-80.
169. Crosnier, C., et al., *Basigin is a receptor essential for erythrocyte invasion by Plasmodium falciparum.* Nature, 2011. **480**(7378): p. 534-7.
170. Douglas, A.D., et al., *Neutralization of Plasmodium falciparum Merozoites by Antibodies against PfRH5.* J Immunol, 2014. **192**(1): p. 245-58.
171. Miao, J., et al., *Puf mediates translation repression of transmission-blocking vaccine candidates in malaria parasites.* PLoS Pathog, 2013. **9**(4): p. e1003268.
172. Eksi, S., et al., *Malaria transmission-blocking antigen, Pfs230, mediates human red blood cell binding to exflagellating male parasites and oocyst production.* Mol Microbiol, 2006. **61**(4): p. 991-8.
173. van Dijk, M.R., et al., *A central role for P48/45 in malaria parasite male gamete fertility.* Cell, 2001. **104**(1): p. 153-64.
174. Stowers, A.W., et al., *A region of Plasmodium falciparum antigen Pfs25 that is the target of highly potent transmission-blocking antibodies.* Infect Immun, 2000. **68**(10): p. 5530-8.
175. Dinglasan, R.R., et al., *Disruption of Plasmodium falciparum development by antibodies against a conserved mosquito midgut antigen.* Proc Natl Acad Sci U S A, 2007. **104**(33): p. 13461-6.
176. Vaccines., m.C.G.o., *A research agenda for malaria eradication: vaccines.* PLoS Med, 2011. **8**(1): p. e1000398.
177. Bett, A.J., et al., *An efficient and flexible system for construction of adenovirus vectors with insertions or deletions in early regions 1 and 3.* Proc Natl Acad Sci U S A, 1994. **91**(19): p. 8802-6.
178. Sutter, G. and B. Moss, *Nonreplicating vaccinia vector efficiently expresses recombinant genes.* Proc Natl Acad Sci U S A, 1992. **89**(22): p. 10847-51.
179. Thomsen, D.R., et al., *Promoter-regulatory region of the major immediate early gene of human cytomegalovirus.* Proc Natl Acad Sci U S A, 1984. **81**(3): p. 659-63.
180. Sutter, G., et al., *A recombinant vector derived from the host range-restricted and highly attenuated MVA strain of vaccinia virus stimulates protective immunity in mice to influenza virus.* Vaccine, 1994. **12**(11): p. 1032-40.
181. Orubu, T., et al., *Expression and cellular immunogenicity of a transgenic antigen driven by endogenous poxviral early promoters at their authentic loci in MVA.* PLoS One, 2012. **7**(6): p. e40167.
182. Chakrabarti, S., J.R. Sisler, and B. Moss, *Compact, synthetic, vaccinia virus early/late promoter for protein expression.* Biotechniques, 1997. **23**(6): p. 1094-7.
183. Mackett, M., G.L. Smith, and B. Moss, *General method for production and selection of infectious vaccinia virus recombinants expressing foreign genes.* J Virol, 1984. **49**(3): p. 857-64.

184. Amalfitano, A., et al., *Production and characterization of improved adenovirus vectors with the E1, E2b, and E3 genes deleted.* J Virol, 1998. **72**(2): p. 926-33.
185. Ewer, K.J., et al., *Protective CD8+ T-cell immunity to human malaria induced by chimpanzee adenovirus-MVA immunisation.* Nat Commun, 2013. **4**: p. 2836.
186. Antrobus, R.D., et al., *Clinical Assessment of a Novel Recombinant Simian Adenovirus ChAdOx1 as a Vectored Vaccine Expressing Conserved Influenza A Antigens.* Mol Ther, 2013.
187. Borthwick, N., et al., *Vaccine-elicited Human T Cells Recognizing Conserved Protein Regions Inhibit HIV-1.* Mol Ther, 2014. **22**(2): p. 464-75.
188. Blanchard, T.J., et al., *Modified vaccinia virus Ankara undergoes limited replication in human cells and lacks several immunomodulatory proteins: implications for use as a human vaccine.* J Gen Virol, 1998. **79 (Pt 5)**: p. 1159-67.
189. Mayr, A., V. Hochstein-Mintzel, and H. Stickl, *Passage history, properties, and applicability of the attenuated vaccinia virus strain MVA.* Infection, 1975. **3**: p. 6-14.
190. Meyer, H., G. Sutter, and A. Mayr, *Mapping of deletions in the genome of the highly attenuated vaccinia virus MVA and their influence on virulence.* J Gen Virol, 1991. **72 (Pt 5)**: p. 1031-8.
191. McCurdy, L.H., et al., *Modified vaccinia Ankara: potential as an alternative smallpox vaccine.* Clin Infect Dis, 2004. **38**(12): p. 1749-53.
192. Xiang, Z.Q., et al., *A replication-defective human adenovirus recombinant serves as a highly efficacious vaccine carrier.* Virology, 1996. **219**(1): p. 220-7.
193. Rodrigues, E.G., et al., *Single immunizing dose of recombinant adenovirus efficiently induces CD8+ T cell-mediated protective immunity against malaria.* J Immunol, 1997. **158**(3): p. 1268-74.
194. Santra, S., et al., *Replication-defective adenovirus serotype 5 vectors elicit durable cellular and humoral immune responses in nonhuman primates.* J Virol, 2005. **79**(10): p. 6516-22.
195. Shott, J.P., et al., *Adenovirus 5 and 35 vectors expressing Plasmodium falciparum circumsporozoite surface protein elicit potent antigen-specific cellular IFN-gamma and antibody responses in mice.* Vaccine, 2008. **26**(23): p. 2818-23.
196. Sridhar, S., et al., *Single-dose protection against Plasmodium berghei by a simian adenovirus vector using a human cytomegalovirus promoter containing intron A.* J Virol, 2008. **82**(8): p. 3822-33.
197. O'Brien, K.L., et al., *Adenovirus-specific immunity after immunization with an Ad5 HIV-1 vaccine candidate in humans.* Nat Med, 2009. **15**(8): p. 873-5.
198. Sedegah, M., et al., *Adenovirus 5-Vectored P. falciparum Vaccine Expressing CSP and AMA1. Part A: Safety and Immunogenicity in Seronegative Adults.* PLoS One, 2011. **6**(10): p. e24586.
199. Tamminga, C., et al., *Adenovirus-5-Vectored P. falciparum Vaccine Expressing CSP and AMA1. Part B: Safety, Immunogenicity and Protective Efficacy of the CSP Component.* PLoS One, 2011. **6**(10): p. e25868.
200. McCoy, K., et al., *The effect of pre-existing immunity to antigens of adenovirus of the human serotype 5 on immune responses of nonhuman primates to vaccine regimens based on human or chimpanzee-derived adenovirus vectors.* J Virol, 2007.
201. Dudareva, M., et al., *Prevalence of serum neutralizing antibodies against chimpanzee adenovirus 63 and human adenovirus 5 in Kenyan Children, in the context of vaccine vector efficacy.* Vaccine, 2009. **27**(27): p. 3501-4.
202. Frahm, N., et al., *Human adenovirus-specific T cells modulate HIV-specific T cell responses to an Ad5-vectored HIV-1 vaccine.* J Clin Invest, 2012. **122**(1): p. 359-67.
203. Sumida, S.M., et al., *Neutralizing antibodies and CD8+ T lymphocytes both contribute to immunity to adenovirus serotype 5 vaccine vectors.* J Virol, 2004. **78**(6): p. 2666-73.
204. Tatsis, N., et al., *Chimpanzee-origin adenovirus vectors as vaccine carriers.* Gene Ther, 2006. **13**(5): p. 421-9.

205. Zhu, J., X. Huang, and Y. Yang, *Innate immune response to adenoviral vectors is mediated by both Toll-like receptor-dependent and -independent pathways.* J Virol, 2007. **81**(7): p. 3170-80.
206. Johnson, M.J., et al., *Type I IFN induced by adenovirus serotypes 28 and 35 has multiple effects on T cell immunogenicity.* J Immunol, 2012. **188**(12): p. 6109-18.
207. Sharma, A., et al., *Comparative analysis of vector biodistribution, persistence and gene expression following intravenous delivery of bovine, porcine and human adenoviral vectors in a mouse model.* Virology, 2009. **386**(1): p. 44-54.
208. Liu, J., et al., *Magnitude and phenotype of cellular immune responses elicited by recombinant adenovirus vectors and heterologous prime-boost regimens in rhesus monkeys.* J Virol, 2008. **82**(10): p. 4844-52.
209. Radosevic, K., et al., *The Th1 immune response to Plasmodium falciparum circumsporozoite protein is boosted by adenovirus vectors 35 and 26 with a homologous insert.* Clin Vaccine Immunol, 2010. **17**(11): p. 1687-94.
210. Barnes, E., et al., *Novel adenovirus-based vaccines induce broad and sustained T cell responses to HCV in man.* Sci Transl Med, 2012. **4**(115): p. 115ra1.
211. Price, P.J., et al., *Modified Vaccinia virus Ankara: innate immune activation and induction of cellular signalling.* Vaccine, 2013. **31**(39): p. 4231-4.
212. Duffy, D., et al., *Neutrophils transport antigen from the dermis to the bone marrow, initiating a source of memory CD8+ T cells.* Immunity, 2012. **37**(5): p. 917-29.
213. Thiele, F., et al., *MVA-infected Dendritic Cells Present CD4+ T-Cell Epitopes by Endogenous MHC Class II Presentation Pathways.* J Virol, 2014.
214. Halliday, J., P. Klenerman, and E. Barnes, *Vaccination for hepatitis C virus: closing in on an evasive target.* Expert Rev Vaccines, 2011. **10**(5): p. 659-72.
215. Tatsis, N., et al., *Multiple immunizations with adenovirus and MVA vectors improve CD8+ T cell functionality and mucosal homing.* Virology, 2007. **367**(1): p. 156-67.
216. Sheehy, S.H., et al., *Phase Ia Clinical Evaluation of the Plasmodium falciparum Blood-stage Antigen MSP1 in ChAd63 and MVA Vaccine Vectors.* Mol Ther, 2011. **19**(12): p. 2269-76.
217. Sheehy, S.H., et al., *Phase Ia Clinical Evaluation of the Safety and Immunogenicity of the Plasmodium falciparum Blood-Stage Antigen AMA1 in ChAd63 and MVA Vaccine Vectors.* PLoS One, 2012. **7**(2): p. e31208.
218. Becker, S.I., et al., *Protection of mice against Plasmodium yoelii sporozoite challenge with P. yoelii merozoite surface protein 1 DNA vaccines.* Infect Immun, 1998. **66**(7): p. 3457-61.
219. Crompton, P.D., et al., *The TLR9 ligand CpG promotes the acquisition of Plasmodium falciparum-specific memory B cells in malaria-naive individuals.* J Immunol, 2009. **182**(5): p. 3318-26.
220. de Cassan, S.C., et al., *The requirement for potent adjuvants to enhance the immunogenicity and protective efficacy of protein vaccines can be overcome by prior immunization with a recombinant adenovirus.* J Immunol, 2011. **187**(5): p. 2602-16.
221. Jain, N.K., et al., *Formulation and stabilization of recombinant protein based virus-like particle vaccines.* Adv Drug Deliv Rev, 2014.
222. Madhusudana, S.N. and R.S. Mani, *Intradermal vaccination for rabies prophylaxis: conceptualization, evolution, present status and future.* Expert Rev Vaccines, 2014. **13**(5): p. 641-55.
223. Marra, F., et al., *A meta-analysis of intradermal versus intramuscular influenza vaccines: immunogenicity and adverse events.* Influenza Other Respir Viruses, 2013. **7**(4): p. 584-603.
224. Belshe, R.B. and W.C. Gruber, *Safety, efficacy and effectiveness of cold-adapted, live, attenuated, trivalent, intranasal influenza vaccine in adults and children.* Philos Trans R Soc Lond B Biol Sci, 2001. **356**(1416): p. 1947-51.

225. Hokey, D.A. and A. Misra, *Aerosol vaccines for tuberculosis: a fine line between protection and pathology.* Tuberculosis (Edinb), 2011. **91**(1): p. 82-5.
226. Carey, J.B., et al., *Microneedle-mediated immunization of an adenovirus-based malaria vaccine enhances antigen-specific antibody immunity and reduces anti-vector responses compared to the intradermal route.* Sci Rep, 2014. **4**: p. 6154.
227. Bruna-Romero, O., et al., *Complete, long-lasting protection against malaria of mice primed and boosted with two distinct viral vectors expressing the same plasmodial antigen.* Proc Natl Acad Sci U S A, 2001. **98**(20): p. 11491-6.
228. Reyes-Sandoval, A., et al., *Prime-boost immunization with adenoviral and modified vaccinia virus ankara vectors enhances the durability and polyfunctionality of protective malaria CD8+ T-cell responses.* Infect Immun, 2010. **78**(1): p. 145-53.
229. Stoute, J.A., et al., *Long-term efficacy and immune responses following immunization with the RTS,S malaria vaccine.* Journal of Infectious Diseases, 1998. **178**(4): p. 1139-1144.
230. Mata, E., et al., *Malaria vaccine adjuvants: latest update and challenges in preclinical and clinical research.* Biomed Res Int, 2013. **2013**: p. 282913.
231. Gordon, D.M., et al., *SAFETY, IMMUNOGENICITY, AND EFFICACY OF A RECOMBINANTLY PRODUCED PLASMODIUM-FALCIPARUM CIRCUMSPOROZOITE-PROTEIN HEPATITIS-B SURFACE-ANTIGEN SUBUNIT VACCINE.* Journal of Infectious Diseases, 1995. **171**(6): p. 1576-1585.
232. Johnson, A.G., *Molecular adjuvants and immunomodulators: new approaches to immunization.* Clin Microbiol Rev, 1994. **7**(3): p. 277-89.
233. Stoute, J.A., et al., *A preliminary evaluation of a recombinant circumsporozoite protein vaccine against Plasmodium falciparum malaria. RTS,S Malaria Vaccine Evaluation Group.* N Engl J Med, 1997. **336**(2): p. 86-91.
234. Bejon, P., et al., *Efficacy of RTS,S/AS01E vaccine against malaria in children 5 to 17 months of age.* N Engl J Med, 2008. **359**(24): p. 2521-32.
235. Bojang, K.A., et al., *Efficacy of RTS,S/AS02 malaria vaccine against Plasmodium falciparum infection in semi-immune adult men in The Gambia: a randomised trial.* Lancet, 2001. **358**(9297): p. 1927-34.
236. Alonso, P.L., et al., *Efficacy of the RTS,S/AS02A vaccine against Plasmodium falciparum infection and disease in young African children: randomised controlled trial.* Lancet, 2004. **364**(9443): p. 1411-20.
237. Forbes, E.K., et al., *T cell responses induced by adenoviral vectored vaccines can be adjuvanted by fusion of antigen to the oligomerization domain of c4b-binding protein.* PLoS One, 2012. **7**(9): p. e44943.
238. de Cassan, S.C. and S.J. Draper, *Recent advances in antibody-inducing poxviral and adenoviral vectored vaccine delivery platforms for difficult disease targets.* Expert Rev Vaccines, 2013. **12**(4): p. 365-78.
239. Iwasaki, A. and R. Medzhitov, *Toll-like receptor control of the adaptive immune responses.* Nat Immunol, 2004. **5**(10): p. 987-95.
240. Wiley, S.R., et al., *Targeting TLRs expands the antibody repertoire in response to a malaria vaccine.* Sci Transl Med, 2011. **3**(93): p. 93ra69.
241. Mullen, G.E., et al., *Enhancement of functional antibody responses to AMA1-C1/Alhydrogel, a Plasmodium falciparum malaria vaccine, with CpG oligodeoxynucleotide.* Vaccine, 2006. **24**(14): p. 2497-505.
242. Near, K.A., et al., *Improved immunogenicity and efficacy of the recombinant 19-kilodalton merozoite surface protein 1 by the addition of oligodeoxynucleotide and aluminum hydroxide gel in a murine malaria vaccine model.* Infect Immun, 2002. **70**(2): p. 692-701.

243. Mullen, G.E., et al., *Enhanced antibody production in mice to the malaria antigen AMA1 by CPG 7909 requires physical association of CpG and antigen.* Vaccine, 2007. **25**(29): p. 5343-7.
244. Ellis, R.D., et al., *A Phase 1 study of the blood-stage malaria vaccine candidate AMA1-C1/Alhydrogel with CPG 7909, using two different formulations and dosing intervals.* Vaccine, 2009. **27**(31): p. 4104-9.
245. Steinhagen, F., et al., *TLR-based immune adjuvants.* Vaccine, 2011. **29**(17): p. 3341-55.
246. Karbach, J., et al., *Therapeutic administration of a synthetic CpG oligodeoxynucleotide triggers formation of anti-CpG antibodies.* Cancer Res, 2012. **72**(17): p. 4304-10.
247. Israeli, E., et al., *Adjuvants and autoimmunity.* Lupus, 2009. **18**(13): p. 1217-25.
248. Ponnudurai, T., et al., *Infectivity of cultured Plasmodium falciparum gametocytes to mosquitoes.* Parasitology, 1989. **98 Pt 2**: p. 165-73.
249. Roestenberg, M., et al., *Comparison of clinical and parasitological data from controlled human malaria infection trials.* PLoS One, 2012. **7**(6): p. e38434.
250. Duncan, C.J. and S.J. Draper, *Controlled human blood stage malaria infection: current status and potential applications.* Am J Trop Med Hyg, 2012. **86**(4): p. 561-5.
251. McCarthy, J.S., et al., *Experimentally induced blood-stage Plasmodium vivax infection in healthy volunteers.* J Infect Dis. **208**(10): p. 1688-94.
252. Hoffman, S.L., et al., *Development of a metabolically active, non-replicating sporozoite vaccine to prevent Plasmodium falciparum malaria.* Hum Vaccin, 2010. **6**(1): p. 97-106.
253. Bejon, P., et al., *Calculation of liver-to-blood inocula, parasite growth rates, and preerythrocytic vaccine efficacy, from serial quantitative polymerase chain reaction studies of volunteers challenged with malaria sporozoites.* J Infect Dis, 2005. **191**(4): p. 619-26.
254. Shekalaghe, S., et al., *Controlled Human Malaria Infection of Tanzanians by Intradermal Injection of Aseptic, Purified, Cryopreserved Plasmodium falciparum Sporozoites.* Am J Trop Med Hyg, 2014. **91**(3): p. 471-80.
255. Mueller, A.K., et al., *Genetically modified Plasmodium parasites as a protective experimental malaria vaccine.* Nature, 2005. **433**(7022): p. 164-7.
256. Roestenberg, M., et al., *Protection against a malaria challenge by sporozoite inoculation.* N Engl J Med, 2009. **361**(5): p. 468-77.
257. Sauerwein, R.W., E.M. Bijker, and T.L. Richie, *Empowering malaria vaccination by drug administration.* Curr Opin Immunol, 2010. **22**(3): p. 367-73.
258. Seder, R.A., et al., *Protection Against Malaria by Intravenous Immunization with a Nonreplicating Sporozoite Vaccine.* Science, 2013.
259. Roestenberg, M., et al., *Long-term protection against malaria after experimental sporozoite inoculation: an open-label follow-up study.* Lancet, 2011. **377**(9779): p. 1770-6.
260. Butler, N.S., et al., *Superior antimalarial immunity after vaccination with late liver stage-arresting genetically attenuated parasites.* Cell Host Microbe, 2011. **9**(6): p. 451-62.
261. Egan, A., et al., *Characterization of human T- and B-cell epitopes in the C terminus of Plasmodium falciparum merozoite surface protein 1: evidence for poor T-cell recognition of polypeptides with numerous disulfide bonds.* Infect Immun, 1997. **65**(8): p. 3024-31.
262. Crotty, S., et al., *Tracking human antigen-specific memory B cells: a sensitive and generalized ELISPOT system.* J Immunol Methods, 2004. **286**(1-2): p. 111-22.
263. Wrammert, J., et al., *Rapid cloning of high-affinity human monoclonal antibodies against influenza virus.* Nature, 2008. **453**(7195): p. 667-71.
264. Osier, F.H., et al., *Naturally acquired antibodies to polymorphic and conserved epitopes of Plasmodium falciparum merozoite surface protein 3.* Parasite Immunol, 2007. **29**(8): p. 387-94.

265. Dobano, C., et al., *Expression of merozoite surface protein markers by Plasmodium falciparum-infected erythrocytes in peripheral blood and tissues of children with fatal malaria.* Infect Immun, 2007. **75**(2): p. 643-52.
266. Draper, S.J., et al., *Enhancing blood-stage malaria subunit vaccine immunogenicity in rhesus macaques by combining adenovirus, poxvirus, and protein-in-adjuvant vaccines.* J Immunol, 2010. **185**(12): p. 7583-95.
267. Chuang, I., et al., *DNA Prime/Adenovirus Boost Malaria Vaccine Encoding P. falciparum CSP and AMA1 Induces Sterile Protection Associated with Cell-Mediated Immunity.* PLoS One, 2013. **8**(2): p. e55571.
268. Reddy, S.B., et al., *High affinity antibodies to Plasmodium falciparum merozoite antigens are associated with protection from malaria.* PLoS One, 2012. **7**(2): p. e32242.
269. Yeom, J.S., et al., *Serum cytokine profiles in patients with Plasmodium vivax malaria: a comparison between those who presented with and without hepatic dysfunction.* Trans R Soc Trop Med Hyg, 2003. **97**(6): p. 687-91.
270. Harpaz, R., et al., *Serum cytokine profiles in experimental human malaria. Relationship to protection and disease course after challenge.* J Clin Invest, 1992. **90**(2): p. 515-23.
271. Hermsen, C.C., et al., *Circulating concentrations of soluble granzyme A and B increase during natural and experimental Plasmodium falciparum infections.* Clin Exp Immunol, 2003. **132**(3): p. 467-72.
272. Berthoud, T.K., et al., *MIG (CXCL9) is a more sensitive measure than IFN-gamma of vaccine induced T-cell responses in volunteers receiving investigated malaria vaccines.* J Immunol Methods, 2009. **340**(1): p. 33-41.
273. Eling, W.M. and P.G. Kremsner, *Cytokines in malaria, pathology and protection.* Biotherapy, 1994. **7**(3-4): p. 211-21.
274. Angulo, I. and M. Fresno, *Cytokines in the pathogenesis of and protection against malaria.* Clin Diagn Lab Immunol, 2002. **9**(6): p. 1145-52.
275. Seder, R.A., P.A. Darrah, and M. Roederer, *T-cell quality in memory and protection: implications for vaccine design.* Nat Rev Immunol, 2008. **8**(4): p. 247-58.
276. Doucett, V.P., et al., *Enumeration and characterization of virus-specific B cells by multicolor flow cytometry.* J Immunol Methods, 2005. **303**(1-2): p. 40-52.
277. Scheid, J.F., et al., *A method for identification of HIV gp140 binding memory B cells in human blood.* J Immunol Methods, 2009. **343**(2): p. 65-7.
278. Weiss, G.E., et al., *High efficiency human memory B cell assay and its application to studying Plasmodium falciparum-specific memory B cells in natural infections.* J Immunol Methods, 2011. **375**(1-2): p. 68-74.
279. Frolich, D., et al., *Secondary immunization generates clonally related antigen-specific plasma cells and memory B cells.* J Immunol, 2010. **185**(5): p. 3103-10.
280. Pinna, D., et al., *Clonal dissection of the human memory B-cell repertoire following infection and vaccination.* Eur J Immunol, 2009. **39**(5): p. 1260-70.
281. Nelson, A.L., E. Dhimolea, and J.M. Reichert, *Development trends for human monoclonal antibody therapeutics.* Nat Rev Drug Discov, 2010. **9**(10): p. 767-74.
282. Drewe, E. and R.J. Powell, *Clinically useful monoclonal antibodies in treatment.* J Clin Pathol, 2002. **55**(2): p. 81-5.
283. Burton, D.R., et al., *Broadly neutralizing antibodies present new prospects to counter highly antigenically diverse viruses.* Science, 2012. **337**(6091): p. 183-6.
284. Wrammert, J., et al., *Broadly cross-reactive antibodies dominate the human B cell response against 2009 pandemic H1N1 influenza virus infection.* J Exp Med, 2011. **208**(1): p. 181-93.

285. Wu, X., et al., *Rational design of envelope identifies broadly neutralizing human monoclonal antibodies to HIV-1.* Science, 2010. **329**(5993): p. 856-61.
286. Saylor, C., E. Dadachova, and A. Casadevall, *Monoclonal antibody-based therapies for microbial diseases.* Vaccine, 2009. **27 Suppl 6**: p. G38-46.
287. Muellenbeck, M.F., et al., *Atypical and classical memory B cells produce Plasmodium falciparum neutralizing antibodies.* J Exp Med, 2013. **210**(2): p. 389-99.
288. Lanzavecchia, A., D. Corti, and F. Sallusto, *Human monoclonal antibodies by immortalization of memory B cells.* Curr Opin Biotechnol, 2007. **18**(6): p. 523-8.
289. Kozbor, D., A.E. Lagarde, and J.C. Roder, *Human hybridomas constructed with antigen-specific Epstein-Barr virus-transformed cell lines.* Proc Natl Acad Sci U S A, 1982. **79**(21): p. 6651-5.
290. Jones, P.T., et al., *Replacing the complementarity-determining regions in a human antibody with those from a mouse.* Nature, 1986. **321**(6069): p. 522-5.
291. Kaluza, B., et al., *A general method for chimerization of monoclonal antibodies by inverse polymerase chain reaction which conserves authentic N-terminal sequences.* Gene, 1992. **122**(2): p. 321-8.
292. McCafferty, J., et al., *Phage antibodies: filamentous phage displaying antibody variable domains.* Nature, 1990. **348**(6301): p. 552-4.
293. Tiller, T., et al., *Efficient generation of monoclonal antibodies from single human B cells by single cell RT-PCR and expression vector cloning.* J Immunol Methods, 2008. **329**(1-2): p. 112-24.
294. Smith, K., et al., *Rapid generation of fully human monoclonal antibodies specific to a vaccinating antigen.* Nat Protoc, 2009. **4**(3): p. 372-84.
295. Trager, W. and J.B. Jensen, *Human malaria parasites in continuous culture.* Science, 1976. **193**(4254): p. 673-5.
296. Miura, K., et al., *Anti-apical-membrane-antigen-1 antibody is more effective than anti-42-kilodalton-merozoite-surface-protein-1 antibody in inhibiting plasmodium falciparum growth, as determined by the in vitro growth inhibition assay.* Clin Vaccine Immunol, 2009. **16**(7): p. 963-8.
297. Biswas, S., et al., *Transgene Optimization, Immunogenicity and In Vitro Efficacy of Viral Vectored Vaccines Expressing Two Alleles of Plasmodium falciparum AMA1.* PLoS One, 2011. **6**(6): p. e20977.
298. Goodman, A.L., et al., *New candidate vaccines against blood-stage Plasmodium falciparum malaria: prime-boost immunization regimens incorporating human and simian adenoviral vectors and poxviral vectors expressing an optimized antigen based on merozoite surface protein 1.* Infect Immun, 2010. **78**(11): p. 4601-12.
299. Dupraz, P. and M. Kobr, *Leader sequences for use in production of proteins*. 2006, Google Patents.
300. Ahlborg, N., et al., *Protective immune responses to the 42-kilodalton (kDa) region of Plasmodium yoelii merozoite surface protein 1 are induced by the C-terminal 19-kDa region but not by the adjacent 33-kDa region.* Infect Immun, 2002. **70**(2): p. 820-5.
301. Hodgson, S.H., et al., *Combining viral vectored and protein-in-adjuvant vaccines against the blood-stage malaria antigen AMA1 - Report on a Phase Ia clinical trial.* Mol Ther, 2014.
302. Bestard, O., et al., *Cross-validation of IFN-gamma Elispot assay for measuring alloreactive memory/effector T cell responses in renal transplant recipients.* Am J Transplant, 2013. **13**(7): p. 1880-90.
303. Maecker, H.T., et al., *Impact of cryopreservation on tetramer, cytokine flow cytometry, and ELISPOT.* BMC Immunol, 2005. **6**: p. 17.
304. Smith, J.G., et al., *Development and validation of a gamma interferon ELISPOT assay for quantitation of cellular immune responses to varicella-zoster virus.* Clin Diagn Lab Immunol, 2001. **8**(5): p. 871-9.

305. Truck, J., et al., *Effect of cryopreservation of peripheral blood mononuclear cells (PBMCs) on the variability of an antigen-specific memory B cell ELISpot.* Hum Vaccin Immunother, 2014. **10**(8): p. 2490-6.
306. Quan, J. and J. Tian, *Circular polymerase extension cloning for high-throughput cloning of complex and combinatorial DNA libraries.* Nat Protoc, 2011. **6**(2): p. 242-51.
307. Sheehy, S.H., et al., *Optimising Controlled Human Malaria Infection Studies Using Cryopreserved Parasites Administered by Needle and Syringe.* PLoS One, 2013. **8**(6): p. e65960.
308. Halliley, J.L., et al., *Peak frequencies of circulating human influenza-specific antibody secreting cells correlate with serum antibody response after immunization.* Vaccine, 2010. **28**(20): p. 3582-7.
309. Capone, S., et al., *Development of chimpanzee adenoviruses as vaccine vectors: challenges and successes emerging from clinical trials.* Expert Rev Vaccines, 2013. **12**(4): p. 379-93.
310. Traore, B., et al., *The TLR9 agonist CpG fails to enhance the acquisition of Plasmodium falciparum-specific memory B cells in semi-immune adults in Mali.* Vaccine, 2009. **27**(52): p. 7299-303.
311. Sallusto, F., et al., *From vaccines to memory and back.* Immunity, 2010. **33**(4): p. 451-63.
312. Sauerwein, R.W., M. Roestenberg, and V.S. Moorthy, *Experimental human challenge infections can accelerate clinical malaria vaccine development.* Nat Rev Immunol, 2011. **11**(1): p. 57-64.
313. Weiss, R., et al., *Differential effects of C3d on the immunogenicity of gene gun vaccines encoding Plasmodium falciparum and Plasmodium berghei MSP1(42).* Vaccine, 2010. **28**(28): p. 4515-22.
314. Zuccala, E.S., et al., *Subcompartmentalisation of proteins in the rhoptries correlates with ordered events of erythrocyte invasion by the blood stage malaria parasite.* PLoS One, 2012. **7**(9): p. e46160.
315. Kafuye-Mlwilo, M.Y., P. Mukherjee, and V.S. Chauhan, *Kinetics of humoral and memory B cell response induced by the Plasmodium falciparum 19-kilodalton merozoite surface protein 1 in mice.* Infect Immun, 2012. **80**(2): p. 633-42.
316. Wykes, M.N., et al., *Plasmodium yoelii can ablate vaccine-induced long-term protection in mice.* J Immunol, 2005. **175**(4): p. 2510-6.
317. Clutterbuck, E.A., et al., *Pneumococcal conjugate and plain polysaccharide vaccines have divergent effects on antigen-specific B cells.* J Infect Dis, 2012. **205**(9): p. 1408-16.
318. Nduati, E.W., et al., *Distinct kinetics of memory B-cell and plasma-cell responses in peripheral blood following a blood-stage Plasmodium chabaudi infection in mice.* PLoS One, 2010. **5**(11): p. e15007.
319. Garcia-Bates, T.M., et al., *Association between magnitude of the virus-specific plasmablast response and disease severity in dengue patients.* J Immunol, 2013. **190**(1): p. 80-7.
320. Moir, S., et al., *Evidence for HIV-associated B cell exhaustion in a dysfunctional memory B cell compartment in HIV-infected viremic individuals.* J Exp Med, 2008. **205**(8): p. 1797-805.
321. Mahanta, A., et al., *Heightened inflammation in severe malaria is associated with decreased IL-10 expression levels and neutrophils.* Innate Immun, 2014.
322. Kyu, S.Y., et al., *Frequencies of human influenza-specific antibody secreting cells or plasmablasts post vaccination from fresh and frozen peripheral blood mononuclear cells.* J Immunol Methods, 2009. **340**(1): p. 42-7.
323. Groom, J.R. and A.D. Luster, *CXCR3 ligands: redundant, collaborative and antagonistic functions.* Immunol Cell Biol, 2011. **89**(2): p. 207-15.
324. Muehlinghaus, G., et al., *Regulation of CXCR3 and CXCR4 expression during terminal differentiation of memory B cells into plasma cells.* Blood, 2005. **105**(10): p. 3965-71.

325. Whiting, D., et al., *Chemokine monokine induced by IFN-gamma/CXC chemokine ligand 9 stimulates T lymphocyte proliferation and effector cytokine production.* J Immunol, 2004. **172**(12): p. 7417-24.
326. Groom, J.R. and A.D. Luster, *CXCR3 in T cell function.* Exp Cell Res, 2011. **317**(5): p. 620-31.
327. Brice, G.T., et al., *Expression of the chemokine MIG is a sensitive and predictive marker for antigen-specific, genetically restricted IFN-gamma production and IFN-gamma-secreting cells.* J Immunol Methods, 2001. **257**(1-2): p. 55-69.
328. Mizuochi, T., et al., *Possible recruitment of peripheral blood CXCR3+ CD27+ CD19+ B cells to the liver of chronic hepatitis C patients.* J Interferon Cytokine Res, 2010. **30**(4): p. 243-52.
329. Cepok, S., et al., *Short-lived plasma blasts are the main B cell effector subset during the course of multiple sclerosis.* Brain, 2005. **128**(Pt 7): p. 1667-76.
330. Achtman, A.H., et al., *Plasmodium chabaudi chabaudi infection in mice induces strong B cell responses and striking but temporary changes in splenic cell distribution.* J Immunol, 2003. **171**(1): p. 317-24.
331. Galson, J.D., et al., *Studying the antibody repertoire after vaccination: practical applications.* Trends Immunol, 2014.
332. Dekosky, B.J., et al., *High-throughput sequencing of the paired human immunoglobulin heavy and light chain repertoire.* Nat Biotechnol, 2013. **31**(2): p. 166-9.
333. Pizarro, J.C., et al., *Crystal structure of the malaria vaccine candidate apical membrane antigen 1.* Science, 2005. **308**(5720): p. 408-11.
334. Igonet, S., et al., *Cross-reactivity studies of an anti-Plasmodium vivax apical membrane antigen 1 monoclonal antibody: binding and structural characterisation.* J Mol Biol, 2007. **366**(5): p. 1523-37.
335. Moody, M.A. and B.F. Haynes, *Antigen-specific B cell detection reagents: use and quality control.* Cytometry A, 2008. **73**(11): p. 1086-92.
336. Bardelli, M., et al., *Ex vivo analysis of human memory B lymphocytes specific for A and B influenza hemagglutinin by polychromatic flow-cytometry.* PLoS One, 2013. **8**(8): p. e70620.
337. Franz, B., et al., *Ex vivo characterization and isolation of rare memory B cells with antigen tetramers.* Blood. **118**(2): p. 348-57.
338. Pinto, D., et al., *A functional BCR in human IgA and IgM plasma cells.* Blood, 2013. **121**(20): p. 4110-4.
339. Jourdan, M., et al., *An in vitro model of differentiation of memory B cells into plasmablasts and plasma cells including detailed phenotypic and molecular characterization.* Blood, 2009. **114**(25): p. 5173-81.
340. Manz, R., et al., *Analysis and Sorting of Live Cells According to Secreted Molecules, Relocated to a Cell-Surface Affinity Matrix.* Proceedings of the National Academy of Sciences of the United States of America, 1995. **92**(6): p. 1921-1925.
341. Townsend, S.E., C.C. Goodnow, and R.J. Cornall, *Single epitope multiple staining to detect ultralow frequency B cells.* J Immunol Methods, 2001. **249**(1-2): p. 137-46.
342. Poulsen, T.R., et al., *Kinetic, affinity, and diversity limits of human polyclonal antibody responses against tetanus toxoid.* J Immunol, 2007. **179**(6): p. 3841-50.
343. Johnson, P.R., et al., *Vector-mediated gene transfer engenders long-lived neutralizing activity and protection against SIV infection in monkeys.* Nat Med, 2009. **15**(8): p. 901-6.
344. Deal, C., et al., *Vectored antibody gene delivery protects against Plasmodium falciparum sporozoite challenge in mice.* Proc Natl Acad Sci U S A, 2014. **111**(34): p. 12528-32.
345. McCoy, L.E. and R.A. Weiss, *Neutralizing antibodies to HIV-1 induced by immunization.* J Exp Med, 2013. **210**(2): p. 209-23.

346. Bouharoun-Tayoun, H. and P. Druilhe, *Plasmodium falciparum malaria: evidence for an isotype imbalance which may be responsible for delayed acquisition of protective immunity.* Infect Immun, 1992. **60**(4): p. 1473-81.
347. Dutta, S., et al., *Mode of action of invasion-inhibitory antibodies directed against apical membrane antigen 1 of Plasmodium falciparum.* Infect Immun, 2005. **73**(4): p. 2116-22.
348. Collins, C.R., et al., *Fine mapping of an epitope recognized by an invasion-inhibitory monoclonal antibody on the malaria vaccine candidate apical membrane antigen 1.* J Biol Chem, 2007. **282**(10): p. 7431-41.
349. Coley, A.M., et al., *Rapid and precise epitope mapping of monoclonal antibodies against Plasmodium falciparum AMA1 by combined phage display of fragments and random peptides.* Protein Eng, 2001. **14**(9): p. 691-8.
350. Coley, A.M., et al., *Structure of the malaria antigen AMA1 in complex with a growth-inhibitory antibody.* PLoS Pathog, 2007. **3**(9): p. 1308-19.
351. Kusi, K.A., et al., *Humoral immune response to mixed PfAMA1 alleles; multivalent PfAMA1 vaccines induce broad specificity.* PLoS One, 2009. **4**(12): p. e8110.
352. Schaerli, P., et al., *CXC chemokine receptor 5 expression defines follicular homing T cells with B cell helper function.* J Exp Med, 2000. **192**(11): p. 1553-62.
353. Havenith, S.H., et al., *CXCR5+CD4+ follicular helper T cells accumulate in resting human lymph nodes and have superior B cell helper activity.* Int Immunol, 2014. **26**(3): p. 183-92.
354. Nutt, S.L. and D.M. Tarlinton, *Germinal center B and follicular helper T cells: siblings, cousins or just good friends?* Nature Immunology, 2011. **12**(6): p. 472-477.
355. Muller, G., U.E. Hopken, and M. Lipp, *The impact of CCR7 and CXCR5 on lymphoid organ development and systemic immunity.* Immunol Rev, 2003. **195**: p. 117-35.
356. Garside, P., et al., *Visualization of specific B and T lymphocyte interactions in the lymph node.* Science, 1998. **281**(5373): p. 96-9.
357. Bishop, G.A. and B.S. Hostager, *The CD40-CD154 interaction in B cell-T cell liaisons.* Cytokine Growth Factor Rev, 2003. **14**(3-4): p. 297-309.
358. Kalled, S.L., *Impact of the BAFF/BR3 axis on B cell survival, germinal center maintenance and antibody production.* Semin Immunol, 2006. **18**(5): p. 290-6.
359. Good-Jacobson, K.L., et al., *PD-1 regulates germinal center B cell survival and the formation and affinity of long-lived plasma cells.* Nat Immunol, 2010. **11**(6): p. 535-42.
360. Linterman, M.A., et al., *IL-21 acts directly on B cells to regulate Bcl-6 expression and germinal center responses.* J Exp Med, 2010. **207**(2): p. 353-63.
361. Zotos, D., et al., *IL-21 regulates germinal center B cell differentiation and proliferation through a B cell-intrinsic mechanism.* J Exp Med, 2010. **207**(2): p. 365-78.
362. Waring, P. and A. Mullbacher, *Cell death induced by the Fas/Fas ligand pathway and its role in pathology.* Immunol Cell Biol, 1999. **77**(4): p. 312-7.
363. Weinstein, J.S., et al., *B cells in T follicular helper cell development and function: separable roles in delivery of ICOS ligand and antigen.* J Immunol, 2014. **192**(7): p. 3166-79.
364. Weber, J.P., F. Fuhrmann, and A. Hutloff, *T-follicular helper cells survive as long-term memory cells.* Eur J Immunol, 2012. **42**(8): p. 1981-8.
365. Morita, R., et al., *Human blood CXCR5(+)CD4(+) T cells are counterparts of T follicular cells and contain specific subsets that differentially support antibody secretion.* Immunity, 2011. **34**(1): p. 108-21.
366. Tsai, L.M. and D. Yu, *Follicular helper T-cell memory: establishing new frontiers during antibody response.* Immunol Cell Biol, 2014. **92**(1): p. 57-63.

367. Spensieri, F., et al., *Human circulating influenza-CD4+ ICOS1+IL-21+ T cells expand after vaccination, exert helper function, and predict antibody responses.* Proc Natl Acad Sci U S A, 2013. **110**(35): p. 14330-5.
368. Schmitt, N., S.E. Bentebibel, and H. Ueno, *Phenotype and functions of memory Tfh cells in human blood.* Trends Immunol, 2014.
369. van der Most, R.G., et al., *Seeking help: B cells adapting to flu variability.* Sci Transl Med, 2014. **6**(246): p. 246ps8.
370. Hale, J.S., et al., *Distinct memory CD4+ T cells with commitment to T follicular helper- and T helper 1-cell lineages are generated after acute viral infection.* Immunity, 2013. **38**(4): p. 805-17.
371. Moon, J.J., et al., *Enhancing humoral responses to a malaria antigen with nanoparticle vaccines that expand Tfh cells and promote germinal center induction.* Proc Natl Acad Sci U S A, 2012. **109**(4): p. 1080-5.
372. Rankin, A.L., et al., *IL-21 receptor is critical for the development of memory B cell responses.* J Immunol, 2011. **186**(2): p. 667-74.
373. Thera, M.A., et al., *Safety and allele-specific immunogenicity of a malaria vaccine in Malian adults: results of a phase I randomized trial.* PLoS Clin Trials, 2006. **1**(7): p. e34.
374. Ellis, R.D., et al., *Phase 1 trial of the Plasmodium falciparum blood stage vaccine MSP1(42)-C1/Alhydrogel with and without CPG 7909 in malaria naive adults.* PLoS One, 2010. **5**(1): p. e8787.
375. Thera, M.A., et al., *A field trial to assess a blood-stage malaria vaccine.* N Engl J Med, 2011. **365**(11): p. 1004-13.
376. Ouattara, A., et al., *Lack of allele-specific efficacy of a bivalent AMA1 malaria vaccine.* Malar J, 2010. **9**: p. 175.
377. Harvey, K.L., et al., *Insights and controversies into the role of the key apicomplexan invasion ligand, Apical Membrane Antigen 1.* Int J Parasitol, 2014.
378. Wright, K.E., et al., *Structure of malaria invasion protein RH5 with erythrocyte basigin and blocking antibodies.* Nature, 2014.
379. Chitnis, C.E. and A. Sharma, *Targeting the Plasmodium vivax Duffy-binding protein.* Trends Parasitol, 2008. **24**(1): p. 29-34.
380. Qiu, X., et al., *Reversion of advanced Ebola virus disease in nonhuman primates with ZMapp.* Nature, 2014.
381. Balazs, A.B., et al., *Broad protection against influenza infection by vectored immunoprophylaxis in mice.* Nat Biotechnol, 2013. **31**(7): p. 647-52.
382. Balazs, A.B. and A.P. West, Jr., *Antibody gene transfer for HIV immunoprophylaxis.* Nat Immunol, 2013. **14**(1): p. 1-5.